ISSN 0021-9673

VOL. 590 NO. 2 JANUARY 31, 1992

THIS ISSUE COMPLETES VOL. 590

JOURNAL OF CHROMATOGRAPHY

INCLUDING ELECTROPHORESIS AND OTHER SEPARATION METHODS

ELSEVIER

JOURNAL OF CHROMATOGRAPHY

INCLUDING ELECTROPHORESIS AND OTHER SEPARATION METHODS

Scope. The *Journal of Chromatography* publishes papers on all aspects of chromatography, electrophoresis and related methods. Contributions consist mainly of research papers dealing with chromatographic theory, instrumental development and their applications. The section *Biomedical Applications*, which is under separate editorship, deals with the following aspects: developments in and applications of chromatographic and electrophoretic techniques related to clinical diagnosis or alterations during medical treatment; screening and profiling of body fluids or tissues with special reference to metabolic disorders; results from basic medical research with direct consequences in clinical practice; drug level monitoring and pharmacokinetic studies; clinical toxicology; analytical studies in occupational medicine.

Submission of Papers. Manuscripts (in English; *four* copies are required) should be submitted to: Editorial Office of *Journal of Chromatography*, P.O. Box 681, 1000 AR Amsterdam, Netherlands, Telefax (+31-20) 5862 304, or to: The Editor of *Journal of Chromatography, Biomedical Applications*, P.O. Box 681, 1000 AR Amsterdam, Netherlands. Review articles are invited or proposed by letter to the Editors. An outline of the proposed review should first be forwarded to the Editors for preliminary discussion prior to preparation. Submission of an article is understood to imply that the article is original and unpublished and is not being considered for publication elsewhere. For copyright regulations, see below.

Publication. The *Journal of Chromatography* (incl. *Biomedical Applications*) has 39 volumes in 1992. The subscription prices for 1992 are:

J. Chromatogr. (incl. *Cum. Indexes, Vols. 551–600*) + *Biomed. Appl.* (Vols. 573–611):
Dfl. 7722.00 plus Dfl. 1209.00 (p.p.h.) (total *ca.* US$ 4880.25)

J. Chromatogr. (incl. *Cum. Indexes, Vols. 551–600*) only (Vols. 585–611):
Dfl. 6210.00 plus Dfl. 837.00 (p.p.h.) (total *ca.* US$ 3850.75)

Biomed. Appl. only (Vols. 573–584):
Dfl. 2760.00 plus Dfl. 372.00 (p.p.h.) (total *ca.* US$ 1711.50).

Subscription Orders. The Dutch guilder price is definitive. The US$ price is subject to exchange-rate fluctuations and is given as a guide. Subscriptions are accepted on a prepaid basis only, unless different terms have been previously agreed upon. Subscriptions orders can be entered only by calender year (Jan.–Dec.) and should be sent to Elsevier Science Publishers, Journal Department, P.O. Box 211, 1000 AE Amsterdam, Netherlands, Tel. (+31-20) 5803 642, Telefax (+31-20) 5803 598, or to your usual subscription agent. Postage and handling charges include surface delivery except to the following countries where air delivery via SAL (Surface Air Lift) mail is ensured: Argentina, Australia, Brazil, Canada, China, Hong Kong, India, Israel, Japan*, Malaysia, Mexico, New Zealand, Pakistan, Singapore, South Africa, South Korea, Taiwan, Thailand, USA. *For Japan air delivery (SAL) requires 25% additional charge of the normal postage and handling charge. For all other countries airmail rates are available upon request. Claims for missing issues must be made within three months of our publication (mailing) date, otherwise such claims cannot be honoured free of charge. Back volumes of the *Journal of Chromatography* (Vols. 1–572) are available at Dfl. 217.00 (plus postage). Customers in the USA and Canada wishing information on this and other Elsevier journals, please contact Journal Information Center, Elsevier Science Publishing Co. Inc., 655 Avenue of the Americas, New York, NY 10010, USA, Tel. (+1-212) 633 3750, Telefax (+1-212) 633 3990.

Abstracts/Contents Lists published in Analytical Abstracts, Biochemical Abstracts, Biological Abstracts, Chemical Abstracts, Chemical Titles, Chromatography Abstracts, Clinical Chemistry Lookout, Current Contents/Life Sciences, Current Contents/Physical, Chemical & Earth Sciences, Deep-Sea Research/Part B: Oceanographic Literature Review, Excerpta Medica, Index Medicus, Mass Spectrometry Bulletin, PASCAL-CNRS, Pharmaceutical Abstracts, Referativnyi Zhurnal, Research Alert, Science Citation Index and Trends in Biotechnology.

See inside back cover for Publication Schedule, Information for Authors and information on Advertisements.

0021-9673/92/$05.00

This issue is printed on acid-free paper.

Printed in the Netherlands

CONTENTS

(Abstracts/Contents Lists published in Analytical Abstracts, Biochemical Abstracts, Biological Abstracts, Chemical Abstracts, Chemical Titles, Chromatography Abstracts, Current Contents/Life Sciences, Current Contents/Physical, Chemical & Earth Sciences, Deep-Sea Research/Part B: Oceanographic Literature Review, Excerpta Medica, Index Medicus, Mass Spectrometry Bulletin, PASCAL-CRNS, Referativnyi Zhurnal, Research Alert and Science Citation Index)

REGULAR PAPERS

Column Liquid Chromatography

Gas Chromatography

(Continued overleaf)

In articles with more than one author, the name of the author to whom correspondence should be addressed is indicated in the article heading by a 6-pointed asterisk (*).

Journal of Chromatography, 590 (1992) 175–188
Elsevier Science Publishers B.V., Amsterdam

CHROM. 23 807

Preparative liquid chromatography

I. Influence of column efficiency on optimum injection conditions under isocratic elution

G. Crétier*, L. Macherel and J. L. Rocca

Laboratoire des Sciences Analytiques (UA CNRS 435), Université Claude Bernard, Lyon I, Bât. 308, 43 Boulevard du 11 Novembre 1918, 69622 Villeurbanne Cédex (France)

(First received October 15th, 1990; revised manuscript received May 30th, 1991)

ABSTRACT

Using a chromatographic simulation algorithm based on the Craig machine, CRAIGSIM, to simulate the chromatogram of a binary mixture, the optimum injection conditions corresponding to the maximum recovered amount of the solute of interest were found to depend on the column efficiency. Generally, the optimum injection concentration is an increasing function of the plate number. Consequences of this behaviour on the scale-up procedure in preparative liquid chromatography are discussed.

INTRODUCTION

The goal of a preparative separation is to recover from a mixture the largest amount of one or several substances at a specified purity. A few years ago, the question was to establish whether the best injection conditions consist in concentration or volume overloading the column, *i.e.*, either using a small injection volume and increasing the injected sample concentration, or maintaining a concentration that lies in the linear part of the solute distribution isotherm and increasing the sample volume. Since then, some published results [1–4] have shown that neither of these two ways is correct: generally, both the injection concentration and the injection volume have to be increased and there are some optimum values of the two parameters for which the recovered amount of the solute of interest is maximum. The detailed study of Katti and Guiochon [2] demonstrated that optimization of injection conditions is essential when the impurity to be eliminated is the second-eluted component.

This work deals with the dependence of the optimum injection conditions on the column efficiency. This issue is of the greatest practical importance when scaling up a separation. Both the analytical and the preparative columns have to generate identical retentions, but generally they do not have the same efficiency. Hence the evolution of the optimum values of the injection parameters with the column plate number has to be known in order to extrapolate accurately the separation optimized on the analytical column to the preparative column. This paper also discusses the phenomena explaining the existence of optimum injection conditions.

This study was carried out on chromatograms simulated by means of a program based on the Craig machine using the mixed Langmuir isotherm (*i.e.*, which considers interactions between solutes during their migration). The validity of this simulation software, called CRAIGSIM, is first examined by comparing qualitatively and quantitatively some of its results with those given by the ideal model [5].

0021-9673/92/$05.00

MODEL

Simulation of the chromatographic process

The simulation algorithm is based on a Craig-type repetitive distribution [6]. The column is replaced with n_c stages connected in series, each stage consisting of a certain volume of mobile phase and a certain volume of stationary phase (Fig. 1). The sample is assumed to have a rectangular concentration–volume profile and is considered to fill a certain number of mobile phase cells approaching the column inlet (Fig. 1a). The first mobile phase cell containing sample is introduced in the first stage (Fig. 1b) and after equilibration of both phases (Fig. 1c) the mobile phase is moved to the second stage, taking along its part of the sample (Fig. 1d). The process is repeated until either the sample amount in the transferred mobile phase cell becomes negligible (Fig. 1e) or the transferred mobile phase cell comes out of the column (Fig. 1f). Then the second transfer

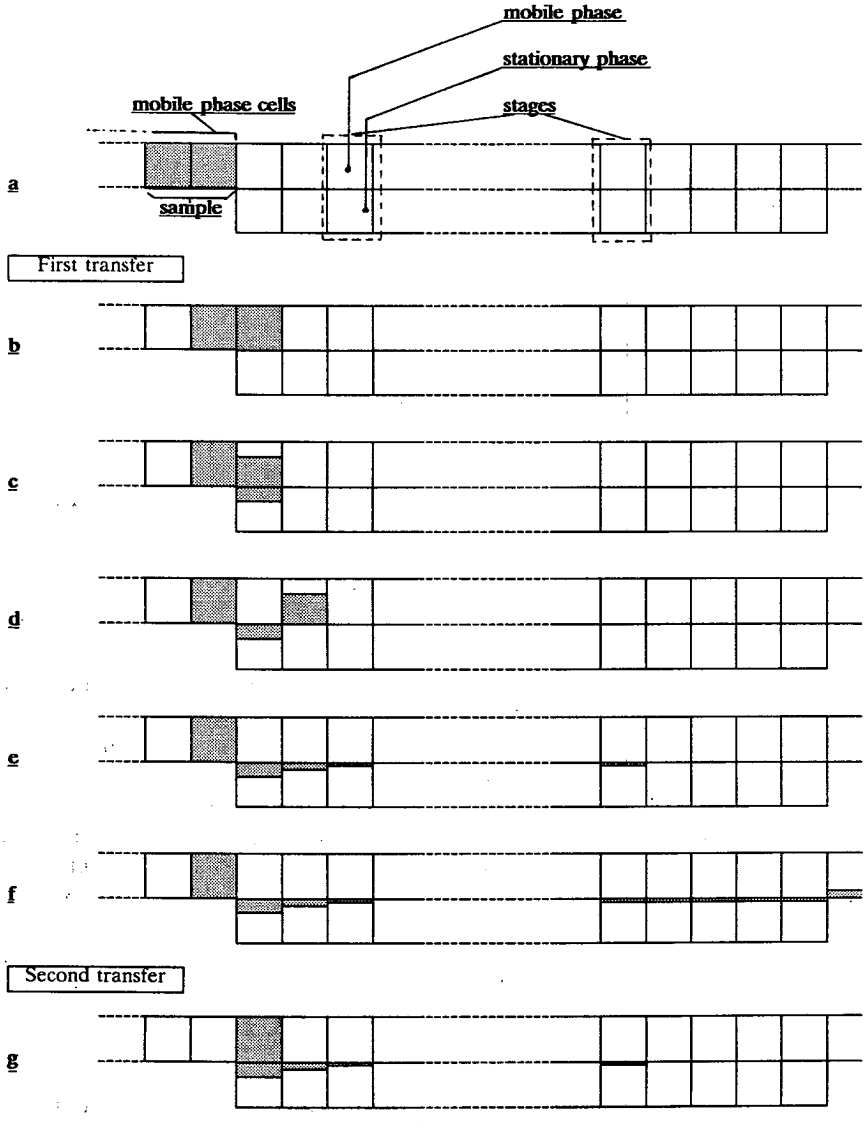

Fig. 1. Schematic diagram of the Craig machine.

is beginning: the second mobile phase cell containing the sample is placed in the first stage, and so on. Consecutive transfers flow the sample downstream. The simulated chromatogram is obtained by plotting the concentration of each solute in the mobile phase of the last stage after the last equilibration *versus* the eluted volume. The process simulates both the retention of solutes and the chromatographic dispersion. The number of theoretical plates N_j (simulated at infinite dilution for solute j) is related to the number of stages n_c by the relationship [6]

$$N_j = (n_c + 1)\frac{1 + k'_j}{k'_j} \quad (1)$$

where k'_j represents the capacity factor of solute j. Hence a given column efficiency can be simulated by adjusting the Craig stage number.

Equilibration of mobile and stationary phases in a stage

The amount of solute j contained in the stage n at the transfer t is

$$Q_{j,n,t} = [\varepsilon C^{m}_{j,n,t} + (1 - \varepsilon)C^{s}_{j,n,t}]\frac{V_c}{n_c} \qquad j = 1 \quad (2a)$$

$$j = 2 \quad (2b)$$

where $C^{m}_{j,n,t}$ is the concentration of solute j in the mobile phase of stage n at transfer t, $C^{s}_{j,n,t}$ is the concentration of solute j in the stationary phase of stage n at transfer t, V_c is the volume of the empty column and ε is the total porosity of the chromatographic bed. $C^{m}_{j,n,t}$ and $C^{s}_{j,n,t}$ with $j = 1$ and $j = 2$ are the four unknowns because, considering the process development, $Q_{j,n,t}$ can be calculated by

$$Q_{j,n,t} = [\varepsilon C^{m}_{j,n-1,t} + (1 - \varepsilon)C^{s}_{j,n,t-1}]\frac{V_c}{n_c} \qquad j = 1 \quad (3a)$$

$$j = 2 \quad (3b)$$

where $C^{m}_{j,n-1,t}$ is the concentration of solute j in mobile phase of stage $n-1$ at transfer t and $C^{s}_{j,n,t-1}$ is the concentration of solute j in stationary phase of stage n at transfer $t-1$.

Mixed Langmuir isotherms are used to describe the solute distribution between the two phases and the interactions between the co-eluting solutes under overload conditions. The distribution of solutes 1 and 2 between the stationary and mobile phases in stage n at transfer t is represented by isotherm equations:

$$C^{s}_{1,n,t} = \frac{a_1 C^{m}_{1,n,t}}{1 + b_1 C^{m}_{1,n,t} + b_2 C^{m}_{2,n,t}} \quad (4a)$$

$$C^{s}_{2,n,t} = \frac{a_2 C^{m}_{2,n,t}}{1 + b_2 C^{m}_{2,n,t} + b_1 C^{m}_{1,n,t}} \quad (4b)$$

where $a_j (j = 1 \text{ or } 2)$ is related to the capacity factor k'_j of solute j according to

$$k'_j = a_j\left(\frac{1 - \varepsilon}{\varepsilon}\right) \quad (5)$$

and b_j ($j = 1$ or 2) is the non-linear coefficient of solute j. $a_j/b_j (j = 1 \text{ or } 2)$ is the saturation concentration of the stationary phase for solute j, *i.e.*, the stationary phase concentration of solute j when its mobile phase concentration is very high. In our study, it is assumed not to depend on the solute ($a_1/b_1 = a_2/b_2$). The corresponding solute amount taken up by the whole stationary phase of the column is called the column saturation capacity and is given by

$$w_s = (1 - \varepsilon)V_c \cdot \frac{a_j}{b_j} \quad (6)$$

The concentrations in the mobile and stationary phases for each solute 1 and 2, $C^{m}_{1,n,t}$, $C^{s}_{1,n,t}$, $C^{m}_{2,n,t}$ and $C^{s}_{2,n,t}$, are calculated by considering the system of the four non-linear equations 2a, 2b, 4a and 4b; the resolution method is described in the Appendix.

EXPERIMENTAL

Computer

Chromatograms were simulated on a PC-AT compatible computer, type NX 386-25 (at 25 MHz) supplied by Unisyx (Paris, France) and equipped with a Model 80387 arithmetic coprocessor. The simulation program was written in TURBO-BASIC from Borland (Scotts Valley, CA, USA).

Simulated conditions

The column simulated was 15 cm × 0.5 cm I.D. with a total porosity ε of 0.8. Consequently, the column dead volume was 2.4 ml. The column plate number was varied from 150 to 900 by changing the stage number n_c from 100 to 600. We simulated the behaviour of two sample mixtures, A and B, of two solutes, 1 and 2. For each binary mixture, Table I gives the coefficients of the solute isotherms a_j and b_j, the solute capacity factors k'_j, the solute relative

TABLE I

CHARACTERISTICS OF THE BINARY MIXTURES CONSIDERED

Mixture	Solute	a_j	b_j (l/mol)	k'_j	k'_2/k'_1	w_s (mmol)
A	1	8	0.8	2	1.5	5.89
	2	12	1.2	3		
B	1	40	8.0	10	1.2	2.95
	2	48	9.6	12		

retention k'_2/k'_1 and the column saturation capacity w_s.

Procedure

Each simulated chromatogram corresponded to a given sample load Q_i injected at a certain total concentration C_i in a certain injection volume V_i ($Q_i = C_i V_i$). For each solute, the program determined the amount $Q_{r,j}$ recovered at 99% purity and calculated the corresponding recovery ratio or yield r_j:

$$r_j = Q_{r,j}/Q_{i,j} \quad (7)$$

where $Q_{i,j}$ is the injected amount of solute j when the injected sample load is Q_i equal to $Q_{i,1} + Q_{i,2}$.

RESULTS AND DISCUSSION

Validation of the present Craig model

Because of interferences between migrating species, peak profiles in multi-component chromatography under overload conditions bear little resemblance to the corresponding single-component peak shapes (Fig. 2). When the two solutes are present simultaneously, the more retained solute tends to push the less retained solute in front of it; this displacement effect is beneficial for the recovery of a large amount of pure solute 1: the main part of solute 1 is eluted as a narrow and concentrated band at the beginning of the chromatogram. The displacement force of solute 2 decreases as its concentration decreases, which explains the tail on the elution profile of solute 1 under the elution profile of solute 2; this latter phenomenon has an adverse effect on the recovery ratio of the more retained compound. The peak front of solute 2 is also swept along by solute 1. The end of the peak profile of solute 2 is similar to the corresponding one without interference.

Such complex peak shapes, which are the result of interfering adsorption behaviour, are qualitatively in very good agreement with numerous published data [3–5,7]. However, in order to establish the

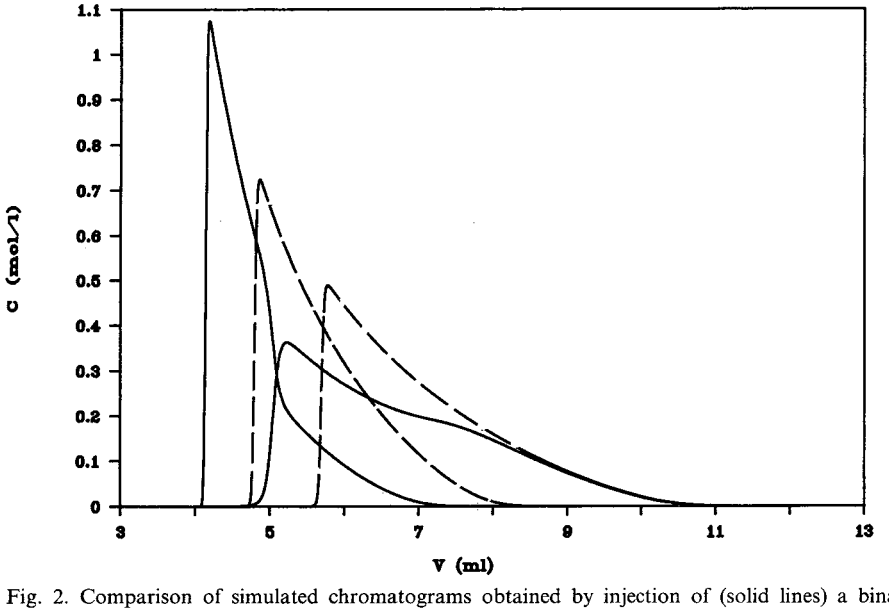

Fig. 2. Comparison of simulated chromatograms obtained by injection of (solid lines) a binary mixture and (dashed lines) the corresponding amounts of single solutes. Mixture A, relative composition 1:1. Q_i = 1.8 mmol = $0.3w_s$; C_i = 2.8 mol/l; n_c = 400.

quantitative validity of our simulation program, CRAIGSIM, we need to compare some chromatograms simulated with it with the corresponding chromatograms given by the ideal model which was previously used as a reference model for describing the heavily overload separation of a binary mixture [8].

The ideal model assumes that the column efficiency is infinite, *i.e.*, the kinetics of mass transfer are so fast that there is a constant equilibrium between the two phases of the chromatographic system. The analytical solution of this ideal model in the case of a binary mixture was recently derived by Golshan-Shirazi and Guiochon [8]; each compound elution profile is composed of discontinuities and continuous parts that are described by the equations given in ref. 8. In Figs. 3–5 corresponding to the same sample amount (1.18 mmol = $0.2w_s$) of three different mixture compositions (1:9, 1:1, 9:1) under different injection conditions, we have superimposed the chromatogram simulated by CRAIGSIM and the peak elution profiles calculated using the analytical solution of the ideal model. The agreement between the ideal chromatogram and the simulated one is very impressive; their overall shapes obviously are very similar; further, there is quantitative agreement for the retention volumes of the discontinuities and the concentrations of the different plateaux. Of course, because of the finite column efficiency simulated by CRAIGSIM, the concentration shocks of the ideal model are slightly eroded, a small amount of band broadening appears at the peak base on each side and the band maximum does not coincide exactly. This close agreement between the two models demonstrates that CRAIGSIM software can be used to predict quantitatively elution profiles for two component separations under overload conditions.

Fig. 3 shows the elution profiles of a 9:1 mixture for a very large injected volume ($V_i = 14.5\sigma_1$, where σ_1 is the standard deviation of the Gaussian peak of solute 1 observed at infinite dilution). The erosion of the top of the rectangular injection band is not complete. The profiles of the two components exhibit two plateaux. For the first peak, the second plateau corresponds to the injected concentration of solute 1 (0.034 mol/l) and the first plateau corresponds to a higher concentration (*ca.* 0.087 mol/l). The more retained solute, which is the major portion of the sample, strongly displaces the less retained

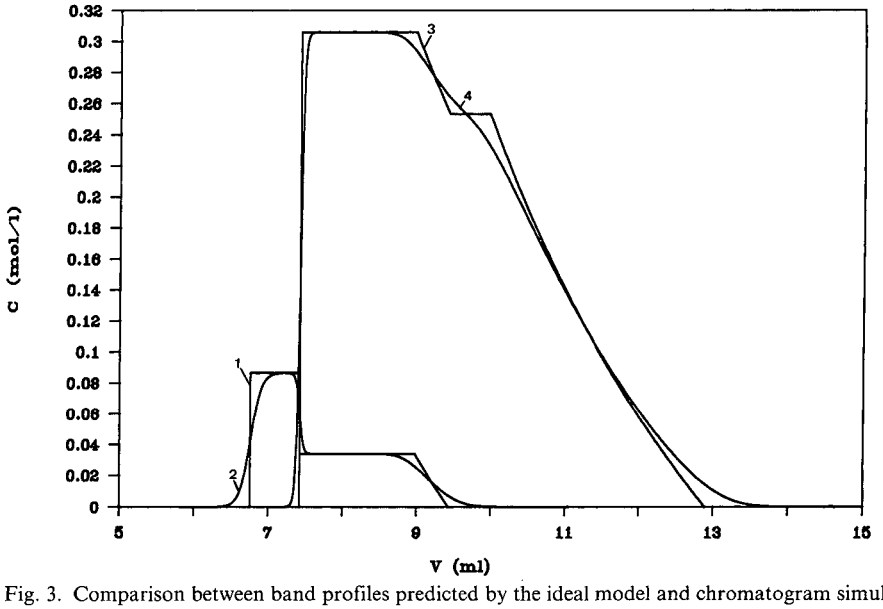

Fig. 3. Comparison between band profiles predicted by the ideal model and chromatogram simulated by CRAIGSIM for a 600-stage column. Mixture A, relative composition 1:9. Q_i = 1.18 mmol = $0.2w_s$; C_i = 0.34 mol/l. Curves: 1 = solute 1, ideal model; 2 = solute 1, CRAIGSIM simulation; 3 = solute 2, ideal model; 4 = solute 2, CRAIGSIM simulation.

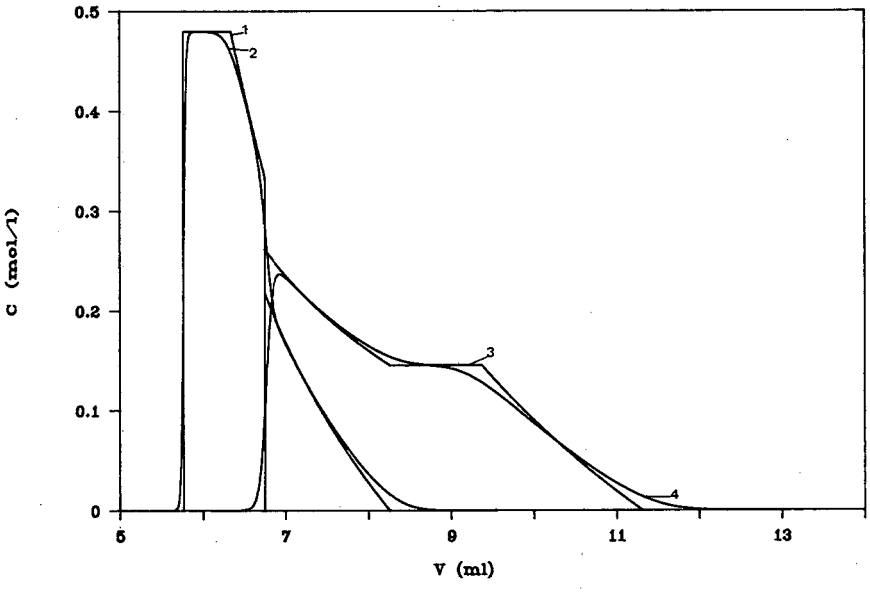

Fig. 4. Comparison between band profiles predicted by the ideal model and chromatogram simulated by CRAIGSIM for a 600-stage column. Conditions as in Fig. 3 except relative concentration of the two solutes = 1:1 and C_i = 0.62 mol/l.

solute and an excrescence, called the "displacement plateau", appears at the front of the profile of the first component. For the second peak, the concentration of the first plateau is equal to the injected concentration of solute 2 (0.306 mol/l) and the second plateau (which has completely disappeared owing to the chromatographic dispersion simulated by CRAIGSIM) corresponds to a lower concentra-

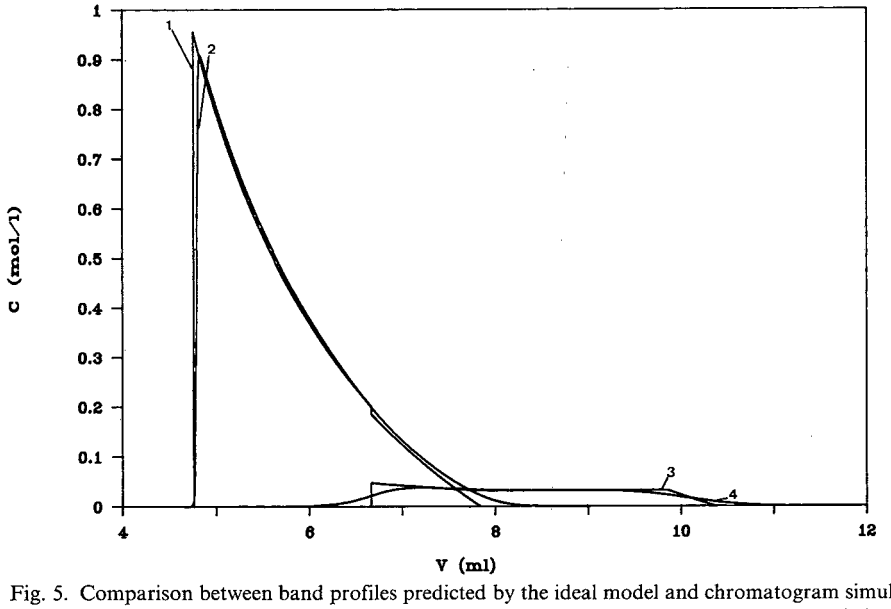

Fig. 5. Comparison between band profiles predicted by the ideal model and chromatogram simulated by CRAIGSIM for a 600-stage column. Conditions as in Fig. 3 except relative concentration of the two solutes = 9:1 and C_i = 1.25 mol/l.

tion (*ca.* 0.253 mol/l). The formation of the second plateau of the second peak, called the "tag-along" plateau, is due to the acceleration of the migration of solute 2 when the two solutes co-elute; the length of this plateau is increased by increasing the relative composition of the first component in the studied mixture (compare Figs. 3, 4 and 5 corresponding to 1:9, 1:1 and 9:1 mixtures, respectively).

In Fig. 5, corresponding to injection of a smaller volume (V_i = 0.94 ml = $3.9\sigma_1$) of a 9:1 mixture, the top of the rectangular band injection is completely eroded. Because solute 2 is the minor component of the sample, the displacement effect of solute 1 by solute 2 is very weak and the plateaux of the first peak are no longer visible.

Design of a preparative separation

We first considered the recovered amount of purified solute as a function of both the recovery yield and the injection conditions. For a given concentration C_i of the injected mixture, the injected amount Q_i, *i.e.*, the injected volume V_i, was gradually increased. In each run, the amount $Q_{r,j}$ of each solute collected at 99% purity was quantified and was plotted against the corresponding recovery yield r_j. This study was carried out for mixture A at relative compositions of 9:1 (Fig. 6) and 1:9 (Fig. 7). These figures confirm the results obtained by Katti and Guiochon [2]: a recovery yield much lower than 100% is often required in order to optimize the recovered amount and the optimum recovery ratio which gives the highest recovered amount for solute 2 is always larger than that for solute 1 (from the 9:1 mixture, 65% for solute 2 instead of 40% for solute 1; from the 1:9 mixture, 97% for solute 2 instead of 50% for solute 1). These plots also show that, except at very large recovery yields, the recovered amount is affected by the sample concentration, whatever the component and the mixture composition considered.

The influence of the sample concentration and the chosen recovery yield on the recovered amount of each 99% pure solute is illustrated in detail for mixture A having relative compositions of 9:1 and 1:9 in Figs. 8 and 9, respectively. At any specified recovery yield, there is an optimum injection concentration for which the recovered amount is maximum. This optimum sample concentration is more or less critically defined. The maximum of the recovered amount is greater when the sample contains much more solute 1 than solute 2, the solute of interest is solute 1 and the acceptable recovery yield is much smaller than 100% (Fig. 8a). Hence under these conditions, the concentration of the injected mixture has to be optimized. In all other instances (Figs. 8b, 9a and 9b), the injection concentration has to be sufficient, but the use of a sample concentration much larger than the optimum does not result in

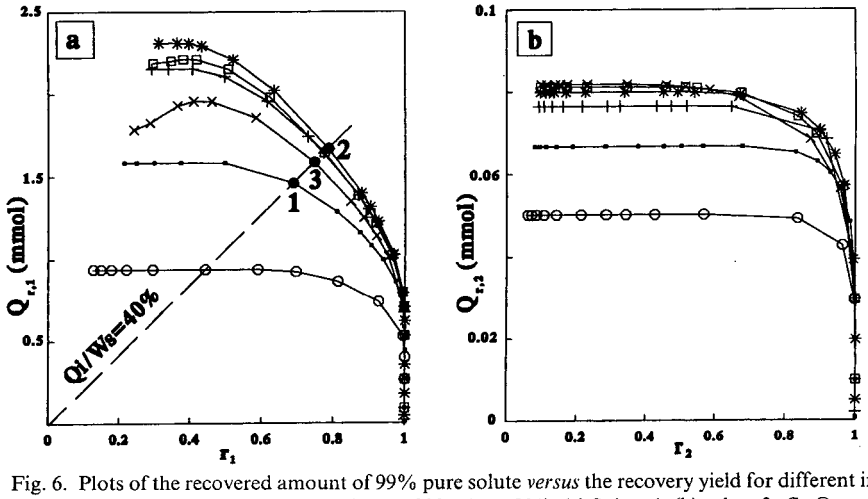

Fig. 6. Plots of the recovered amount of 99% pure solute *versus* the recovery yield for different injected sample concentrations. Mixture A, relative composition 9:1. n_c = 600 (N_1 = 902; N_2 = 801). (a) Solute 1; (b) solute 2. C_i: ○ = 0.6; ■ = 1.7; + = 5; ✳ = 12.5; □ = 25; × = 50 mol/l.

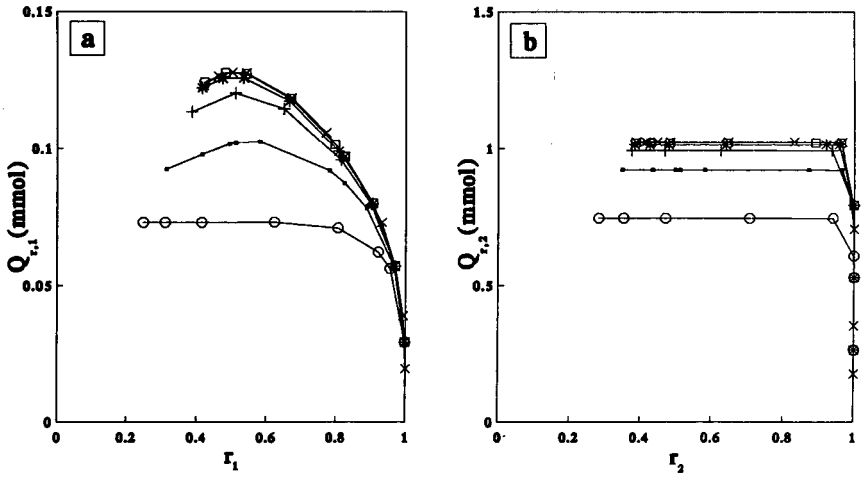

Fig. 7. Plots of the recovered amount of 99% pure solute *versus* the recovery yield for different injected sample concentrations. Conditions as in Fig. 6, except relative composition of the mixture = 1:9.

a large decrease in the recovered amount. Fig. 9b shows that the recovered amount of solute 2 from the 1:9 mixture is identical for recovery yields of 80% and 50%, whatever the injection concentration. This result was foreseeable from Fig. 7b, which demonstrates that, at any sample concentration, the recovered amount of solute 2 from the 1:9 mixture remains maximum as long as the recovery ratio is kept below 97%.

Reprocessing of an impure substance from a preceding chromatographic run is generally expensive and the optimum recovery ratio for the minimum production cost is rarely smaller than 80% [9]. Consequently, although a yield of 40% corresponds to the maximum amount of solute 1 recovered from the 9:1 mixture (Fig. 6a), it is unrealistic in practice. However, under these recovery conditions, the optimum injection concentra-

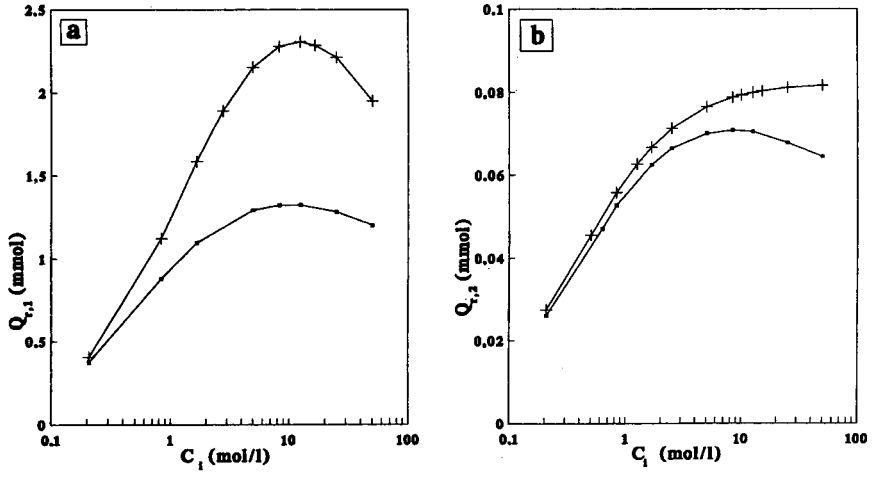

Fig. 8. Plots of the recovered amount of each 99% pure solute *versus* the sample concentration for different recovery yields. Mixture A, relative composition 9:1. n_c = 600 (N_1 = 902; N_2 = 801). (■) r_j = 90%; (+) r_j = 40%. (a) Solute 1; (b) solute 2.

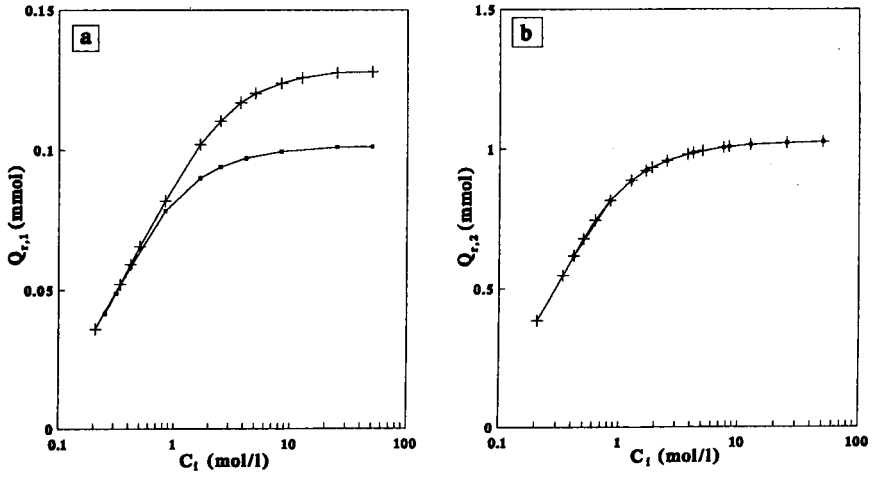

Fig. 9. Plots of the recovered amount of each 99% pure solute *versus* the sample concentration for different recovery yields. Mixture A, relative composition 1:9. n_c = 600 (N_1 = 902; N_2 = 801). (■) r_j = 80%; (+) r_j = 50%. (a) Solute 1; (b) solute 2.

tion is critical and, for clarity reasons, we report the results of the study of the effect of the column efficiency on the optimum injection conditions only in that case. For different column plate numbers, the variations of the recovered amount of 99% pure solute 1 from the 9:1 mixture as a function of both the sample concentration and the injection volume are plotted in Fig. 10. The recovered amount increases with increasing column plate number. The optimum concentration corresponding to the maximum recovered amount is also an increasing function of the column efficiency (Fig. 10a). It increases from 4 to 12.5 mol/l when the stage number of the column is increased from 100 to 600 but, for an injection of 12.5 instead of 4 mol/l on the 100-stage column, the recovered amount of solute 1 decreases by no more than 12%. For 90% recovery of solute 1 from the 9:1 sample, the use on the 100-stage column

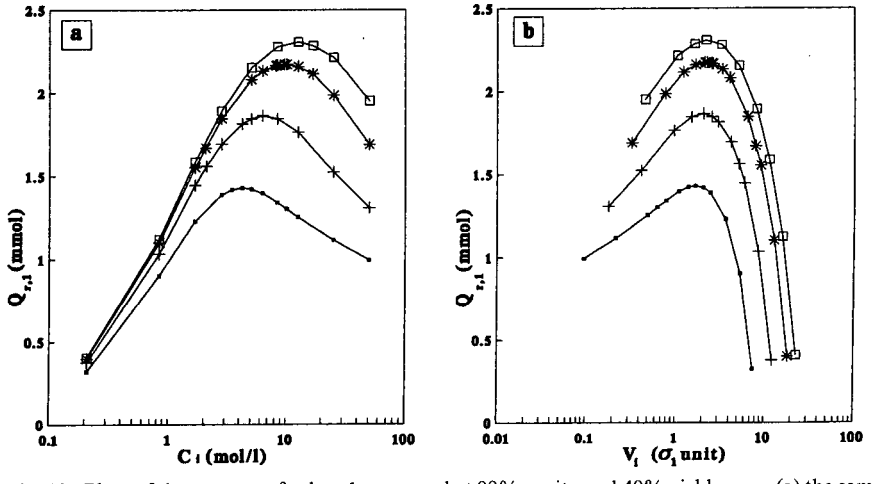

Fig. 10. Plots of the amount of solute 1 recovered at 99% purity and 40% yield *versus* (a) the sample concentration and (b) the injection volume for different column efficiencies. Mixture A, relative composition 9:1. (■) n_c = 100 (N_1 = 152; N_2 = 135); (+) n_c = 200 (N_1 = 302; N_2 = 268); (✳) n_c = 400 (N_1 = 602; N_2 = 535); (□) n_c = 600 (N_1 = 902; N_2 = 801).

of the same injection concentration that is optimum for the 600-stage column results in a decrease of only 4% in the recovered amount (results not shown). In other words, when scaling a separation, if necessary, the injection concentration optimized on the analytical column can be used on the preparative column, which usually contains a smaller number of theoretical plates. Then, the injection volume has to be adjusted directly on the preparative column.

Fig. 10b shows that the optimum injection volume, corresponding to the maximum recovered amount and expressed in standard deviations of the Gaussian peak observed at infinite dilution of the first solute, can be considered to be independent of the column efficiency. It varies from $1.6\sigma_1$ to $2.2\sigma_1$ when the column stage number ranges from 100 to 600, but a decrease of only 1.5% in the recovered amount is incurred when the sample is injected on the 100-stage column in a volume of $2.2\sigma_1$. Consequently, in scale-up operation, the value of the reduced injection volume V_i/σ_1 can first be optimized on the analytical column and then, without taking any risks, this optimum value can be adopted for the preparative column in order to adjust the injection amount.

Phenomena governing the optimum injection conditions

In order to understand the phenomena that explain the existence of the optimum injection conditions, we examined the influence of the sample concentration on the chromatogram corresponding to a given injected amount of mixture A at a relative composition of 9:1 (Fig. 11). The elution volume of

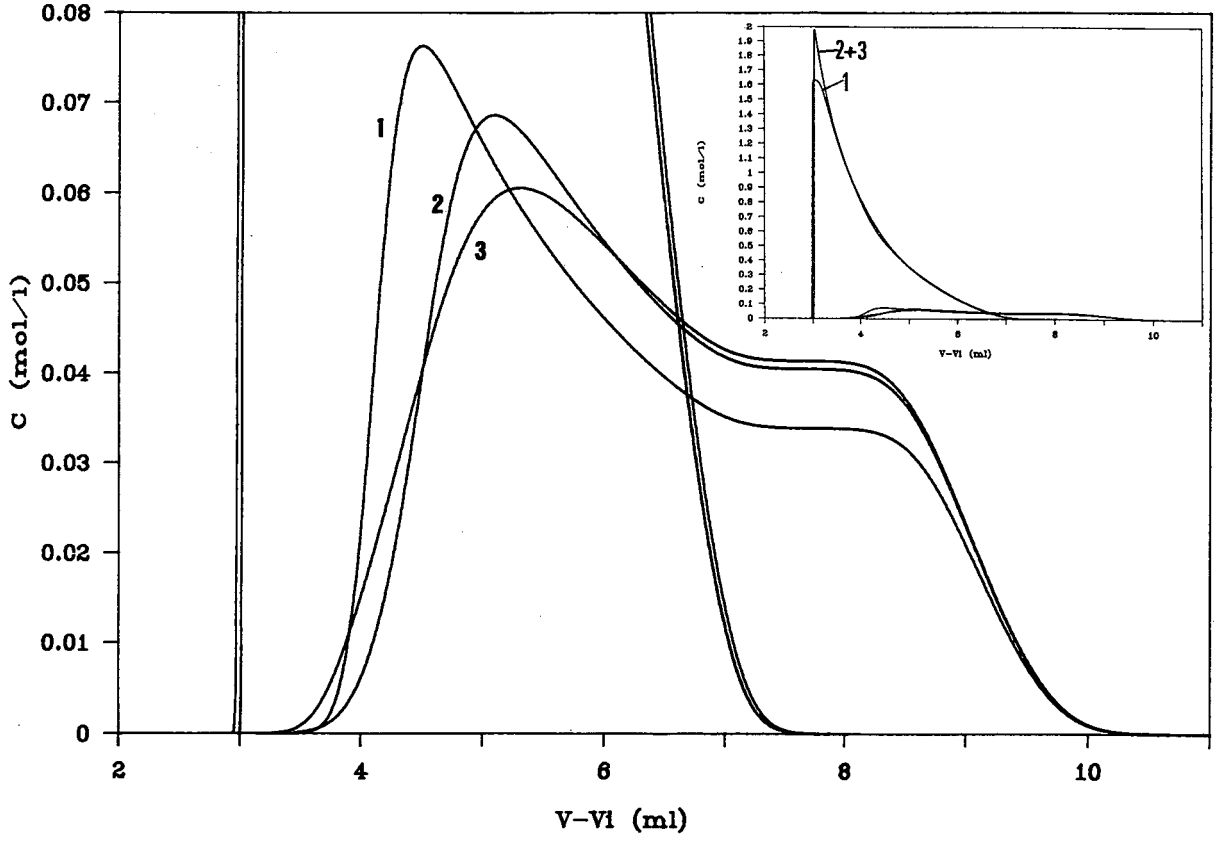

Fig. 11. Enlargement of the second peak for three chromatograms corresponding to the same injected amount, $Q_i = 2.4$ mmol $= 0.4w_s$, of mixture A at a relative composition of 9:1 (the global chromatograms are presented in the inset). $n_c = 600$ ($N_1 = 902$; $N_2 = 801$). Profile: (1) $C_i = 1.7$ mol/l; (2) $C_i = 12.5$ mol/l; (3) $C_i = 50$ mol/l. The elution volume is adjusted by subtracting the injection volume.

this set of chromatograms is adjusted by subtracting the injection volume. The injected sample amount is 2.4 mmol, *i.e.*, 40% of the column saturation capacity. Elution profile 2 corresponds to the optimum injection concentration for the recovery of the first-eluted solute (C_i = 12.5 mol/l, data point 2 in Fig. 6a). Elution profiles 1 and 3 are obtained for a smaller injected concentration (data point 1 in Fig. 6a) and a larger concentration (data point 3 in Fig. 6a), respectively. Because the relative composition of solute 2 in the mixture is small, the tag-along effect is very strong [8]; the co-elution of the two solutes accelerates the migration of the front of the second solute and results in the formation of the plateau on the peak of solute 2. When we successively consider chromatograms 1–3, the injected concentration is increased and the injected volume is decreased because the injected amount is kept constant. The height of the tag-along plateau for the second component increases with increasing the injection concentration. Because the smaller the relative concentration of the second component the more important is the tag-along effect, the acceleration of the migration is larger for the front base of the second component, corresponding to low concentrations, than for its front top, corresponding to larger concentrations; hence the decrease in the width of the second component with decreasing injection volume is smaller at the peak base (compare elution profiles 1 and 2). This phenomenon becomes more marked as the injected concentration is increased and finally results in band broadening at the front base of the second component, which elutes faster in the chosen representation (compare elution profiles 2 and 3). The decrease in the recovered amount of the 99% pure first component for a large injected concentration of the 9:1 mixture (data point 3 in Fig. 6a) is a consequence of this additional band broadening of the second-component front.

Fig. 12 shows that the same phenomena occur with sample mixture corresponding to a lower separation factor. It superposes the chromatograms obtained for the same load of the 9:1 mixture B, Q_i = 0.59 mmol = $0.2w_s$, injected at three different concentrations, C_i = 0.08, 1.2 and 62.5 mol/l. In these experiments, the resolution at infinite dilution is equal to 1.2 instead of 1.7 for mixture A in Fig. 11. As the injection concentration is increased, the band broadening pattern seems to be qualitatively very similar to that observed for mixture A (compare Figs. 11 and 12). Quantitatively, the recovered amount of 99% pure solute 1 for the 1.2 mol/l

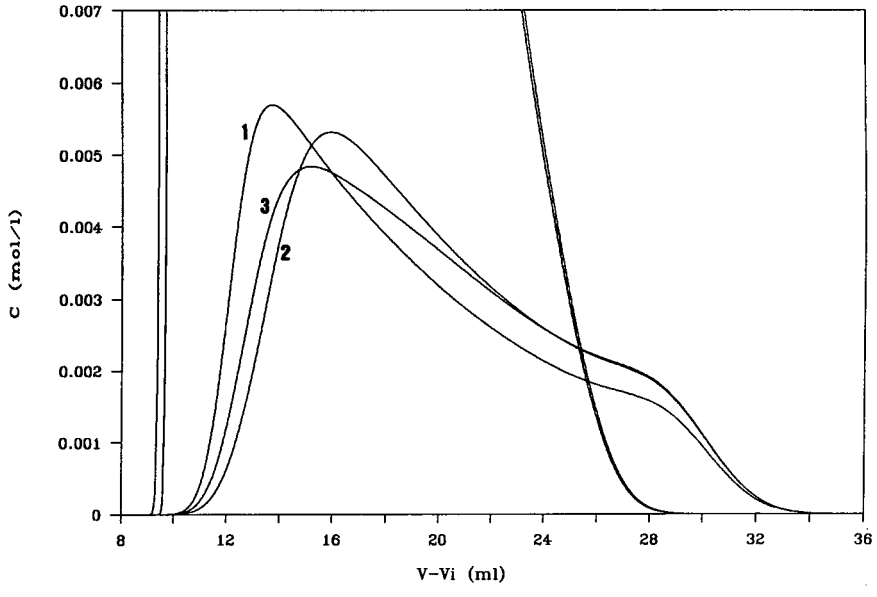

Fig. 12. Enlargement of the second peak for three chromatograms corresponding to the same injected amount, Q_i = 0.59 mmol = $0.2w_s$, of mixture B at a relative composition of 9:1. n_c = 500 (N_1 = 551; N_2 = 543). Profile: (1) C_i = 0.08 mol/l; (2) C_i = 1.2 mol/l; (3) C_i = 62.5 mol/l. The elution volume is adjusted by subtracting the injection volume.

injection exceeds that for the 0.08 and 62.5 mol/l injections, namely 0.274 mmol for C_i = 1.2 mol/l to 0.197 and 0.239 mmol for C_i = 0.08 and 62.5 mol/l, respectively. Hence the value of 1.2 mol/l is optimum. The corresponding recovery yield of solute 1 is 51.8%.

The effect of the column efficiency on the optimum injection concentration giving the highest recovered amount is shown in Fig. 13. The sample is mixture A at the relative composition 9:1. The injected amount is kept equal to 2.4 mmol ($0.4w_s$) and each curve plots, for a specified column plate number, the amount of the first solute recovered at 99% purity against the injected sample concentration. The result previously observed is found: the optimum injection concentration corresponding to the curve maximum is an increasing function of the column efficiency. It seems to become infinite for the column of infinite efficiency simulated by the ideal model. Under the latter conditions, the peak fronts are vertical; the bottom and the top of the peak front of the second component co-elute with the same concentration of the first component; consequently, they are subjected to the same tag-along effect and, when the injection concentration is increased, the front bottom of the second peak is no longer affected by an additional band broadening detrimental to the recovered amount of the first component.

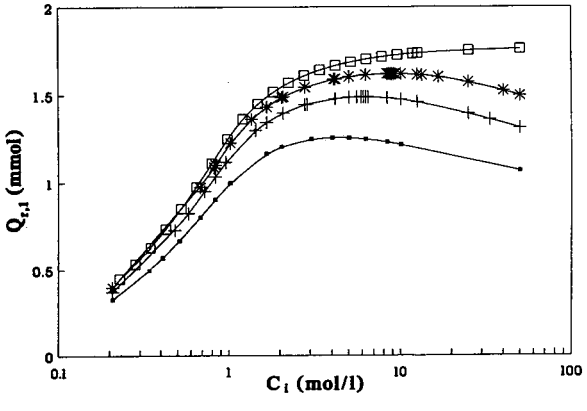

Fig. 13. Plot of the recovered amount of 99% pure solute 1 *versus* the injected sample concentration for different column efficiencies. Mixture A, relative composition 9:1. Q_i = 2.4 mmol = $0.4w_s$. (■) n_c = 100 (N_1 = 152; N_2 = 135); (+) n_c = 200 (N_1 = 302; N_2 = 268); (∗) n_c = 400 (N_1 = 602; N_2 = 535); (□) ideal model (N_1 and N_2 are infinite).

CONCLUSIONS

The chromatogram of a binary mixture simulated by the Craig model CRAIGSIM is very close to that described by the ideal model. The predictions of CRAIGSIM seem to be quantitative. Hence it was possible to simulate accurately preparative separations and to discuss quantitatively the influence of different parameters such as sample amount, injection volume, injected concentration and column plate number on recovery yield and recovered solute amount at a specified purity.

This work confirms that there are optimum injection conditions corresponding to the maximum recovered amount when the solute of interest is both the first-eluted component and the major portion of the sample [1,3], *i.e.*, when the tag-along effect is strong [4]. In all other instances, the results reported by Knox and Pyper [10] seem to be confirmed: for a given sample load, band broadening can be considered to be a minimum and independent of the injection volume up to a critical value of this volume; this explains why the recovered amount at a given purity and yield is maximum and approximately constant as long as the sample concentration exceeds a certain value.

Another conclusion from this study is that solute–solute interactions and chromatographic dispersion are not independent phenomena and that the optimum value of the injection parameters is affected by the column efficiency. In practice, the optimum injection volume can be considered to be directly proportional to the standard deviation of the peak at infinite dilution. The optimum injection concentration is increased with increasing column plate number.

Consequently, in scaling up a separation, two approaches are possible:

(i) When the plate number is different for the two columns, optimization requires three steps: first, the optimum injection volume for the analytical column is experimentally determined; second, the optimum injection volume for the preparative column is calculated from that of the analytical column and the standard deviation of the peak at infinite dilution for the two columns; third, the injectable load is directly adjusted on the preparative column by injecting optimum volumes of successively more concentrated solutions until the preparative specifications of purity and yield are reached.

(ii) When the two columns have the same efficiency, the optimum injection concentration is identical for the two columns. Hence both injection parameters, volume and concentration, are optimized on the analytical column; the optimum injection volume is calculated as described in (i).

SYMBOLS

a_j origin slope of Langmuir isotherm ($j = 1$ or 2)
b_j coefficient of non-linearity in Langmuir isotherm equation ($j = 1$ or 2) (l/mol)
C_i injected sample concentration (mol/l)
$C^m_{j,n,t}$ concentration of solute j ($j = 1$ or 2) in the mobile phase part of stage n at transfer t (mol/l)
$C^s_{j,n,t}$ concentration of solute j ($j = 1$ or 2) in the stationary phase part of stage n at transfer t (mol/l)
F_j parameter defined by eqns. A3 and A4 for $j = 1$ and 2, respectively
k'_j capacity factor of solute j at infinite dilution ($j = 1$ or 2)
l_k element of a converging sequence defined in Appendix (mol/l)
m_k element of a converging sequence defined in Appendix (mol/l)
n_c number of stages in the Craig machine algorithm
N_j number of theoretical plates calculated on solute j at infinite dilution ($j = 1$ or 2)
p_k element of a converging sequence defined in Appendix (mol/l)
q_k element of a converging sequence defined in Appendix (mol/l)
Q_i injected sample amount (mmol)
$Q_{i,j}$ injected amount of solute j ($j = 1$ or 2), (mmol)
$Q_{j,n,t}$ amount of solute j ($j = 1$ or 2) in stage n at transfer t (mmol)
$Q_{r,j}$ recovered amount of solute j ($j = 1$ or 2) (mmol)
r_j recovery yield of solute j ($j = 1$ or 2)
V_c volume of the empty column (ml)
V_i injected volume (ml)
V_m column dead volume (ml)
w_s saturation capacity of the column (mmol)
ε column total porosity
σ_1 standard deviation of the Gaussian peak of solute 1 at infinite dilution (ml)

ACKNOWLEDGEMENT

This work was supported by CEDI SA (Compagnie Européenne d'Instrumentation, Lannemezan, France) within the context of a "CIFRE convention" (No. 0570/88).

APPENDIX

Calculation of concentration of solute 1 and 2 in both phases of a stage

From eqns. 2a, 2b, 4a and 4b, we can write

$$C^m_{1,n,t} = \frac{b_2\varepsilon(C^m_{2,n,t})^2 + [(1-\varepsilon)a_2 + \varepsilon - b_2F_2]C^m_{2,n,t} - F_2}{b_1(F_2 - \varepsilon C^m_{2,n,t})} \quad \text{(A1)}$$

$$C^m_{2,n,t} = \frac{b_1\varepsilon(C^m_{1,n,t})^2 + [(1-\varepsilon)a_1 + \varepsilon - b_1F_1]C^m_{1,n,t} - F_1}{b_2(F_1 - \varepsilon C^m_{1,n,t})} \quad \text{(A2)}$$

with

$$F_1 = \frac{Q_{1,n,t}n_c}{V_c} \quad \text{(A3)}$$

$$F_2 = \frac{Q_{2,n,t}n_c}{V_c} \quad \text{(A4)}$$

Considering eqns. 2a and A3, the following inequalities can be written:

$$0 \leqslant C^m_{1,n,t} \leqslant \frac{F_1}{\varepsilon} \quad \text{(A5)}$$

$C^m_{1,n,t}$ is equal to 0 and F_1/ε when solute 1 is totally retained and non-retained, respectively.

Then, from eqns. A1 and A5, we obtain

$$0 \leqslant \frac{b_2\varepsilon(C^m_{2,n,t})^2 + [(1-\varepsilon)a_2 + \varepsilon - b_2F_2]C^m_{2,n,t} - F_2}{b_1(F_2 - \varepsilon C^m_{2,n,t})} \leqslant \frac{F_1}{\varepsilon} \quad \text{(A6)}$$

from which it can be demonstrated that

$$l_1 \leqslant C^m_{2,n,t} \leqslant m_1 \quad \text{(A7)}$$

with $0 \leqslant l_1 \leqslant m_1 \leqslant F_2/\varepsilon$. Substitution of eqn. A2 in eqn. A7 leads to

$$p_1 \leqslant C^m_{1,n,t} \leqslant q_1 \quad \text{(A8)}$$

with $0 \leqslant p_1 \leqslant q_1 \leqslant F_1/\varepsilon$. The calculation is then

iterated: substitution of eqn. A1 in eqn. A8 leads to

$$l_2 \leqslant C^{m}_{2,n,t} \leqslant m_2 \tag{A9}$$

with $0 \leqslant l_1 \leqslant l_2 \leqslant m_2 \leqslant m_1 \leqslant F_2/\varepsilon$, and substitution of eqn. A2 in eqn. A9 leads to

$$p_2 \leqslant C^{m}_{1,n,t} \leqslant q_2 \tag{A10}$$

with $0 \leqslant p_1 \leqslant p_2 \leqslant q_2 \leqslant q_1 \leqslant F_1/\varepsilon$, and so on.

At the kth iteration $l_k \leqslant C^{m}_{2,n,t} \leqslant m_k$ and $p_k \leqslant C^{m}_{1,n,t} \leqslant q_k$, where the sequences l_k and m_k and the sequences p_k and q_k converge to $C^{m}_{2,n,t}$ and $C^{m}_{1,n,t}$, respectively. m_k and q_k are considered to be equal to $C^{m}_{2,n,t}$ and $C^{m}_{1,n,t}$, respectively, when $(m_k - l_k)/l_k \leqslant$ lim and $(q_k - p_k)/p_k \leqslant$ lim, lim being fixed *a priori*. $C^{s}_{1,n,t}$ and $C^{s}_{2,n,t}$ are then calculated from eqns. 4a and 4b.

REFERENCES

1 G. Crétier and J. L. Rocca, *Sep. Sci. Technol.*, 22 (1987) 1881.
2 A. Katti and G. Guiochon, *Anal. Chem.*, 61 (1989) 982.
3 V. Svoboda, *J. Chromatogr.*, 464 (1989) 1.
4 J. Newburger and G. Guiochon, *J. Chromatogr.*, 484 (1989) 153.
5 G. Guiochon and S. Ghodbane, *J. Phys. Chem.*, 92 (1988) 3682.
6 B. L. Karger, L. R. Snyder and Cs. Horváth, *An Introduction to Separation Science*, Wiley-Interscience, New York, 1973, p. 110.
7 L. R. Snyder, J. W. Dolan and G. B. Cox, *J. Chromatogr.*, 483 (1989) 63.
8 S. Golshan-Shirazi and G. Guiochon, *J. Phys. Chem.*, 93 (1989) 4143.
9 R. M. Nicoud and H. Colin, *LC·GC Int.*, 3, No. 2 (1990) 28.
10 J. H. Knox and H. M. Pyper, *J. Chromatogr.*, 363 (1986) 1.

Journal of Chromatography, 590 (1992) 189–196
Elsevier Science Publishers B.V., Amsterdam

CHROM. 23 753

Chromatographic effects of residual amino groups on liquid chromatographic stationary phases derived from aminopropyl-silica gel

Dajing Ji and John R. Jezorek*

Department of Chemistry, University of North Carolina at Greensboro, Greensboro, NC 27412-5001 (USA)

(First received July 23rd, 1991; revised manuscript received September 17th, 1991)

ABSTRACT

Low-capacity phenylazo-8-quinolinol-silica gel (QSG) stationary phases were made by two different procedures. The first began with an aminopropyl-silica gel (APSG), which was converted to nitrobenzamide-silica gel (NBSG) by amidization with *p*-nitrobenzoyl chloride. The second began with the direct preparation of the NBSG using nitrobenzamidesilane. Retention data for several organic analytes were obtained on APSG and on the NBSG and QSG phases made by both procedures. Anomalously high capacity factors were obtained for *p*-nitrobenzoic acid on the NBSG material obtained from APSG, indicating the presence of unreacted aminopropyl anion-exchange sites. Only after reamidization of the NBSG using more vigorous conditions did the retention data approach that on the NBSG made by the second method. Even then, the opposite order of elution of *p*-nitrobenzoic and benzoic acids on the two NBSG and QSG phases indicated that vestiges of amino groups remained on the materials made from the APSG. Several chromatographic and chemical characterization methods confirmed the presence of residual aminopropyl groups.

INTRODUCTION

Chemical modification of surfaces by means of silane coupling agents is employed in many areas of commerce such as the textile, coatings and material composites industries [1,2]. In science and technology, silane-modified solids such as electrodes [2–4], heterogeneous catalysts [2–5] and gas and liquid-chromatographic stationary phases [6,7] are being increasingly employed.

Aminopropylsilane is a commonly used surface-modification reagent. Many organic and biochemical species are directly or indirectly "coupled" to the surface in question via a covalent bond with the amino group at the end of the propyl spacer arm [8], and therefore understanding and control of alkylamine surface chemistry [9] is very important. In fact, one of the early uses of this silane coupling agent was for the immobilization of enzymes on silica gel [10]. Aminopropylsilane has also been used for the production of silica gel-bonded "amino" columns for carbohydrate separations and for the parent modified silica gel from which a variety of stationary phases have been produced [8], including chiral phases [11].

In most of these situations little attention, if any, has been given to whether the amio group is fully reacted with the species with which it is to be coupled. A few studies have found, however, that some of the original amino groups did remain unreacted, for example, in the production of picramidopropyl-silica gel [12,13] or silica gel-immobilized cyclodextrins [14], a stationary phase on which anomalously large retention of organic acids was noticed.

Aminopropyl-silica gel (APSG) has been used in our laboratory for some time [15–17] as the parent material from which propylamido-substituted phenylazo-8-quinolinol-silica gel (QSG) is made [18]. The amino group is reacted with *p*-nitrobenzoyl chloride to yield nitrobenzamide-silica gel (NBSG). The nitro group is reduced to aminobenzamide-silica gel (ABSG) from which the diazonium

0021-9673/92/$05.00

salt-silica gel (DSSG) is made. This material is then coupled with 8-quinolinol to give the QSG phase. Several years ago, we developed a shortened route to QSG which employs triethoxysilylpropyl-*p*-nitrobenzamide to yield NBSG in one step on reaction with silica gel. Subsequent reactions are the same as for the longer method. We had assumed that the final QSG was the same whether APSG or NBSG was the parent material [19] until two columns made by each method were used to separate a series of organic analytes [20]. In that work, organic acids were found to have substantially longer retention times on the columns which were made from aminopropyl-silica gel than on those made from the nitrobenzamide material. We speculated that residual basic amino groups were responsible for the anomalously large retention of the organic acids [20]. In a more recent study, QSG phases made from both parent species were employed for the separation of mixed-class analytes, including inorganic anions. Very high retention values for the anions were obtained on the APSG-derived QSG [21]. It appeared likely that residual protonated amino groups were acting as anion exchangers for both inorganic anions and ionized organic acids [21].

The purpose of this study was to confirm these suspicions and to show that stationary phases produced from aminopropyl parent materials may well exhibit chromatographic results traceable to analyte interaction with residual amino or protonated amino groups, even at low coverages. In this study packing materials produced from both aminopropyl- and nitrobenzamide-silica gel were chromatographically compared, and the presence of residual amino groups was confirmed for phases produced from APSG.

EXPERIMENTAL

Apparatus

The chromatographic system consisted of a Beckman (Fullerton, CA, USA) Model 100-A pump and Model 153 single-wavelength (254 nm) detector. Nitrate analyte was monitored on an ISCO (Lincoln, NE, USA) Model V^4 detector at 210 nm. Columns, packing procedures and general chromatographic conditions have been described previously [16,17,20].

Spectroscopic studies employed a Varian (Sunnyvale, CA, USA) DMS-100 spectrometer for UV–VIS and a Perkin-Elmer (Norwalk, CT, USA) Model 272 for flame atomic absorption spectrometric work.

Silylations employed a Coulter Ultrasonic (Hialeah, FL, USA) Model CE-12 80-W ultrasonic cleaning bath.

Reagents and solutions

The stationary phase support material was Adsorbosil-LC, a preparative-grade, 10-μm diameter, 60-Å pore, 480 m^2 g^{-1} irregular silica from Applied Science (Alltech) (Deerfield, IL, USA). Fines were removed by stirring about 13 g of the material into 250 ml of water and drawing off the top 100 ml of slurry with a 100-ml pipet after 15 min of settling. The procedure was repeated twice, with 100 ml of fresh water added after each removal of fines.

Water was purified with a Barnstead (Dubuque, IA, USA) NANOpure four-cartridge system using feed water doubly deionized by the departmental system. High-performance liquid chromatographic (HPLC)-grade methanol was used for all chromatography and ACS-grade methanol for synthetic and column-packing work. Acetate buffers were made from HPLC-grade sodium acetate and Instra-Analyzed acetic acid, both from J. T. Baker (Phillipsburg, NJ, USA). Analytes were of analytical-reagent grade and about 10^{-3}–10^{-4} *M* solutions were made up in methanol or mobile phase. Analytes and mobile phases were filtered through 0.45-μm membrane filters.

Triethylamine and *p*-nitrobenzoyl chloride were of Puriss grade (>99.5%) from Fluka (Ronkonkoma, NY, USA). 3-Aminopropyltriethoxysilane (Hülls/Petrarch, Bristol, PA, USA) was distilled before use at 3 Torr and 69.5°C. Trimethylsilylimidazole (TMSI) (Hülls/Petrarch) was used as received. All other reagents were of ACS grade and used as received from various suppliers.

Stationary phase synthesis

The 8-quinolinol-modified silica gels (QSG) were made by two different routes. The first (method I) begins with an aminopropyl-modified material (APSG), which is converted into nitrobenzamide-silica gel (NBSG) by amidization of the propylamine with *p*-nitrobenzoyl chloride [15,18,22]. The NBSG is subsequently converted into an amino-

benzamide-silica gel (ABSG) by sodium dithionite reduction of the nitro group. A diazonium salt-silica gel (DSSG) is next prepared from the ABSG in nitrous acid and the DSSG is coupled to 8-quinolinol in ethanol solution. NBSG and QSG phases derived from APSG parent material (synthetic method I) are designated by the suffix I.

Method II employs triethoxysilylpropyl-*p*-nitrobenzamide silylation of silica gel to eliminate the lengthy amidization step and yield NBSG directly [19]. Subsequent reactions are the same as for method I. Stationary phases prepared from NBSG made by method II are designated by the suffix II.

The APSG synthesis was performed in hexane, and used ultrasound rather than the usual refluxing approach [23]. About 13 g of sized Adsorbosil was wet with 60 ml of dried hexane and then 0.28 g of distilled aminopropylsilane was added with a syringe. The flask was placed in an ordinary laboratory ultrasonic cleaning bath and sonicated for 2 h at about 48°C. The resulting APSG was washed with hexane and methanol and cured in a vacuum oven at 85°C for 3 h. The 0.28 g of silane used would yield a 100-μmol g^{-1} APSG if fully reacted.

A solution of 80 ml of dried chloroform containing 0.44 g of *p*-nitrobenzoyl chloride and 0.4 g of triethylamine was added to about 6.8 g of APSG. The mixture was sonicated for 14 h. The resulting NBSGI was washed with chloroform, methanol, 1 *M* hydrochloric acid and methanol. The residual silanol sites on the NBSGI were end-capped using hydroxyl group-selective TMSI. About 80 ml of a 5% (v/v) hexane solution of TMSI were mixed with the NBSGI and sonicated for 3 h. The capped NBSGI was washed with hexane, *n*-propanol and methanol.

The capped NBSGI was reacted a second time with *p*-nitrobenzoyl chloride to convert aminopropyl groups more completely to the amide. About 60 ml of chloroform containing 0.9 g of the benzoyl chloride and 1 ml of triethylamine were added to about 6 g of the capped NBSGI and sonicated for 5 h, then an additional 1 g of the acid chloride and 1 ml of triethylamine were added and sonication was continued for another 10 h. This re-amidized NBSGI was washed with chloroform, methanol, 0.5 *M* hydrochloric acid, water and methanol. Subsequent reactions to yield QSGI were performed as described previously [15,18,22].

NBSGII was prepared from 5 g of sized Absorbosil to which 60 ml of a hexane solution of 0.23 g of recrystallized nitrobenzamide-silane were added [21]. The mixture was sonicated for 4 h. The NBSGII was washed with hexane, acetone and methanol and cured in a vacuum oven at 90°C for 8 h. The theoretical coverage of the silica by nitrobenzamide groups based on the above amounts is 130 μmol g^{-1}. The NBSGII was capped as described above. Subsequent reactions to produce QSGII were performed as described previously [15,18,22].

Capacity determination

Determination of nitrogen by elemental analysis of APSG, NBSG and QSG was performed by Desert Analytics (Tucson, AZ, USA).

Batch extraction of copper(II) by APSG and QSG was performed as described previously [15–17,24], with copper determination by atomic absorption spectrometry.

The coverage of silica by aminopropyl groups was also determined by reaction with salicylaldehyde to produce the silica-bound Schiff's base [8,9] with UV determination of unreacted reagent at 326 nm. A 1–2-fold measured excess of $1.0 \cdot 10^{-2}$ *M* salicylaldehyde in 100% ethanol was added to 0.1 g of APSG and the mixture was shaken for 30 min. The yellow Schiff's-base product was filtered off and the filtrate and ethanol washings were diluted to the range $1 \cdot 10^{-4}$–$4 \cdot 10^{-4}$. The UV absorbance of this and of the original solution was measured and the amount of bound reagent determined by difference. The calibration line had a correlation coefficient of 0.9999 and a slope of $3.98 \cdot 10^{-3}$ l mol^{-1} cm^{-1} (zero intercept).

The capacity of QSG phases was also obtained by determining the amount of 8-quinolinol that remained after the coupling reaction with DSSG. A measured (1–2-fold excess) of a $2.0 \cdot 10^{-2}$ *M* 8-quinolinol solution in 95% ethanol was used for the coupling reaction. The QSG was filtered off and washed with ethanol. The combined filtrate and washings were diluted to the range $2.0 \cdot 10^{-4}$–$5 \cdot 10^{-4}$ *M* for UV determination at 309 nm. The difference between the original and final 8-quinolinol amounts gave a value for the QSG quinolinol coverage. The calibration line in the concentration range above had a correlation coefficient of 0.99999 and a slope of $2.66 \cdot 10^{-3}$ l mol^{-1} cm^{-1} (zero intercept).

RESULTS AND DISCUSSION

The chromatographic behavior of QSG phases prepared from APSG differed from that prepared from NBSGII parent material in two separate studies in this laboratory. Organic acids with pK_a values of 3–5 were found by deBot *et al.* [20] to exhibit capacity factors 3–10 times larger on APSG-derived QSGs than on NBSGII-derived phases of comparable 8-quinolinol coverage. Thompson and Jezorek [21] observed k' values for chloride, bromide, perchlorate and nitrate to be ten times larger on QSGI than on QSGII. These QSG phases had the same copper(II) uptake capacity, again indicating comparable 8-quinolinol coverage.

The pH of the aqueous–organic mobile phases in these two studies ranged from 3 to 5, as measured in the mobile phase itself. Primary akylamines in homogeneous solution exhibit pK_b values around 3–4, while the bound aminopropl groups of ASPG appear to be weaker bases, with pK_b values around 6–7 [24]. Nevertheless, any residual aminopropyl groups which did exist on the method I-derived phases used in these two studies were probably protonated under the mobile phase conditions employed.

In the present study, two QSG phases of similar 8-quinolinol coverage were prepared, one by method I and the other by method II, and chromatographic comparisons of these phases and of APSG, NBSGI and NBSGII were made. The APSG coverage was observed to be 100 μmol g^{-1} by elemental analysis and about 80 μmol g^{-1} based on copper (II) extraction (assuming a 2:1 copper to amino ligand stoichiometry) [24–26]. NBSGI (made from the above APSG) had an original coverage by benzamide groups of 50 μmol g^{-1}, and about 70 μmol g^{-1} after the second amidization reaction, based on elemental nitrogen analysis. NBSGII (made directly with nitrobenzamide-silane) had a benzamide coverage of about 60 μmol g^{-1} by elemental analysis. QSGI (APSG parent material) exhibited a quinolinol coverage of 89 μmol g^{-1} by elemental analysis, 99 μmol g^{-1} by UV determination of unreacted 8-quinolinol and 116 μmol g^{-1} by copper(II) extraction (assuming a 2:1 copper to 8-quinolinol stoichiometry [27]). QSGII (NBSGII parent material) exhibited a coverage of 51 μmol g^{-1} by elemental analysis, 37 μmol by 8-quinolinol UV determination and 58 μmol g^{-1} by copper(II) extraction. Although it is very likely that high-capacity APSG may not react completely with *p*-nitrobenzoyl chloride to give NBSG because of steric constraints, it is reasonable to consider that complete reaction of a low-capacity APSG would routinely occur. Therefore, we deliberately prepared a low-capacity APSG phase (ca. 100 μmol g^{-1}) to see if, even then, residual amino groups remained after the usual synthesis procedure. We used organic chromatographic analytes that were neutral, basic and acidic, and methanol–aqueous acetate mobile phases from pH 4 to 6 to observe the pH dependence of analyte retention.

Various analytes were run on the 100 μmol g^{-1} APSG ("amino") column. Capacity factors for aniline, benzoic acid and *p*-nitrobenzoic acid as a function of pH are shown in Fig. 1. The difference in behavior of the two acids is probably due to their differing acidities. The aqueous pK_a values of benzoic and *p*-nitrobenzoic acid are 4.2 and 3.6, respectively. Therefore, in the pH 4.2 mobile phase, most

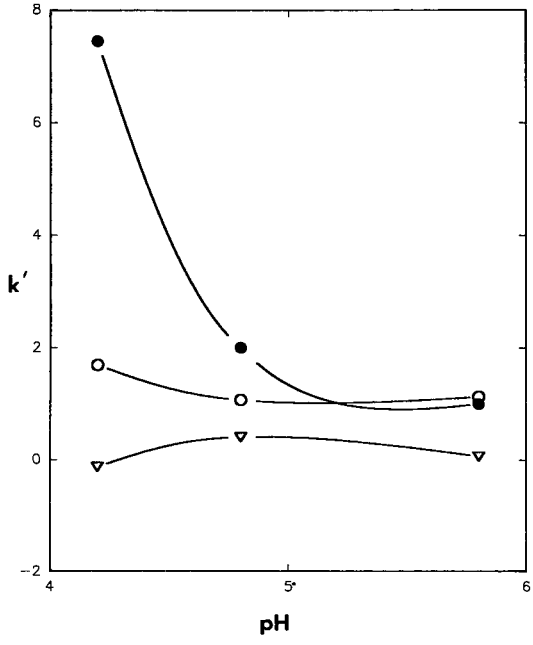

Fig. 1. Capacity factor on the APSG column as a function of pH. Mobile phases: methanol–water–0.1 *M* acetate buffer (50:25:25); pH 3.4 acetate buffer yielded apparent mobile phase pH of 4.2, pH 4.0 buffer an apparent pH of 4.8 and pH 5.0 buffer an apparent pH of 5.8. ● = *p*-Nitrobenzoic acid; ○ = benzoic acid; ▽ = aniline.

of the *p*-nitrobenzoic acid is ionized and much or most of the benzoic is neutral. The anionic form of the *p*-nitrobenzoic acid interacts via an anion-exchange mechanism with the protonated amino groups. The decrease in k' for *p*-nitrobenzoic and the absence of a k' increase for benzoic acid with a pH increase, even though it is more ionized at higher pH, is due to a competitive anion-exchange process with acetate ions in the mobile phase. Based on the aqueous pK_a value of acetic acid of 4.8, most of the acetate species are ionized at pH 5.8. At pH 4.2 most are protonated and therefore neutral. The anion-exchange behavior of the *p*-nitrobenzoic acid and the acetate competition for exchange sites at higher pH were further illustrated by obtaining k' values of the two acids and the neutral phenol species, still at pH 5.8, but at a five-fold lower acetate concentration (0.0046 *M*) than was used for the data in Fig. 1 (0.023 *M*). The expected lack of ionic strength dependence for phenol was indeed found, but k' for the two acids approximately doubled, from 3.3 to 7.9 for benzoic and from 3.1 to 7.5 for *p*-nitrobenzoic acid. Neutral species such as phenol or aniline and positively charged species such as the anilinium ion, which may exist at the lower pH values employed here, clearly show little or no pH or ionic strength dependence, but the benzoic acid–*p*-nitrobenzoic acid pair is a sensitive indicator of anion-exchange interactions in the pH region used here.

Similar tests for anion-exchange interactions were used with the NBSG phases. One column was packed with NBSGI. This material was made from the APSG discussed above using the usual threefold excess of *p*-nitrobenzoyl chloride. A second column was filled with NBSGII which, of course, can contain no residual amino groups. Capacity factors on NBSGI for several analytes at three pH values are given in Table I; k' values for benzoic acid, *p*-nitrobenzoic acid and aniline are plotted *versus* pH in Fig. 2A. Similar data on the NBSGII column (*ca.* 60 μmol g^{-1}) also are given in Table I and in Fig. 2B. The analytes exhibit typical reversed-phase behavior on the NBSGII phase, that is, a small k' decrease for the acids due to increased ionic character and mobile phase solubility at the higher pH values. The anomalously high k' for *p*-nitrobenzoic acid on NBSGI indicates the presence of unreacted aminopropyl groups. This was confirmed by the same experiment as was used with the APSG phase, namely repeating the chromatography on both NBSG columns at pH 5.8, but in a mobile phase with a fivefold lower acetate concentration. No change in k' was observed for any analyte on the NBSGII column, but the two test acids exhibited larger k' values in the less ionic mobile phase on the NBSGI column; the benzoic acid k' changed from 0.4 at the higher to 0.7 at the lower acetate concentration, while the *p*-nitrobenzoic k' changed from 0.5 to 1.0. These results again indicate an anion-

TABLE I

RETENTION OF SEVERAL ANALYTES ON NBSGI AND NBSGII IN THREE MOBILE PHASES

All mobile phases: methanol–water–0.1 *M* acetate buffer (50:25:25); pH 3.4 acetate buffer yielded an apparent mobile phase of 4.2, pH 4.0 buffer an apparent pH of 4.8 and pH 5.0 buffer an apparent pH of 5.8.

Analyte	Capacity factor, k'					
	NBSGI[a]			NBSGII		
	pH 4.2	pH 4.8	pH 5.8	pH 4.2	pH 4.8	pH 5.8
Aniline	0.20	0.33	0.40	0.73	0.60	0.67
2-Chloroethylbenzene	1.87	1.80	1.87	5.13	5.27	5.20
Naphthalene	2.07	2.07	2.13	5.40	5.53	5.53
Phenol	0.47	0.47	0.47	0.93	0.93	1.00
Benzoic acid	1.40	1.07	0.40	1.33	0.67	0.33
p-Nitrobenzoic acid	4.67	1.87	0.47	0.93	0.53	0.20

[a] Coverage by nitrobenzamide groups is about 50 μmol g^{-1} based on nitrogen determination; derived from APSG in Fig. 1.

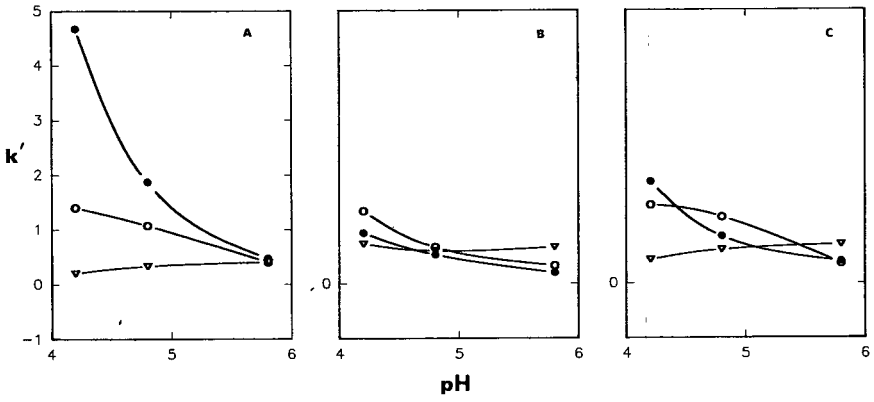

Fig. 2. Capacity factor on the NBSG columns as a function of pH. (A) NBSGI column; (B) NBSGII column; (C) NBSGI column after second amidization reaction. Mobile phases as in Fig. 1. ● = *p*-Nitrobenzoic acid; ○ = benzoic acid; ▽ = aniline.

exchange interaction on NBSGI, the phase made from APSG parent material.

This conclusion was confirmed by some characterization studies on the packing materials themselves, as discussed later, and by two other chromatographic experiments. First, nitrate ion was used as an analyte on both NBSG phases, exhibiting a k' of about +0.5 on NBSGI but about −0.4 on NBSGII (possibly owing to an ion-exclusion mechanism causing elution before the solvent peak). The retention of nitrate also indicates an anion-exchange interaction on the NBSGI. Some of this phase was reacted a second time with *p*-nitrobenzoyl chloride, but with a tenfold instead of the threefold excess of acid chloride that has been used previously [16,18,22]. The results are shown in Fig. 2C. The large decrease in k' for *p*-nitrobenzoic acid clearly indicates that most of the residual amino groups were amidized in this second reaction. However, the fact that benzoic acid still exhibited a k' smaller than that of the stronger *p*-nitrobenzoic acid implies that some residual amino groups remain. The more highly ionized acid is more soluble in the aqueous mobile phase, and should be less retained, as it is on NBSGII (Fig. 2B). A tenfold decrease in the acetate concentration in the mobile phase resulted in no k' change at pH 4.8 for aniline, phenol or even benzoic acid; *p*-nitrobenzoic acid still exhibited an increase in k' of about 0.4, indicating again that some vestiges of anion-exchange behavior remained even after re-amidization of the original NBSGI. Again, no k' change for any analyte on NBSGII was found as a result of the decrease in mobile phase acetate concentration.

The capacity factors of all analytes were less than unity on both QSGI and QSGII, probably as a result of partial loss of trimethylsilyl capping groups and their retentive capacity in the 2 *M* hydrochloric acid used in the diazotization reaction. Little or no pH dependence was observed for the several analytes used, with the exception of the two test acids. Again, both benzoic and *p*-nitrobenzoic acid exhibited a decrease in k' with increase in pH on both columns, as expected, owing to the solubility increase (Fig. 3). However, although the k' values are small, that for *p*-nitrobenzoic is still larger than that of benzoic acid on QSGI, but k' is smaller on QSGII, as reversed-phase behavior would predict. Again, residual aminopropyl groups are probably the cause of the opposite elution order of benzoic and *p*-nitrobenzoic acids on the two QSG phases.

A control experiment was run to determine whether residual amino groups could in fact survive the harsh reaction conditions of the diazonium salt preparation and so remain on a QSG phase. It has been suggested that aliphatic amines can be diazotized, but that the product is not stable and decomposes by losing a molecule of nitrogen [28]. Others claim that, below pH 3, reaction with nitrous acid does not occur [29]. We subjected a 60 μmol g^{-1} APSG sample to the diazonium salt reaction (sodium nitrite in 2 *M* hydrochloric acid) and then added the product to an alcoholic 8-quinolinol solution.

Columns were packed with both the original and

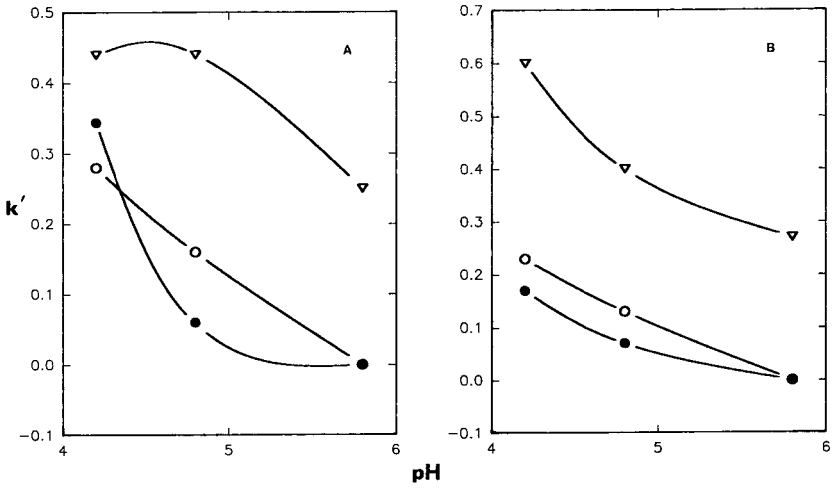

Fig. 3. Capacity factor on the QSG columns as a function of pH. (A) QSGI column; (B) QSGII column. Mobile phases as in Fig. 1. ● = *p*-nitrobenzoic acid; ○ = benzoic acid; ▽ = aniline.

treated APSG and several chemical tests were also run on these materials. Capacity factors for several analytes are given in Table II. These indicate little or no loss of amino groups. Copper(II) and salicylaldehyde [8,9] uptake reactions and elemental analysis also indicated that most of the amino groups remained. Copper uptake was 23 and 21 μmol g^{-1} of APSG, salicylaldehyde uptake was 65 and 43 μmol g^{-1} and nitrogen elemental analysis results were 0.15% and 0.16% on the original and treated APSG, respectively. UV spectrophotometry of the 8-quinolinol solution before and after the coupling reaction indicated that essentially no quinolinol ligand was coupled; indeed, only a slight pinkish tint of the diazotized, 8-quinolinol-treated APSG was observed, whereas the yellow silica-bound Schiff's base was evident on reaction of the treated APSG with salicylaldehyde. It appears that under these reaction conditions the aminopropyl groups do not form diazonium salts but do survive the diazotization reaction and remain on QSG phases.

Because of the low capacity of the stationary phases used here, chemical tests to detect unreacted aminopropyl groups on the NBSG and, especially, QSG, were not conclusive. Elemental analysis for nitrogen gave values of 0.14, 0.21, 0.24 and 0.48 %N for APSG, NBSGI, NBSGI after the second reaction with *p*-nitrobenzoyl chloride and QSGI, respectively. These results imply phase capacities of about 100, 50 and 70 μmol g^{-1} of bonded groups

TABLE II

RETENTION DATA ON ORIGINAL AND TREATED APSG COMPARED WITH QSGI

Mobile phase: methanol–water–0.1 *M* acetate buffer (pH 3.4) (50:25:25) (apparent pH 4.2).

Analyte	Capacity factor, k'		
	Original APSG	Treated APSG	QSGI
Benzoic acid	3.2	2.5	0.28
p-Nitrobenzoic acid	12.5	12.1	0.34
Phenol	0.0	0.0	0.19
Aniline	0.0	0.0	0.44

for APSG, NBSGI and the re-amidized NBSGI, indicating that 50 and 30 μmol g^{-1} of NH_2 groups remained on the two NBSGI materials. Chromatographic capacity factors of *p*-nitrobenzoic acid on the above three materials are about 8, 5 and 1, respectively, however, indicating that most of the amine groups have been amidized after the second reaction. The nitrogen determination has a standard deviation of 0.02–0.05% absolute [30], and is clearly not very reliable for low-capacity phases such as these.

It would appear from this study that following literature directions for the amidization of alkylamines may well leave unreacted amino groups which can affect later chemistry or chromatography. This is alsmost certainly what happened in the two previous studies in our laboratory [20,21]. Precautions need to be taken to mininize this possibility if alkylamino materials are used as parent species to couple some group to a solid surface. Longer reaction times and more concentrated reactant species might be used, and the resulting product should be checked for residual amino groups. Alternatively, if an azo-coupled material is desired, the amide (NBSG) can be obtained with silylpropyl-*p*-nitrobenzamide [19], eliminating the possibility of residual amino groups altogether.

ACKNOWLEDGEMENT

The author thanks the University of North Carolina at Greensboro Research Council for partial support of this work.

REFERENCES

1 E. P. Plueddemann, *Silane Coupling Agents*, Plenum, New York, 1982.
2 D. E. Leyden and W. T. Collins (Editors), *Chemically Modified Surfaces in Science and Industry*, Gordon & Breach, New York, 1987.
3 M. Umana, D. R. Rolinson, R. Nowak, P. Daum and R. W. Murray, *Surf. Sci.*, 101 (1980) 295.
4 R. W. Murray, *Acc. Chem. Res.*, 13 (1980) 135.
5 T., J. Pinnavaia, J.G.-S. Lee and M. Abedini, in D. E. Leyden and W. T. Collins (Editors), *Silylated Surfaces*, Gordon & Breach, New York, 1980, p. 333.
6 K. K. Unger, *Porous Silica*, Elsevier, Amsterdam, 1979, Ch. 6.
7 C. H. Lochmüller, in D. E. Leyden and W. T. Collins (Editors), *Silylated Surfaces*, Gordon & Breach, New York, 1980, p. 231.
8 T. G. Waddell, D. E. Leyden and D. M. Hercules, in D. E. Leyden and W. T. Collins (Editors), *Silylated Surfaces*, Gordon & Breach, New York, 1980, p. 55.
9 T. G. Waddell, D. E. Leyden and M. T. DeBello, *J. Am. Chem. Soc.*, 103 (1981) 5303.
10 G. G. Guilbault, *Analytical Uses of Immobilized Enzymes*, Marcel Dekker, New York, 1984.
11 W. H. Pirkle, M. H. Hyun and B. Banks, *J. Chromatogr.*, 316 (1984) 585.
12 L. Nondek and R. Ponec, *J. Chromatogr.*, 294 (1984) 175.
13 L. Nondek, P. Dienstbier and R. Reriche, *J. High Resolut. Chromatogr. Chromatogr. Commun.*, 11 (1988) 217.
14 K. Fujimura, M. Kitagawa, H. Takayanagi and T. Ando, *J. Chromatogr.*, 350 (1985) 371.
15 C. Fulcher, M.A. Crowell, R. Bayliss, K. B. Holland and J. R. Jezorek, *Anal. Chim. Acta*, 129 (1981) 29.
16 G. J. Shahwan and J. R. Jezorek, *J. Chromatogr.*, 256 (1983) 39.
17 C. H. Risner and J. R. Jezorek, *Anal. Chim. Acta*, 186 (1986) 233.
18 J. M. Hill, *J. Chromatogr.*, 76 (1973) 455.
19 J. R. Jezorek, K. H. Faltynski, L. G. Blackburn, P. J. Henderson and D. H. Medina, *Talanta*, 32 (1985) 763.
20 S. A. deBot, J. R. Jezorek and M. E. Hager, *J. Chromatogr.*, 465 (1989) 249.
21 H. W. Thompson and J. R. Jezorek, *Anal. Chem.*, 63 (1991) 78.
22 K. F. Sugawara, H. H. Weetall and G. D. Schucker, *Anal. Chem.*, 50 (1974) 489.
23 S. V. Ley and C. M.R. Low, *Ultrasound in Synthesis*, Springer, Berlin, 1989.
24 J. R. Jezorek, C. Fulcher, M. A. Crowell, R. Bayliss, B. Greenwood and J. Lyon, *Anal. Chim. Acta*, 131 (1981) 223.
25 L. W. Burggrat, D. S. Kendall, D. E. Leyden and F. J. Pern, *Anal. Chim. Acta*, 129 (1981) 19.
26 R. G. Masters and D. E. Leyden, *Anal. Chim. Acta*, 98 (1978) 9.
27 J. Tang, *Masters Thesis*, University of North Carolina at Greensboro, Greensboro, NC, 1991.
28 J. March, *Advanced Organic Chemistry*, Holden-Day, San Francisco, CA, 3rd ed., 1985, p. 570.
29 N. Kornblum and D. C. Iffland, *J. Am. Chem. Soc.*, 71 (1949) 2137.
30 R. C. Johnson, Desert Analytics, personal communication.

Journal of Chromatography, 590 (1992) 197–202
Elsevier Science Publishers B.V., Amsterdam

CHROM. 23 727

Chemically modified resins for solid-phase extraction

Jeffrey J. Sun and James S. Fritz*

Ames Laboratory–D.O.E. and Department of Chemistry, Iowa State University, Ames, IA 50011 (USA)

(First received May 3rd, 1991; revised manuscript received August 20th, 1991)

ABSTRACT

The packings most widely used for solid-phase extraction are hydrophobic and make poor surface contact with aqueous samples unless the resins are first treated with an activating organic solvent such as methanol. Insertion of an acetyl- or hydroxymethyl group into a porous polystyrene–divinylbenzene resin provides a more hydrophilic surface that is easily wetted by water alone. Small columns of the chemically modified resins were found to be very efficient for the solid-phase extraction of many types of organic solutes from aqueous samples. Comparative recovery studies showed that the modified resins are superior to both silica packings and unmodified organic resins for the solid-phase extraction of organic compounds, and especially for polar organics such as phenols.

INTRODUCTION

Solid-phase extraction (SPE) is now widely used for the preconcentration and clean-up of analytical samples, for the purification of various chemicals and for applications such as the removal of toxic or valuable substances from a variety of predominantly aqueous solutions. Typical applications include methods for the determination of trace amounts of pesticides [1,2], determination of trace organic contaminants in water [3,4], analysis of industrial waste waters [5], determination of azaarenes in water [6], evaluation of porous polymers [7], isolation of organic compounds from ground water [8], sampling of priority pollutants in waste water [9], collection and concentration of environmental samples [10] and pretreatment of urine samples [11,12].

For analytical purposes, SPE is usually performed using a small column or cartridge containing an appropriate packing. Membranes loaded with appropriate resins have also been used for SPE [13]. Following uptake of extractable solutes from a predominately aqueous sample, it is common practice to elute the adsorbed materials from the resin with a small amount of an organic solvent.

Chemically bonded silica, usually with a C_{18} or C_8 organic group, is by far the most commonly used material for SPE. Use has also been made of porous polystyrene or other polymeric resins in SPE. Graphitized carbon black has been used for the concentration of agricultural chemicals [14] and phenols [15] from water. It was stated that the carbon black appears to function as an anion exchanger and as a non-specified adsorbent.

Chemically bonded silica and porous polystyrene resins have several shortcomings for use in SPE. (1) While silica itself is hydrophilic, the hydrocarbon chains make the surface hydrophobic. The consequence is poor surface contact with predominantly aqueous solutions. Porous polystyrene resins also have a hydrophobic surface. (2) Pretreatment of the SPE materials with an activating solvent (such as methanol, acetone or acetonitrile) must be used to obtain better surface contact with the aqueous solution being extracted. However, the activating solvent can be gradually leached out of the resin, thereby causing the extraction to become ineffective. This is particularly true if the SPE column inadvertently becomes dry, causing air to be sucked into the column. (3) Many types of organic compounds are incompletely extracted from predominantly aqueous solutions. This is especially true with chemically

0021-9673/92/$05.00

bonded silica packings [3,7,9]. These drawbacks can be largely overcome by use of a new type of chemically derivatized resin.

In this work, new chemically modified polystyrene–divinylbenzene resins were prepared which are hydrophilic and easily wetted by water while still keeping their extraction ability. Various organic compounds were tested by SPE using these modified resins. The recovery results were compared with those using C_{18} silica and underivatized polystyrene–divinylbenzene resins. The new resins showed superior recoveries for test compounds in SPE.

EXPERIMENTAL

Reagents and chemicals

The reagents and solvents used for the derivatization reactions were of analytical-reagent grade and were dried with molecular sieves. Laboratory-distilled water was further purified using a Barnstead Nanopure II System (Sybron Barnstead, Boston, MA, USA).

Several chemically modified resins were prepared from porous, cross-linked polystyrene materials. Amberchrome 161 (Supelco, Bellefonte, PA, USA) is spherical with an average particle size of *ca.* 50 μm and a surface area of *ca.* 720 m^2/g. Sarasep resin (Sarasep, Santa Clara, CA, USA) has an average particle size of *ca.* 10 μm and a surface area of *ca.* 415 m^2/g.

The acetyl derivative was prepared as follows. To 5.1 g of resin add 30 ml of carbon disulphide, 9.5 g of anhydrous aluminum chloride and 5.5 g of acetyl chloride (added dropwise). Keep at 50°C for 24 h and stir with a magnetic stirrer bar from time to time through the whole reaction. Pour the final product into ice–water. Filter with filter-paper to isolate the resin, wash with acetone, methanol and water until clean, then dry. The presence of a carbonyl group was proved by a strong band at 1690 cm^{-1} on the spectrum obtained by Fourier transform IR spectrometry with a pellet of powdered potassium bromide and resin. The concentration of $-COCH_3$ groups on the resin was found to be 1.2 mmol/g by oxygen elemental analysis.

The hydroxymethyl derivative was prepared as follows. Add 1.2 g of paraformaldehyde, 16 ml of acetic acid and 4 ml of acetic anhydride to 5.2 g of resin. Stir with a stirrer bar for a few minutes, then add 6.0 g of anhydrous zinc chloride and keep at 60°C overnight with stirring from time to time. Filter the resin, rinse with methanol then heat with methanol–concentrated hydrochloric acid (90:10) for 1 h with stirring from time to time. Wash the final product with methanol and dry with aspiration. The concentration of $-CH_2OH$ groups on the resin was determined as 1.3 mmol/g by oxygen elemental analysis.

Apparatus and components

The apparatus used for solid-phase extraction is shown in Fig. 1. The small columns were packed with *ca.* 100 mg of resin. The C_{18} silica SPE column was obtained from Alltech (Deerfield, IL, USA). This column was 55 × 6 mm I.D., packed to a bed height of 8–10 mm with resin of 40 μm particle size. Derivatized and underivatized Amberchrome 161 resins were packed dry to a bed height of 12 mm into empty 55 × 6 mm I.D. plastic columns obtained from P. J. Cobert Assoc. (St. Louis, MO, USA). Each column contained polyethylene frits to support and cover the resins. Because of the smaller particle size (10 μm), the bed height of the Sarasep resin was only about 10 mm, packed in a 55 × 6 mm I.D. plastic column. Each SPE column was connected to a laboratory-made reservoir by an adaptor (P. J. Cobert Assoc.). The flow-rate of the sample solution from the reservoir was controlled by air pressure applied to the top of the reservoir.

The organic compounds eluted from SPE column with ethyl acetate were collected and then analyzed using an HP 5880A gas chromatograph with a flame ionization detector, an HP 5880A Series Level 4 integrator and an HP 7673A automatic sampler (Hewlett-Packard, Avondale, PA, USA). The gas chromatographic columns used were J&W fused-silica capillary megabore DB-5 and minibore DB-1 (Alltech) and Supelco (Bellfonte, PA, USA) fused-silica capillary columns.

A Bruker FT-IR 98 instrument (USA Bruker Instruments, San Jose, CA, USA) was used for structure determination.

Procedure for SPE

Prior to their initial use, columns were cleaned by passing through them small amounts of methanol, ethyl acetate and acetonitrile, then drying. Approxi-

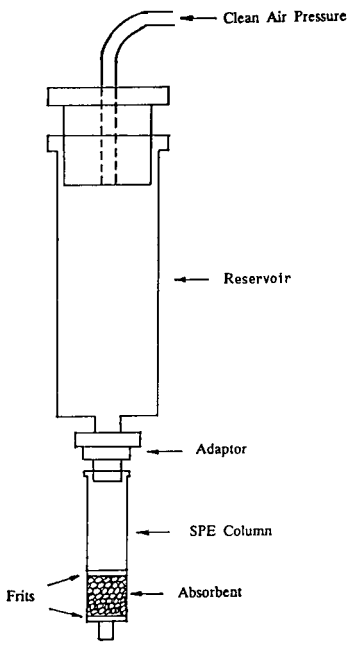

Fig. 1. Solid-phase extraction apparatus.

mately 1 ml of methanol was added to the SPE column just before each sample run to serve as an "activating" solvent.

Samples were prepared by adding a dilute methanol solution of several organic test compounds to 20 ml of water so that the concentration of each test compound would be about 5 ppm. This sample was then added to the reservoir and the air pressure was adjusted to give a sample flow-rate of 5 ml/min through the column. The column was then washed with 1 ml of pure water and air was blown through the column for a few seconds.

The SPE column was disconnected from the reservoir and 1 ml of ethyl acetate was added. The column was again connected to the reservoir and gentle air pressure was applied to make the ethyl acetate pass through the column in *ca.* 1 min. The eluate was collected in a small vessel with a syringe cap. A measured volume of internal standard was added to the vessel, which was capped immediately and agitated to mix well.

The vessel was placed in the automatic sampler of the gas chromatograph. A 1-μl aliquot was injected. Nitrogen carrier gas was used at a flow-rate of 15 ml/min, and a splitting ratio of 1:40 was used. Temperature programming was employed. Recoveries were calculated as average values ($n > 2$) by comparing the relative peak heights of collected samples with samples not subjected to SPE.

RESULTS AND DISCUSSION

Selection of resins

In a previous study, various hydrophilic functional groups were chemically atrached to the benzene rings of porous, cross-linked polystyrene resins [16]. When used for high-performance liquid chromatographic separations of typical organic compounds, the derivatized resins gave slightly shorter retention times for relatively non-polar organic solutes, but appreciably longer retention times for more polar test compounds such as phenols. Of the resins studied, the acetyl resin showed the best ability to retain phenols. The resin with a hydroxymethyl group also retained phenols more strongly than the underivatized resin. These results suggest that organic resins containing a hydrophilic group should strongly retain almost all types of test compounds from a predominantly aqueous solution, as in SPE.

Our dry acetyl or hydroxymethyl resin is quickly and easily wetted by water. This can be demonstrated by placing a small amount of the dry resin in a test-tube and adding water. The resins make good surface contact with the water and sink to the bottom. In contrast, dry, underivatized resin or dry C_{18} silica is not wetted by water and the hydrophobic particles clump together and tend to float on the suface of the water. This suggests that the acetyl or hydroxymethyl resin can be used in SPE from aqueous solutions without any pretreatment with an "activating" organic solvent.

The efficiency of porous resins used in SPE varies with the porosity, those with the largest surface area giving the greatest retention [17]. Amberchrome 161 is a spherical, cross-linked polystyrene resin with an unusually high surface area (720 m^2/g) and should therefore be well suited for SPE. Another polystyrene resin with a surface area of around 415 m^2/g was also available for testing. Preliminary experiments showed that most organic test compounds are easily eluted from these resins with an organic solvent such as ethyl acetate.

TABLE I

RECOVERIES OF PHENOLS, AROMATIC COMPOUNDS AND POLYHYDROXY AROMATIC COMPOUNDS BY SPE UNDER WET AND DRY LOADING CONDITIONS

Compound	Recovery (%)							
	C_{18} Si		Amberchrome		Amberchrome $-CH_2OH$		Amberchrome $-COCH_3$	
	Wet	Dry	Wet	Dry	Wet	Dry	Wet	Dry
Phenol	6	<3	91	3	94	75	100	93
p-Cresol	16	4	91	12	98	88	101	94
p-Ethylphenol	66	15	96	37	99	97	101	99
2-Nitrophenol	45	17	93	47	95	96	96	96
3-Nitrophenol	<5	<5	81	<5	85	75	93	73
4-Nitrophenol	<5	<5	87	<5	86	77	87	85
2,4-Dimethylphenol	71	21	95	42	97	96	100	98
4-*tert.*-Butylphenol	83	49	88	50	96	90	100	95
Anisole	78	58	91	56	94	95	98	96
Aniline	9	<5	94	26	96	90	100	96
Benzyl alcohol	10	<5	92	17	98	85	99	99
Nitrobenzene	54	27	92	51	96	96	100	97
2,4-Dinitrofluorobenzene	44	4	83	23	96	92	98	94
o-Hydroxyacetophenone	88	67	85	54	95	94	96	94
Isopentyl benzoate	84	60	72	73	89	84	96	85
Diethyl phthalate	90	70	87	58	96	84	100	90
Average	47	26	89	35	94	88	98	93
Catechol	0	0	72	0	89	9	75	30
Resorcinol	0	0	61	0	88	0	97	95
o-Methylresorcinol	0	0	83	0	97	16	99	96
Hydroquinone	0	0	26	0	72	0	87	81
Methylhydroquinone	0	0	77	0	98	5	99	94
Phloroglucinol	0	0	0	0	24	0	56	42

Recovery of test compounds

Various resins were compared for use in the SPE of different organic compounds from aqueous solution. The apparatus used is shown in Fig. 1. Derivatized and underivatized Amberchrome 161 resins were compared with each other and with a widely used C_{18} silica material.

Results for SPE and subsequent elution of the organic test compounds (about 5 ppm in aqueous solution) are summarized in Table I for phenols, aromatic compounds and polyhydroxyphenols. The "wet" designation refers to the usual procedure in which the SPE column is first treated with a 1–2 ml of methanol as an "activating" organic solvent before introduction of the aqueous sample. The recovery of the organic compounds was much higher using Amberchrome 161 than with the C_{18} silica material. However, the recovery of test compounds was still higher for the derivatized Amberchrome 161 resins, with the acetyl derivative giving the highest recovery in every case.

Sometimes a short column (or cartridge) used for SPE inadvertently becomes dry, causing air to be sucked in. This could cause part or all of the activating solvent to be lost from the resin bed. The efficiency of the various resins for SPE was tested after passing air through a column for several minutes to remove the water and activating solvent. Then the sample was added and the recoveries of test compounds were determined as before. These results, denoted as "dry", are also given in Table I. There is a marked decrease in the recoveries for both the C_{18} silica and the Amberchrome. However, the recoveries on the hydroxymethyl and acetyl resins

TABLE II

THE RECOVERIES (%) OF ALIPHATIC AND PYRIDINE COMPOUNDS UNDER WET SPE COLUMN LOADING CONDITIONS

Compound	C_{18} Si	Amber-chrome 161	Amber-chrome 161 $-COCH_3$
Pentanone	20	91	97
Octanone	91	89	98
Hexyl acetate	85	70	92
Mesityl oxide	58	76	98
Ethyl crotonate	76	74	97
Hexenyl acetate	72	59	85
3-Picoline	41	92	97
3-Ethylpyridine	76	95	97
Average	65	81	95

are only slightly below those obtained under normal conditions where an organic activating solvent is used. These results demonstrate the superior ability of the hydrophilic resins to make intimate contact with aqueous solutions without resorting to the use of an adsorbed organic solvent.

In Table II results are given for several aliphatic compounds and substituted pyridines. Again, the recoveries are much higher on Amberchrome 161 than on C_{18} silica, but the recoveries are highest on the acetyl Amberchrome 161 SPE column. When air was passed through each column before addition of the aqueous sample, the average recoveries were as follows: C_{18} silica, 50.5%; Amberchrome 161, 50.9%; and acetyl Amberchrome 161, 91.2%.

TABLE III

RECOVERIES (%) OF PHENOLS AND POLYHYDROXYPHENOLS USING 10-μm POLYSTYRENE (PS) RESINS UNDER WET SPE COLUMN LOADING CONDITIONS

Compound	PS	PS–$COCH_3$
Phenol	24	98
p-Cresol	91	100
2,4-Dinitrofluorobenzene	100	100
3-Nitrophenol	82	102
Catechol	1	40
Hydroquinone	0	14
2-Methylresorcinol	8	80
Methylhydroquinone	4	59

TABLE IV

COMPARISON OF DIFFERENT ACETYL RESINS FOR SPE

Amberchrome 161: *ca.* 720 m^2/g surface area and 50 μm average particle size. Sarasep: *ca.* 415 m^2/g surface area and 10 μm average particle size.

Compound	Recovery (%)		
	C_{18} Si	Amberchrome 161	Sarasep
Benzene	41	86	85
Toluene	75	85	88
Indene	73	84	85
Naphthalene	68	79	79
Anthracene	59	67	71
Phenol	7	98	97
p-Cresol	33	100	99
Dibutyl phthalate	66	84	88
Average	53	85	87

The effect of hydrophilic substituents was further tested by comparing resins from different sources. A highly cross-linked, spherical polystyrene resin was obtained from Sarasep. This resin has an average particle size of 10 μm and a surface area of 415 m^2/g, which is appreciably lower than that of the Amberchrome 161 resins.

The results in Table III show significantly higher recoveries on the acetyl resin than on the underivatized resin for all the compounds tested. The results for the four phenols on the acetyl Sarasep resin are comparable to those obtained on the acetyl Amberchrome resin (Table I). However, recoveries of the polyhydroxyphenols are lower on the acetyl Sarasep than on the acetyl Amberchrome resin. This may be due to the smaller surface area of the Sarasep resin.

Several organic compounds (0.7–7 ppm in water) were selected to compare the recoveries obtained with the acetyl derivatives of the Amberchrome 161 and Sarasep resins. The recoveries were similar, as shown in Table IV. Again, the recoveries with the C_{18} silica material were much lower.

CONCLUSIONS

Incorporation of a hydrophilic group into a porous polymeric resin enables excellent surface contact to be made with an aqueous sample without resorting to any pretreatment of the resin with an

organic solvent. Aromatic and other relatively non-polar organic compounds are taken up from aqueous solutions almost as strongly by the derivatized as by the underivatized resins. More polar compounds (particularly phenols) are retained more strongly by the resins with a hydrophilic group, especially when the resin bears an acetyl group.

The surface area of a porous resin seems to have a major effect on its efficiency for SPE. The better recovery of test compounds by polymeric resins compared with bonded-phase silica resins could be due in part to the significantly higher surface area of the polymeric resins.

ACKNOWLEDGEMENTS

We thank John Naples of Rohm and Haas for the Amberchrome 161 resin and Doug Gjerde of Sarasep for the 10-μm polystyrene resins used in this research. Ames Laboratory is operated for the US Department of Energy under Contract No. W-7405-Eng-82. This work was supported by the Director of Energy Research, Office of Basic Energy Sciences.

REFERENCES

1 C. H. Marvin, I. D. Brindle, C. D. Hall and M. Chiba, *Anal. Chem.*, 62 (1990) 1495.
2 G. A. Junk and J. J. Richard, *Anal. Chem.*, 60 (1988) 451.
3 G. A. Junk, J. J. Richard, M. D. Grieser, D. Witiak, J. L. Witiak, M. D. Arguello, R. Vick, H. J. Svee, J. S. Fritz and G. V. Calder, *J. Chromatogr.*, 99 (1974) 745.
4 A. Tateda and J. S. Fritz, *J. Chromatogr.*, 152 (1978) 329.
5 M. W. F. Nielen, U. A. Th. Brinkman and R. W. Frei, *Anal. Chem.*, 57 (1985) 806.
6 T. R. Steinheimer and M. G. Ondrus, *Anal. Chem.*, 58 (1986) 1839.
7 C. E. Rostad, W. E. Pereira and S. M. Ratcliff, *Anal. Chem.*, 56 (1984) 2856.
8 A. Przyjazny, *J. Chromatogr.*, 346 (1985) 61.
9 E. Chladek and R. S. Marano, *J. Chromatogr. Sci.*, 22 (1984) 313.
10 A. W. Wolkoff and C. Creed, *J. Liq. Chromatogr.*, 4 (1981) 1459.
11 C. P. Richard and D. J. Bisch, *GC · LC*, 7 (1989) 972.
12 D. Bourquin and R. Breuneisen, *J. Chromatogr.*, 414 (1987) 187.
13 D. F. Hagen, C. G. Markell and G. A. Schmitt, *Anal. Chim. Acta*, 236 (1990) 157.
14 A. Bacaloni, G. Goretti, A. Lagana, B. Petronio and M. Rotatori, *Anal. Chem.*, 52 (1980) 2033.
15 C. Borra, A. Di Corcia, M. Marchetti and R. Samperi, *Anal. Chem.*, 58 (1986) 2048.
16 J. J. Sun and J. S. Fritz, *J. Chromatogr.*, 522 (1990) 95.
17 J. N. King and J. S. Fritz, *Anal. Chem.*, 57 (1985) 1016.

Journal of Chromatography, 590 (1992) 203–213
Elsevier Science Publishers B.V., Amsterdam

CHROM. 23 752

High-performance liquid chromatography and supercritical fluid chromatography of monosaccharides and polyols using light-scattering detection

Chemometric studies of the retentions

L. Morin-Allory* and B. Herbreteau

Laboratoire de Chimie Bioorganique et Analytique (LCBA), URA CNRS 499, Université d'Orléans, BP 6759, 45067 Orléans Cedex 2 (France)

(First received February 19th, 1991; revised manuscript received September 17th, 1991)

ABSTRACT

Twelve sugars and polyols were analyzed using high-performance liquid chromatographic (HPLC) and supercritical fluid chromatographic (SFC) systems with silica and bonded silica stationary phases with the help of an evaporative light-scattering detector. The separation capacities of the two techniques are discussed. The retention data were studied using different chemometric methods (automatic classification, factor analysis). They clearly show that SFC and HPLC have the same retention process for these compounds and that is the sum of only two mathematically independent physico-chemical phenomena.

INTRODUCTION

Sugars and polyols (sugar alcohols) are widespread compounds found in our biotope. Their use in the food processing, pharmaceutical, cosmetic and chemical industries make them very important from an economic point of view. Thus many studies on their separation by chromatographic methods have been carried out [1–4]. These studies have revealed many difficulties, due principally to two features of these products: their retention mechanism is badly defined, making the development of a new separation difficult, and their detection is not possible or too weak with the UV detectors commonly used in high-performance liquid chromatography (HPLC) and supercritical fluid chromatography (SFC).

For several years, our group has been working on these types of compounds [5–7] using a detection technique which is less common but perfectly suitable for them, namely evaporative light-scattering detection. Recently this method of detection was adapted to SFC [8,9] in our laboratory. This is the only detection compatible with polar modifiers in the supercritical fluid phase for solutes which do not absorb in the UV region. Another advantage is that gradient elution can be used in either HPLC or SFC.

This paper concerns the retention results obtained with an isocratic eluent for twelve monosaccharides and polyols on twelve normal-phase chromatographic systems, seven in SFC and five in HPLC. In HPLC an eluent system whose polarity is close to that of the carbon dioxide–methanol mixtures used in SFC was chosen. This was necessary for an objective comparison of the two techniques and an interpretation of the mechanisms because this type of system (eluent–stationary phase) has not yet been studied much. Various statistical analytical methods [10] are used, such as the hierarchical ascending classification (HAC) and factor analysis (FA).

0021-9673/92/$05.00

These methods have been used in our laboratory to analyse the retentions and selectivities of other solutes in other chromatographic systems [11,12]. This allows the establishment of the factors linking the retention in these systems, a better understanding of the "true" complexity of the problem and a clearer visualization of convergences and divergences, and hence the respective advantages, of HPLC and SFC for the separation of these types of products.

EXPERIMENTAL

Apparatus

SFC. Carbon dioxide, kept in a cylinder with an eductor tube connected to a Waters (Milford, MA, USA) Model M45 pump, was passed through a cooling bath (−30°C). The pump head was cooled (0°C) to improve efficiency. The flow-rates and the weight percentages of carbon dioxide and methanol given in the tables and figures have been corrected to take into account the pumping yield and the pump-head temperature. Polar modifier (methanol) was added using a Jasco (Tokyo, Japan) Model 2510 pump. The two solvents were mixed in a Knauer (Berlin, Germany) dynamic mixer. The column temperature (40°C) was controlled with a water-bath. The loop of a Rheodyne (Cotati, CA, USA) Model 7125 valve was immersed in the same water-bath.

A Sedex 45 evaporative light-scattering detector (Sedere, Vitry sur Seine, France) was used with a special interface for the SFC (Sedere). It was connected to a Shimadzu (Kyoto, Japan) CR5A calculator.

HPLC. The chromatographic system consisted of a Gilson (Villiers le Bel, France) Model 303 isocratic pump, a Rheodyne 20-μl sample loop, an Sedex 45 evaporative light-scattering detector and a Shimadzu CR3A calculator.

Columns

The following columns were used: 10-μm LiChrospher Diol (250 × 4.6 mm I.D.), 10-μm LiChrospher Diol (125 × 4 mm I.D.), 5-μm LiChrosorb CN (150 × 4.6 mm I.D.) and 10-μm LiChrospher CN (250 × 4.6 mm I.D.), all from Merck (Darmstadt, Germany), Zorbax CN (150 × 4.6 mm I.D.), Zorbax Phenyl (150 × 4.6 mm I.D.), Zorbax NH_2 (150 × 4.6 mm I.D.), Zorbax TMS (250 × 4.6 mm I.D.), and Zorbax Sil (250 × 4.6 mm I.D.), all from DuPont (Wilmington, DE, USA), 5-μm RSil NO_2 (250 × 4.6 mm I.D.) from RSL (Eke, Belgium) and 10-μm μBondapak CN (150 × 3.9 mm I.D.) from Waters.

Chemicals and reagents

Carbon dioxide (Air Liquide, Paris, France) was of B 50 grade and was flushed through molecular sieves before the pump. Pestipur-grade methanol was purchased from SDS (Vitry, France) for use as a polar modifier. Only a few grades of methanol are suitable as polar modifiers with a light-scattering detection system in SFC and must always be tested before use. Dichloromethane was of HiPerSolv grade (BDH, Poole, UK). Distilled water (Cooperation Pharmaceutique Francaise, Etampes, France) was used throughout.

The solutes (analytical-reagent grade) were dissolved in chloroform–methanol or in pure methanol. The chloroform–methanol mixture was preferable to avoid problems such as band broadening and peak splitting caused by high elution strength solvents.

Data processing

Microcomputers were used for data treatment using commercial programs [13] or specially adapted programs from publications [14,15].

RESULTS AND DISCUSSION

The compositions of the mobile phases differed from one system to another. The compositions for each column had to be adjusted in order to obtain peak shapes as correct as possible, pressures compatible with our devices and to have capacity factors (k') in a suitable range (usually 0.8–10) for every product [9]. A few SFC experiments, using large amounts of methanol in the mobile phase, were performed under subcritical conditions but no dramatic changes concerning selectivity were observed between subcritical or supercritical conditions. Although carbon dioxide is compressible under the conditions applied, the mean density of the carbon dioxide–methanol fluids, calculated from the supplier's data, is quite constant (0.84–0.89). A list of these systems is given in Table I.

TABLE I

LIST OF THE CHROMATOGRAPHIC SYSTEMS

System	Stationary phase	Dimensions (length × I.D.) (mm)	Mobile phase	Composition	Flow-rate (ml/min)	Pressure (p.s.i.)
SYS 1	Zorbax CN	150 × 4.6	CO_2–CH_3OH	93.5:6.5	4.35	3700
SYS 2	μBondapak CN	150 × 3.9	CO_2–CH_3OH	95.9:4.1	3.37	3900
SYS 3	LiChrosorb CN	150 × 4	CO_2–CH_3OH	96.4:3.6	3.35	3900
SYS 4	LiChrospher CN	150 × 4	CO_2–CH_3OH	95.4:4.6	2.97	3000
SYS 5	LiChrospher Diol	250 × 4	CO_2–CH_3OH	83.7:16.3	1.79	3900
SYS 6	RSil NO_2	250 × 4.6	CO_2–CH_3OH	87:13	3.8	3500
SYS 7	Zorbax Phenyl	150 × 4.6	CO_2–CH_3OH	85.7:14.3	3.48	3000
SYS 8	Zorbax NH_2	150 × 4.6	CH_2Cl_2–CH_3OH	65:35	1	
SYS 9	LiChrospher Diol	125 × 4	CH_2Cl_2–CH_3OH	87:13	1	
SYS 10	RSil NO_2	250 × 4.6	CH_2Cl_2–CH_3OH	80:20	1	
SYS 11	Zorbax TMS	250 × 4.6	CH_2Cl_2–CH_3OH	70:30	1	
SYS 12	Zorbax Sil	250 × 4.6	CH_2Cl_2–CH_3OH–H_2O	80:19.8:0.2	1.5	

Table II gives the capacity factors for the twelve compounds with the twelve systems. Direct interpretations and drawing inferences from this type of table are difficult. Fig. 1 presents a graphical representation of these k' values, providing new information. In addition to overall of these k' values among the various systems, abnormal points appear (*e.g.*, xylitol and mannitol in systems 1 and 3) and some retention inversions may be noted. However, this graphical representation does not allow the quantification of these specificities and also hides a large part of the information.

From a practical viewpoint, the chromatographer is essentially interested in the separation capacities

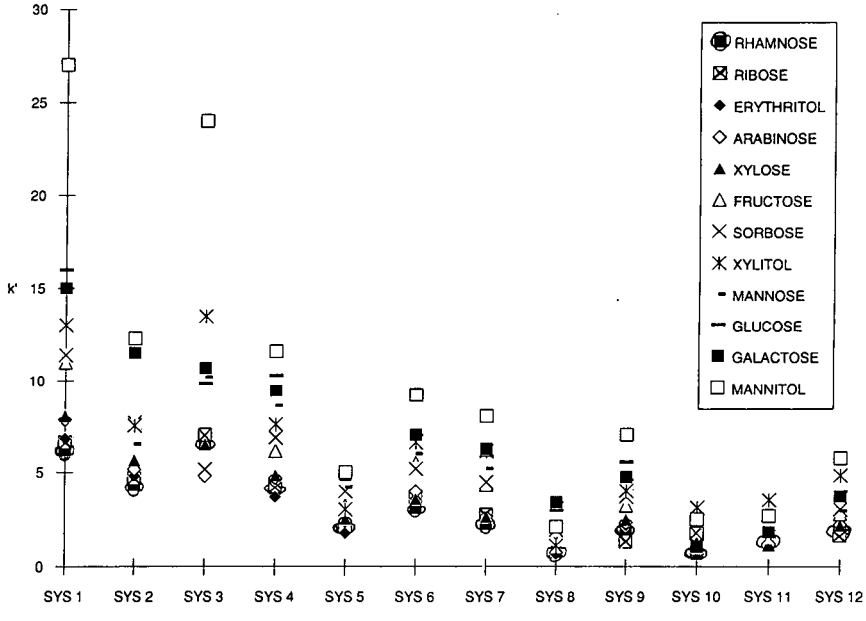

Fig. 1. Capacity factors of the twelve products on the twelve chromatographic systems.

TABLE II
CAPACITY FACTORS OF TWELVE PRODUCTS ON TWELVE CHROMATOGRAPHIC SYSTEMS

System	L-Rhamnose	D-Ribose	*m*-Erythritol	L-Arabinose	D-Xylose	D-Fructose	L-Sorbose	Xylitol
SYS 1	6.2	6.6	6.8	7.8	8	11	11.4	13
SYS 2	4.33	4.67	4.83	5.17	5.67	7.67	7.67	7.5
SYS 3	6.5	7	5	4.83	6.5	5.17	5.17	13.5
SYS 4	4.14	4.28	3.71	4.71	4.86	6.14	6.86	7.57
SYS 5	2.22	2.11	1.78	2.44	2.55	3.22	4	3.05
SYS 6	3.1	3.7	3.6	4	3.6	5.5	5.2	6.6
SYS 7	2.26	2.76	2.62	2.65	2.67	4.35	4.5	6.12
SYS 8	0.882	0.824	0.706	1.82	1.18	2.12	1.94	1.12
SYS 9	2.04	1.32	2.2	2.36	2.52	3.24	3.72	4.04
SYS 10	0.724	1.76	1.24	0.793	0.724	1.07	1.07	3.14
SYS 11	1.13	1.36	1.45	1.45	1.23	1.82	1.59	3.55
SYS 12	1.85	1.65	2.5	2.25	2.2	2.8	3.05	4.85

of a new system. The best criterion would be the calculation of the resolution of every potential pair included in this group of products on each system. In this way the highest resolution system (for this group of products) could be determined and a definitive conclusion could be drawn. However, this would imply the optimization of each chromatographic system. Another problem is linked to this approach, namely that to calculate easily the efficiency of the system, Gaussian or near-Gaussian peaks are required. This is not always the case with these products [9], so we limited ourselves to calculating all the selectivities. For each system we calculated the selectivities (α) of the 66 potential pairs and Table III gives the number of selectivities greater than 1.2, 1.5, 1.7 and 2. These values illustrate, for a system, the more or less regular distribution of the k' values within the range of values. It is obvious that a system giving high values is more likely to separate a given pair than a system giving low values when their efficiencies are equivalent.

Fig. 2 gives a graphical representation of these values, thus allowing an overview of these results. It is worth noting that greater homogeneity of the values is obtained with the supercritical systems compared with the HPLC systems. The average values are slightly greater with HPLC than with SFC, but this is not really significant as indicated by the averages and standard deviations of these values (Table III). Efficiencies are generally slightly higher with SFC, which allows separations with lower selectivities. Therefore, it is not possible to conclude that one of these two systems has an intrinsic advantage over the other, but rather that they are simply complementary. For example, it is worth noting that the products are separable on CN phases in SFC, whereas this is difficult, or even impossible,

TABLE III
NUMBER OF PAIRS OF PRODUCTS WITH A SELECTIVITY GREATER THAN 1.2, 1.5, 1.7 and 2 ON TWELVE SYSTEMS

The last three pairs of lines give the average and standard deviation of these values in SFC, HPLC and SFC + HPLC.

System	$\alpha > 1.2$	$\alpha > 1.5$	$\alpha > 1.7$	$\alpha > 2$
1	51	37	31	20
2	48	35	23	15
3	54	37	30	23
4	52	35	25	18
5	51	34	24	15
6	47	32	22	8
7	49	38	30	21
8	54	47	36	27
9	55	40	33	21
10	48	30	26	21
11	41	20	16	10
12	54	33	22	14
Av. (SFC)	50.29	35.43	26.43	17.14
S.D. (SFC)	2.25	1.92	3.50	4.64
Av. (HPLC)	50.40	34.00	26.60	18.60
S.D. (HPLC)	5.31	9.14	7.26	5.95
Av. (total)	50.33	34.83	26.50	17.75
S.D. (total)	3.84	6.12	5.39	5.28

D-Mannose	D-Glucose	D-Galactose	D-Mannitol
15	16	15	27
6.5	12	11.5	12.3
10.2	9.83	10.7	24
8.57	10.3	9.43	11.6
4.22	4.89	4.88	5
6	7	7	9.2
5.2	5.91	6.25	8
3.41	3	3.41	2.12
4.6	5.56	4.76	7
0.896	0.896	1.07	2.52
1.54	1.64	1.82	2.68
2.95	4	3.72	5.75

in HPLC on the same stationary phases. All the trials we made on these phases with these kinds of mobile phases gave broad peaks with very bad selectivities.

Thermodynamic approach

A comparison of the retention based on the plot of log k'_{ij} *vs.* log k'_{ij} for all the products i on systems j and j' can be made [16,17]. Depending on the relationship between ΔG_j and $\Delta G_{j'}$ (the Gibbs free energy of the transport of the solutes between the mobile and the stationary phases), the slope $a_{jj'}$ and the correlation coefficient $r_{jj'}$ of the regression line log $k'_j = a_{jj'}$ *log* $k'_{j'}$ + constant may vary. If the Gibbs free energies in the two systems j and j' are identical for all the products i, then $a_{jj'}$ and $r_{jj'}$ ought to be close to 1. The retention is called homoenergetic (the same). If these energies are proportional, the correlation coefficient is always close to 1 but the slope is different, and then the retention is called

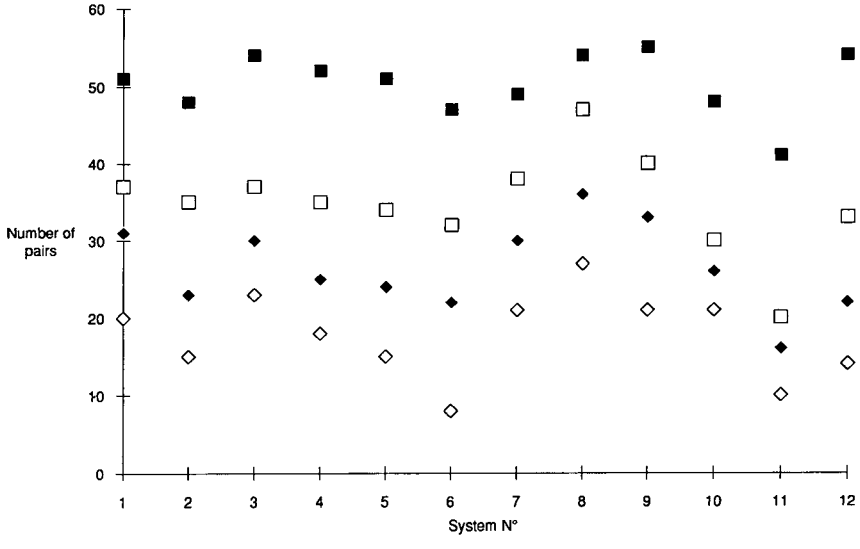

Fig. 2. Representation for the twelve systems of the number of pairs of products with a selectivity greater than (■) 1.2, (□) 1.5, (◆) 1.7 and (◇) 2.

	SYS 1	SYS 2	SYS 3	SYS 4	SYS 5	SYS 6	SYS 7	SYS 8	SYS 9	SYS 10	SYS 11
SYS 2	3	.	.	.	.	.	.	.	.	.	.
SYS 3	3	3	.	.	.	.	.	.	.	.	.
SYS 4	2 (1.12)	3	3	.	.	.	.	.	.	.	.
SYS 5	3	3	3	1 (0.91)	.	.	.	.	.	.	.
SYS 6	2 (1.27)	3	3	2 (0.85)	3	.	.	.	.	.	.
SYS 7	1 (0.99)	3	3	2 (0.86)	3	2 (0.78)	.	.	.	.	.
SYS 8	3	3	3	3	3	3	3	.	.	.	.
SYS 9	2 (0.88)	3	3	3	3	3	3	3	.	.	.
SYS 10	3	3	3	3	3	3	3	3	3	.	.
SYS 11	3	3	3	3	3	3	3	3	3	3	.
SYS 12	3	3	3	3	3	3	3	3	3	3	3

Fig. 3. Comparison of retentions for the 66 pairs of systems. 1 = Homoenergetic; 2 = homeoenergetic; 3 = heteroenergetic. The slope is given in parentheses.

homeoenergetic (similar). If these energies are not proportional then the correlation coefficient is different from 1 and the retention is heteroenergetic (different).

Fig. 3 shows the result of these regressions for all 66 pairs of systems. It is clear that the retentions are mainly heteroenergetic (58 pairs compared with only 6 homeoenergetic and 2 homeoenergetic pairs). This result corroborates the difficulties in the interpretation and prediction process of the retention of the carbohydrates and polyols on such chromatographic systems. However, from another point of view, it is difficult to accept so many different processes for the retention of very similar products on similar chromatographic systems. The limitation of this classification is due to the criterion chosen. The regression analysis is a global approach. For example, it cannot interpret either a specific interaction of a product with a system or the diversity of the chromatographic variables and therefore it gives a bad correlation coefficient. It is for these reasons that the following statistical procedures are more efficient.

Classification approach

Hierarchical ascending classification (HAC) [18] is a statistical method which successively groups together p objects, represented in an N-dimensional observation space, in $p-1$, $p-2$, ..., 2, 1 groups according to their similarity. The programs select the two objects which are the closest to one another, then create a group and replace it with a new point located at its centroid. The procedure is repeated with $p-1$, $p-2$, ..., points until all the objects are agglomerated. The result is presented in the form of a classification tree (dendogram). Several criteria are available to define the inter-object "distance". The average Euclidian distance on raw or reduced data was used because it is straightforward, close to the requirements for developing new separations, and the most natural for quantitative data [19]. This global technique has the advantage of clearly underscoring and even quantifying the similarity between the objects. The lower the agglomeration level is, the closer the objects are; the higher this level is, the more dissimilar the objects are. The basic difference between the classification and the thermodynamic approach is its pragmatic aspect. The aim is not to search for links between the mathematical criteria and the physico-chemical phenomena, but rather a more comprehensible representation of reality.

Our data can be considered as the coordinates of twelve products in a space of twelve chromatographic systems with the products being the objects and the similarity of their retention on this set of chromatographic systems is visualized.

However, these data can also be considered as the coordinates of twelve chromatographic system in a space of twelve products and then the similarity of the chromatographic system in relation to their action on this products is visualized.

Products in the space of systems

In this case, the Euclidian distance on the raw data was selected as a criterion. The classification tree is presented in Fig. 4. The agglomeration level is indicated near each vertical line.

Well known similarities appear, *e.g.*, glucose and

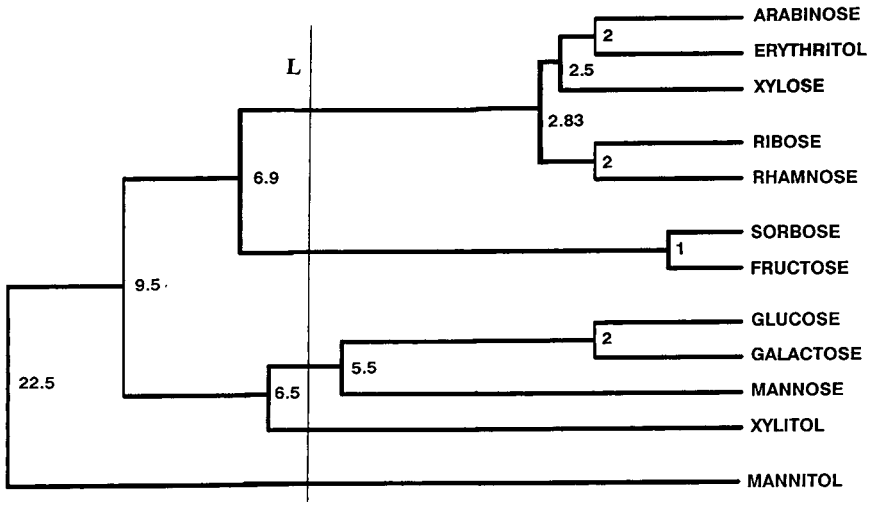

Fig. 4. Classification tree of the twelve products. The vertical line L indicates the partitioning into five groups.

galactose, and xylose and arabinose. It is also worth noting agglomerations which are less obvious: fructose and sorbose (two ketohexoses) are closer to pentoses than to aldohexoses. The division into five classes, dilineated by the line L (Fig. 4), certainly provides the most interesting information as it can be correlated with very simple chemical criteria, *e.g.*, the number of hydroxyl groups on the molecule and its family.

class 1: mannitol	alcohol	6 OH
class 2: glucose, galactose, mannose	aldose	5 OH
class 3: xylitol	alcohol	5 OH
class 4: fructose, sorbose	ketose	5 OH
class 5: other products	sugars and alcohol	4 OH

One can reasonably interpret the proximity of ketohexoses and pentoses by the very poor accessibility of the hydroxyl group located at the C-2 of the furanose form, which leads these molecules to interact with the mobile and stationary phases in a way that is closer to that of the pentoses than that of the aldohexoses. These results indeed show the global influence of the number of hydroxyl groups of the molecule, *i.e.*, its polar area, but it remains a global approach that does not take into account the specific interactions of a system with certain products.

Systems in the space of products

In this case, the agglomeration criterion selected is the Euclidian distance of the reduced data in order to eliminate the scale effect due to products having high retentions (mainly polyols). The classification tree is represented in Fig. 5.

The first noteworthy fact is the non-separation of the SFC and HPLC systems. SFC has been claimed to be superior than HPLC for compounds less polar than sugars. However, regarding selectivity in our experiments, it is clear that there is nothing special about a sub- or supercritical mobile phase in that it is no different from any other mobile phase. The four CN phases in SFC form a group opposed to the other systems but with notable differences within this group (the agglomeration level between the

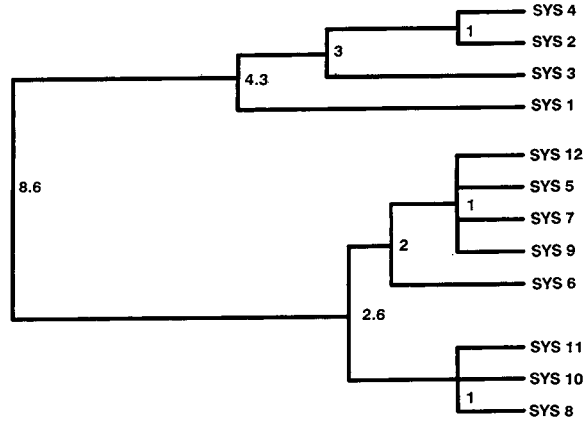

Fig. 5. Classification tree of the twelve systems.

Zorbax CN phase and the other CN phases is equal to 4.3, *i.e.*, the penultimate level). It is also worth noting stranger parallels: LiChrospher Diol HPLC and SFC, Zorbax Sil HPLC and Zorbax Phenyl SFC (SYS 5, 9, 7 and 12) are very similar (level 1). It is not possible to conclude that the mobile or the stationnary phases systematically have a stronger influence because, *e.g.*, the RSil NO_2 in SFC and HPLC systems (SYS 6 and 10) are dissimilar (Level 2.6) and, in contrast, the LiChrospher Diol SFC and HPLC systems (SYS 5 and 9) are very similar (level 1). Contrary to what has been done for the products in the space of systems, it is not possible to classify logically these systems, which are globally very dissimilar. This is in accordance with the results of the thermodynamic approach which indicated a strong complexity of the retentions.

Principal component analysis

Principal component analysis (PCA) is a factor analysis method allowing the exploration of the complete data space and the reduction of this space into a subspace with a much smaller dimension but which still contains the maximum amount of information. The principles, the mathematical bases and the applications to chemical data of these analyses are well known and perfectly explained especially by Malinowski and Howery [20]. Their applications in analytical chemistry are numerous [21] and we have already applied then to chromatographic data [11]. As for the classification, the products in the space of systems or the systems in the space of products can be analysed. The major difficulty in this analysis is choosing the proper number of dimensions in order to keep the maximum amount of information and to eliminate the background noise. We jointly used the imbedded error function (*IE*) and Malinowski's indicator [20], while taking into account the percentage of explained inertia and the comparison between the original matrix and the one reconstituted with the selected eigenvectors.

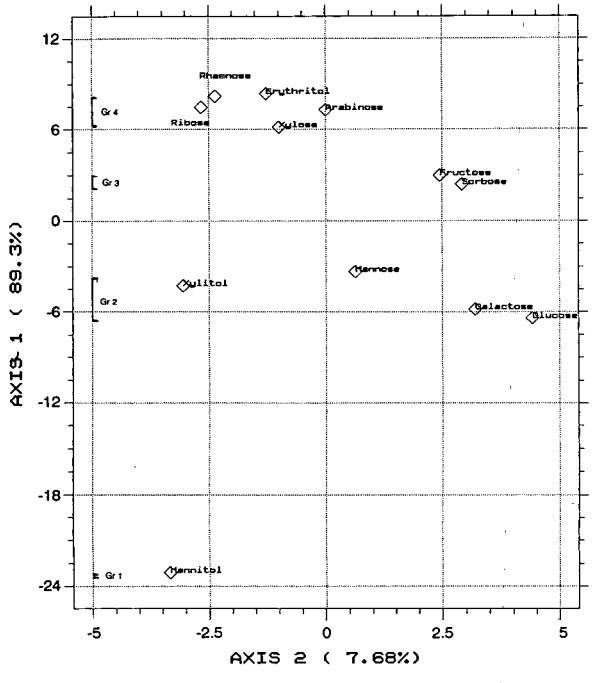

Fig. 6. Projection of the twelve products on the main PCA plane.

PCA of products in the space of systems

The analysis of the k' table of the products in the space of the chromatographic systems was carried out by using the simplest criterion: a canonical metric centred on the mean. The first two components contribute 89.3% and 7.68%, respectively, to the total inertia. The difference between the original and the reconstituted matrices is small and the introduction of additional components does not notably improve it. One can conclude that reduction to a two-dimensional space is possible without a notable loss of information. The plane represents 97% of the inertia of the twelve dimensional initial space and therefore gives a simplified representation, virtually exact, of the relative position of the products in the original space.

Fig. 6 represents a projection of these twelve products on this plane. One notices clusters similar to that with HAC (five groups), but it is much more interesting to note the projections on the two axes, each of which is mathematically independent. On axis 1 (which explains 89.3% of the retention) only four groups can be distinguished: (1) mannitol with six OH, (2) the aldohexoses with five OH and the alcohol with five OH, (3) the products with four OH and, between these two last groups, (4) the ketohexoses with four accessible OH plus one not very accessible OH groups. This proves that this axis, and hence the major part of the retention, are directly linked to the number of accessible OH groups in the molecule and therefore to its polar surface.

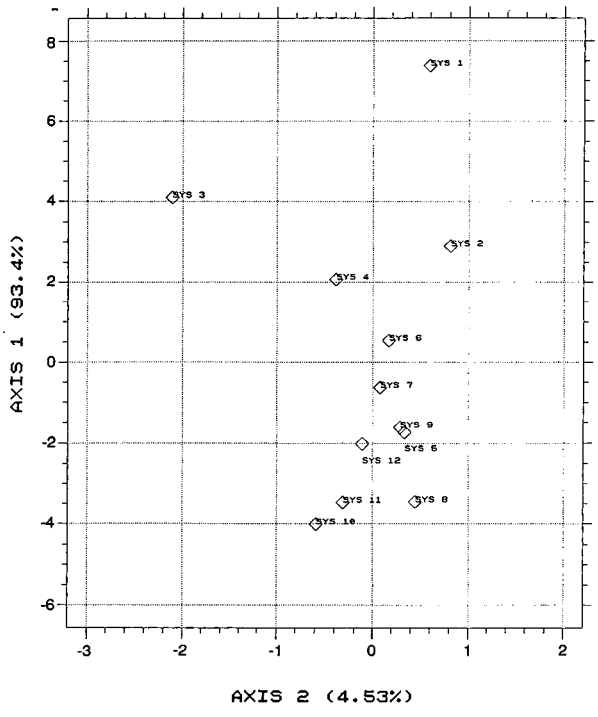

Fig. 7. Projection of the twelve systems on the main PCA plane.

The second axis is smaller (7.68%) and its interpretation is more difficult. One notices mainly an opposition between the hexoses and a group constituted by the alcohols, rhamnose and especially ribose. It is the effect represented by this axis which causes the non-regularity of the retention because although the ratio of the influences is equal to 89:8 for the overall systems, it varies from one system to another. For example, if axis 1 is sufficient to explain the retention of systems 1 or 12 whose correlation with that axis is greater than 0.95, the influence of axis 2 is very important for the systems 3, 8, 10 and 11. Finding a physico-chemical correlation with this axis is difficult. A differentiation between the open forms of the alcohols and the cyclic forms of hexoses can be considered but cannot explain the position of some pentoses on this axis. Such assumptions should be confirmed by structural and conformational studies of the products connected to a rotational study of the two main axes. At present the real conformations of these products in the injection solvent and the kinetics of conversion from one form into another at the time of the transfer from the injection solvent to the eluent phase are unknown, but will be studied.

PCA of systems in the space of products

In a similar way, we can analyse the systems in the space of products. For the same reason as for HAC, we shall use a standardized metric centred on the mean. The two first components contribute 93.4% and 4.5%, *i.e.*, 98% of the total inertia. The other axes, the contributions of which to inertia are very small, do not improve the representation. The plane (Fig. 7) formed by these first two axes is then sufficient to represent the quasi-total amount of information. A clustering made from this plane is in close agreement with the result of HAC.

Axis 1 allows the separation of the CN phases from the others, which is also in agreement with the conclusions of the HAC. It clearly indicates the specificity of these systems. Axis 2 is mainly created by the opposition between one system (LiChrosorb CN) and the others. Its contribution to inertia is only 4.5%, a low value, and a corrective effect of the importance of axis 1 is probable. Giving a physico-chemical explanation to this classification is not really possible with the present state of our knowledge of these systems.

The most significant and most interesting fact, however, is the explanation given by the two factors obtained in the two PCA to the incoherence underlined at the beginning of this paper. Therefore, the variation in the retentions of these similar compounds on similar systems is not due to many different mechanisms but rather to the combination of only two mathematically independent phenomena. The proportions of these phenomena vary from one product to another and from one system to another. This simplicity in the decomposition of the mechanism is even more impressed if these results are compared with those obtained previously [17]. With a homogeneous set of compounds (chalcones), seven significant factors for the interpretation of the retention on eleven chromatographic systems were found, which corresponds to a much greater complexity.

Correspondence factor analysis

Correspondence factor analysis is a factor analysis method allowing the determination of the

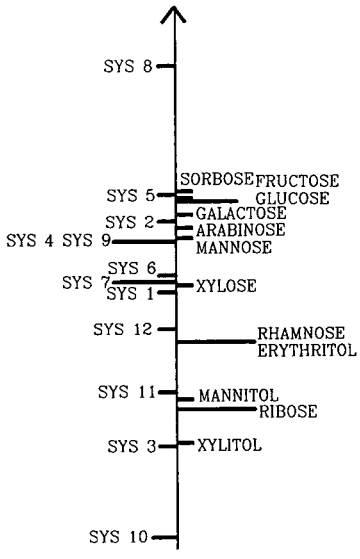

Fig. 8. Projection of products and systems on the main CFA axis.

factors causing the deviation from the state of independence [22] using the χ^2 distance criterion. The number of significant factors in CFA is equal to the number of significant PCA factors minus one because the first one is embedded in the state of independence. One limitation of CFA is the need to have homogeneous data. The major advantages are the possibility of representing the rows and columns of the data matrix on the same space and interpreting the proximity of a row and a column as a specific interaction causing the deviation from proportionality.

Two PCA factors indicate one CFA factor alone. This allows all space to be represented in one-dimensional space, *i.e.*, a line (Fig. 8).

Classification of products is similar to that obtained on axis two of PCA. The deviation from proportionality is caused by specific interactions between certain products (mainly sugar alcohols and some pentoses) and certain systems (SYS 10, 3 and 11). The physical interpretation is not simple; what is the common factor between LiChrosorb CN in SFC and RSil NO_2 and Zorbax TMS in HPLC? It is interesting to note that these interactions were observed not only with alcohols but also with certain pentoses. This proves once again the necessity for a better understanding of the real conformation of these products in the injection solvent and mobile phase, in addition to the solvation state of both the stationary phases and products. This knowledge makes it possible to transform pragmatic information given by these statistical analyses into a rational interpretation.

CONCLUSIONS

The use of a particular system of detection allowed us to obtain a homogeneous set of data on the retention of sugars and polyols in HPLC and SFC. The statistical analysis of the results allows a better definition of the information contained in these data.

First, when we considered the retention mechanism and the separation abilities, neither of the two systems (HPLC, SFC) clearly differed and rather the two techniques are complementary.

However, the most significant fact is that the apparent complexity of the retention mechanisms of these products in these systems is simply caused by the combination of two independent factors, one directly connected to the number of accessible OH groups on the solutes and the other, well quantified, not physico-chemically interpreted.

The knowledge of the components of this retention allows a better choice of which chromatographic system to use for a particular problem. The joint use of HPLC and SFC with a light-scattering detector make it possible to solve frequent separation problems with this set of compounds. This aspect is currently being investigated, principally the interactions between the mobile and stationary phases and the products, to obtain a physico-chemical meaning of these two axes. This information will allow a correct prediction of the retention of a product on a new system using the retention of this product on other systems.

ACKNOWLEDGEMENTS

The authors thank Professor M. Dreux for many fruitful discussions.

REFERENCES

1 L. A. Verhaar and B. F. M. Kuster, *J. Chromatogr.*, 220 (1981) 313.
2 A. Meunier, M. Caude and R. Rosset, *Analusis*, 14 (1986) 363.

3 P. E. Shaw, *Handbook of Sugar Separation in Foods by HPLC*, CRC Press, Boca Raton, FL, 1988.
4 M. Verzele, G. Simoens and F. Van Damme, *Chromatographia*, 23 (1987) 292.
5 M. Lafosse, M. Dreux, L. Morin-Allory and J. M. Colin, *J. High Resolut. Chromatogr. Chromatogr. Commun.*, 8 (1985) 41.
6 M. Lafosse, M. Dreux and L. Morin-Allory, *J. Chromatogr.*, 404 (1987) 95.
7 L. Morin-Allory, B. Herbreteau, M. Lafosse and M. Dreux, *J. High Resolut. Chromatogr.*, 13 (1990) 343.
8 M. Lafosse, P. Rollin, C. Elfakir L. Morin-Allory, M. Martens and M. Dreux, *J. Chromatogr.*, 505 (1990) 191.
9 B. Herbreteau, M. Lafosse, L. Morin-Allory and M. Dreux, *J. Chromatogr.*, 505 (1990) 299.
10 D. L. Massart, B. G. M. Vandeginste, S. N. Deming, Y. Michotte and L. Kaufman, *Chemometrics: a Textbook*, Elsevier, Amsterdam, 1988.
11 B. Walczak, M. Dreux, J. R. Chrétien, L. Morin-Allory, M. Lafosse and G. Félix, *J. Chromatogr.*, 464 (1990) 237, and previous papers in the series.
12 B. Walczak, M. Dreux and J. R. Chrétien, *Chromatographia*, 29 (1990) 259.
13 *STATPC*, B. Bleuse-Trillon, Orléans, 1989.
14 T. Foucart, *Analyse Factorielle*, Masson, Paris, 2nd ed., 1985.
15 T. Foucart, A. Bensaber and R. Garnier, *Méthodes Pratiques de la Statistique*, Masson, Paris, 1987.
16 W. Melander, J. Stoveken and Cs. Horváth, *J. Chromatogr.*, 199 (1980) 35.
17 G. Walczak, L. Morin-Allory, M. Lafosse, M. Dreux and J. R. Chrétien, *J. Chromatogr.*, 395 (1987) 183.
18 H. Jambu and H. O. Lebeaux, *Classification Automatique pour l'Analyse des Données*, Dunod, Paris, 1978.
19 G. Saporta, *Probabilités, Analyse des Données et Statistique*, Technip, Paris, 1990.
20 E. R. Malinowski and D. C. Howery, *Factor Analysis in Chemistry*, Wiley, New York, 1980.
21 S. D. Brown, *Anal. Chem.*, 62 (1990) 84.
22 J. Benzécri, *L'Analyse des Données*, Vol. 2, Dunod, Paris, 1973.

Journal of Chromatography, 590 (1992) 215–222
Elsevier Science Publishers B.V., Amsterdam

CHROM. 23 740

Determination of carboxylic acids, sugars, glycerol and ethanol in wine and grape must by ion-exchange high-performance liquid chromatography with refractive index detection

M. Calull, R. M. Marcé and F. Borrull*

Departament de Química, Universitat de Barcelona, Pça. Imperial Tarraco 1, 43005 Tarragona (Spain)

(First received May 28th, 1991; revised manuscript received September 10th, 1991)

ABSTRACT

Method to determine the major carboxylic acids, sugars, glycerol and ethanol in wine and grape must was developed using an ion-exchange column and refractive index detector. A solid-phase extraction method with a strong anion exchanger was used to determine these compounds in sweet wines and in grape musts. With this method it is possible to determine malic acid in sweet wines and in grape musts without interference from sugars. This high-performance liquid chromatographic method was compared with standard methods of analysis. There was good agreement in the accuracy and precision of the compared methods.

INTRODUCTION

Chromatographic methods are considered to be valid alternatives to enzymatic methods for the determination of carboxylic acids in wine as all the carboxylic acids can be determined chromatographically with a shorter analysis time and with similar accuracy [1,2].

Of the various high-performance liquid chromatographic (HPLC) techniques, reversed-phase HPLC [1–7] and ionic-exchange HPLC [1,8–13] are the most often used. The latter has several advantages over the reversed-phase methods, such as the possibility of determining the carboxylic acids simultaneously with fructose, glucose, glycerol and ethanol when a refractive index (RI) detector is used. The sensitivity of this method is not very high, but it is sufficient to determine these compounds in wine samples.

When ion-exchange HPLC is used to determine these compounds, poor resolution between glucose, malic acid and fructose is obtained. When the concentration of the two sugars is high, it is impossible to determine malic acid correctly. For this reason, various workers [1,11] have applied this method to dry wine samples only using IR detection, with which it is possible to determine malic acid. However, the identification and determination of organic acids in grape musts is impossible with this method because the high concentration of sugars requires a dilution of the sample before injection, and the carboxylic acids cannot be detected at such low concentrations.

The different behaviour of sugars, glycerol and ethanol compared with carboxylic acids allows the separation of these compounds using a solid-phase extraction by ion exchange. In this work, LC-SAX tubes (quaternary amine bonded silica with strong anion exchange) (Supelco) were used to separate the sample into two fractions, neutral and acidic. Once this separation has been carried out, it is possible to determine the carboxylic acids in wine or grape must independently of the concentration of sugars.

This separation method gives a determination of

0021-9673/92/$05.00

malic acid which is more similar to that obtained by enzymatic methods than to that obtained by the direct HPLC method without extraction.

EXPERIMENTAL

High-performance liquid chromatography

The samples were analysed using a Model LC-9A Shimadzu pump, a Shimadzu RID-6A detector and an ION-300 (300 × 7.8 mm) column containing a cation-exchange polymer in the ionic hydrogen form, with a GC-801 ion guard column (Interaction). The column was operated at 74°C using 0.013 *M* sulphuric acid as the mobile phase and a flow-rate of 0.6 ml/min.

Standard solution

The experiment was carried out with a standard solution of the main carboxylic acids found in wine and grape must (tartaric, lactic, malic, acetic, citric and succinic acids, Aldrich Chemicals) and glucose, fructose, glycerol and ethanol (R.A. quality, Merck) at concentrations of 2.5 g/l, except for ethanol, which was prepared at 5% (v/v).

Grape must and wines

Various red and white grape musts and wines from the Tarragona region of Spain were used. All the samples were supplied by the Institut Calatà de la Vinya i del Vi, where all the standard analyses were performed. The grape must samples were stored at 2–4°C after sterile filtration.

Sample preparation procedures

Three simple procedures depending on the products to be determined, were followed before the injection of the samples into the chromatograph.

Procedure A. All samples were filtered with a 0.45-μm nylon membrane (mSI Micron Separations).

Procedure B. To prolong the life of the column, it is necessary to remove the phenolic compounds in the red wines, and grape musts. This is achieved using a C_{18} Sep-Pak cartridge (Waters Assoc.). When a white grape must or wine is analysed, only dilution of the sample is required to obtain good results. The C_{18} Sep-Pak cartridge was activated by a recommended method [14] with 1 ml of methanol–water (10:90) then 1 ml of the wine sample was passed through the Sep-Pak cartridge, followed by 1.5 ml of 0.005–0.0025 *M* sulphuric acid.

Procedure C. To separate the neutral compounds from the acidic compounds, a 3-ml Supelclean LC-SAX (strong anion exchange) tube (Supelco) was used. First, the tube was conditioned with 5 ml of Milli-Q water and then 0.5 ml of sample diluted 1:2, previously adjusted to pH 7–8 with 10 *M* sodium hydroxide solution, was slowly passed through the extraction tube. To obtain a good recovery of the neutral compounds, it is necessary to elute these compounds with 1 ml of water if a wine sample is analysed, and 2 ml of water if a grape must is analysed. The final volumes obtained are 1.5 ml for the wine samples and 2.5 ml for the grape must samples.

To elute the acidic compounds, two 0.5-ml aliquots of 0.5 *M* sulphuric acid were passed through the tube. Two small aliquots of eluent generally elute the compounds of interest more efficiently than one larger aliquot.

To determine the sugars in grape must samples, only a 1:50 dilution is necessary to determine glucose and fructose.

Chemical methods used as comparisons with HPLC

Citric acid, L-malic acid, glucose, fructose and glycerol were determined enzymatically using the Boehringer UV method [15]. Tartaric acid was determined by titration [16].

RESULTS AND DISCUSSION

In a previous paper [13] the optimization of an ion-exchange HPLC separation with an RI detector for the determination of the major carboxylic acids, sugars, glycerol and ethanol in wine samples with various chemometric methods was reported. The best chromatographic conditions obtained with an ION-300 column were: flow-rates, 0.6 ml/min; mobile phase 0.013 *M* sulphuric acid; and column temperature, 74°C.

Fig. 1 shows the chromatogram obtained for a standard mixture using these conditions. Good resolution between the different peaks was obtained, except for the glucose, malic acid and fructose peaks. In samples with high sugar concentrations (sweet wines and grape musts), the malic acid peak was completely masked by the high concentration

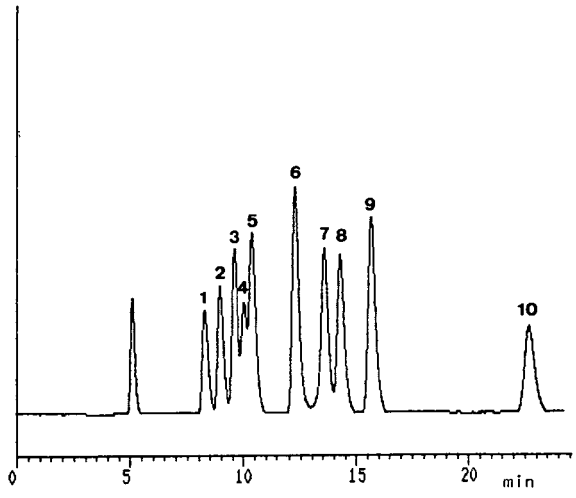

Fig. 1. Chromatogram of a standard solution. Peaks: 1 = Citric acid; 2 = tartaric acid; 3 = glucose; 4 = malic acid; 5 = fructose; 6 = succinic acid; 7 = lactic acid; 8 = glycerol; 9 = acetic acid; 10 = ethanol.

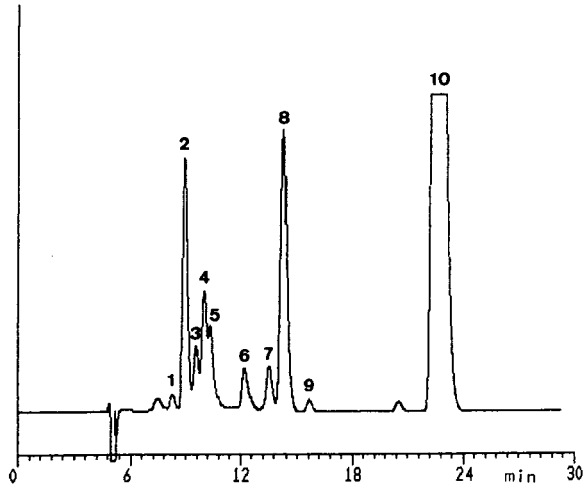

Fig. 2. Chromatogram of wine without SAX treatment. Peaks as in Fig. 1.

of glucose and fructose. However, when a grape must was analysed, the dilution of the sample which was necessary to determine the sugars made it impossible to determine carboxylic acids in the same injection. The determination of tartaric and citric acids can be achieved without dilution of the must, but the determination of malic acid is impossible.

If the method is applied to samples with high sugar contents, it is necessary to separate glucose and fructose from the malic acid before chromatographic determination. This separation is possible using a Supelclean LC-SAX (strong anion exchange) column to remove the acidic fraction (containing citric acid, tartaric acid, malic acid, succinic acid, lactic acid and acetic acid) from the neutral fraction (containing glucose, fructose, glycerol and ethanol). The use of a Sep-Pak cartridge to eliminate the coloured compounds is recommended by several workers [3,17] when red wines are analysed.

The volume of sample and the volume and concentration of the sulphuric acids passed through the cartridge to obtain a good recovery of the compounds were optimized. The volumes of sample and sulphuric acid studied were between 0.5 and 1.5 ml and the concentration of sulphuric acid was between 0.005 and 0.0025 *M*. The best results were obtained when the volume of sample was 1 ml, followed by 1.5 ml of 0.0025 *M* sulphuric acid.

Table I shows the results obtained for a red wine spiked with different standard solutions to determine the recovery values and the influence of the concentration on these values. A good recovery was obtained (> 90%) and changes in the concentration of sulphuric acid did not affect the recovery.

A study of the repeatability of the method and its reproducibility between days was performed. The results obtained are given in Table II. The repeatability study under these conditions gave relative standard deviations ranging from 0.58 to 5.15% and reproducibilities between 1.13 and 5.62%.

The linearity of the response of the HPLC method was evaluated using a range of concentrations of each standard component. All components had a good linear response over the studied concentration range and can be quantified by an external standard. The linearity ranges were: citric acid, 0.05–1 g/l; tartaric acid, 0.1–6 g/l; malic acid, 0.05–6 g/l; succinic acid, 0.05–2.5 g/l; lactic acid, 0.1–5 g/l; acetic acid, 0.05–2 g/l; glucose and fructose, 0.1–4 g/l; glycerol, 0.2–10 g/l; and ethanol, 0.5–15% (v/v).

The chromatogram obtained for a wine with a low sugar content without SAX treatment can be seen in Fig. 2. The peaks corresponding to citric, tartaric, succinic, lactic and acetic acids, glycerol and ethanol have a good resolution and can be determined, but poor resolution was obtained with this column for glucose, malic acid and fructose.

TABLE I

RECOVERY STUDY OF SEP-PAK TREATMENT FOR A RED WINE

Compound	Concentration (g/l)				
	In wine	Added	Calculated	Found	Recovery (%)
Citric acid	0.145	0.155	0.300	0.295	99.5
	0.145	0.305	0.450	0.435	96.6
	0.145	0.510	0.655	0.590	90.4
Tartaric acid	2.780	1.200	3.980	4.045	101.6
	2.780	2.405	5.185	5.275	101.8
	2.780	4.005	6.785	6.725	99.1
Malic acid	1.515	0.605	2.120	2.135	100.8
	1.515	2.425	3.940	3.950	100.4
	1.515	4.040	5.555	5.395	97.1
Succinic acid	0.875	0.460	1.335	1.280	96.0
	0.875	0.925	1.800	1.720	95.7
	0.875	1.540	2.415	2.285	94.7
Lactic acid	1.625	0.505	2.130	2.295	107.8
	1.625	0.950	2.575	2.630	102.3
	1.625	1.895	3.520	3.430	97.4
Acetic acid	0.455	0.200	0.655	0.660	100.9
	0.455	0.620	1.075	0.995	92.6
	0.455	1.035	1.490	1.425	95.8
Glucose	1.175	0.605	1.780	1.770	99.5
	1.175	1.215	2.390	2.400	100.5
	1.175	2.025	3.200	3.150	98.5
Fructose	0.300	0.605	0.905	0.975	108.1
	0.300	1.210	1.515	1.680	111.0
	0.300	2.020	2.320	2.465	106.4
Glycerol	8.785	1.810	10.595	10.870	102.6
	8.785	3.620	12.405	12.675	102.2
	8.785	6.300	15.085	13.945	92.5
Ethanol[a]	14.021	1.000	15.021	15.312	101.9
	14.021	2.500	16.521	16.734	101.3
	14.021	4.000	18.021	18.453	102.4

[a] Expressed as % (v/v).

They can be identified, although the accuracy of the determination is a function of the integration criteria used.

Fig. 3 shows the chromatogram obtained when the wine sample is passed through a SAX tube. In the region corresponding to glucose, malic acid and fructose, only one peak appears, corresponding to malic acid. At the end of the chromatogram a small peak appears corresponding to glycerol together with another peak corresponding to ethanol, showing a high concentration in the wine. The extraction of glycerol and ethanol is not quantitative with the solid-phase extraction.

Fig. 4 shows the neutral compounds after SAX extraction, when a higher fraction of glycerol and ethanol compounds appear. In the first zone there are three peaks, corresponding to neutral compounds. One possible identification was assigned to glucose, malic acid and fructose, assuming a poor extraction of the malic acid, but in accuracy study,

TABLE II

STUDY OF BETWEEN-DAY REPEATABILITY AND REPRODUCIBILITY OF SEP-PAK TREATMENT FOR A RED WINE

Compound	Repeatability (n = 10)		Reproducibility (n = 10)	
	Mean (g/l)	R.S.D. (%)	Mean (g/l)	R.S.D. (%)
Citric acid	0.16	2.22	0.16	2.30
Tartaric acid	2.64	0.91	2.73	2.81
Malic acid	1.38	2.07	1.43	3.36
Succinic acid	0.92	1.87	0.87	1.32
Lactic acid	1.65	0.58	1.64	1.63
Acetic acid	0.41	2.84	0.44	3.38
Glucose	1.08	3.84	1.16	4.31
Fructose	0.39	5.15	0.33	5.62
Glycerol	8.53	0.78	8.62	1.13
Ethanol[a]	13.84	0.96	13.91	1.43

[a] Expressed as % (v/v).

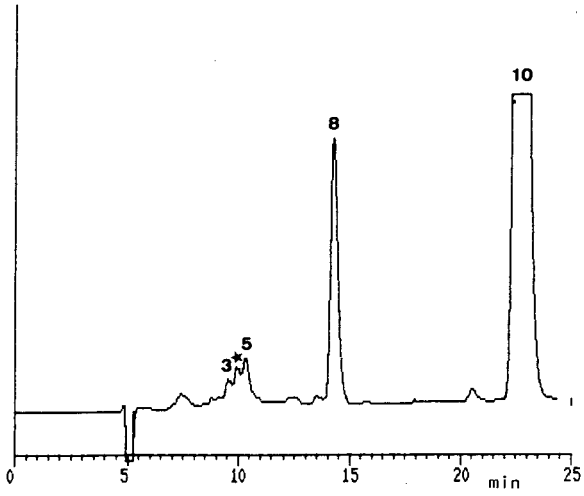

Fig. 4. Chromatogram of neutral fraction of wine sample after SAX treatment. ★ = Unknown peak; other peaks as in Fig. 1.

comparing the results obtained by various chromatographic methods and the enzymatic method, the peak appeared between glucose and fructose and was assigned to another unknown neutral compound.

When a grape must is analysed, only a dilution of the sample is required to determine the sugar compounds (Fig. 5). In this instance, only a small peak corresponding to the main acid present in grape must, tartaric acid, appears before the glucose and fructose peaks. If acidic compounds are analysed, the extraction of sugars with the SAX cartridge is required. Fig. 6 shows the chromatogram obtained after SAX treatment, when citric, tartaric and malic acids can be assigned and quantified.

The method was validated by determining the re-

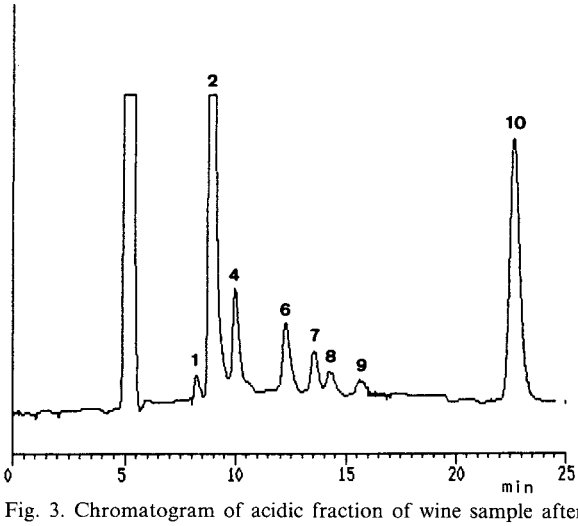

Fig. 3. Chromatogram of acidic fraction of wine sample after SAX treatment. Peaks as in Fig. 1.

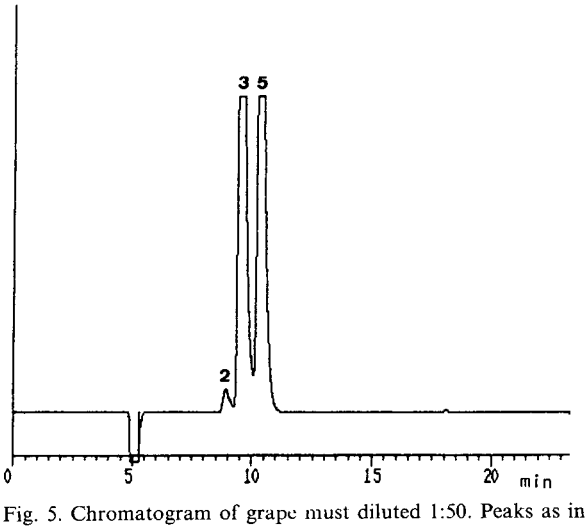

Fig. 5. Chromatogram of grape must diluted 1:50. Peaks as in Fig. 1.

TABLE III

STUDY OF BETWEEN-DAY REPEATABILITY AND REPRODUCIBILITY OF SAX TREATMENT FOR A WHITE WINE

Compound	Repeatability (n = 10)		Reproducibility (n = 10)	
	Mean (g/l)	R.S.D. (%)	Mean (g/l)	R.S.D. (%)
Citric acid	0.15	2.98	0.15	3.23
Tartaric acid	3.59	2.22	3.53	2.81
Malic acid	0.83	2.48	0.84	2.74
Succinic acid	0.73	3.10	0.72	3.61
Lactic acid	0.63	4.14	0.63	4.87
Acetic acid	0.18	3.51	0.17	3.82
Glucose	0.58	1.58	0.59	2.81
Fructose	0.68	4.11	0.68	4.60
Glycerol	4.95	2.57	4.98	2.98

peatability, reproducibility, recovery and accuracy. Table III shows the results obtained for repeatability and between-day reproducibility of the analytical method. The study of repeatability showed a relative standard deviation between 1.58 and 4.14% and a between-day reproducibility of 2.74–4.87%.

Recovery analysis after SAX treatment was performed on a white wine. This wine was spiked with various amounts of each component. For malic acid the results were compared with those of a non-spiked sample, deducting the amount added from the amount in the wine, because it was not possible to determine malic acid without SAX treatment due to the co-elution of an unknown peak. The results are shown in Table IV as a percentage of recovery. The recovery was greater than 88% for citric, tartaric and malic acids. The other three carboxylic

TABLE IV

STUDY OF THE RECOVERY OF ACIDS AFTER SAX TREATMENT

Compound	Concentration (g/l)				
	In wine (g/l)[a]	Added	Calculated	Found	Recovery (%)
Citric acid	0.083	0	0.083	0.082	99.4
	0.083	0.083	0.166	0.161	97.0
	0.083	0.166	0.249	0.237	95.2
	0.083	0.416	0.499	0.466	93.3
Tartaric acid	1.742	0	1.742	1.666	95.6
	1.742	0.127	1.869	1.712	91.6
	1.742	0.254	1.996	1.842	92.3
	1.742	0.632	2.374	2.149	90.5
Malic acid[b]	–	0	–	0.343	–
	–	0.101	–	0.432	88.1
	–	0.202	–	0.531	93.1
	–	0.505	–	0.791	88.7
Succinic acid	0.372	0	0.372	0.337	90.6
	0.372	0.146	0.518	0.460	88.8
	0.372	0.293	0.665	0.600	90.2
	0.372	0.731	1.103	0.888	80.5
Lactic acid	0.531	0	0.531	0.548	103.1
	0.531	0.127	0.658	0.612	93.0
	0.531	0.255	0.786	0.704	89.6
	0.531	0.637	1.168	0.903	77.3
Acetic acid	0.180	0	0.180	0.177	98.3
	0.180	0.081	0.261	0.242	92.7
	0.180	0.162	0.342	0.303	88.6
	0.180	0.406	0.586	0.459	78.3

[a] Amount in wine diluted 1:2.

[b] See results and discussion for explanation.

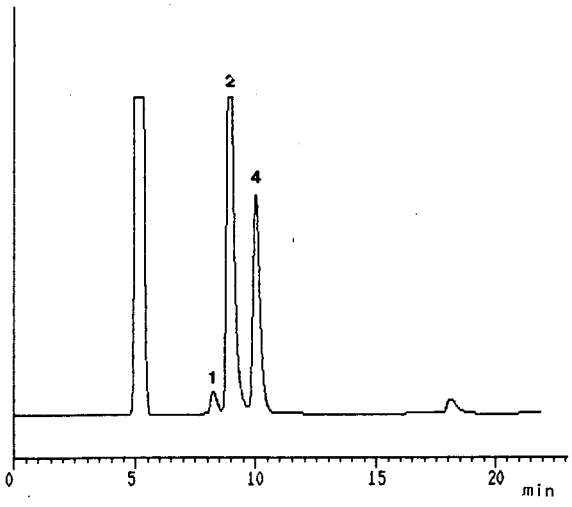

Fig. 6. Chromatogram of acidic fraction of grape must after SAX treatment. Peaks as in Fig. 1.

acids, succinic, acetic and lactic acid, have a poor recovery if their concentration is high, but this is not a problem in these wine samples and their recovery was good after SAX treatment. However, if these compounds are present in large concentrations, the determination must be carried out without SAX extraction (direct method) or dilution of the wine samples.

To determine the accuracy of the method the results obtained by the direct method (without SAX treatment), by the method with SAX treatment and by standard method [15,16] for wine and grape must were compared (Table V). Citric, tartaric and malic acids were not determined by the direct method because of the dilution necessary to quantify the sugars. A good accuracy was obtained for the two chromatographic methods, but this was less for malic acid. The high value obtained for malic acid in the direct method confirms the existence of another unknown peak with the same retention time. In this instance, the best results were obtained when the SAX treatment was used. If a grape must is analysed, only after SAX treatment is it possible to determine citric, malic and tartaric acids in the same injection and the results are similar to those obtained by the enzymatic method.

To confirm the better determination of malic acid after SAX treatment compared with the direct method, various wine and must samples were analysed and their results compared with those obtained by the enzymatic method. In the direct method the criteria of integration considered were the valley bases. The results can be seen in Table VI. This high value for malic acid in the direct method

TABLE V

RESULTS OBTAINED BY THE DIRECT METHOD WITHOUT SAX TREATMENT (A), WITH SAX TREATMENT (B) AND WITH THE STANDARD METHODS (C)

Compound	Concentration (g/l)		
	A	B	C
Wine			
Citric acid	0.15	0.15	0.15[b]
Tartaric acid	3.8	3.6	3.6[c]
Malic acid	1.15	0.83	0.80[b]
Succinic acid	0.81	0.73	–
Lactic acid	0.64	0.63	
Acetic acid	0.20	0.18	–
Glycerol	5.0	4.9	4.7[b]
Glucose	0.55	0.58	0.52[b]
Fructose	0.69	0.68	0.67[b]
Must			
Citric	ND[a]	0.28	0.24[b]
Tartaric acid	ND	4.9	4.8[c]
Malic acid	ND	3.33	3.39[b]
Glucose	133	122	129[b]
Fructose	93	86	90[b]

[a] ND = not determined by this method.
[b] Enzymatic method.
[c] Titration method.

TABLE VI

DETERMINATION OF MALIC ACID IN WINE AND MUST SAMPLES BY THE DIRECT METHOD WITHOUT SAX TREATMENT (A), WITH SAX TREATMENT (B) AND WITH THE STANDARD METHODS (C)

Sample	Concentration (g/l)		
	A	B	C
White wine (René Barbier)	1.10	0.83	0.80
White wine (Colombard-Verdú)	3.01	2.69	2.84
White wine (Chardonnay-Batea)	3.05	2.78	2.84
Red wine (Garnatxa-Riudabella)	0.73	0.55	0.53
Red wine (Garnatxa-Riudabella)	0.86	0.62	0.58
White must (Chardonnay-Verdú)	ND[a]	3.33	3.74
Red must (Ull de llebre-Barberà)	ND	3.41	3.58

[a] ND = not determined by this method.

was noted by Frayne [1]; it is a neutral compound co-eluting with the malic acid peak.

CONCLUSIONS

Ion-exchange chromatography with RI detection is a good alternative method to determine carboxylic acids, sugars, glycerol and ethanol in wine samples, but if malic acid is to be determined, SAX treatment is required to obtain better results. The compounds were separated and quantified by this method in less than 25 min.

ACKNOWLEDGEMENTS

The authors thank J. Guardiola and C. Masqué at the Institut Català de la Vinya i del Vi for the wine and grape must samples supplied and the standard analysis, and Caixa de Barcelona "Ajuts a la Recerca" for financial support.

REFERENCES

1 R. F. Frayne, *Am. J. Enol. Vitic.*, 37 (1986) 176.
2 R. M. Marcé, M. Calull, R. M. Marcé, F. Borrull and F. X. Rius, *Chromatographia*, 29 (1990) 54.
3 D. Tusseau and C. Benoit, *J. Chromatogr.*, 395 (1987) 323.
4 E. Mentasti, M. C. Gennaro, C. Sarzanini, C. Barochi and M. Savigliano, *J. Chromatogr.*, 322 (1985) 177.
5 M. C. Polo, F. Barahona and I. Cáceres, *Connais. Vigne Vin*, 3 (1986) 175.
6 F. Caccamo, G. Carfagnini, A. Di Corcia and R. Samperi, *J. Chromatogr.*, 362 (1986) 47.
7 R. M. Marcé, M. Calull, F. Borrull and F. X. Rius, *Am. J. Enol. Vitic.*, 41 (1990) 289.
8 A. Schneider, V. Gerbi and M. Redoglia, *Am. J. Enol. Vitic.*, 38 (1987) 151.
9 J. Haginaka, J. Wakai, H. Yadua and T. Nomura, *J. Chromatogr.*, 447 (1988) 373.
10 J. P. Goiffon, A. Blanchere and C. Reminiac, *Analusis*, 13 (1985) 218.
11 P. Pfeiffer and F. Radler, *Z. Lebensm.-Unters.-Forsch*, 181 (1985) 24.
12 J. D. McCord, E. Trousdale and D. D. Y. Ryu, *Am. J. Enol. Vitic.*, 35 (1984) 28.
13 M. Calull, E. López, R. M. Marcé, J. C. Olucha and F. Borrull, *J. Chromatogr.*, 589 (1991) 151.
14 D. Woo, L. Treat-Clemons and R. M. Patel, *Application Note*, Interaction Chemicals, 1989.
15 Boehringer Mannheim, *Methods of Enzymatic Food Analysis 82/83*, Gebr. Parcus, Munich, 1982.
16 *Official Methods of Analysis*, Association of Official Analytical Chemists, Washington DC, 13th ed., 1980, pp. 153–572.
17 R. Badoud and G. Pratz, *J. Chromatogr.*, 360 (1986) 119.

Journal of Chromatography, 590 (1992) 223–233
Elsevier Science Publishers B.V., Amsterdam

CHROM. 23 738

Mass spectrometric and gas and high-performance liquid chromatographic behaviour of an impurity in 2,5-hexanedione

A. Sturaro*, G. Parvoli, S. Zanchetta and L. Doretti

Servizio di Sicurezza del Lavoro e Protezione Sanitaria del CNR, Corso Stati Uniti 4, 35020 Padova (Italy)

G. Gori and G. B. Bartolucci

Istituto di Medicina del Lavoro, Università di Padova, Via Facciolati 71, 35127 Padova (Italy)

(First received May 15th, 1991; revised manuscript received September 3rd, 1991)

ABSTRACT

The analysis of 2,5-hexanedione, a metabolic compound of several industrial solvents, is normally carried out using gas chromatographic (GC) or GC–mass spectrometric (MS) techniques. This work, with the aim of verifying the possibility of determining the diketone by means of a high-performance liquid chromatographic (HPLC) method with UV detection, illustrates the importance of the choice of a 2,5-hexanedione standard for the determination of the diketone response factor. In some commercial diketone samples the presence of an impurity, which may interfere with the analysis of the target analyte, was ascertained. This impurity showed GC and HPLC behaviour similar to that of 2,5-hexanedione, but gave a very different UV response. This impurity was identified as 3-methylcyclopent-2-enone by means of MS, GC–MS, HPLC–photodiode-array detection, IR and UV spectrometry. The structure was confirmed by comparing the chromatographic, mass and ultraviolet data of the unknown compound with those of a synthesized reference sample. The well known difficulty in determining 2,5-hexanedione by HPLC with UV detection was reconfirmed owing to its low molar absorptivity.

INTRODUCTION

Occupational exposure to *n*-hexane and related compounds has been reported as causing peripheral neuropathies [1] and this disease in workers is due to 2,5-hexanedione (2,5-HD), the ultimate and most abundant metabolite resulting from the breakdown of this type of solvent [2]. The biological monitoring of exposure is normally done by measuring the diketone in hydrolysed urine using gas chromatography (GC) or GC–mass spectrometry (MS) [3,4]. The application of GC to biological samples is complicated owing to the need for extraction and concentration procedures involving the transfer of the target compound into an organic solvent.

Reversed-phase high-performance liquid chromatography (HPLC) may, however, be a valid alternative to GC owing to the sample characteristics and therefore many workers have tried to develop an HPLC method suitable for the detection of C_6 metabolites [5,6]. The main drawback to HPLC is the low molar absorptivity (ε) of 2,5-HD in UV detection; moreover, the presence in the commercial compound of an impurity with high ε and similar gas and liquid chromatographic behaviour may be a further source of error.

We and others [7] have tried, without success, to repeat the HPLC–UV method proposed by Marchiseppe *et al.* [6] for the detection of 2,5-HD in spiked samples. The proposed wavelength of 233 nm seems to be unsuitable for identifying this metabolite, because the absorbance in that UV range cannot be

0021-9673/92/$05.00

attributed with certainty to 2,5-HD. The need to obtain the correct UV spectrum and, consequently, the absorbance maximum of 2,5-HD led to the conviction that some commercial products should be studied.

EXPERIMENTAL

Chemicals

2,5-Hexanedione samples were purchased from Aldrich (Steinheim, Germany), Merck, (Darmstadt, Germany), Eastman Kodak (Rochester, NY, USA) and Carlo Erba (Milan, Italy). HPLC-grade water, methanol and 2,4-dinitrophenylhydrazine and all other analytical-reagent grade chemicals were obtained from Aldrich.

Synthesis of standards

3-Methylcyclopent-2-enone. According to the literature procedure [8], acetonylacetone (3.1 g) was added rapidly to a boiling solution of sodium hydroxide (0.25 g) in water (25 ml). After refluxing for 20 min, the brown solution was cooled to room temperature and extracted with diethyl ether (3 × 20 ml). The extracts were washed with water (2 × 1 ml), dried and evaporated. The crude reaction product, analysed by GC–MS, gave a mass spectrum corresponding to 3-methylcyclopent-2-enone.

2,4-Dinitrophenylhydrazone. According to the literature procedure [9], 2,4-dinitrophenylhydrazine was added to a sample of 2,5-HD enriched in 3-methylcyclopent-2-enone (3-MCP) by means of vacuum distillation (b.p. 76–80°C/25 mmHg), giving a yellow-orange precipitate. The filtered solid was washed with hot water–ethanol (3:2, v/v) and successively introduced into a cold-finger condenser in order to separate the 2,4-dinitrophenylhydrazone derivative of 3-MCP from that of 2,5-HD using their different fusion temperatures of 181 and 257°C, respectively [8,10]. The sample introduced directly into the ion source of the mass spectrometer gave a parent ion at *m/z* 276, corresponding to the calculated molecular weight of the derivative.

HPLC apparatus and conditions

All the measurements were performed with a Waters (Milford, MA, USA) high-performance liquid chromatographic system consisting of a Model 600 E MS pump, a Rheodyne manual loop injector with a 20-μl sample loop, a Model 990 plus MS photodiode-array (PDA) detector operating in the 200–330 nm range and a Model 990 plotter.

The acquisition and the elaboration of the data were carried out with an NEC (Boxborough, MA, USA) APC IV computer. The HPLC column employed was a Nova-Pak RP-18 stainless-steel column (150 mm × 3.9 mm I.D.) with spherical particles of 4 μm (Waters).

Separations were carried out by using methanol–water (40:60, v/v) as the mobile phase at a constant flow-rate of 0.6 ml min^{-1} and at room temperature. The HPLC solvents were degassed with helium. The injection volume for all the samples was 20 μl.

The PDA detector conditions were wavelength scan 200–330 nm, scan rate 1 s, detector sensitivity 1 a.u.f.s. and resolution 1.4 nm.

GC–MS apparatus and conditions

The measurements were performed using a Hewlett-Packard GC–MS system consisting of a Model 5890 gas chromatograph equipped with a 25 m × 0.31 mm I.D. fused-silica capillary column coated with Ultra-2 (cross-linked 5% phenylmethylsilicone; layer thickness 0.52 μm) (Hewlett-Packard, Palo Alto, CA, USA) and a Model 5971 A mass spectrometer. An HP 59970 C data system was used for data acquisition and editing.

For GC separations the column temperature was programmed from 50°C (isothermal for 3 min) at 10°C min^{-1} to 150°C (maintained for 3 min). The injector and transfer line temperatures were 260 and 280°C, respectively.

The MS conditions were electron energy 70 eV, emission current 300 μA and ion source temperature 176°C. Mass spectra were recorded by cyclically scanning from 40 to 250 mass units with a total cycle time of 0.49 s and a solvent delay of 3 min. The injection volume was 1 μl in splitless conditions (0.2 min).

UV apparatus

The UV spectra were recorded with a Hitachi (Tokyo, Japan) Model U-3200 spectrophotometer in the range 210–400 nm and 1 a.u.f.s. using methanol as solvent.

MS apparatus

The mass spectrum of the 3-MCP derivative was

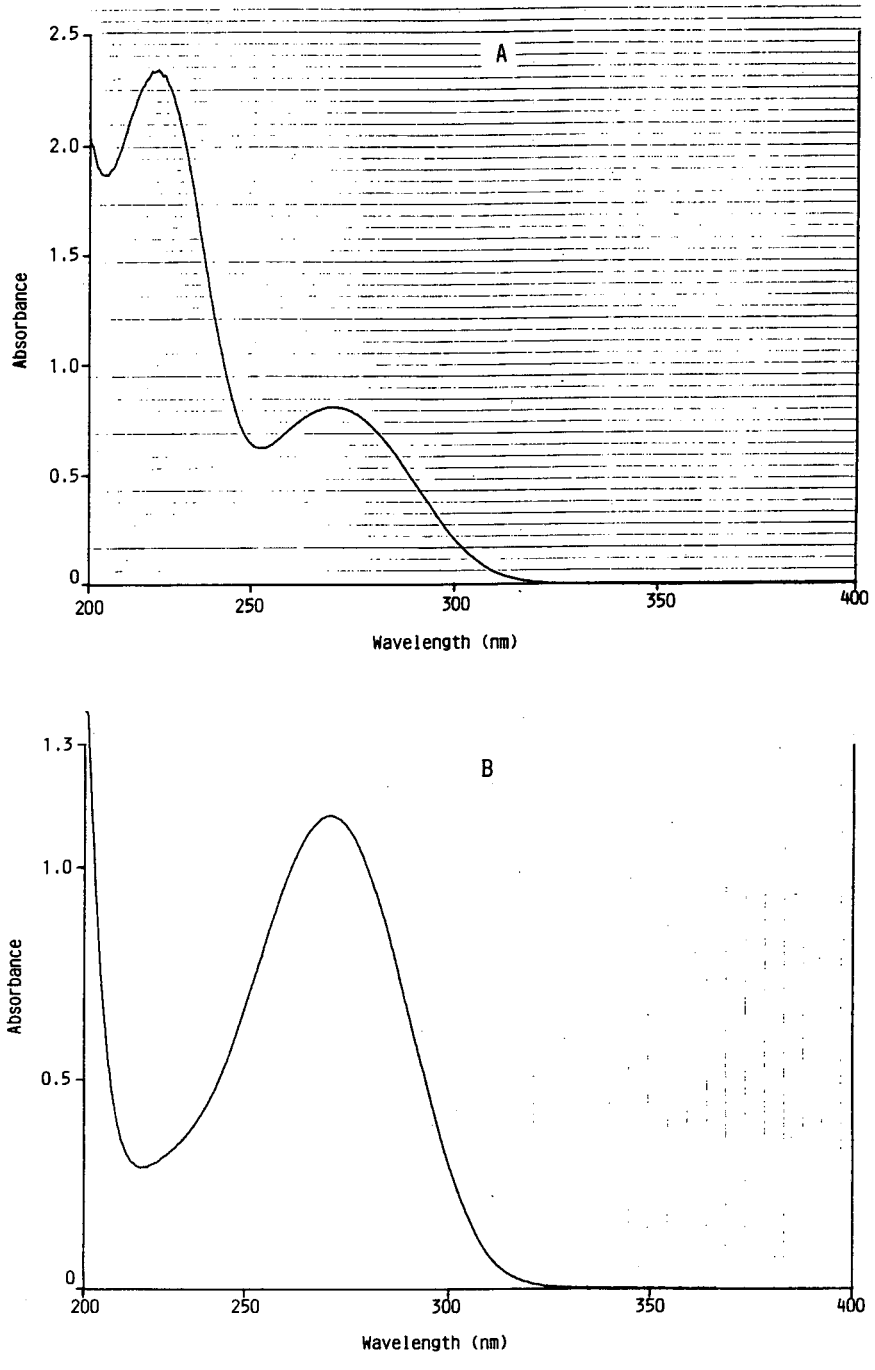

Fig. 1. UV spectra of 2,5-hexanedione from (A) Carlo Erba and (B) Eastman Kodak in methanol, recorded from 210 to 400 nm with a Hitachi U-3200 spectrophotometer.

obtained using a VG-ZAB2F mass spectrometer operating in the electron impact mode (70 eV, 200 μA, source temperature 280°C). The sample was introduced directly into the ion source.

IR apparatus

The IR spectrum of the neat crude reaction product of 3-MCP was recorded with a Perkin-Elmer (Norwalk, CT, USA) Model 682 infrared spectrophotometer in the range 2000–400 cm^{-1} on a potassium bromide disc.

RESULTS AND DISCUSSION

The UV absorption spectra (in methanol) of four commerical 2,5-HD compounds showed a considerable difference in the range 210–400 nm (Fig. 1). Fig. 1A shows two absorbance maxima at 270.4 and 226.6 nm, whereas Fig. 1B shows only one UV peak at 270.4 nm for two samples of the same compound, but of different brands.

The injection of 2,5-HD solution with the double absorption maximum (12 g/l) into the HPLC sys-

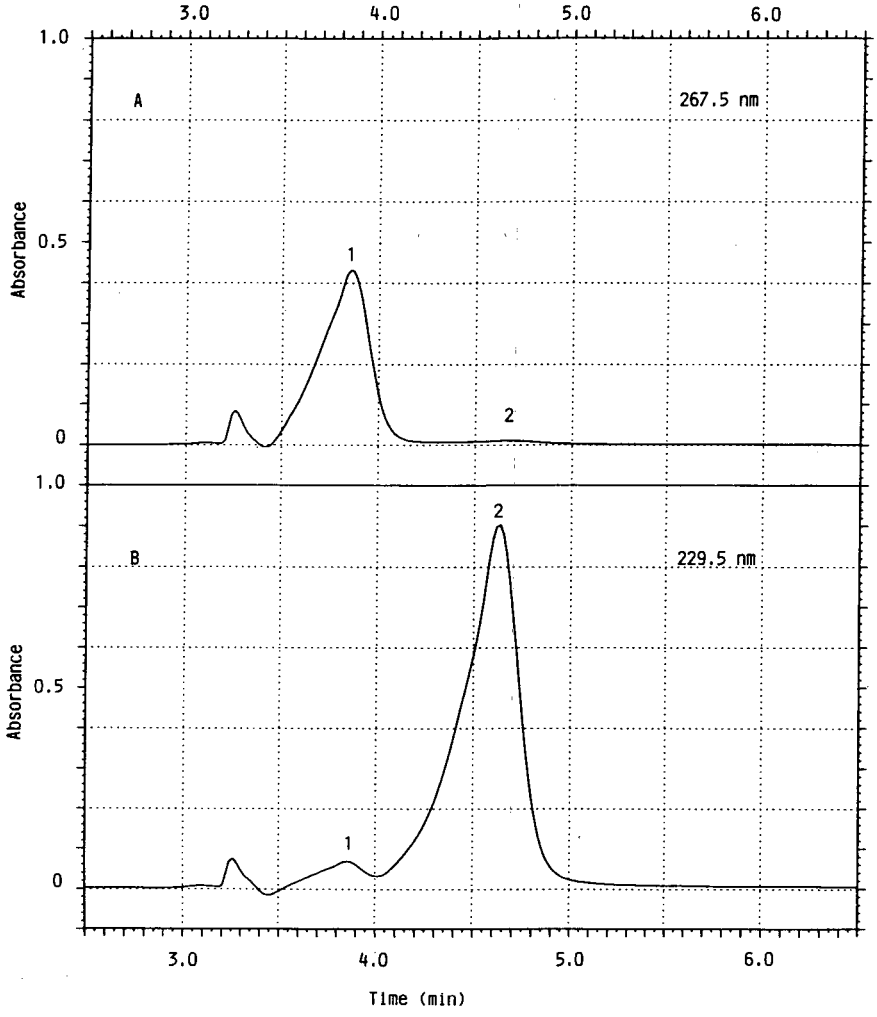

Fig. 2. Reversed-phase HPLC–PDA analysis of Aldrich 2,5-hexanedione sample (12 g/l) in water. Detection: (A) 267.5 nm; (B) 229.5 nm.

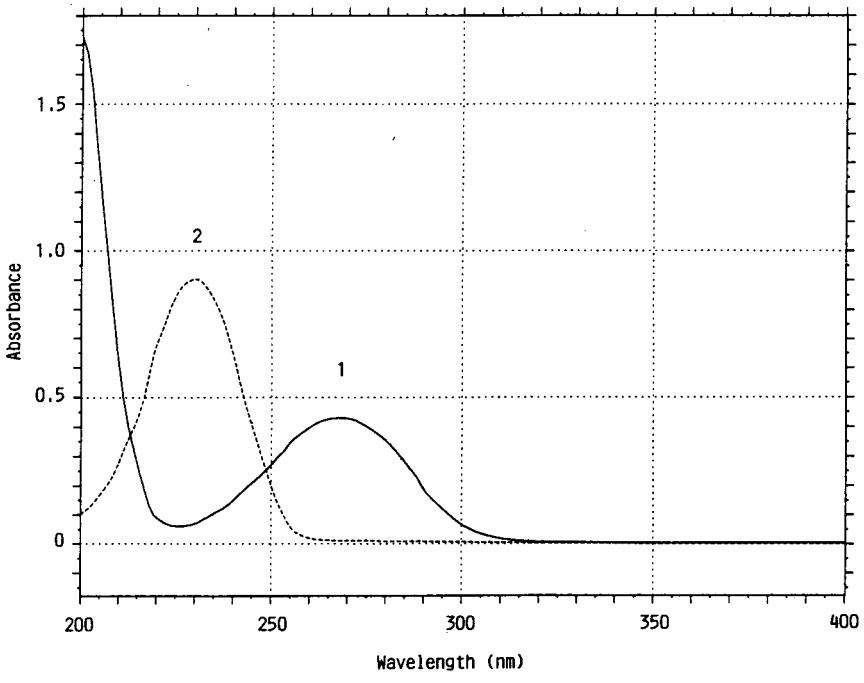

Fig. 3. UV spectra recorded with PDA detector of peaks 1 and 2 from Fig. 2.

tem gave a chromatogram with two separate chromatographic peaks (Fig. 2), to which the UV spectra reported in Fig. 3 corresponded. Comparison of the UV spectra indicated that the 267.5- and 229.5-nm absorbance maxima were independent of each other and seemed to belong to two different compounds. Assuming that one maximum must be assigned to 2,5-HD, the other could belong to another compound with a similar absorbance. To identify the interfering compound, four different commercial 2,5-HD samples were analysed without dilution using the GC–MS system, for which the signal intensity attributed to each peak is strictly dependent on the amount present. All the chromatograms obtained (Fig. 4) showed, close to a very intense peak which could be attributed unequivocally to 2,5-HD owing to its intensity and its mass spectrum, another small peak with reproducible retention times and different abundances.

The mass spectrum relating to the chromatographic peak (arrowed, Fig. 4) was attributed from a library search as having a high probability of being 3-MCP [11]. In fact, the mass spectra of the other reported isomers of the 3-MCP showed the following evident differences: 2-methylcyclopent-2-enone had the base peak at *m/z* 67 and the relative fragment ions at *m/z* 81 were not very abundant (10%); cyclohex-2-enone showed the base peak at *m/z* 68 and 2,5-dimethylfuran, with a very intense $[M-H]^+$ peak, had a retention time of about 2 min under the same GC conditions. Moreover, according to *Beilstein* [12], the 3-MCP compound was the only methylcyclopentenone isomer that is synthesized from 2,5-HD. In order to confirm the preliminary information obtained from the library search, the compound was synthesized in accordance with the literature procedure [8].

The crude reaction product, analysed by GC–MS, showed that 3-MCP was the more abundant product (Fig. 5) and had a mass spectrum identical with that reported in the literature [11], while the IR spectrum of the above sample gave the same absorption peaks with similar reciprocal intensities of those reported in the literature for technical 3-MCP [13]. The IR absorption maxima are shown in Fig. 6.

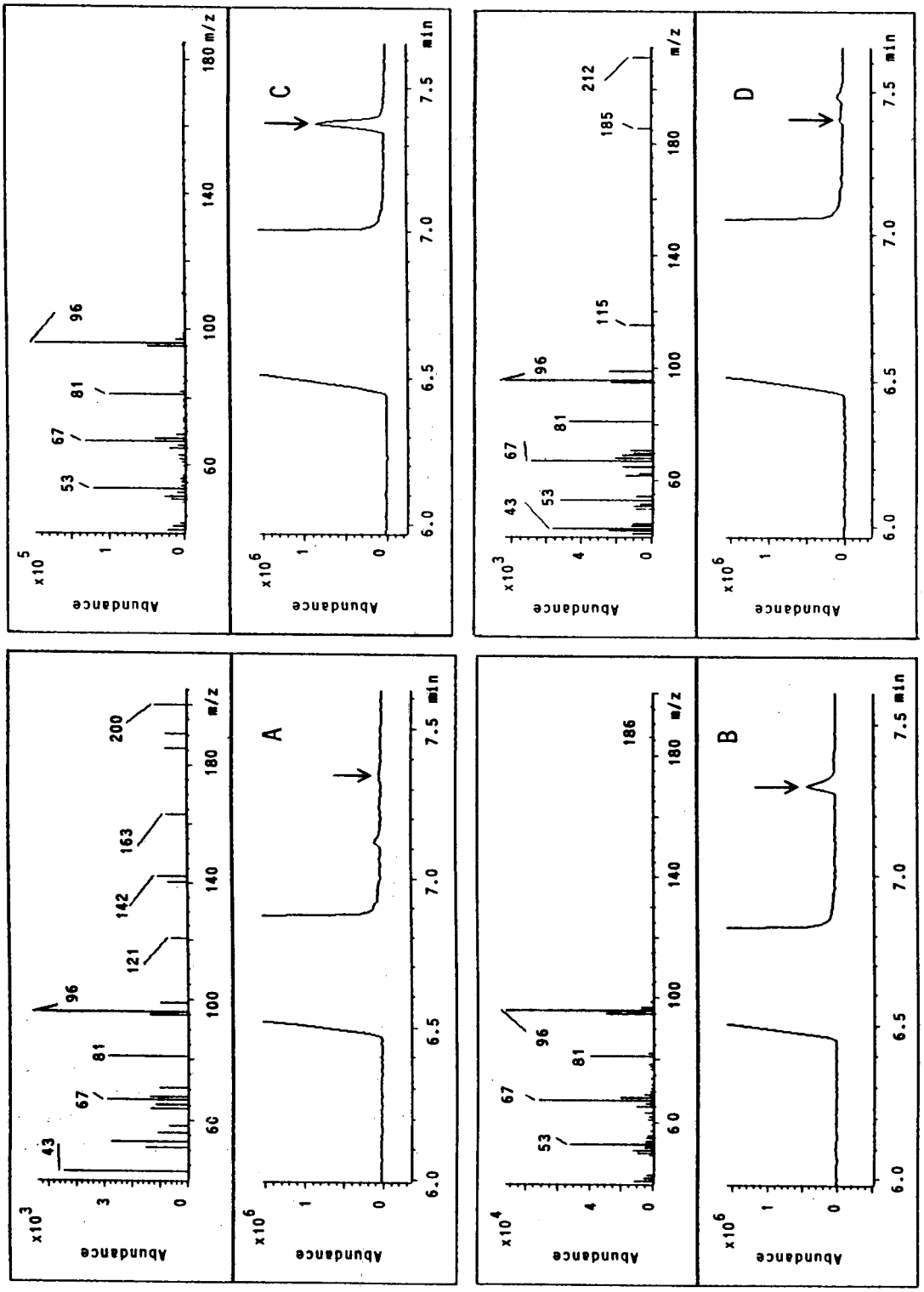

Fig. 4. GC–MS and relative mass spectra of impurity present in different 2,5-hexanedione samples: (A) Eastman Kodak; (B) Aldrich; (C) Carlo Erba, (D) Merck.

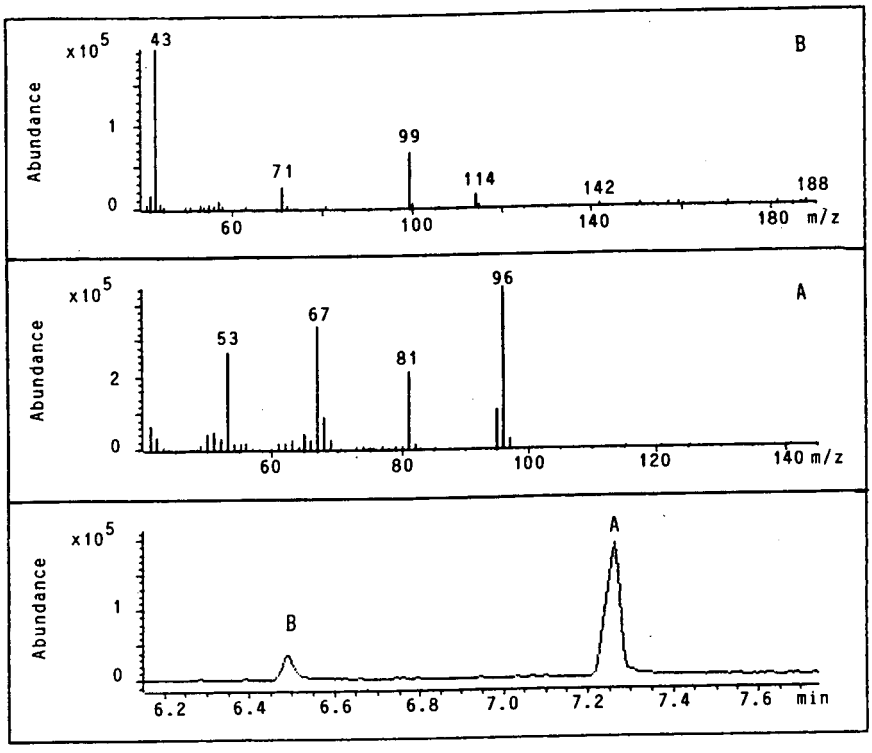

Fig. 5. GC–MS of crude reaction product and mass spectra of (A) synthesized 3-methylcyclopent-2-enone and (B) 2,5-hexanedione.

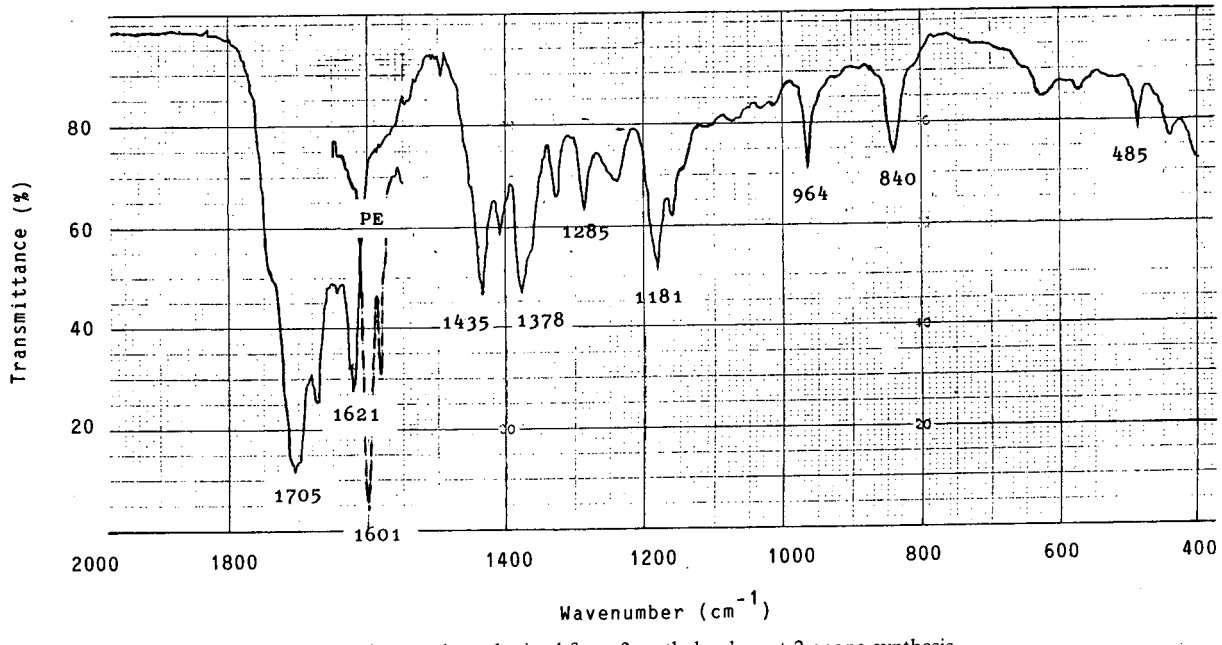

Fig. 6. IR spectrum of neat crude reaction product obtained from 3-methylcyclopent-2-enone synthesis.

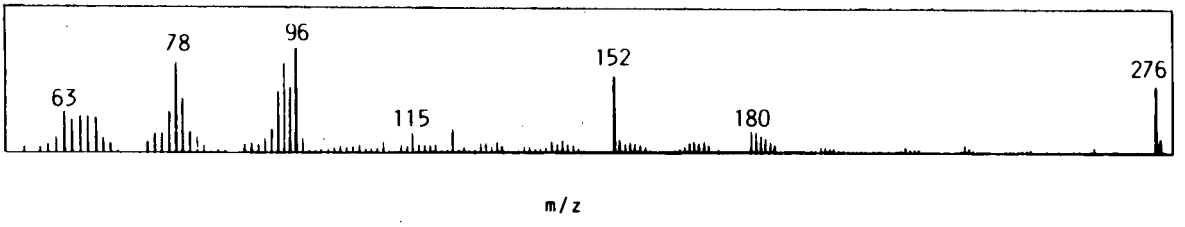

Fig. 7. Electron impact mass spectrum of 2,4-dinitrophenylhydrazone derivative of 3-methylcyclopent-2-enone (*m/z* 276) contained in the commercial 2,5-hexanedione sample.

On the basis of the MS and GC data, it was concluded that 3-MCP is generally present in commercial 2,5-HD samples. For further confirmation that the impurity was 3-MCP, the 2,4-dinitrophenylhydrazone derivative was prepared, as described under Experimental, and then analysed using a VG-ZAB 2F mass spectrometer. The resulting spectrum gave a value of *m/z* 276 for the parent ions, as reported in Fig. 7.

The presence of this compound in 2,5-HD can be explained by considering the following decomposition scheme (Me = methyl):

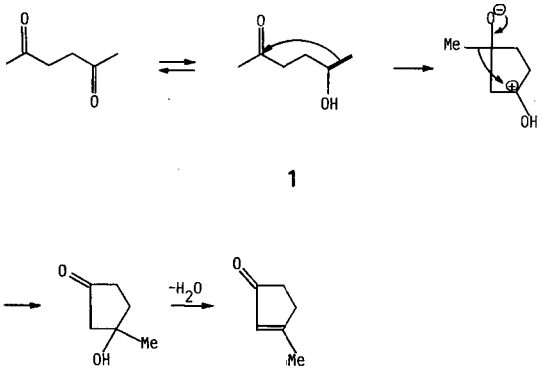

The enol form **1** is the driving force for the subsequent rearrangements, and the cyclization and the successive loss of water lead to the formation of 3-MCP. The different 3-MCP concentrations in the four different 2,5-HD samples seem to be independent of the declared purity (97–98%), but they appear to be closely linked to the specific synthesis process. In fact, the other unreported impurities present in the 2,5-HD samples analysed were all different compounds, while 3-MCP was common to all four samples. Fig. 4 demonstrates that this impurity, in the concentrations found in the four commercial samples, does not affect the GC–MS detection of the principal compound, but plays a very important role in the analytical technique when UV detectors are used. In order to verify the possibility of carrying out a correct determination of 2,5-HD by means of HPLC–UV detection, it appears to be of great importance not only to assign the correct UV spectrum to 2,5-HD, but also to know the exact HPLC and UV behaviour of 3-MCP.

The three-dimensional chromatogram of the synthesized compound (Fig. 8) showed the presence of only one peak with a retention time and UV spectrum that could be superimposed over the second peak in the commercial 2,5-HD chromatogram (Fig. 9), whereas the mixture of two samples (1:1, v/v) gave rise to a chromatogram (Fig. 10) in which

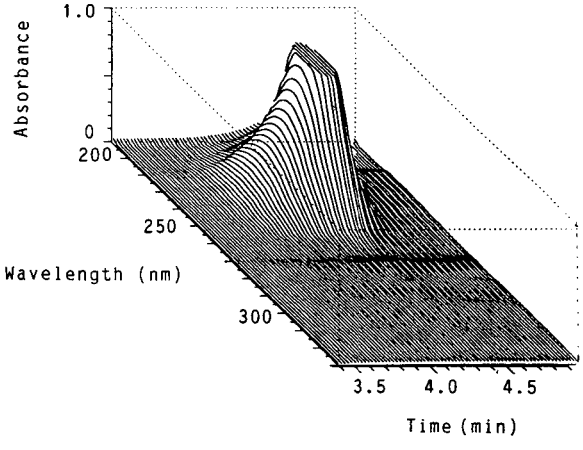

Fig. 8. Three-dimensional HPLC–PDA of synthesized 3-methylcyclopent-2-enone sample.

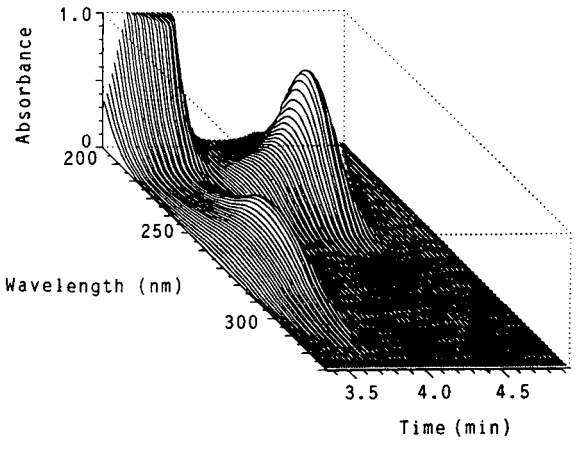

Fig. 9. Three-dimensional HPLC–PDA of Aldrich 2,5-hexanedione sample (12 g/l).

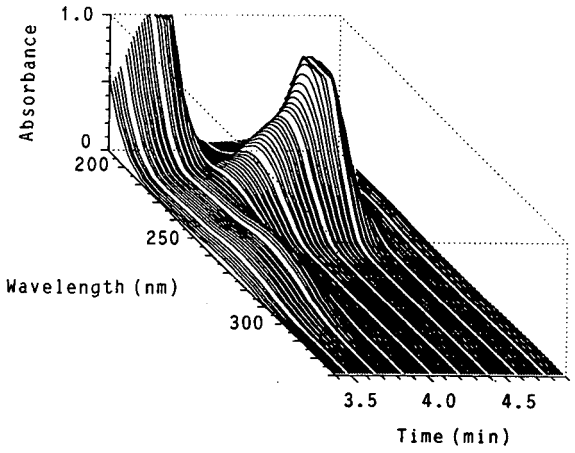

Fig. 10. Three-dimensional HPLC–PDA of synthesized 3-methylcyclopent-2-enone and Aldrich 2,5-hexanedione (12 g/l) mixture (1:1, v/v).

a decrease in the first peak and an increase in the second peak with respect to the above two chromatograms were evident.

Comparison of the HPLC–PDA and GC–MS results for the same sample showed the different instrumental responses for the two compounds (Figs. 2 and 11).

In the HPLC–UV system, the molar absorptivity greatly influenced the response factor of the analyte and therefore a strong signal was associated with a small concentration of 3-MCP owing to its high ε, unlike 2,5-HD. The two values of ε are 18 150 and 123 for 3-MCP and 2,5-HD, respectively [8,14], emphasizing that a 2,5-HD concentration 147 times

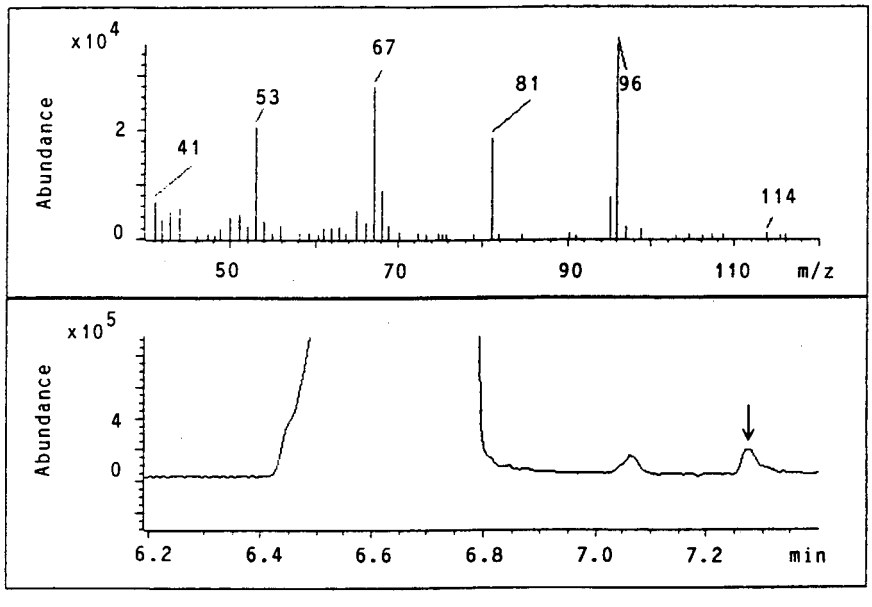

Fig. 11. GC–MS of Aldrich 2,5-hexanedione sample (12 g/l).

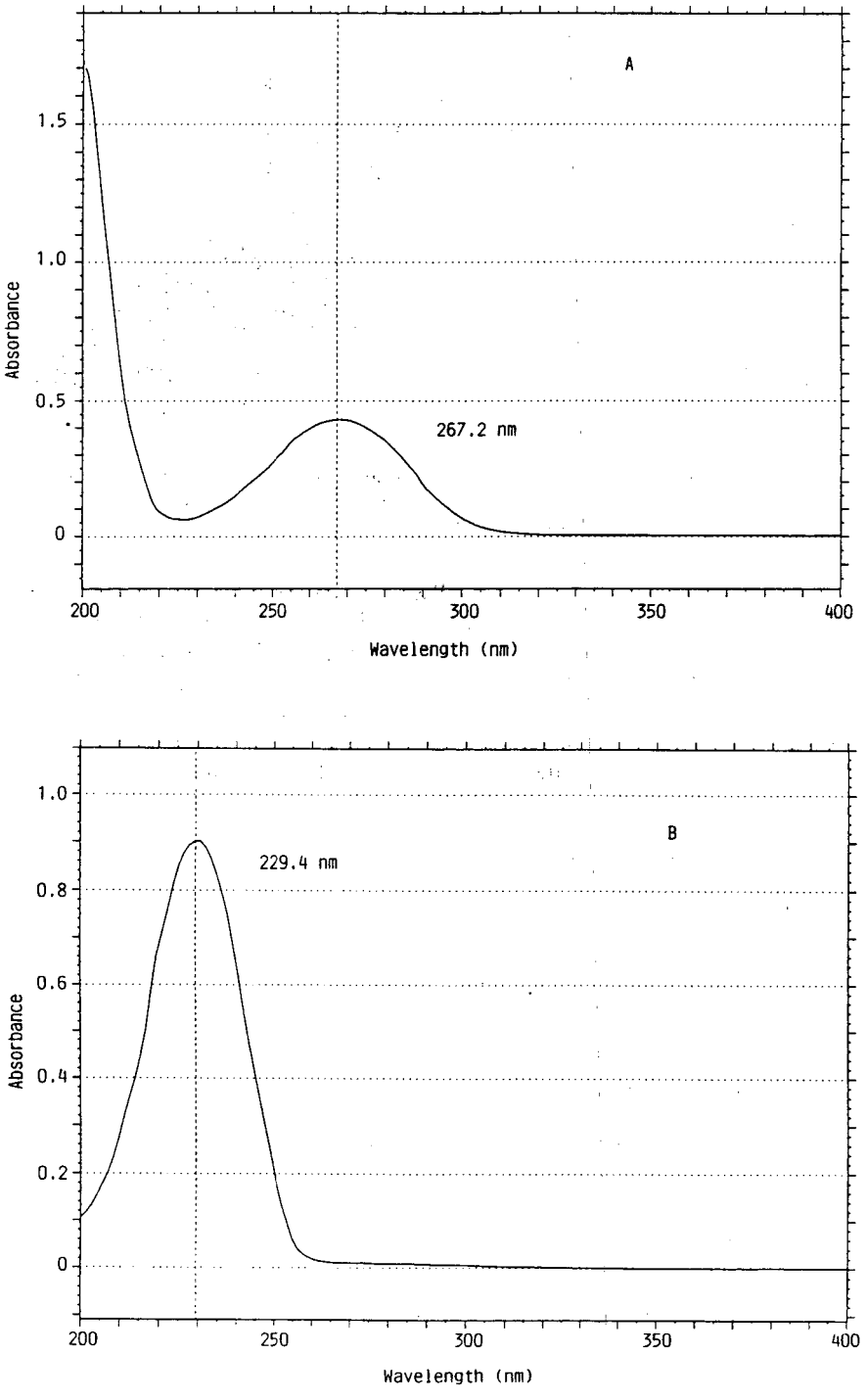

Fig. 12. UV spectra recorded with PDA detector of pure (A) 2,5-hexanedione and (B) 3-methylcyclopent-2-enone and respective wavelengths of maximum absorption.

higher than that of 3-MCP would give rise to two UV chromatographic peaks of similar intensity if measured at the respective absorption maxima.

All the above data allowed the UV spectra shown in Fig. 12A and B to be attributed unequivocally to 2,5-HD and 3-MCP and consequently to establish the correct wavelength for the UV detection of the metabolite, which was found to be 267 nm.

CONCLUSIONS

The use of independent chromatographic and detection techniques allowed the identification of the 3-MCP compound present as an impurity in four different commercial 2,5-HD samples. This compound of high ε may constitute a misleading interference in the UV detection of 2,5-HD in standard solutions and therefore a wavelength of 233 nm does not seem suitable for HPLC–UV analysis because at this value the 2,5-HD is undetectable.

It is the opinion of the authors that any HPLC–UV procedure used to determine directly metabolic 2,5-HD in urine is not a particularly accurate, specific or sensitive method owing to the low molar absorptivity and low concentration levels of the diketone. The HPLC method with UV detection would show a better performance if 2,5-HD underwent a pre- or post-column derivatization by reaction with a specific chromophore so as to increase the molar absorptivity and shift the UV detection window to a range less troubled by the many compounds present in the urine matrix.

REFERENCES

1 C. Cianchetti, G. Abbritti, G. Perticoni, A. Siracusa and F. Curradi, *Br. J. Ind. Med.*, 39 (1976) 1151.
2 L. Perbellini, F. Brugnone and I. Pavan, *Toxicol. Appl. Pharmacol.*, 53 (1980) 220.
3 L. Perbellini, F. Tagliaro, S. Maschio, A. Zedde and F. Brugnone, *Med. Lav.*, 77 (1986) 628.
4 N. Fendtke and H. M. Bolt, *Int. Arch. Occup. Environ. Health*, 57 (1986) 143.
5 A. A. Nomeir and M. B. Abou-Donia, *Anal. Biochem.*, 151 (1985) 381.
6 I. Marchiseppe, M. Valentino, V. Stocchi and M. Governa, *J. Chromatogr.*, 495 (1989) 288.
7 M. Zordan, personal communication.
8 R. M. Acheson and S. R. Robinson, *J. Chem. Soc.*, (1952) 1127.
9 B. S. Furniss *et al.*, *Vogel's Textbook of Practical Organic Chemistry Including Quantitative Organic Analysis*, Longman, Harlow; 4th ed., 1978, p. 1149.
10 B. S. Furniss *et al.*, *Vogel's Textbook of Practical Organic Chemistry Including Quantitative Organic Analysis*, Longman, Harlow, 4th ed., 1978, p. 1232.
11 *NBS/NIH/EPA/MSDC Data Base, MS Libraries*, Hewlett-Packard, Palo Alto, CA, 1988.
12 *Beilstein*, Vol. 7.
13 C. J. Pouchert, *The Aldrich Library of FT-IR Spectra*, Aldrich, Milwaukee, WI, 1st ed., 1985, p. 446.
14 R. C. Weast and M. J. Astle (Editors), *CRC Handbook of Chemistry and Physics*, CRC Press, Boca Raton, FL, 59th ed., 1978, p. C-335.

Journal of Chromatography, 590 (1992) 235–240
Elsevier Science Publishers B.V., Amsterdam

CHROM. 23 748

High-performance liquid chromatographic determination of 2-furaldehyde in spirits

Filippo Lo Coco

Istituto di Chimica, Università di Udine, Via Cotonificio 108, 33100 Udine (Italy)

Luciano Ceccon*

Dipartimento di Economia e Merceologia delle Risorse Naturali e della Produzione, Università di Trieste, Via Valerio 6, 34127 Trieste (Italy)

Clemente Valentini

Laboratorio Chimico Compartimentale delle Dogane di Venezia, Via Ca' Marcello 15, 30172 Mestre (Italy)

Veronica Novelli

Istituto di Chimica, Università di Udine, Via Cotonificio 108, 33100 Udine (Italy)

(First received May 30th, 1991; revised manuscript received September 19th, 1991)

ABSTRACT

Official methods for the determination of 2-furaldehyde in spirits involve for a spectrophotometric evaluation, which is characterized by poor specificity. Gas chromatographic evaluations have also been proposed, which offer a much higher sensitivity, particularly when capillary columns are used. In this paper a high-performance liquid chromatographic (HPLC) method based on the formation of the 2,4-dinitrophenylhydrazones of carbonyl compounds and subsequent reversed-phase separation of these derivatives is described. Derivatization is carried out by utilizing an acidic solution of 2,4-dinitrophenylhydrazine in acetonitrile. Precipitation of the derivatives is avoided, and direct injection of the sample into the HPLC system is allowed. The determination offers a high specificity and a detection limit of the order of 10^{-8} mol/l. Accuracy and reproducibility data are presented.

INTRODUCTION

The determination of 2-furaldehyde (F) in alcoholic beverages represents an interesting goal not only in analytical respects, but also with regard to regulatory implications. Current Italian regulations, for example, fix very strict limits for the presence of F in spirits. They state that F must be absent, or present only in trace amounts, in spirits of both domestic production and import [1]. On the contrary, French regulations state that the lower limit of F allowed in genuine cognac must be 1 g per 100 l of ethanol, corresponding to 4 mg/l of sample [2]. However, F is produced by pentoses during wine and cereal distillation, and also during barrel storage of spirits such as whisky and cognac, and therefore, F is certainly present in these types of products.

The classical method for the determination of F in alcoholic beverages is based on a spectrophotometric evaluation, the only one provided by the official AOAC methods [3]. In this procedure, the UV absorbance of the solution obtained by steam distillation of the sample is measured. This procedure

0021-9673/92/$05.00

is characterized by poor specificity, as other carbonyl compounds present in the sample may contribute to the absorbance [2].

Gas chromatographic procedures have also been proposed; they offer a much higher sensitivity, particularly when capillary columns are used [4,5].

In recent years, high performance liquid chromatographic (HPLC) methods have also been developed based on the determination of F either without derivatization [2,6] or after preparation of a derivative which allows the sensitivity of the method to be improved [7].

In this paper an HPLC method is described that is based on the formation of the 2,4-dinitrophenylhydrazones (DNPH-ones) of carbonyl compounds by addition of an excess of an acidic solution of 2,4-dinitrophenylhydrazine (DNPH) in acetonitrile. The DNPH-ones obtained are then separated by reversed-phase HPLC and determined with spectrophotometric detection.

EXPERIMENTAL

Standards and reagents

2-Furaldehyde (Prolabo) was doubly distilled and kept in a refrigerator at 0–4°C. 2,4-Dinitrophenylhydrazine (Prolabo) was purified by successive crystallizations with HPLC-grade methanol and kept in a refrigerator at 0–4°C. Perchloric acid (70%) was obtained from Prolabo and acetonitrile and absolute ethanol (HPLC-grade) from Carlo Erba. Water was distilled, deionized and then further purified with a Milli-Q system (Millipore).

2,4-Dinitrophenylhydrazine solution. Reagent solution containing 2.5×10^{-3} mol/l of 2,4-dinitrophenylhydrazine was prepared in acetonitrile.

2-Furaldehyde standard solutions. A stock standard solution containing 10^{-2} mol/l of F was prepared in ethanol–water (40:60, v/v). By successive dilutions with the ethanol–water mixture, working standard solutions containing down to 10^{-7} mol/l of F were prepared.

Calibration graph

A 5-ml volume of F working standard solution and 4 ml of DNPH solution were transferred into a 10-ml glass-stoppered volumetric flask, a few drops of perchloric acid were added to pH 2 and the volume was made up to the mark with DNPH solution. The solution was kept on a magnetic stirrer at room temperature for at least 25 min, then 10 μl of the solution were immediately injected into the HPLC system.

Sample preparation

The same procedure described under *Calibration graph* was applied to a 5-ml volume of sample instead of F working standard solution.

Determination of recoveries of 2-furaldehyde

To 2.5 ml of a sample of brandy were added 2.5 ml of F working standard solution containing from 2×10^{-3} down to 2×10^{-7} mol/l of F. The solution obtained was processed as described under *Sample preparation.*

High-performance liquid chromatography

A Spectra-Physics Model 8700 high-performance liquid chromatograph, equipped with a Knauer Model 8700 variable-wavelength spectrophotometric detector and a 10-μl loop, was used. A Supelcosil LC-18 stainless-steel column (250 × 4.6 mm I.D.; film thickness 5 μm) was employed.

Analyses were carried out isocratically at room temperature with acetonitrile–water (65:35, v/v) as eluent at a flow-rate of 1 ml/min. The spectrophotometric detector was set at 388 nm. Peak areas were determined by means of a Spectra-Physics Model 4270 integrator.

RESULTS AND DISCUSSION

Optimization of the derivatization step

In recent years, HPLC has been employed to determine F in several real samples, particularly fruit juices [8–11] and spirits [2,6,7]. The determination may be carried out without preliminary derivatization, but usually the preparation of a derivative is to be preferred. In fact, the selectivity and sensitivity of the method may be enhanced by introducing a suitable chromophore into the molecule [7]. The most widely utilized derivative is the corresponding DNPH-one; it is usually obtained by adding an excess of DNPH aqueous solution in the presence of hydrochloric acid. Nevertheless, the utilization of an acetonitrile DNPH solution offers the advantage of obtaining a solution of the derivative that may be injected directly into the HPLC system [12]. Long

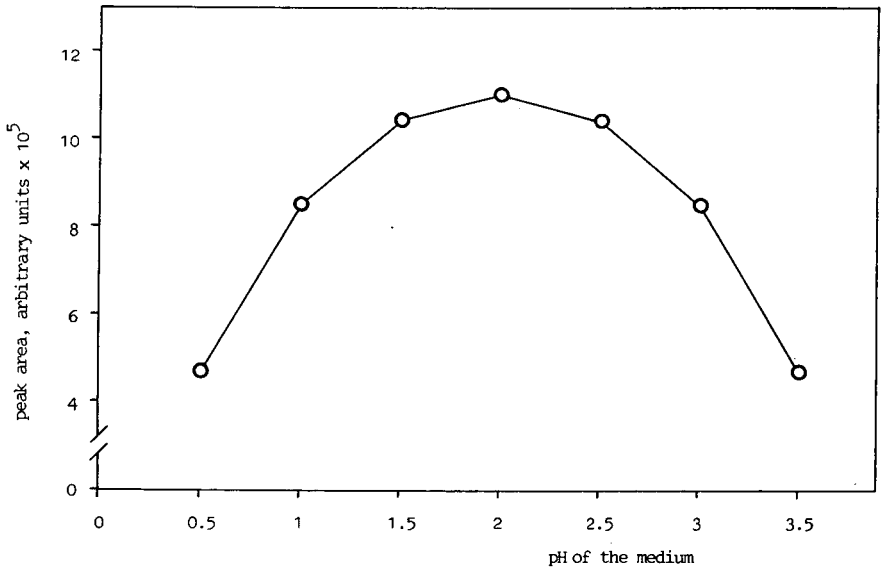

Fig. 1. Conversion of 2-furaldehyde to its 2,4-dinitrophenylhydrazone as a function of the acidity of the medium. 2,4-Dinitrophenylhydrazine-to-2-furaldehyde molar ratio = 2.5; reaction time = 30 min.

and tedious steps, such as filtration and washing of the derivatives obtained in aqueous solution and preparation of a derivative solution in a suitable solvent before the HPLC determination, may therefore be avoided [12]. The use of perchloric acid instead of hydrochloric acid is due to its higher solubility in acetonitrile [12].

In our case, the derivatization step was optimized at room temperature with respect to the DNPH to F molar ratio, the perchloric acid concentration of the medium and the reaction time. For this purpose, the amount of the derivative obtained was evaluated on F standard solutions. The F standard solutions were prepared by employing ethanol–water

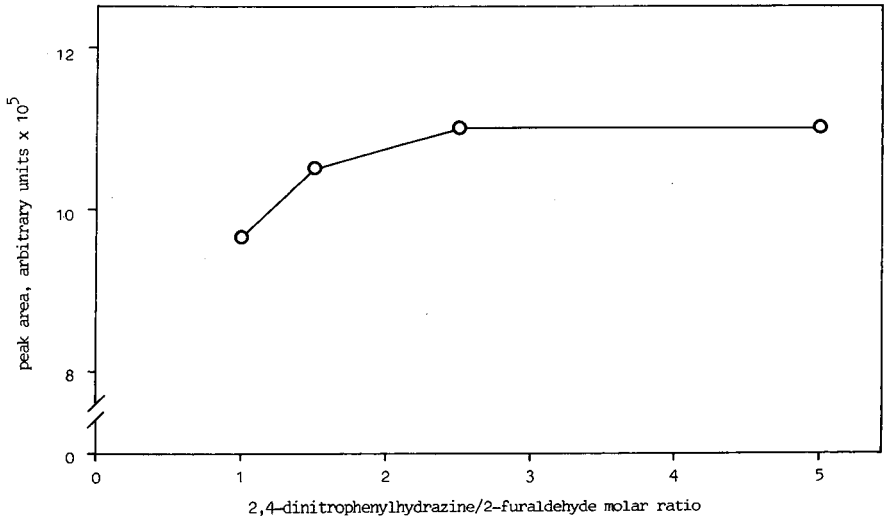

Fig. 2. Conversion of 2-furaldehyde to its 2,4-dinitrophenylhydrazone as a function of the 2,4-dinitrophenylhydrazine-to-2-furaldehyde molar ratio. pH of the medium = 2; reaction time = 30 min.

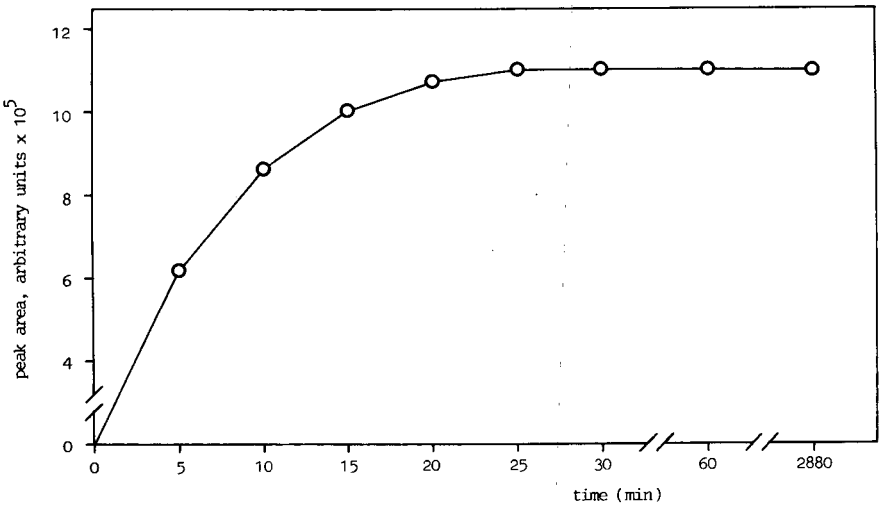

Fig. 3. Conversion of 2-furaldehyde to its 2,4-dinitrophenylhydrazone as a function of reaction time. 2,4-Dinitrophenylhydrazine-to-2-furaldehyde molar ratio = 2.5; pH of the medium = 2.

(40:60, v/v). This mixture simulates natural matrices as much as possible. The results obtained are shown in Figs. 1–3.

As can be seen, the reaction is quantitative when the reagent to analyte ratio is at least 2.5:1 and the acidity of the medium, as evaluated with a pH meter, is about 2. Under these conditions, F is quantitatively converted into its DNPH-one within 25 min. A similar result was obtained previously by Selim [13] for the derivatization of propionaldehyde. The derivative obtained is stable at room temperature for at least 48 h.

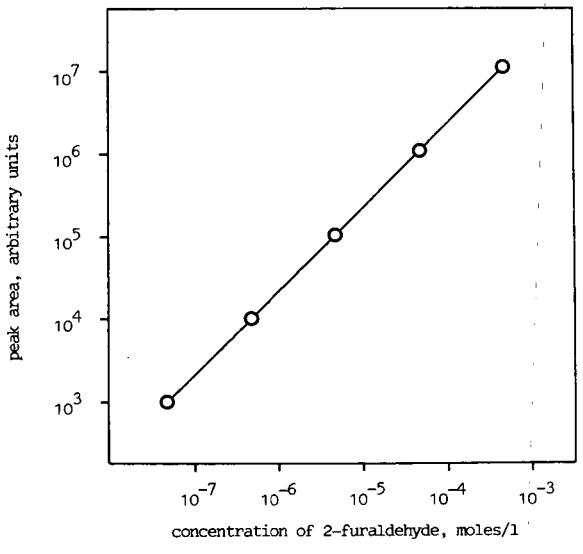

Fig. 4. Calibration graph of peak area of the 2,4-dinitrophenylhydrazone of 2-furaldehyde *versus* concentration of 2-furaldehyde. 2,4-Dinitrophenylhydrazine-to-2-furaldehyde molar ratio = 2.5; pH of the medium = 2; reaction time = 30 min.

Calibration

The calibration graph was obtained by employing standard solutions of F under optimum experimental conditions as described in the preceding section, and is shown in Fig. 4. A straight line was obtained over a wide range of examined concentrations, which represent values typically found in real samples. By setting the detector wavelength at the maximum absorbance of the F derivative, it is possible to determine the detection limit as $3\sigma/S$ [14], where S is the sensitivity, which is $2.23 \cdot 10^{10}$ as obtained from the calibration graph, and σ is the peak threshold of the integrator, which was set by us at 100. The detection limit is therefore $1.3 \cdot 10^{-8}$ M.

Specificity, recovery and reproducibility

The method shows a high specificity because, under the described conditions, the F derivative is well separated with respect to the other carbonyl compounds present in the sample under examination. As an example, Fig. 5 shows a typical separation

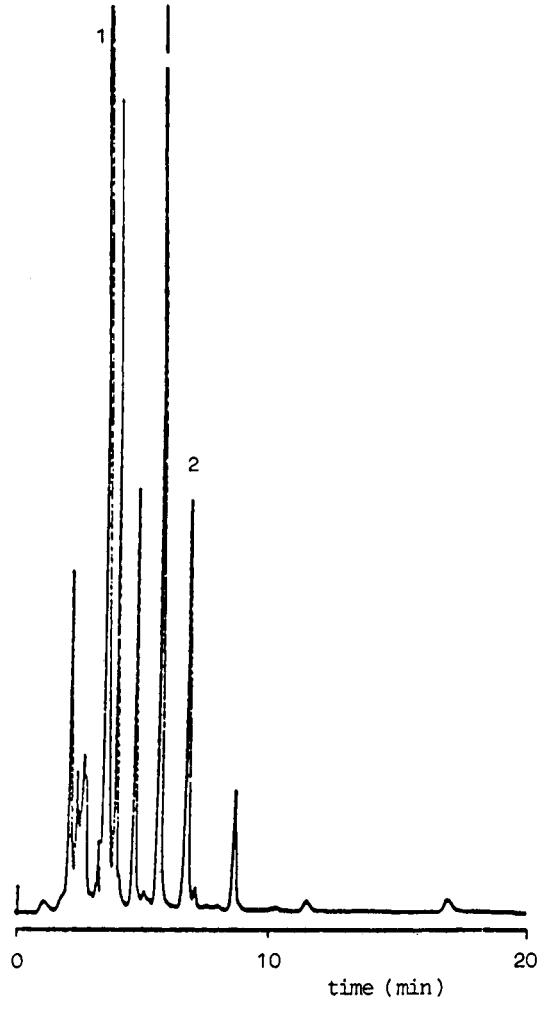

Fig. 5. HPLC separation of the 2,4-dinitrophenylhydrazones of carbonyl compounds from a sample of whisky. For conditions, see Experimental. Peaks: 1 = 2,4-dinitrophenylhydrazine; 2 = 2,4-dinitrophenylhydrazone of 2-furaldehyde.

obtained on a sample of a 12-year-old whisky. DNPH must be at least 20 times more concentrated than the analyte to be determined in the analyses of real samples, as an aliquot of the reagent is employed in the derivatization of the other carbonyl compounds present, in particular of acetaldehyde. In all the samples so far examined, a 1:20 ratio between F and DNPH was sufficient, as a large peak of the DNPH excess appears in the chromatogram.

Recovery was evaluated by adding different levels of F to a sample of brandy. The sample was selected on the basis of its low F content ($4.4 \cdot 10^{-7}$ mol/l), one of the lowest levels among those which we found in real samples. The results obtained are shown in Table I. Recoveries ranged from 98 to 100%.

TABLE I

RECOVERY OF 2-FURALDEHYDE ADDED TO BRANDY

Concentration of 2-furaldehyde (mol/l)			
Originally present	Added	Found	Recovery (%)
$2.2 \cdot 10^{-7}$	$1.0 \cdot 10^{-7}$	$3.2 \cdot 10^{-7}$	100
$2.2 \cdot 10^{-7}$	$1.0 \cdot 10^{-6}$	$1.21 \cdot 10^{-6}$	99
$2.2 \cdot 10^{-7}$	$1.0 \cdot 10^{-5}$	$1.00 \cdot 10^{-5}$	98
$2.2 \cdot 10^{-7}$	$1.0 \cdot 10^{-4}$	$9.91 \cdot 10^{-5}$	99
$2.2 \cdot 10^{-7}$	$1.0 \cdot 10^{-3}$	$9.92 \cdot 10^{-4}$	99

Reproducibility was evaluated by carrying out the determination six times on the same sample of whisky over a period of 48 h. The average concentration of F was $5.6 \cdot 10^{-5}$ mol/l, with a standard deviation of $1.6 \cdot 10^{-6}$ mol/l and a relative standard deviation of 2.78%.

Application

The procedure was applied to the determination of F in different spirits and the results are summarized in Table II. F was found in higher concentrations in samples such as cognac and whisky, that is, samples usually stored in barrels.

TABLE II

CONCENTRATIONS OF 2-FURALDEHYDE FOUND IN SOME SPIRITS

Spirit	Concentration of 2-furaldehyde (mol/l)	Spirit	Concentration of 2-furaldehyde (mol/l)
Cognac 1	$1.2 \cdot 10^{-5}$	Brandy 2	$4.4 \cdot 10^{-7}$
Cognac 2	$1.5 \cdot 10^{-5}$	Vodka 1	$8.9 \cdot 10^{-7}$
Cognac 3	$6.3 \cdot 10^{-5}$	Vodka 2	$1.1 \cdot 10^{-6}$
Cognac 4	$3.9 \cdot 10^{-5}$	Whisky 1	$5.6 \cdot 10^{-5}$
Brandy 1	$2.8 \cdot 10^{-6}$	Whisky 2	$7.9 \cdot 10^{-5}$

REFERENCES

1 Ministerial Decree (August 3, 1983), *Official Gazette of the Republic of Italy*, 240 (September 1, 1983) 7077.
2 H. J. Jeuring and F. J. E. M. Kuppers, *J. Assoc. Off. Anal. Chem.*, 63 (1980) 1215.
3 *Official Methods of Analysis of the Association of Official Analytical Chemists*, AOAC, Arlington, VA, 15th ed., 1990, Sec. 960.16.
4 M. Masuda, M. Yamamoto and Y. Asakura, *J. Food Sci.*, 50 (1985) 264.
5 K. MacNamara, *J. High Resolut. Chromatogr. Chromatogr. Commun.*, 7 (1984) 641.
6 H. E. Frischkorn, M. Wanderley-Casado and C. G. B. Frischkorn, *Z. Lebensm.-Unters.-Forsch.*, 174 (1982) 117.
7 E. Puputti and P. Lehtonen, *J. Chromatogr.*, 353 (1986) 163.
8 J. E. Marcy and R. L. Rouseff, *J. Agric. Food Chem.*, 32 (1984) 979.
9 S. Bloeck, A. Kreis and O. Stanek, *Alimenta*, 25 (1986) 23.
10 H. S. Lee, R. L. Rouseff and S. Nagy, *J. Food Sci.*, 51 (1986) 1075.
11 Z.-F. Li, M. Sawamura and H. Kusunose, *Agric. Biol. Chem.*, 52 (1988) 2231.
12 F. Lipari and S. J. Swarin, *J. Chromatogr.*, 247 (1982) 297.
13 S. Selim, *J. Chromatogr.*, 136 (1977) 271.
14 D. L. Massart, A. Dijkstra and L. Kaufman, *Evaluation and Optimization of Laboratory Methods and Analytical Procedures*, Elsevier, Amsterdam, 1978.

Journal of Chromatography, 590 (1992) 241–245
Elsevier Science Publishers B.V., Amsterdam

CHROM. 23 766

Specific detection of acetyl-coenzyme A by reversed-phase ion-pair high-performance liquid chromatography with an immobilized enzyme reactor

Susumu Yamato*, Masaharu Nakajima, Hiroyuki Wakabayashi and Kenji Shimada

Department of Analytical Chemistry, Niigata College of Pharmacy, 5-13-2 Kamishin'ei-cho, Niigata 950-21 (Japan)

(First received July 2nd, 1991; revised manuscript received September 25th, 1991)

ABSTRACT

A selective chromatographic detection system for the determination of acetyl-coenzyme A (CoA) is reported. The short-chain acyl-CoA thioesters were separated by reversed-phase ion-pair high-performance liquid chromatography (HPLC), and then acetyl-CoA was selectively detected on-line with an immobilized enzyme reactor (IMER) as a post-column reactor. Thio-CoA liberated enzymatically from acetyl-CoA was determined spectrophotometrically after reaction with Ellman's reagent in the reagent stream. The IMER with phosphotransacetylase had a substrate specificity sufficient to determine acetyl-CoA and was active and stable in the mobile phase containing methanol and the ion-pair reagent. The calibration graph was linear between 0.2 and 10 nmol, with a detection limit of 0.05 nmol. This HPLC system with detection by IMER allows the selective identification and determination of acetyl-CoA in a mixture of acetoacetyl-CoA and 3-hydroxy-3-methylglutaryl-CoA, which are difficult to separate with ion-pair HPLC.

INTRODUCTION

Owing to the significance of coenzyme A (CoA) and its thioesters in metabolic regulation, several modifications of the reversed-phase high-performance liquid chromatographic (HPLC) method with ultraviolet (UV) detection for determining short-chain acyl-CoA esters have been published [1–6]. Acetyl-CoA plays an important role as the acetyl donor in the biosynthesis of acetylcholine, acetyl-L-carnitine and *N*-acetylserotonin. Working with an analytical approach for determining acetyl-CoA, a rapid and reliable flow injection technique has been reported with immobilized phosphotransacetylase (PTA) as a catalytic reactor [7].

Immobilized enzyme reactors (IMERs) are powerful analytical tools in flow injection analysis (FIA), with high selectivity and economy [8]. The application of IMERs for reaction detection systems in HPLC is another application in the analytical flow mode [9–11]. Although the on-line combination of HPLC separation and detection with an IMER provides high sensitivity and analytical selectivity, the effect on the activity and stability of the IMER towards organic modifiers in the mobile phase must be taken into consideration. Bowers and co-workers [9,12] examined the effect of the organic solvents methanol, ethanol, acetonitrile and ethylene glycol on immobilized β-glucuronidase, and observed that the organic modifiers in the mobile phase exert a reductive effect on the activity and stability of the immobilized enzyme.

In a previous paper, it was reported that immobilized PTA has a marked stability to changes in temperature and methanol concentration, and it has been shown that immobilized PTA retains its activity even in 60% methanol [7]. In this study, immobilized PTA was used in a post-column reaction detection system in HPLC, and this paper discusses the usefulness of this HPLC system with detection by IMER, that is, the selective determination of acetyl-CoA in a mixture of short-chain acyl-CoA esters.

0021-9673/92/$05.00

EXPERIMENTAL

Materials

CoA, acetyl-CoA and other acyl-CoA esters were obtained from Sigma (St. Louis, MO, USA). PTA (acetyl-CoA:orthophosphate acetyltransferase, EC 2.3.1.8, 11 660 U/mg of protein) from *Bacillus stearothermophilus* was purchased from Seikagaku Kogyo (Tokyo, Japan), 5,5′-dithiobis (2-nitrobenzoic acid) (DTNB; Ellman's reagent) and glutathione (reduced) from Wako (Osaka, Japan) and AF-Tresyl Toyopearl 650 gel ($-CH_2OSO_2CH_2CF_3$ residue; 100 μmol/g of dry gel) from Tosoh (Tokyo, Japan). The ion-pairing reagent, tetra-*n*-butylammonium phosphate (TBAP), was from Nacalai Tesque (Kyoto, Japan). HPLC-grade methanol was purchased from Kanto Chemical (Tokyo, Japan).

Immobilized enzyme reactor

The detailed procedure for the preparation of immobilized PTA has been described previously [7]. The immobilized PTA was packed into a stainless-steel column (10 × 4 mm I.D.) and used as the IMER for FIA and HPLC. The active groups of the gel (AF-Tresyl Toyopearl 650) without enzyme to be bonded were entirely blocked with 0.1 *M* Tris–HCl buffer (pH 8.0) containing 0.5 *M* sodium chloride. The gel was then packed into another column of the same size and was used as a blank column.

Apparatus and procedures

The flow system for the FIA mode was almost the same as that reported previously [7], except that a blank column was constructed, as shown in the upper panel of Fig. 1. The carrier stream [30 m*M* Na_2HPO_4 as the substrate, 15 m*M* $(NH_4)_2SO_4$ as the enzyme activator and 0.1 m*M* DTNB as the colour-producing reagent in 0.1 *M* borate buffer (pH 7.5)] was pumped by a Shimadzu LC-6A pump (Kyoto, Japan) at a flow-rate of 1 ml/min. A 25-μl sample was introduced into the carrier stream through a Rheodyne Model 7125 injector (Cotati, CA, USA) with a 100-μl sample loop. CoA enzymatically liberated from acetyl-CoA by passage through the IMER was reacted with DTNB in the carrier stream. The columns with PTA [IMER, E(+)] and without PTA [the blank column, E(−)] were thermostated in an oven (CTO-6A, Shimadzu); the mixing coil tubing was 35 cm × 0.25 mm I.D. The six-port switching valve (FCV-2AH, Shimadzu), controlled by a system controller (SCL-6A, Shimadzu), was used for column switching. The change in absorbance at 412 nm was monitored with a spectrophotometer (SPD-6AV, Shimadzu) equipped with an 8-μl flow cell. The chromatogram and integration were obtained with an integrator (C-R4A, Shimadzu). A trace amount of DTNB-reactive thiol compounds in the samples was corrected by subtracting the peak height or peak area obtained with the blank column, E(−), from those obtained with the IMER, E(+). The HPLC mode with the IMER detection system used is shown in the lower panel of Fig. 1.

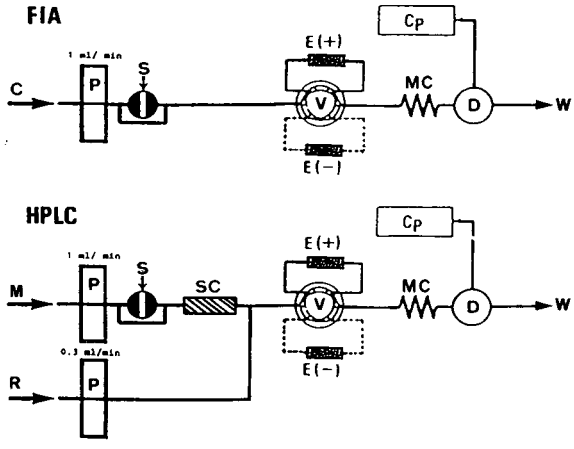

Fig. 1. Schematic diagrams of the FIA and HPLC systems with IMER detection. P = pump; S = sample injector; SC = separation column; V = switching valve; MC = mixing coil; D = detector; Cp = computing integrator; M = mobile phase; R = reagent solution; E(+) = immobilized enzyme column; E(−) = blank column without immobilized enzyme.

An analytical column (15 cm × 6 mm I.D., Capcell Pak C_8, SG type, 5-μm particle, Shiseido, Tokyo, Japan) was used in the FIA flow mode described above. The mobile phase was pumped by a Shimadzu LC-6A pump at a flow-rate of 1 ml/min, and sample solutions of 25 μl were injected through a Rheodyne injector. After the separation of the compounds on the analytical column at ambient temperature, the reagent solution or distilled water was introduced through a T-piece with an another pump (LC-6A, Shimadzu) at a flow-rate of 0.3 ml/min. When the distilled water was pumped in, the column effluent was monitored by UV absorption

at 254 nm. When the reagent solution containing the enzyme substrate, the enzyme activator and the colour-producing reagent were introduced to the flow, the absorbance was monitored at 412 nm.

Preparation of mobile phase and reagent solution

The mobile phase solvents consisted of the ion-pairing reagent (TBAP) and methanol. Two mixtures, namely, 2 m*M* TBAP (pH 6.4) in methanol–water (42:58) and 2 m*M* TBAP (pH 6.5) in methanol–water (45:55), were used throughout this study. The pH was adjusted with 1% H_3PO_4. The solvents were filtered through 0.4-μm pore size filters (Fuji Photo Film, Tokyo, Japan) and degassed. The concentration of the reagent solution used for the HPLC system with IMER detection was twice that of the carrier stream, *i.e.* the reagent solution contained 60 m*M* Na_2HPO_4, 30 m*M* $(NH_4)_2SO_4$ and 0.2 m*M* DTNB in 0.2 *M* borate buffer, pH 7.5.

RESULTS AND DISCUSSION

Effects of ion-paired reagent and methanol on IMER activity

The reversed-phase ion-pair chromatographic (RP-IPC) technique using the ion-pairing reagent TBAP and methanol reported by Baker and Schooley [2,6] provided a rapid isocratic separation of CoA, acetyl-CoA and other acyl-CoA thioesters. If our immobilized PTA is used as the IMER in a RP-IPC system, it is necessary to evaluate the level of the enzymatic activity of the IMER in the presence of TBAP and methanol. The effects of the concentrations of TBAP and/or methanol on the IMER activity were examined using the FIA flow system and the carrier stream, as described under *Apparatus and procedures*. The TBAP had no inhibiting or acitvating effect on the IMER at concentrations less than 4 m*M* in the carrier tested. The effects of methanol on the IMER activity were studied in the presence of 2 m*M* TBAP. A decrease in the relative response with an increasing concentration of methanol was observed. When the carrier stream contained 2 m*M* TBAP and 25% methanol, the enzymatic activity of the IMER was 65% of its original level. This decreased effect was assumed (as reported earlier) not to be enzyme inactivation but to result from a decrease in the rate of the enzymatic reaction [7].

Substrate specificity of the IMER

The enzyme specificity of the IMER was also examined using the FIA flow system, in which the formation of CoA from a series of related acyl-CoAs at a concentration of 2.5 nmol per 25-μl injection was measured. The activities obtained from peak-area and peak-height measurements were corrected by subtracting the values with the blank column from those with the IMER; the relative responses are given in Table I.

The IMER, as far as tested, can catalyse the transfer reaction of acetyl-CoA, propionyl-CoA and isobutyryl-CoA. Other acyl-CoAs were not catalysed. When the acetyl-CoA of the substrate was injected together with acetoacetyl-CoA and 3-hydroxy-3-methylglutaryl-CoA (HMG-CoA), with 2.5 nmol of each component per 25-μl injection, no inhibitory activity was observed. These results show that neither acetoacetyl-CoA nor HMG-CoA had any competitive effect against the catalytic reaction of the IMER for acetyl-CoA.

Chromatographic separation and specific detection of acetyl-CoA

The separation of CoA and other acyl-CoA esters was performed with a reversed-phase ion-paired

TABLE I

ENZYMATIC ACTIVITY OF IMMOBILIZED ENZYME REACTOR (IMMOBILIZED PHOSPHOTRANSACETYLASE)

Enzymatic activity was measured using the FIA flow system. Samples contained 2.5 nmol of each ingredient per 25-μl injection. Each value is expressed as the mean of five experiments. A trace amount of DTNB-reactive thiol compounds in the samples was corrected. See text for details.

Sample	Relative activity (%)	
	Peak area	Peak height
Acetyl-CoA	100	100
Acetoacetyl-CoA	0.7	0.9
3-Hydroxy-3-methylglutaryl-CoA (HMG-CoA)	0	0
Propionyl-CoA	96.4	96.5
n-Butyryl-CoA	0.3	0.6
Isobutyryl-CoA	16.8	17.1
Acetyl-CoA + acetoacetyl-CoA	101.5	99.2
Acetyl-CoA + HMG-CoA	99.3	100.9
Acetyl-CoA + acetoacetyl-CoA + HMG-CoA	100.5	98.7

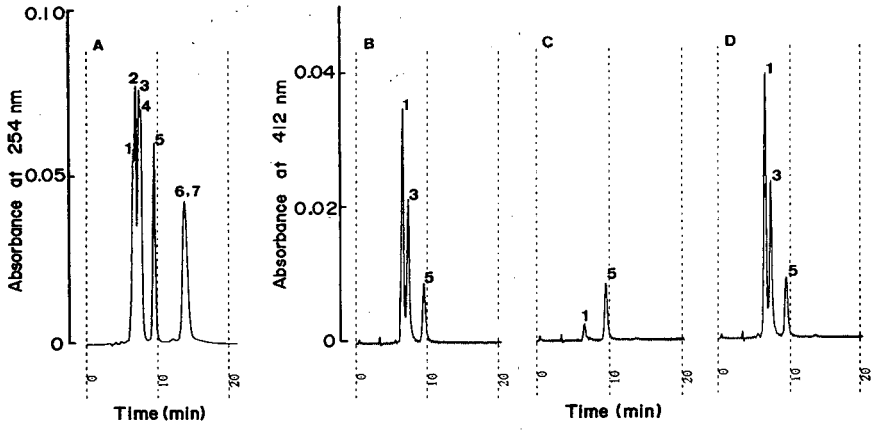

Fig. 2. Chromatograms of reversed-phase ion-pair HPLC with (A) ultraviolet detection at 254 nm and (B)–(D) visible detection at 412 nm. Samples comprised mixtures of acyl-CoAs at a concentration of 2.5 nmol per 25-μl injection. Samples in (A) and (D) contained CoA, acetyl-CoA, acetoacetyl-CoA, HMG-CoA, propionyl-CoA, *n*-butyryl-CoA and isobutyryl-CoA; in (B), CoA, acetyl-CoA, propionyl-CoA and *n*-butyryl-CoA; and in (C), acetoacetyl-CoA, HMG-CoA, propionyl-CoA and isobutyryl-CoA. Peaks: 1 = CoA; 2 = acetoacetyl-CoA; 3 = acetyl-CoA; 4 = HMG-CoA; 5 = propionyl-CoA; 6 = isobutyryl-CoA; 7 = *n*-butyryl-CoA. Mobile phase, 0.002 *M* TBAP, pH 6.4, in methanol–water (42:58).

system. The mobile phase was pumped at a flow-rate of 1.0 ml/min and distilled water was introduced through a T-piece with another pump at a flow-rate of 0.3 ml/min. The column effluent was monitored at 254 nm. The separation conditions onto a Capcell Pak C_8 column were selected on the basis of the excellent results reported previously, for which 50 m*M* TBAP was used [6]. TBAP is an expensive and corrosive reagent, so its concentration was reduced to 2 m*M*. At this low TBAP concentration, acetyl-CoA was weakly adsorbed to the column, and was therefore readily eluted from the column with the lower methanol concentration. The lower methanol concentration was also favourable for the functioning of the IMER. At the lower pH, acetyl-CoA had a long retention time, but, at pH values below 5.5, the activity and the stability of the IMER were decreased. Consequently, a mobile phase was selected consisting of 2 m*M* TBAP (pH 6.4) in methanol–water (42:58).

A typical chromatogram of a mixture of acyl-CoA esters monitored at 254 nm is shown in Fig. 2A. Although CoA and the six acyl-CoA esters in the samples were eluted within 15 min, the resolution of acetyl-CoA (peak 3) from acetoacetyl-CoA (peak 2) and HMG-CoA (peak 4) presented considerable difficulties. Isobutyryl-CoA and *n*-butyryl-CoA (peaks 6 and 7) were co-eluted. The pumping of distilled water was replaced with reagent solution pumping, and the column effluent passing through the IMER was monitored at 412 nm. As Fig.2 B–D shows, the IMER could selectively detect acetyl-CoA (peak 3) and propionyl-CoA (peak 5), but not the other acyl-CoA esters. This selective detection is in accord with the data shown in Table I. Peak 1 in Fig. 2C, which has a retention time corresponding to CoA, is assumed to be the contamination or degradation product originating from acetoacetyl-CoA.

Quantitative chromatograms were obtained by injecting samples containing various amounts of acetyl-CoA (peak 3) in a definite amount of glutathione (peak 1) and CoA (peak 2). As shown in Figs. 3A–E, the peak of acetyl-CoA increased linearly with increasing amounts of acetyl-CoA injected into the HPLC system with IMER detection. In contrast, when the sample solution identical with that used in Fig. 3D was injected into the system and the blank column was used in place of the IMER, no acetyl-CoA peak was detected (Fig. 3F).

Calibration graph, precision and stability

A calibration graph for acetyl-CoA, obtained by measurement of the peak area, was linear over the range 0.2–10 nmol per 25-μl injection. The detection limit was 0.05 nmol at a signal-to-noise ratio of

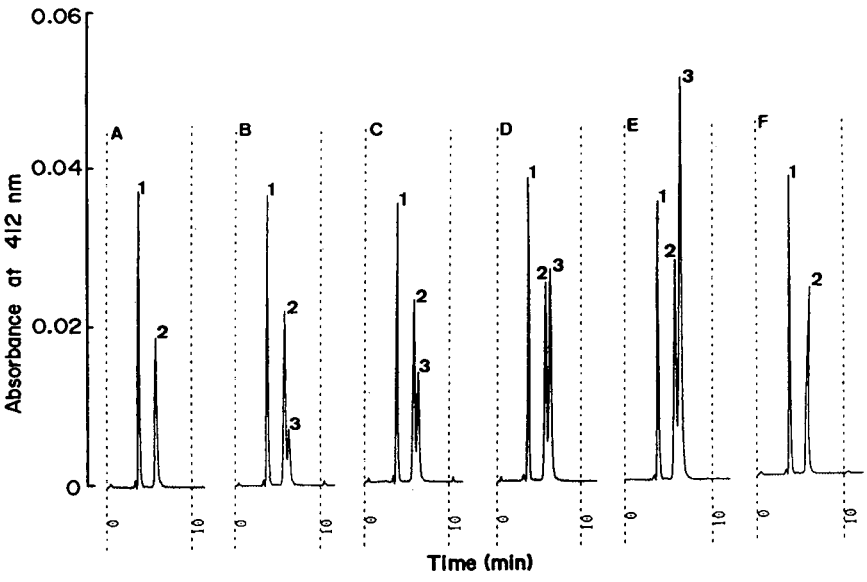

Fig. 3. Typical chromatograms for the selective determination of acetyl-CoA using the HPLC system with IMER detection. Samples comprised various amounts of acetyl-CoA: (A) none; (B) 0.625 nmol per 25-μl injection; (C) 1.25 nmol per 25-μl injection; (D) 2.5 nmol per 25-μl injection; (E) 5 nmol per 25-μl injection; (F) 2.5 nmol per 25-μl injection, each in a definite amount of glutathione (1 nmol per 25-μl injection) and CoA (1.25 nmol per 25-μl injection). Peaks: 1 = glutathione; 2 = CoA; 3 = acetyl-CoA. Mobile phase, 0.002 *M* TBAP, pH 6.5, in methanol–water (45:55).

3. The regression equations and the correlation coefficients (r) were $y = 233.38x - 8.81$, $r = 0.9994$ ($n = 30$) for peak area (mV · S) and $y = 9.63x + 0.21$, $r = 0.9987$ ($n = 30$) for peak height (mV). The intra-assay relative standard deviation (R.S.D.) was 2.8% (1 nmol per 25-μl injection, $n = 9$). The IMER retained 80–85% of its original activity after 1 month with repeated use for 5 h per day, even using in the organic modifier (methanol) at 40°C.

The HPLC system with IMER detection described here provides a simple, rapid and selective method for determining acetyl-CoA. The sensitivity should be further increased if a thiol-specific electrochemical detection system [13,14] is used.

ACKNOWLEDGEMENT

We thank Ms. J. Takigawa for her assistance in the early stages of this work.

REFERENCES

1 M. T. King, P. D. Reiss and N. W. Cornell, *Methods Enzymol.* 166 (1988) 70.
2 F. C. Baker and D. A. Schooley, *Methods Enzymol.* 72 (1981) 41.
3 B. E. Corkey, M. Brandt, R. J. Williams and J. R. Williamson, *Anal. Biochem.*, 118 (1981) 30.
4 N. Takeyama, D. Takagi, K. Adachi and T. Tanaka, *Anal. Biochem.*, 158 (1986) 346.
5 R. E. Dugan, M. J. Schmidt, G. E. Hoganson, J. Steele, B. A. Gilles and A. L. Shug, *Anal. Biochem.*, 160 (1987) 275.
6 F. C. Baker and D. A. Schooley, *Anal. Biochem.*, 94 (1979) 417.
7 S. Yamato and K. Shimada, *Anal. Chim. Acta*, 232 (1990) 281.
8 J. Ruzicka and E. H. Hansen, *Flow Injection Analysis*, Wiley, New York, 2nd ed., 1988.
9 L. D. Bowers, in I. S. Krull (Editor), *Reaction Detection in Liquid Chromatography*, Marcel Dekker, New York, 1986, Ch. 4, p. 195.
10 H. Jansen and R. W. Frei, in K. Zech and R. W. Frei (Editors), *Selective Sample Handling and Detection in High-Performance Liquid Chromatography, Part B*, Elsevier, Amsterdam, 1989, Ch. 5, p. 208.
11 K. Shimada, T. Oe and T. Nambara, *J. Chromatogr.*, 492 (1989) 345.
12 L. D. Bowers and P. R. Johnson, *Biochim. Biophys. Acta*, 661 (1981) 100.
13 R. Saetre and D. L. Rabenstein, *Anal. Chem.*, 50 (1978) 276.
14 J. P. Richie and C. A. Lang, *Anal. Biochem.*, 163 (1987) 9.

Journal of Chromatography, 590 (1992) 247–253
Elsevier Science Publishers B.V., Amsterdam

CHROM. 23 751

Purification of pro- and eukaryotic superoxide dismutases by charge-controlled hydrophobic chromatography

Marlis Grunow and Wulfdieter Schöpp*

Bereich Biochemie der Sektion Biowissenschaften, Universität Leipzig, Talstrasse 33, O-7010 Leipzig (Germany)

(First received May 17th, 1991; revised manuscript received September 17th, 1991)

ABSTRACT

The process of purifying superoxide dismutases was simplified using charge-controlled hydrophobic chromatography on 10-carboxydecyl Sepharose. In only one chromatographic step following ammonium sulphate precipitation, Fe-containing superoxide dismutase from *Pseudomonas putida* and Cu,Zn-containing superoxide dismutase from bovine erythrocytes were purified with an overall yield of about 70% to electrophoretic homogeneity. The specific activities of the crystalline enzyme preparations were expressed in McCord and Fridovich units and were 3000 and 3200 U/mg, respectively.

INTRODUCTION

Superoxide dismutase (SOD, EC 1.15.1.1) catalyzes the disproportionation of superoxide anion radical ($O_2^{\cdot-} + O_2^{\cdot-} + 2H^+ \rightarrow H_2O_2 + O_2$) to protect cells from oxygen toxicity caused by superoxide and other species of oxygen derived from it. This important enzyme is found in nearly all aerobic organisms as well as in some anaerobic ones. SODs are classified by their prosthetic metal into Cu, Zn-, Fe- and Mn-containing enzymes. Cu,Zn-SOD is localized mainly in the cytosol of eukaryotes and presents an independent line of descent. Different in structure from this type are the Fe- and Mn-SODs, which are present in prokaryotes; the latter are also present in mitochondria (for a review see ref. 1).

Owing to their broad distribution, SODs have been isolated and characterized from many organisms. With only a few exceptions [2–7] the described purification techniques conventionally involve ammonium sulphate fractionation, ion-exchange chromatography and gel filtration. Usually more than five steps are necessary to obtain homogeneous enzyme.

Because of the experimental and therapeutic importance, particularly of Cu,Zn-SOD, simple isolation procedures with high yields are of great practical interest.

In 1976 we reported on a special type of hydrophobic chromatography using 10-carboxydecyl Sepharose (CD-Sepharose) as a support [8]. The coupled ligand first implied that this Sepharose derivative specifically binds enzymes with hydrophobic active centers, such as alcohol dehydrogenase [8]. However, further investigations have shown that other oxidoreductases as well as enzymes of other classes, including transferases, lyases and hydrolases, can also be adsorbed to CD-Sepharose [9]. These data offer the possibility of expanding the use of this technique to the purification of pro- and eukaryotic SODs.

EXPERIMENTAL

Reagents

The sources of chemicals were as follows: xanthine oxidase, bovine serum albumin, xanthine and Coomassie brilliant blue G250, Serva (Heidelberg, Germany); cytochrome c, Biomed (Krakow, Poland); 11-aminoundecanoic acid, Fluka (Buchs, Switzerland); nitroblue tetrazolium chloride (NBT), Chemapol (Prague, Czechoslovakia); riboflavin,

0021-9673/92/$05.00

Reanal (Budapest, Hungary); Sepharose 4B, Pharmacia (Uppsala, Sweden).

The chemicals for the electrophoretic experiments were products of Ferak (Berlin, Germany).

CD-Sepharose was prepared as described previously [8].

Enzyme assay and electrophoresis

SOD activity was measured by the xanthine/xanthine oxidase/cytochrome c assay of McCord and Fridovich [10] using a Beckman DK 2A spectrophotometer. Enzymatic activity is shown in McCord and Fridovich units [10].

Polyacrylamide gel electrophoresis on 8% gels was performed according to Davies [11]. Zones of protein were localized by staining with Coomassie brilliant blue G250 [12]. The detection of enzyme activity on the gels was carried out by the photochemical procedure of Beauchamp and Fridovich [13]. Sodium dodecylsulphate polyacrylamide gel electrophoresis (SDS-PAGE) was performed by the method of Weber and Osborn [14].

Determination of protein concentration

The method of Kalb and Bernlohr [15] was employed for the determination of protein concentration. In the case of the purified enzyme solutions the protein concentration was determined according to the method of Lowry *et al.* [16] with bovine serum albumin as standard.

Purification procedure

Prokaryotic SOD was purified using the Fe-containing enzyme of a *Pseudomonas putida* strain [17]. Eukaryotic Cu,Zn-SOD was isolated from bovine erythrocytes.

Pseudomonas putida BL 1 was grown on *n*-hexane as a carbon source as previously reported [18]. Cells were collected by centrifugation and suspended in 0.05 *M* sodium phosphate buffer pH 7.0 to obtain an optical density of A_{600} (1 cm) = 20. This suspension was cooled to −80°C and held at this temperature for about 4 h. Thawing was performed at 30°C. After 2 h of incubation at the same temperature cell debris was removed by centrifugation at 13 000 *g* for 30 min. Almost all the SOD activity was recovered in the clarified cell extract. The protein was precipitated by adding solid ammonium sulphate to reach 90% saturation. SOD was extracted from the pellet with an ammonium sulphate solution of lower concentration (depending on the composition of the protein extract between 50 and 60% saturation).

The SOD-containing fractions were directly applied to a CD-Sepharose column (10 cm × 2 cm I.D.) equilibrated with an ammonium sulphate solution. Elution of SOD activity was achieved by washing the column at a flow-rate of 0.4–0.7 ml/min with solutions of decreasing salt concentration at 20°C (fraction volume 20 ml). The SOD-containing fractions were concentrated and dialyzed against 90% saturated ammonium sulphate yielding crystalline SOD preparations.

For the isolation of the Cu,Zn-SOD, Tsuchihashi fractionation (chloroform/ethanol treatment) was performed to remove haemoglobin as described in ref. 10. The Tsuchihashi supernatant was lyophilized and dissolved in an ammonium sulphate solution of 65% saturation. Chromatography on CD-Sepharose was performed as described above.

All operations with the exception of the chromatographic steps were carried out at 4°C. The ammonium sulphate solutions used during the purification procedures contained 0.05 *M* disodium hydrogenphosphate.

RESULTS AND DISCUSSION

Purification of SOD from Pseudomonas putida

The cell-free extract was brought to 90% saturation with solid ammonium sulphate. After standing overnight in the cold the precipitated protein was collected by centrifugation (15 000 *g*, 30 min). Approximately 90% of the total SOD activity was extracted by stirring the precipitate twice for 10 min with an ammonium sulphate solution of 60% saturation. After centrifugation (15 000 *g*, 30 min) the two clear supernatants were pooled and diluted with 0.05 *M* sodium phosphate buffer pH 8.0 to reach an ammonium sulphate concentration of 50% saturation. The solution was applied to a CD-Sepharose column, previously equilibrated with an ammonium sulphate solution of the same concentration. Under these conditions SOD activity was quantitatively adsorbed onto the Sepharose derivative. A discontinuous gradient of ammonium sulphate (50% to 40% saturation) was then applied to the column, decreasing the salt concentration in

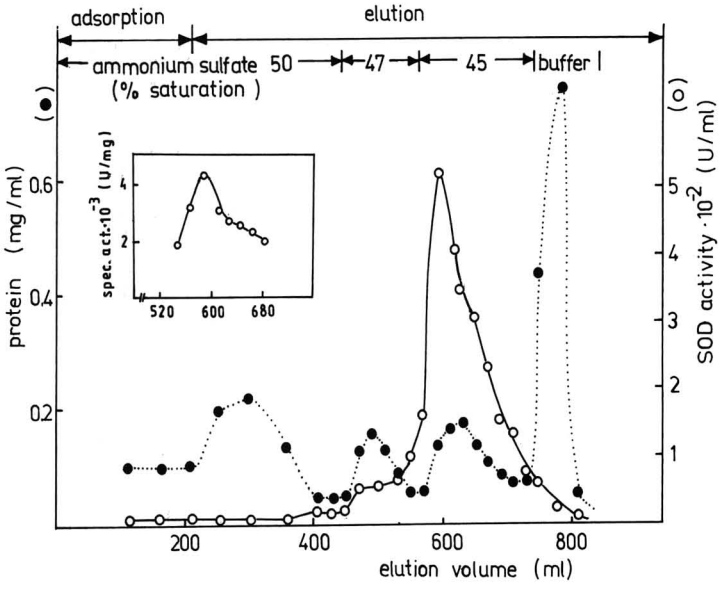

Fig. 1. CD-Sepharose chromatography of Fe-SOD from *Pseudomonas putida*. A 210-ml aliquot of the supernatant of the ammonium sulphate extract (1700 mg, 59 · 10^3 U) was applied to the CD-Sepharose column.

small steps if the protein concentration in the eluates decreased below 0.06 mg/ml. SOD was eluted with an ammonium sulphate solution of 45% saturation (Fig. 1). Fractions containing more than 5% of the total SOD activity were pooled and concentrated to 10 ml on a small column (2.5 cm × 2 cm I.D.) of CD-Sepharose as follows. The pooled fractions were brought to 55% saturation with solid ammonium sulphate and adsorbed on the equilibrated column (55% saturation). Elution was performed with 0.05 *M* sodium phosphate buffer pH 8.0. After discarding a volume of 5 ml the total SOD activity was removed from the column in only one fraction of 10 ml. For storage the enzyme was

TABLE I

PURIFICATION OF Fe-CONTAINING SOD FROM *PSEUDOMONAS PUTIDA*

Step	Volume (ml)	Total protein (mg)	Total activity (U)	Specific activity (U/mg)	Purification (fold)	Recovery (%)
Crude extract[a]	615	1660	59 552	36	1	100
Ammonium sulphate extraction						
Supernatant 60% saturation 1.	110	154	35 642	231	6.4	95
2.	100	60	20 933	349	9.6	
CD-Sepharose chromatography	200	19	48 237	2486	69	81
Concentration on CD-Sepharose	10	14	41 091	2935	80	69
SOD preparation in crystalline state	5	13.5	40 500	3000	83	68

[a] Crude extract was prepared from a 7-l culture of *Pseudomonas putida* cells with an optical density of A_{600} (1 cm) = 1.7. The cells were harvested and disrupted as described in the Experimental section.

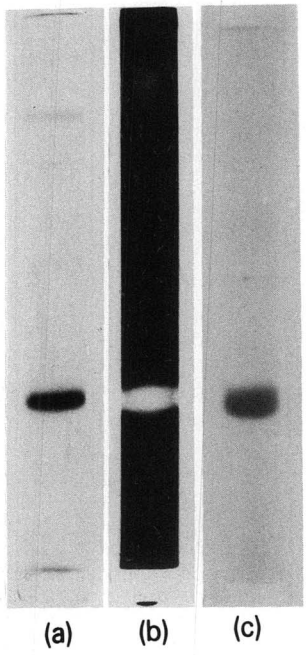

Fig. 2. Polyacrylamide gel electrophoresis of crystalline Fe-SOD from *Pseudomonas putida* in 8% gels under non-denaturing (a,b) and denaturing (c) conditions: (a) 30 μg of SOD stained for protein with Coomassie brilliant blue G250; (b) 5 μg of SOD stained for activity with the photochemical/NBT procedure; (c) 20 μg of SOD were incubated for 5 min at 95°C in the presence of 1% SDS and 1% β-mercaptoethanol and subjected to SDS-PAGE.

dialyzed against 90% saturated ammonium sulphate solution. At 4°C and a protein concentration of about 2 mg/ml no decrease of enzyme activity was observed over a period of 12 months. The results of the purification procedure are summarized in Table I. The recovery of 70% of the total SOD activity is very high in comparison with conventional purification procedures for prokaryotic SOD. The reported yields are as a rule below 40% [19–27]. Generally hydrophobic chromatography seems to be a useful technique to purify SODs. Gregory and co-workers [7,28,29], who used phenyl-Sepharose as carrier material, reported recoveries of 71–99% SOD activity for this single step. As the complete purification procedures include one or two additional chromatographic steps, the overall yields were in the range of 60%.

Because of the high specific activity of SOD in the crude extract of *Pseudomonas putida* [17], only 85-fold purification yielded homogeneous protein. Fig. 2a and b shows the electrophoretic patterns on 8% gels without SDS. A single protein band was observed, corresponding to the activity zone. The enzyme was also homogeneous as judged by SDS-PAGE (Fig. 2c). The specific activity of the purified enzyme was 3000 U/mg, which is of the same order of magnitude as described for some other Fe-containing SODs [19–27].

To obtain protein crystals, purified SOD (7 mg/ml) was dissolved in an ice-cold 53% saturated ammonium sulphate solution. Single crystals appeared after 1–2 days of storage at 25°C (Fig. 3).

Purification of SOD from bovine erythrocytes

Changing the conditions, CD-Sepharose is also suitable for purifying Cu,Zn-containing SOD. However, binding of eukaryotic SOD to the carrier required higher ammonium sulphate concentrations. The supernatant from the Tsuchihashi frac-

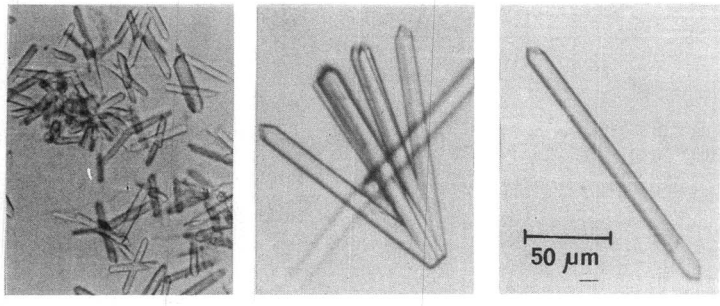

Fig. 3. Microphotograph of crystalline Fe-SOD from *Pseudomonas putida*.

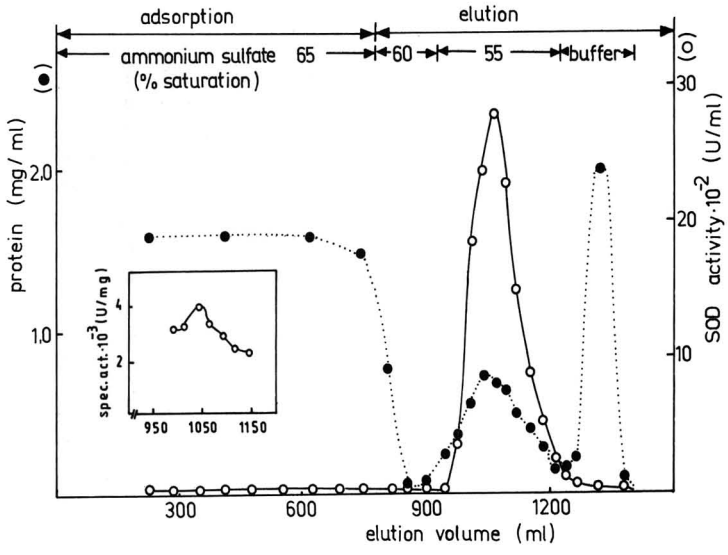

Fig. 4. CD-Sepharose chromatography of Cu,Zn-SOD from bovine erythrocytes. A 1300-ml aliquot of lyophilized Tsuchihashi supernatant was dissolved in 65% saturated ammonium sulphate, clarified by filtration and applied to the CD-Sepharose column (770 ml, 1900 mg, 300 · 10^3 U).

tionation was lyophilized and the dried protein was redissolved in 65% saturated ammonium sulphate. The solution was percolated over filter paper and then applied to a CD-Sepharose column previously equilibrated with the same salt concentration (Fig. 4). Elution and concentration of SOD activity were done as described in the case of the Fe-SOD. The Cu,Zn-containing enzyme, however, was eluted

TABLE II

PURIFICATION OF Cu,Zn-SOD FROM BOVINE ERYTHROCYTES

Step	Volume (ml)	Total protein (mg)	Total activity (U)	Specific activity (U/mg)	Purification (fold)	Recovery (%)
Hemolysate[a]	1830	250 000	316 235[b]	1.3[c]	1	100
Supernatant from Tsuchihashi fractionation	1300	2 080	316 235	150	115	100
Lyophilized Tsuchihashi supernatant in 65% saturated ammonium sulphate	770	1 885	300 000	159	122	94
CD-Sepharose chromatography	175	95	286 600	2950	2269	91
Concentration on CD-Sepharose	20	85	275 000	3235	2488	87
Crystalline SOD preparation	12	84	268 800	3200	2461	85

[a] Hemolysate was prepared from 1 l of packed red cells.
[b] Not estimated.
[c] Because haemoglobin interferes with the SOD test, the activity of the haemoglobin-free extract was used to calculate the specific activity.

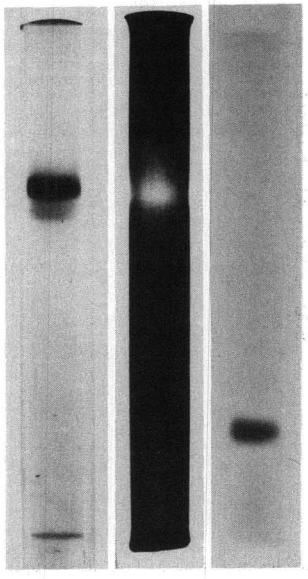

Fig. 5. Polyacrylamide gel electrophoresis of purified Cu,Zn-SOD from bovine erythrocytes in 8% gels under non-denaturing (a,b) and denaturing (c) conditions: (a) 30 μg of SOD stained for protein with Coomassie brilliant blue G250; (b) 5 μg of SOD stained for activity with the photochemical/NBT procedure; (c) 20 μg of protein were incubated for 5 min at 95°C in the presence of 1% SDS and 1% β-mercaptoethanol and subjected to SDS-PAGE.

from CD-Sepharose using 55% saturated ammonium sulphate. The results of the purification are summarized in Table II. The enzyme showed a 2400-fold purification with a yield of 85%. The specific activity of the purified enzyme was 3200 U/mg. The concentrated enzyme was stored under 90% saturated ammonium sulphate at 4°C. No loss of enzyme activity could be detected during 12 months. Homogeneity of the purified Cu,Zn-SOD was analyzed by PAGE. The electrophoretic patterns of the native enzyme show two bands, which correspond to the area of activity staining (Fig. 5a and b). These are the typical charge isomeric forms of Cu,Zn-SOD purified from erythrocytes [30]. SDS-PAGE demonstrates only one band (Fig. 5c).

CONCLUSION

In the present study we describe a special type of hydrophobic chromatography for the purification of prokaryotic as well as eukaryotic SODs. By using this technique we were able to improve the process of purification with respect to the time required, the number of purification steps and the yield. The mechanism of this chromatography was unknown till now. We suggest that conformational changes induced by variation of the ammonium sulphate concentration alter the affinity of the enzymes for the Sepharose derivative [9]. As single proteins show differences in the binding as well as elution behaviour, it is possible to separate a special enzyme from other proteins in one chromatographic step. Additionally the high concentration of structure-forming anions present at all purification steps causes stabilization of enzyme activity. The overall yields of active SOD were approximately 70%.

With the same chromatographic technique we also purified the Fe-containing SOD from *Pseudomonas testosteroni* and the Cu,Zn-containing SOD from human erythrocytes to electrophoretic homogeneity [17].

It should be pointed out that the support prepared by coupling 11-aminoundecanoic acid to cyanogen bromide-activated Sepharose was used for more than 25 preparations within 1 year with the same success. Sufficient regeneration was obtained by washing the columns with distilled water. From our experience with the preparation of other enzymes [9], the reproducibility of the purification results was influenced by the composition of the protein extract applied to the column [17].

REFERENCES

1 H. M. Steinman, in W. Oberley (Editor), *Superoxide dismutase*, Vol. 1, CRC Press, Boca Raton, FL, 1982, pp. 11–68.
2 K. Maejima, K. Miyata and K. Tomoda, *Agric. Biol. Chem.*, 47 (1983) 1537–1543.
3 R. J. Weselake, Sh. L. Chesney, A. Petkau and A. D. Friesen, *Anal. Biochem.*, 155 (1986) 193–197.
4 M. Miyata-Asano, K. Ito, H. Ikeda and S. Sekiguchi, *J. Chromatogr.*, 370 (1986) 501–507.
5 I. Bianchi, *Eur. Pat.*, EP 112 2990 A2 (1984).
6 K. Miyata, *Jpn. Pat.*, JP 589686 A (1983).
7 E. M. Gregory and Ch. H. Dapper, *Arch. Biochem. Biophys.*, 220 (1983) 293–300.

8 W. Schöpp, M. Grunow, H. Tauchert and H. Aurich, *FEBS Lett.*, 68 (1976) 198–202.
9 W. Schöpp, M. Grunow, K. Stolarski, A. Schäfer, D. Knopp and R. Lorenz, *J. Chromatogr.*, 376 (1986) 359–374.
10 J. M. McCord and I. Fridovich, *J. Biol. Chem.*, 244 (1969) 6049–6055.
11 B. J. Davies, *Ann. N.Y. Acad. Sci.*, 121 (1964) 404–427.
12 W. Diezel, St. Liebe, G. Kopperschläger and E. Hofmann, *Acta Biol. Med. Germ.*, 28 (1972) 27–30.
13 C. Beauchamp and I. Fridovich, *Anal. Biochem.*, 44 (1971) 276–287.
14 K. Weber and M. Osborn, *J. Biol. Chem.*, 244 (1969) 4406–4412.
15 V. F. Kalb and R. W. Bernlohr, *Anal. Biochem.*, 28 (1977) 362–371.
16 O. H. Lowry, N. Y. Rosebrough, A. L. Farr and R. J. Randall, *J. Biol. Chem.*, 193 (1964) 265–275.
17 M. Grunow, *Dissertation B*, Karl-Marx-Universität Leipzig, 1988.
18 S. Vorberg, W. Schöpp and H. Tauchert, *Monatsh. Chem.*, 114 (1983) 563–569.
19 F. Yost and I. Fridovich, *J. Biol. Chem.*, 248 (1973) 4905–4908.
20 F. Yamakura, *Biochim. Biophys. Acta*, 422 (1976) 280–294.
21 A. Anastasi, J. V. Bannister and W. H. Bannister, *Int. J. Biochem.*, 7 (1976) 541–546.
22 E. C. Hatchikian and Y. A. Henry, *Biochimie*, 59 (1977) 153–161.
23 J. B. Baldensperger, *Arch. Microbiol.*, 119 (1978) 237–244.
24 S. Kanematsu and K. Asada, *Arch. Biochem. Biophys.*, 185 (1978) 473–482.
25 S. Kanematsu and K. Asada, *FEBS Lett.*, 91 (1978) 94–98.
26 B. Meier, D. Barra, F. Bossa, L. Calabrese and G. Rotilio, *J. Biol. Chem.*, 257 (1982) 13977–13980.
27 E. Kusonose, K. Ichihara, Y. Noda and M. Kusonose, *J. Biochem.*, 80 (1976) 1343–1352.
28 K. B. Barkley and E. M. Gregory, *Arch. Biochem. Biophys.*, 280 (1990) 192–200.
29 E. M. Gregory, *Arch. Biochem. Biophys.*, 238 (1985) 83–89.
30 A. Gärtner and U. Weser, *Biomimetic and Bioorganic Chemistry II*, Akademie-Verlag, Berlin, 1986, pp. 1–61.

Journal of Chromatography, 590 (1992) 255–261
Elsevier Science Publishers B.V., Amsterdam

CHROM. 23 746

Rapid, two-step purification process for the preparation of pyrogen-free murine immunoglobulin G_1 monoclonal antibodies

Edith A. Neidhardt, Michael A. Luther and Michael A. Recny*

PROCEPT, Inc., 840 Memorial Drive, Cambridge, MA 02139 (USA)

(First received July 22nd, 1991; revised manuscript received September 16th, 1991)

ABSTRACT

A cost-efficient process was specifically designed for the preparation of gram amounts of highly pure murine immunoglobulin (Ig) G_1 monoclonal antibodies (mAbs). This rapid, simple and scalable purification process employs a unique binding and elution protocol for IgG_1 mAbs on a silica-based, mixed-mode ion-exchange resin followed by conventional anion-exchange chromatography. mAbs are bound to BakerBond ABx medium at pH 5.6 directly from serum-supplemented hybridoma culture supernatants. Contamining proteins and nucleic acids are removed by an intermediate wash at pH 6.5, followed by the specific elution of IgG_1 mAbs with 100 m*M* Tris–HCl (pH 8.5). The mAb eluate is then loaded directly on to QAE-Sepharose Fast Flow medium and eluted with 10 m*M* sodium phosphate buffer (pH 7.4), containing 150 m*M* sodium chloride. The resulting IgG_1 mAbs are greater than 98% pure, free from measurable endotoxin, formulated in a physiological buffer and suitable for *in vivo* applications.

INTRODUCTION

Exciting developments in monoclonal antibody (mAb) technology over the past several years have increased the demand for large amounts of highly pure, non-pyrogenic mAbs suitable for *in vivo* diagnostic and therapeutic usage [1–5]. This demand has led to the design of a variety of chromatographic matrices for the isolation of mAbs from both hybridoma cell culture supernatants and ascites fluids. Typically, mAbs are present as minor protein components in serum-supplemented hybridoma culture media and require extensive purification in order to remove serum proteins, nucleic acids, pyrogens and other non-proteinaceous contaminants prior to use as *in vivo* reagents. Classic methodologies for mAb purification often employ the use of ion-exchange, hydrophobic interaction (HIC) and hydroxyapatite resins [4–8]. These matrices require both labor-intensive method development and purification processes that utilize multiple chromatographic steps to assure a suitably pure, pyrogen-free product.

Affinity-based matrices employing both protein A and protein G have gained widespread acceptance for their ability to specifically purify mAbs from many different species and subclasses [9]. Although the use of these resins can result in preparations of > 90% pure mAb in a single step, disadvantages such as their high cost, relatively harsh elution conditions and the potential for leaching of the affinity ligand make these resins less desirable than conventional matrices for designing an economical process for the preparation of gram amounts of highly pure mAbs. In particular, when the desired mAb is a murine immunoglobulin (Ig) G_1 subtype, protein A affinity resins are less useful owing to the lack of binding specificity for this murine mAb isotype at neutral pH [9].

Recently, the silica-based mixed-mode ion exchange medium BakerBond ABx has been successfully used to isolate murine and rat IgG_1 mAbs

0021-9673/92/$05.00

from ascites and cell culture supernatants with purities similar to those obtained with either protein A or protein G resins [10,11]. This paper describes a novel and exceptionally cost-efficient process employing both ABx and QAE-Sepharose Fast Flow media for the purification of murine IgG_1 mAbs from serum-containing cell-culture supernatants. This rapid, two-step procedure utilizes a unique ABx binding and elution protocol designed specifically for the purification of murine IgG_1 mAbs, followed by a second chromatographic step on QAE-Sepharose Fast Flow medium to further purify, concentrate and depyrogenate the mAb preparation for potential *in vivo* applications.

EXPERIMENTAL

Monoclonal antibodies

Anti-LFA3 mAb was purified from cell-culture supernatants harvested from a hybridoma cell line (ATTC HB205) grown in CellPharm hollow-fiber bioreactors (CD Medical, Miami Lakes, FL, USA). Tissue culture medium was composed of α-MEM supplemented with L-glutamine (4 m*M*), penicillin (50 units/ml), streptomycin (50 mg/l) and 5% fetal bovine serum (FBS). The anti-Lewis mAb was purchased from Helix Biocore (Minneapolis, MN, USA) as a 5% FBS-supplemented RPMI harvest from the hybridoma cell line grown in suspension culture.

Liquid chromatography

All chromatographic procedures were performed on a Pharmacia FPLC system that had been depyrogenated with 0.1 *M* NaOH as described by the manufacturer. All buffers were made with USP-grade reagents, when available, prepared with Sterile Water For Injection (SWFI) (Baxter Healthcare, Miami, FL, USA), and sterile filtered using Millipore HV 0.22-μm membranes. BakerBond ABx medium (J.T. Baker, Phillipsburg, NJ, USA) and Pharmacia QAE-Sepharose Fast Flow medium (Pharmacia–LKB, Piscataway, NJ, USA) were depyrogenated according to the protocols described by the respective manufacturers prior to use.

mAb characterization

mAb purity was analyzed by sodium dodecyl sulfate–polyacrylamide gel electrophoresis (SDS–PAGE) [12] under reducing and non-reducing conditions using either 12% precast or 4–20% gradient precast minigels (Bio-Rad Labs., Richmond, CA, USA). Total protein was determined using the absorption coefficient of 1.4 ml mg^{-1} cm^{-1} at 280 nm [13]. The amount of IgG_1 mAb was determined by employing a sandwich enzyme-limited immunoassay (ELISA) as follows: NUNC maxiSorb 96-well microtiter plates (Cat. No. 468667) were coated with 300 ng of goat anti-mouse whole IgG (Sigma, St. Louis, MO, USA; M8642) in phosphate-buffered saline (PBS), pH 7.2. Plates were blocked with 2% bovine serum albumin (BSA) in PBS for 2 h at 25°C. Aliquots of 100 μl containing IgG_1 cell-culture supernatants, purified mAbs or IgG_1 standard (murine IgG_1 monoclonal anti-human IgM, clone SA-DA4; Fisher Scientific, Pittsburgh, PA, USA) in the range 0.5–20 ng/ml were added and incubated for 2 h at 37°C. Plates were washed with PBS–0.05% Tween 20 and incubated with 100 μl of goat anti-mouse IgG_1 conjugated to alkaline phosphatase (Southern Biotech Assoc., Birmingham, AL, USA; Cat. No. 0101-04; diluted 1:500 in 2% BSA–PBS) for 2 h at 37°C. After washing, the plates were developed for 10 min with 100 μl of DNP substrate [1 mg/ml of *p*-nitrophenyl phosphate in diethanolamine, pH 8.9] and read at 405 nm.

Isoelectric focusing (IEF)

IEF was performed using Serva ultra-thin gels having a p*I* range from 3 to 10. The cathode buffer consisted of 23 m*M* L-arginine free base, 4 m*M* L-lysine, 2 *M* ethylenediamine and 0.1 *M* NaOH and the anode buffer was 25 m*M* L-aspartic acid, 25 m*M* L-glutamic free acid and 0.1 *M* phosphoric acid. Gels were prefocused (1700 V, 5 mA, 4 W) for 25 min. Protein samples were focused at 200 V, 5 mA, 4 W for 90 V h followed by 1700 V, 5 mA, 4 W for 5500 V h. Gels were fixed in 20% trichloroacetic acid (TCA) for 10 min and protein samples were rendered visible by staining with Serva Blue GW for 15 min. Gels were cleared with water.

Fluorescence-activated cell sorting (FACS) analysis

The functionality of the mAbs was examined by FACS analysis of cells bearing the respective antigens.

Limulus amebocyte lysate (LAL) assay

Endotoxin units were measured using a chromogenic LAL assay purchased from Whittaker Bioproducts (Walkersville, MD, USA). All buffers were routinely tested for acceptable endotoxin levels [<0.25 endotoxin units (EU)/ml] prior to chromatographic experiments.

RESULTS AND DISCUSSION

The purpose of this study was to develop a rapid, simple, scalable and economical process for the preparation of gram amounts of highly pure, pyrogen-free murine monoclonal IgG_1 mAbs which can be used for *in vivo* applications. Ideally, this process would consist of a minimum number of chromatographic steps that could be performed in series without subjecting the mAbs to either dialysis or diafiltration. The presence of high concentrations of albumin and other contaminating proteins in serum-supplemented cell culture supernatants requires that the initial step of the process employ a chromatographic resin having a high capacity, selectivity and specificity for mAbs. The final step of the process should depyrogenate, concentrate and formulate the mAbs in a physiological buffer, thereby making them suitable for potential *in vivo* applications. In addition, the entire chromatographic process should be performed in an environment that maintains sterility and prevents contamination by exogenous endotoxins.

A number of mAbs from different species have been successfully purified using BakerBond ABx medium, a mixed-mode ion-exchange chromatographic resin [2–5,10,11]. ABx medium was developed for process-scale chromatography with properties such as a high capacity for protein binding, good flow characteristics and excellent chemical and physical stability. This resin binds a wide variety of antibodies, while exhibiting weak affinity for albumin, transferrin and other serum proteins at selected pHs and ionic strengths [2–5]. The unique combination of the silica-based, hydrophilic polymer backbone paired with zwitterionic and weakly hydrophobic side-groups capitalizes on the principles outlined by the multi-point interaction hypothesis [14,15], which suggests that the summation of weak forces such as electrostatic, hydrophobic and hydrogen-bonding forces can significantly enhance the affinity for the ligand of interest.

Most protocols for the purification of murine IgG_1 mAbs from serum-based cell culture supernatants and ascites using ABx resin require that a significant dilution of the starting medium be made in order to effectively bind the antibody of interest [2–5,10]. Elution of the mAb is usually accomplished by applying linear or stepwise salt gradients to the column at or near neutral pH. For example, Ross *et al.* [10] have reported the isolation of murine IgG_1 mAbs from ascites using ABx chromatography where the ascites fluid is diluted with four volumes of 2-(N-morpholino)ethanesulfonic acid (MES) buffer (pH 5.6) and eluted with a linear gradient from 0 to 1 *M* sodium acetate (pH 7.0). Although the resulting mAb preparation is $>95\%$ pure, the high ionic strength of the ABx eluate is incompatible with subsequent anion-exchange chromatographic steps. Therefore, we sought to develop unique binding and elution conditions for murine IgG_1 mAbs which minimize initial sample manipulation and avoid the use of salt gradients. Thus, one could eliminate the need for a dialysis, diafiltration or a significant dilution step prior to anion-exchange chromatography.

The binding efficiency of IgG_1 mAbs present in both diluted and undiluted conditioned cell culture supernatants from two different hybridoma cell lines was compared on ABx. The diluted supernatants were prepared by diluting fivefold with 25 m*M* MES (pH 5.6), while the undiluted supernatants were adjusted to 50 m*M* MES (pH 5.6) using a stock solution of 1.0 *M* MES (pH 4.0). No difference in IgG_1 binding efficiency was detected when the diluted or undiluted supernatants from either of the two different hybridoma cell lines were compared, based on determination of the mouse IgG_1 present in the flow-through fraction by ELISA. This was surprising, considering the significant difference in conductivity between the diluted (2 mS/cm) and undiluted (10 mS/cm) hybridoma cell culture supernatants.

Once the initial parameters for binding of IgG_1 mAbs to ABx had been established, we investigated conditions for specifically eluting the mAbs, whereby the ionic strength of the elution buffer would be compatible with a subsequent anion-exchange chromatographic step. A linear gradient from 0 to 100% buffer B (15 m*M* sodium acetate–35 m*M* sodium

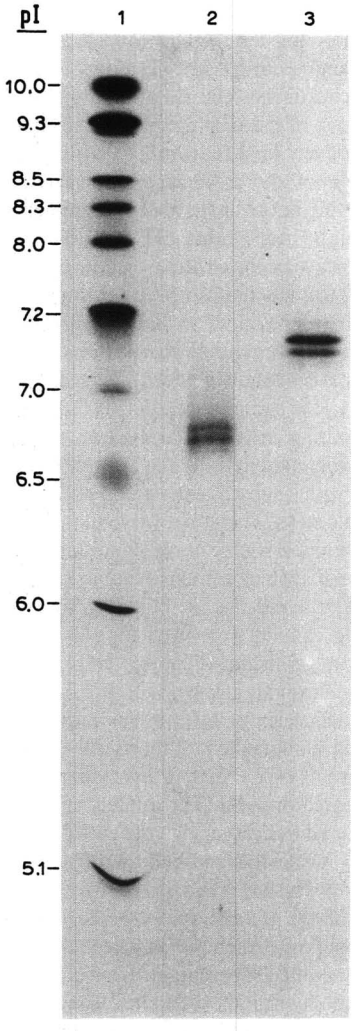

Fig. 1. IEF analysis of purified IgG_1 mAbs. Lanes: 1 = p*I* standards; 2 and 3 = anti-LFA3 and anti-Lewis mAbs, respectively. A 20-μg amount of purified mAb was loaded for each corresponding lane.

phosphate–700 m*M* ammonium sulfate, pH 7.5), where buffer A is 50 m*M* MES (pH 5.6), showed that both IgG_1 mAbs eluted between 35% and 50% buffer B. Eluting stepwise with 25% buffer B was sufficient to recover >90% of the applied mAbs with >90% purity, as determined by SDS-PAGE. However, under these conditions, the high ionic strength of the eluate was not compatible with a subsequent anion-exchange chromatographic step.

The characteristics of the ABx resin, such as a predominance of anionic or cationic side-chains and a relatively narrow pH range within which mAbs bind to the matrix [2–4] suggested to us that a strong buffer with pH >7.5 could also be effective in eluting IgG_1 mAbs from ABx. We observed that both 100 m*M* HEPES buffer (pH 7.5) and 100 m*M* sodium phosphate buffer (pH 7.8) were capable of eluting each of these two mAbs from ABx. However, precipitation of the mAbs was detected in the leading fractions of the mAb eluates using either of these two buffers. Precipitation of the mAbs appeared to be pH dependent, as the fractions from the leading edge of the mAb eluate had a pH between 6.0 and 7.0, while the trailing fractions (which exhibited no precipitation) had a pH of 7.5. The appearance of a precipitate was not entirely unexpected, as the pH of these eluates was near the isoelectric point of both mAbs (Fig. 1). In contrast, no precipitation of either mAb was observed when the ABx column was eluted with 100 m*M* Tris–HCl buffer (pH 8.5). By stepwise eluting the ABx resin with a strong buffer at a pH significantly above the isoelectric point of the mAb ($\geqslant$ 1.5 pH units), precipitation of the mAb was avoided and the mAb eluate is in a buffer compatible for direct application to a sterile, pyrogen-free anion-exchange column.

Based on these results, cell-culture supernatants containing *ca.* 1.0 g of mAb (3 mg IgG_1/ml) from two different hybridoma cell lines were adjusted to 50 m*M* MES (pH 5.6) and loaded directly on to separate columns packed with 100 ml of BakerBond Prepscale 40-μm ABx. Based on the quantitative murine IgG_1 ELISA, ABx exhibited a binding capacity of *ca.* 15 mg mAb/ml resin for undiluted cell culture supernatants containing 5% FBS at pH 5.6. Contaminating proteins were removed by washing the column by stepwise adjustment with 10% buffer B (100 m*M* Tris–HCl, pH 8.5), where buffer A is 50 m*M* MES (pH 5.6). This intermediate washing step (resulting pH of 6.5) was very important as it also facilitated the removal of significant amounts of DNA and/or RNA non-specifically bound to the resin (Table I). Both mAbs were specifically eluted with 100 m*M* Tris–HCl (pH 8.5) (100% buffer B) and collected aseptically in sterile, pyrogen-free

TABLE I

MAB PURIFICATION SUMMARY

Condition/step	Total protein (mg)	Total mAb (mg)	Purity (%)	Recovery (%)	Absorbance ratio (260/280 nm)	Endotoxin (units/mg)
Hybridoma supernatant (ABx load)	9980	1050	10	100	1.2	20
ABx flow-through	8670	40	N.D.	3	N.D.	N.D.
ABx wash	1310	10	N.D.	1	N.D.	N.D.
ABx eluate/QAE load	850	850	>90	85	1.5	3.8
QAE-Sepharose wash	80	0	N.D.	N.D.	1.5	N.D.
QAE-Sepharose eluate	800	800	>98	80	1.8	<0.25

containers. Average mAb recoveries using this protocol were *ca.* 85% based on a murine IgG_1 ELISA, with protein purities $\geqslant$90% (as judged by SDS-PAGE) (Fig. 2). Pyrogen levels were also reduced significantly by over five fold for both mAb samples (Table I).

In order to assure a purity of >98% and a preparation which was free from detectable pyrogens, a second process step was developed to meet the above criteria and to concentrate and formulate the purified mAbs for *in vivo* studies. QAE-Sepharose Fast Flow and BakerBond MAb media are anion-exchange resins which have a high binding capacity for antibodies (8–10 mg/ml resin) and bacterial endotoxins, and display good flow characteristics [3,4,16]. For anion-exchange chromatography,

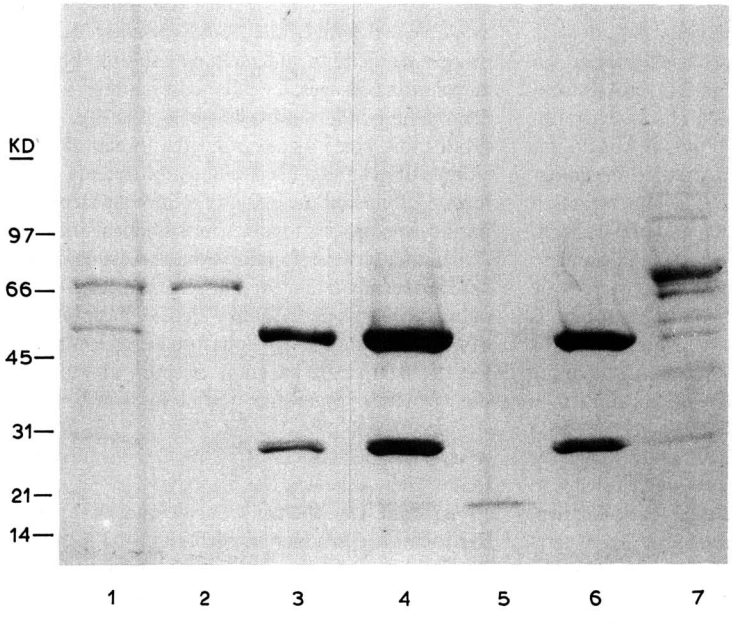

Fig. 2. SDS-PAGE of mAb purification by ABx and QAE-Sepharose Fast Flow. Lanes: 1 = initial ABx load from hybridoma culture supernatants; 2 = ABx flow-through; 3 = 100 m*M* Tris (pH 8.5) eluate from ABx column; 4 = QAE-Sepharose Fast Flow load (ABx eluate); 5 = QAE-Sepharose Fast Flow intermediate wash step; 6 = PBS eluate of QAE-Sepharose Fast Flow; 7 = 300 m*M* NaCl eluate of QAE-Sepharose Fast Flow. kD = kilodalton.

QAE-Sepharose Fast Flow was chosen based on the ability to elute the purified mAbs with an isotonic phosphate buffer. Each mAb eluate was diluted twofold with SWFI to reduce the conductivity to less than 2 mS/cm and applied to 150 ml of sterile, pyrogen-free QAE-Sepharose Fast Flow medium equilibrated in 10 m*M* sodium phosphate buffer (pH 7.4). The resin was washed extensively with equilibration buffer (>10 column volumes) to remove loosely bound contaminants, and the mAbs were recovered by stepwise elution with 10 m*M* sodium phosphate buffer (pH 7.4) containing 150 m*M* NaCl. Recoveries for each mAb were between 85 and 90% based on the murine IgG_1 ELISA, with purities >98% as judged by SDS-PAGE. Endotoxin levels were reduced further by ten fold (in comparison with the levels after ABx chromatography) to less than 0.25 EU/ml. The 280/260 nm absorbance ratio increased from 1.5 following ABx chromatography to 1.8 after chromatography on QAE-Sepharose Fast Flow, indicating the removal of additional nucleic acids contaminants (Table I). Most of the remaining protein contaminants remain bound to QAE-Sepharose Fast Flow and can be eluted by a 300 m*M* NaCl wash (Fig. 2).

Protein A medium has also been utilized to achieve >90% purity for murine IgG_1 mAbs from cell culture supernatants in a single chromatographic step [9,17]. However, murine IgG_1 mAbs do not have a high affinity for protein A under physiological conditions [18]. Therefore, the ionic strength must be raised above 1.0 *M* NaCl, and preferably to 3 *M* NaCl, and the pH adjusted to 9.0 in order to achieve quantitative binding. For large-scale processes, this pH and ionic strength adjustment is cumbersome and may lead to mAb aggregation or precipitation as the medium is titrated through the isoelectric point of the mAb. The mAb can then be eluted from protein A medium by decreasing both the pH and ionic strength, but after this step the ionic strength of the eluate is too high (owing to residual NaCl in the binding buffer) for subsequent chromatography on anion-exchange resins. Therefore, an intermediate manipulation such as dialysis, diafiltration or a significant dilution is required to reduce the conductivity of the eluate sufficiently in order to achieve effective binding on anion-exchange resins. An alternative to diafiltration of protein A purified mAbs would be to utilize hydrophobic interaction chromatography (HIC) as a second step, whereby the mAb sample is bound to an HIC matrix in high salt at neutral pH and eluted from the HIC resin by lowering the ionic strength of the buffer [3,7]. However, when this method was employed with the both anti-LFA3 and anti-Lewis IgG_1 mAbs, the samples were dilute (<200 μg/ml) and the recovery was poor (<50%), thus requiring an extra concentration step to be performed under sterile, pyrogen-free conditions prior to use. These observations, combined with the relatively low capacity of protein A for murine IgG_1 mAbs (*ca.* 3 mg mAb/ml protein A Fast Flow Sepharose), and the much higher cost, make protein A-based media less attractive than ABx for the initial step in large-scale mAb purification processes.

The economics of this large-scale chromatographic process for the purification of murine IgG_1 mAbs are worth noting. Using the protocol described here, the cost of purifying *ca.* 1 g of mAb in a single experimental run using 75 ml of ABx medium (assuming a capacity of 15 mg mAb/ml resin) is *ca.* 30 times less than using 350 ml of protein A Fast Flow Sepharose from the most economical source available. Although one could certainly use less protein A medium and employ multiple binding and elution passages, the labor cost required to conduct numerous runs must be included in the overall production cost, aside from the practical constraints of pH and ionic strength adjustments which must be done and the inability to link the steps of a purification process together in a practical and convenient manner. In summary, the process described here takes advantage of both the excellent chromatographic properties and the cost-efficient nature of both ABx and QAE-Sepharose Fast Flow media for the routine preparation of gram amounts of highly pure, pyrogen-free murine IgG_1 mAbs.

ACKNOWLEDGEMENTS

We thank Dr. Michael Concino and Dr. Charles Sardonini for production of the anti-LFA3 mAb, Kristin Esenther for FACS analysis, Janelle Harings for excellent technical assistance, Maria Knoppers and Dr. Sanjay S. Khandekar for many helpful discussions and Dr. David R. Nau for a critical review of the manuscript prior to publication. Equal contributions to this work were made by E. A. N. and M. A. L.

REFERENCES

1 F. M. Brodsky, *Pharm. Res.*, 5 (1988) 1–9.
2 D. R. Nau, *BioChromatography*, 1 (1986) 82–94.
3 D. R. Nau, *BioChromatography*, 4 (1989) 4–18.
4 D. R. Nau, in: W. Hancock (Editor), *High Performance Liquid Chromatography in Biotechnology*, Wiley, New York, 1990, pp. 399–530.
5 D. R. Nau, *BioChromatography*, 5 (1990) 62–73.
6 C. Williams, in C. A. Williams (Editor), *Methods in Immunology and Immunochemistry*, Vol. 1, Academic Press, New York, 1967, pp. 307–385.
7 B. Pavlu, U. Johansson, C. Nyhlen and A. Wichman, *J. Chromatogr.*, 359 (1986) 449–460.
8 L. J. Crane, in L. B. Schnook (Editor), *Monoclonal Antibody Production Techniques and Applications*, Marcel Dekker, New York, 1987, pp. 139–171.
9 M. D. P. Boyle and K. J. Reis, *Biotechnology*, 5 (1987) 697–702.
10 A. H. Ross, D. Herlyn and H. Koprowski, *J. Immunol. Methods*, 102 (1987) 227–231.
11 F.-M. Chen, G. S. Naeve and A. L. Epstein, *J. Chromatogr.*, 444 (1988) 153–164.
12 E. K. Laemmli, *Nature (London)*, 227 (1970) 680–685.
13 G. L. Peterson, *Methods Enzymol.* 91 (1983) 95–119.
14 F. E. Regnier, *LC·GC*, 5 (1987) 962–967.
15 M. T. W. Hearn, *J. Chromatogr.*, 418 (1987) 3–26.
16 G. Sofer, *Bio/Technology*, 3 (1984) 1035–1038.
17 E. Harlow and D. Lane, *Antibodies: a Laboratory Manual*, Cold Spring Harbor Laboratory, Cold Spring Harbor, NY, 1988, pp. 309–312.
18 P. L. Ey, S. J. Prowse and C. R. Jenkin, *Biochemistry*, 15 (1978) 429–436.

Journal of Chromatography, 590 (1992) 263–270
Elsevier Science Publishers B.V., Amsterdam

CHROM. 23 750

Determination of metal ions by on-line complexation and ion-pair chromatography

Heli Sirén* and Marja-Liisa Riekkola

Department of Chemistry, University of Helsinki, Vuorikatu 20, SF-00100 Helsinki (Finland)

(First received November 6th, 1989; revised manuscript received June 24th, 1991)

ABSTRACT

An ion-pair chromatographic method utilizing on-line complexation and ion-pair formation in a post-column reactor was developed for the determination of copper, palladium, cobalt and iron in mixtures. The system features a reversed-phase column and a second eluent line feeding the ligand reagent, connected after the column via a T-piece, to a mixer and through that to a knitted tubing reactor. The ion-pair former was added to the eluent before the column and the ligand after it. The separation was studied using a binary eluent system containing cetyltrimethylammonium bromide (CTMABr) or tetradecyltrimethylammonium bromide (TDTMABr) in water–methanol (99:1, v/v) as ion-pair former and methanol. In addition, water–methanol (99:1, v/v) containing 1-nitroso-2-naphthol-6-sulphonate (126NNS) as ligand was added to the eluent, through the T-piece, after the column. Mixing of the two eluents took place in the mixer. Methanol was used both isocratically and in gradient addition. Selective UV–VIS detection of the metal–126NNS ion pairs was at wavelengths 230, 260, 310 and 400 nm and their identification was effected in wavelength range 190–600 nm. The metal complex formation in the aqueous methanol eluent evidently governed the retention of the ion pairs, while the selectivity of the method was provided by the different rates of reaction of the metal, the ligand and the ion-pair former in the mixer–reactor system. The detector response for copper, palladium, cobalt and iron was linear up to concentrations of 10 μM. In spiked water–methanol samples the detection limits for these metals ranged from $1 \cdot 10^{-3}$ to 1 mg/l. When the on-line complexation and ion-pair formation method was tested with nickel, mercury and zinc, the results proved that these ion pairs were unstable. Because of the insufficient reproducibility of the absorption intensities of these metal ion pairs, their qualitative study could be performed only in the pH range 7–8. The method was successfully applied to real samples after removal of the organic material.

INTRODUCTION

A number of papers have been published on the use of ion-pair chromatography (IPC) for the separation and determination of metals [1–8]. Because metals in a complex matrix are difficult to detect directly in low concentrations, on the basis of their UV–VIS absorption, pre- and post-column derivatization with an absorbing ligand is often applied as an effective approach to the problem [4].

The mechanism by which metal complex ion pairs are separated in ion-pair chromatography is complicated owing to both metal complex and ion-pair formation. Separation depends on the extraction constants of the ion pairs (K_{ex}), on the ratio of the solid phase and the eluent in the column (V_s/V_m) and, via pH, on the dissociation constant of the ligands (pK_a), the ionic strength of the eluent and temperature.

Column application of strong ligands, such as those containing nitrogen and sulphur atoms in the molecule, offers new possibilities for metal analysis. If the ligand is added after the column, metal complex stability is enhanced and ion-exchange reactions and insolubility effects are minimized. By optimizing separation and detection independently, greater freedom and effectiveness can be obtained in analytical methods [4,6].

Derivatization on-line within the system has a number of advantages over off-line derivatization, but steps need to be taken to avoid broadening in the on-line reactor. There have been several discussions in the literature on the theoretical basis for minimizing band broadening, such as when open-tubular

0021-9673/92/$05.00

reactors are geometrically deformed by helical coiling of the tube to give minimum retention of the components [9,10]. A knitted reactor has the added advantage that peak tailing is minimized.

In this study, we introduced an on-line derivatization method for metal ions, in which the metals are injected into an eluent containing a quaternary ammonium bromide in methanol–water solution and after the column are further combined with a ligand solution. The metals are separated as their ion pairs, consisting of metal–1-nitroso-2-naphthol-6-sulphonate complexes combined under carefully controlled elution conditions with an organic ammonium compound.

The method was developed using mixtures of Cu(II), Pd(II), Co(II) and Fe(II) ions and tested using mixtures of Cu(II), Co(II), Fe(II), Ni(II), Hg(II) and Zn(II) ions. The tests were performed with two real samples, namely nutrient sticks and health drinks containing several of the metal ions. The ligand used for the complex formation, 1-nitroso-2-naphthol-6-sulphonate (126NNS) (as the sodium salt), is UV–VIS absorbing and the ion-pair former, either cetyltrimethylammonium bromide (CTMABr) or tetradecyltrimethylammonium bromide (TDTMABr), is UV absorbing.

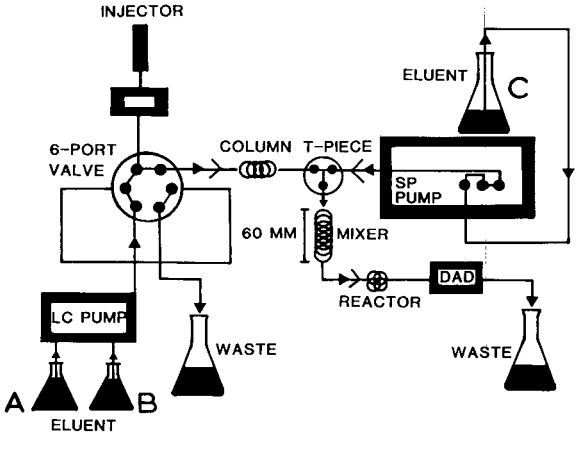

Fig. 1. Schematic diagram of the on-line derivatization technique. Eluent system: (A) ion-pair former solution, (B) methanol and (C) ligand solution. Components: LC pump (HP1090), SP pump (Spectra-Physics), six-port switching valve, column, mixer tube filled with acid-washed glass-wool, reactor (PTFE tubing, 3 or 5 m) and a diode-array detector (DAD).

EXPERIMENTAL

Apparatus

A Hewlett-Packard Model 1090 liquid chromatograph fitted with an HP 1040A diode-array detector was used together with an HP 85B microcomputer. An HP 3392A integrator was employed for data storage and reporting. A PTFE (Habia PTFE tubing, transparent, 300 or 500 mm × 0.3 mm I.D. × 0.86 mm O.D.) laboratory designed reactor was maintained at 25°C in the column oven. The mixer, a steel tube (30 mm × 4.6 mm I.D.), was laboratory made and filled with glass-wool (Supelco, acid washed). An SP8810 precision isocratic pump (Spectra-Physics) was used on-line for the ligand flow. The columns were an HP LiChrosorb RP-18 (30 mm × 3 mm I.D., film thickness 5 μm, N = 38 100 m^{-1}) and an Asahipak ODP-50 (150 mm × 4.6 mm I.D., film thickness 5 μm, N = 16 800 m^{-1}) (Fig. 1).

Standard metal solutions

Stock solutions were prepared by dissolving copper(II) perchlorate (G. F. Smith, Quality 1) and palladium (II), iron(II), cobalt(II), zinc(II), chromium(II), nickel(II), mercury(II), magnesium(II) and (II) chloride (Merck, analytical-reagent grade) in distilled, demineralized water. The samples were filtered before use.

Ligand solution

The sodium salt of 1,2-naphthaquinone-6-sulphonate was synthesized as described in the literature [11]. A stock solution was prepared in water–methanol (99:1, v/v) and diluted before use.

Mobile phases in HPLC

The eluents were (A) 0.008 mM CTMABr in water–methanol (99:1, v/v) or 0.008 mM TDTMABr in water–methanol (99:1, v/v) [4], (B) methanol and (C) 0.165 mM sodium 126NNS in water–methanol (99:1, v/v) containing 0.008 mM ion-pair former (CTMABr or TDTMABr) (see Fig. 1). Eluents were bubbled with helium for 15 min and filtered through 0.45-μm fluoromembranes (ACRO LC 13) before use.

Chromatographic procedures

The UV–VIS diode-array detector was operated

at 230, 260, 310 and 400 nm, with a reference wavelength of 550 nm. Identifications of the metal ion pairs were made using the wavelength range 190–600 nm. The oven temperature was 25°C. The samples were manually injected using a 5-μl loop capillary. The flow-rate of the mobile phase from the first pump (LC pump) was 0.5 ml/min, and that of the ligand solution from a second pump (SP pump) was 0.3 ml/min. When the flow-rate of the mobile phase was changed to 0.7 ml/min, that of the ligand solution was increased to 0.5 ml/min.

Calculations. Chromatographic retention times were calculated as the averages of triplicate determinations. The retention time, t_0, of water–methanol (50:50, v/v) was taken as the unretained peak. The capacity factor, k', was calculated from the retention time of the solute, t_R, according to the equation $k' = (t_R - t_0)/t_0$.

Pretreatment of real samples. Health drinks (Pfrimmer, Germany), containing (per 100 g) 0.47 mg of Cu, 4.24 mg of Fe, 85 mg of Mg, 0.59 mg of Mn and 0.70 mg of Cr, and nutrient sticks (Kemira, Espoo, Finland), containing (per kg) 1 mg of Cu, 1 mg of Zn and 1 mg of Fe, were wet digested with 2 ml of concentrated perchloric acid plus 5 ml of concentrated nitric acid on a sand-bath at 195°C for 5 h. The reagent blank solutions were prepared in the same way as the samples. The samples were eluted through prewashed (with methanol and water) Sep-Pak C_{18} columns (Millipore–Waters).

RESULTS AND DISCUSSION

Retention behaviour

Preliminary studies with liquid–liquid extraction and spectrophotometric detection [12] showed that copper, palladium, cobalt and iron easily form complexes with 126NNS (pK_a 7.29) in different molar ratios depending on the pH of the aqueous solution. The metal complexes were easily extracted as ion pairs into organic solvents, but quantitative extraction was obtained only in a controlled pH range [12]. In addition, all the metal complexes were simultaneously extracted into organic solvents in the pH range 7–8.

As the ligand solution was introduced only after the column (see Fig. 1), the metals could not have been retained on the column in the form of metal complexes. The column material was coated with the ammonium compound which, like the metal ions, was in cation form. It therefore seems improbable that the metals were separated from each other during their passage through the column. They nevertheless appeared to be retained longer when polymer material was used, which suggests that the material had some anionic ability to retain them, independent of their molecular weight or ionic charge. These considerations led us to conclude that the retention and separation of the metal complex ion pairs were primarily dependent on the metal complex and ion-pair formation constants. Possibly, also, there was a thin layer of ammonium compound covering the material of the mixer and the PTFE tubing and having some retention effect.

Formation of the metal complexes was registered on the monitor: the metal complex ion pairs were detected one by one as they eluted to the diode-array detector, and their UV–VIS spectra were compared with library spectra. The purities of the absorption spectra were checked from the slopes and the apex of the spectra to confirm that the chromatographic conditions were good.

The chromatographic behaviour of the ion pairs depended essentially on the properties of the mobile phases and the formation and stability of the metal–126NNS complexes [4]. In this and our earlier studies [4,12–14], the reaction conditions for on-line formation of metal–126NNS complex ion pairs were optimized by manipulations of solvent effects, pH and ionic strength of the mobile phase mixture, and the concentrations of metal, ligand ions and the ammonium salt. Flow-rates of the eluent containing methanol and the ion-pair former (A and B in Fig. 1) and of the ligand solution containing the ion-pair former (C in Fig. 1) influenced the conditions to be optimized for the quantitative complexation and the metal complex ion-pair formation. The pH of the HPLC eluent was maintained between 7 and 8 to ensure optimum metal complex formation with 126NNS. This pH range also provided the best conditions for the formation of metal complexes in the eluent in desired molar ratios [12].

The eluent composition has a clear effect on the retention of the ion pairs (Figs. 2–5). Fig. 3 shows the capacity factors of the copper–, palladium–, cobalt– and iron–126NNS ion pairs to decrease linearly with increasing methanol concentration of the eluent. As the hydrophobicity of the ion pairs

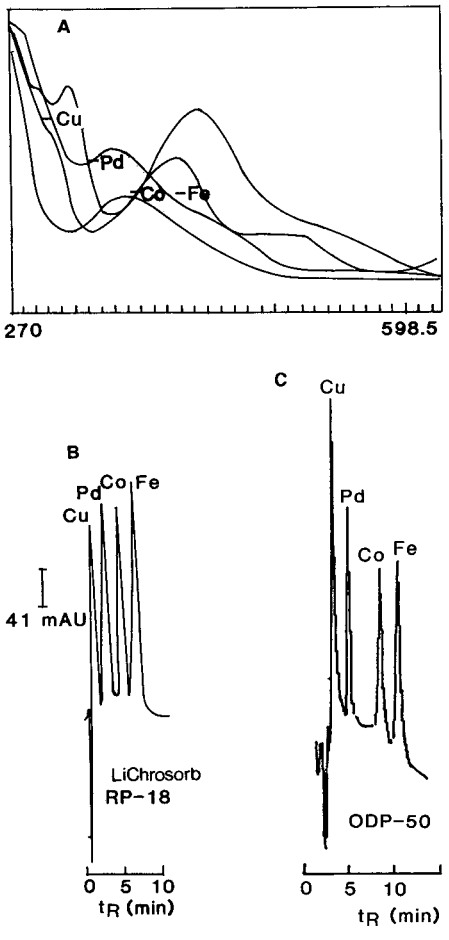

Fig. 2. Liquid chromatogram of metal ion pairs separated on ODP-50 column. (A) UV–VIS spectra of the metal ion pairs; corresponding chromatograms on (B) LiChrosorb RP-18 and (C) ODP-50. Eluent system as described under Experimental; methanol gradient, 95% (5 min) to 100% (3 min); flow-rates, (B) from LC pump 0.7 ml/min and from SP pump 0.5 ml/min; (C) from LC pump 0.5 ml/min and from SP pump 0.3 ml/min; ion-pair former, TDTMABr; length of the reactor, 5 m; detection wavelengths, 310 and 400 nm.

decreases from iron to copper, the solute retention increases in this order. The longer retention of the compounds with increased concentration of ion-pair former and with decrease in the methanol concentration was independent of the column material, *i.e.*, of octadecyl-substituted silica (LiChrosorb RP-18) and the polymer-based material end-capped with octadecyl groups (ODP-50). The ion pairs eluted more slowly, however, when the polymer material

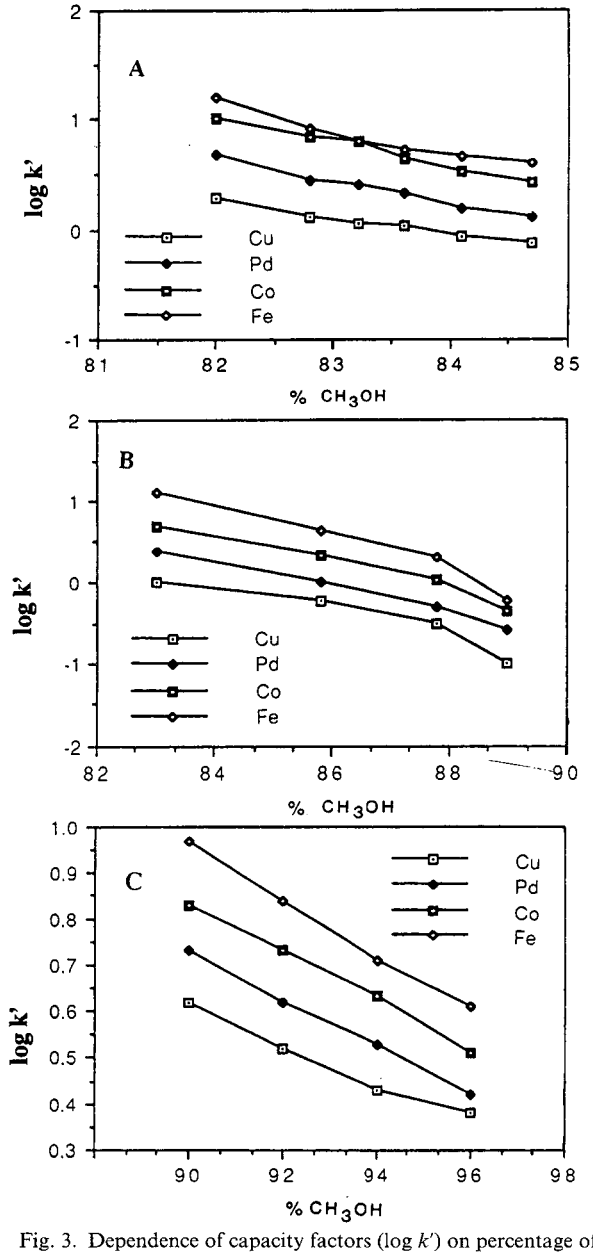

Fig. 3. Dependence of capacity factors (log k') on percentage of methanol, (A) with LiChrosorb RP-18 column; (B) without column; (C) with ODP-50 column. On-line derivatization of metal cations. Flow-rates of the eluents as in Fig. 2B. Ion-pair former, CTMABr; length of the reactor, 3 m; detection wavelength, 260 nm.

was used (Fig. 3), and a higher methanol concentration was needed to produce the same effect. If the ion-pair former concentration was higher than 0.200

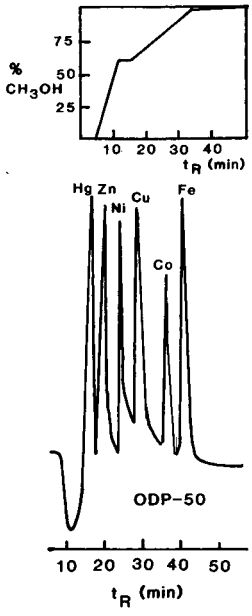

Fig. 4. Liquid chromatogram of separation of metal cations complexed with 126NNS anions and ion-paired with CTMABr. Column material, ODP-50; flow-rates of the eluents as in Fig. 2B; length of the reactor, 5 m; detection wavelength, 310 nm.

m*M*, the compounds did not elute in a reasonable time. The ligand concentration was kept as low as possible to minimize the background absorbance.

In reversed-phase ion-pair chromatography, addition of an organic ion to the system easily disturbs the chemical equilibrium in the mobile phase. This results in migrating zones of the different eluent compounds involved in the disturbance. If, for example, only one eluent component is visible to the detector, these zones will appear as negative system peaks in the visible absorption region (wavelengths below 450 nm); usually these peaks are seen in the first part of the chromatograms as in Figs. 2 and 4–6. The UV–VIS absorption of a system peak is negatively orientated on the monitor.

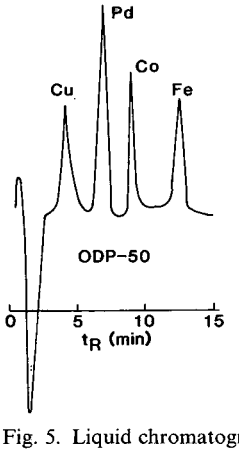

Fig. 5. Liquid chromatographic separation of metal ions as ion pairs on ODP-50 column. Gradient elution with methanol from 85% (3 min) to 95% (5 min); flow-rates, from LC pump 0.5 ml/min, from SP pump 0.3 ml/min; length of reactor, 5 m; detection wavelength, 310 nm.

Samples and technique

Conditions for the study were optimized by injecting spiked water samples into the line. The eluent flowing through the column contained only water, the ion-pair former and methanol; the ligand solution with the organic ammonium salt was continuously added to the system, through a T-piece, after the column (see Fig. 1). We assume, then, that the metal complexes, and also the ion pairs, were formed in the mixer–reactor system. The metal complexes formed after the column where the metal ions were combined with the ligand solution containing the ion-pair former. The different metal complexes, completed as ion pairs, were then separated according to their extractability [12], which was confirmed with liquid–liquid extraction studies by calculating their log K_{ex} values: Cu (13.79) > Pd (12.22) ≈ Co (12.39) > Fe (11.81).

On-line methods

As seen in Fig. 2, cobalt, copper, iron and palladium ions introduced as their salts were separated as their ion pairs by the IPC reactor system on LiChrosorb RP-18 and ODP-50 columns. It can be assumed, however, on the basis of our systematic studies and the literature [15], that the metal cations were not noticeably separated from each other in the column, although slight separation of copper and palladium was evident on the ODP column. The column worked more as a pressure regulator than a separator, providing the low flow-rates necessary for the formation of metal–126NNS complexes.

The reactor knitted from PTFE tubing provides good separation of the metal complex ion pairs, evidently because the reaction time in the mixer and the knitted reactor is long enough for metal complex formation [12] and subsequent ion-pair formation.

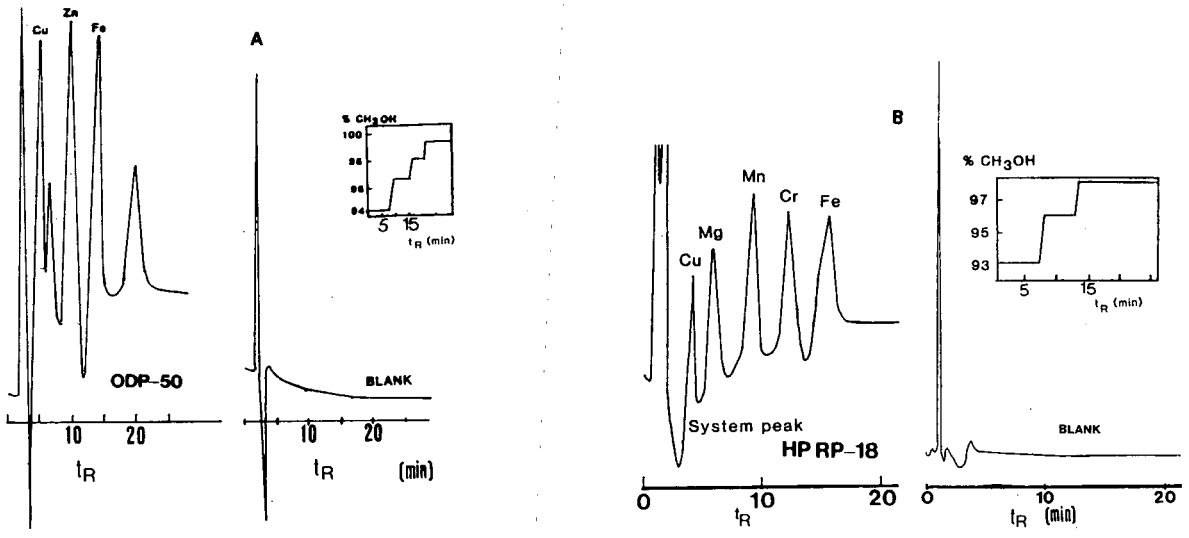

Fig. 6. Liquid chromatographic separation of metal ions by on-line derivatization technique. (A) Nutrient sticks and the reagent blank (see Experimental); column, ODP-50; flow-rates, from LC pump 0.7 ml/min and from SP pump 0.5 ml/min. (B) Health drinks and the reagent blank (see Experimental). Column, LiChrosorb RP-18; flow-rates, from LC pump 0.5 ml/min and from SP pump 0.3 ml/min; length of the reactor, 5 m; detection wavelength, 260 nm. Concentrations of metals: (A) 1 mg/l and (B) 4.7 mg/l Cu, 42 mg/l Fe, 850 mg/l Mg, 5.9 mg/l Mn and 7.0 mg/l Cr.

As can be seen in Fig. 3, the LiChrosorb RP-18 and ODP-50 columns improve the separation of the metal compounds, without effecting significant separation of the metal ions as shown by tests without a column. However, the selectivity is better with than without the column. Moreover, methanol affects the capacity factors less with the column than without it, as can be seen from the slopes of the straight lines. Although the LiChrosorb RP-18 column was good and short enough for our work, it was replaced with a five times longer ODP-50, column, which decreased the flow-rate of the mobile phase. The mixer contributes by homogenizing the eluents containing the ligand solution and the ion-pair former in water and methanol. Without the mixer the metal complex formation would be inefficient and detection of the compounds poor.

Elution

The elution order was copper, palladium, cobalt and iron. In isocratic elution the copper ion pair eluted within a few minutes and the iron ion pair in about 20 min. With an ammonium compound and methanol both present in the eluent, it was also possible to carry out gradient experiments in which the percentage of methanol was gradiently increased.

Equilibrium requirements

No attempt was made to mask the excess of ligand in the eluent by the addition of extra metal ions because the complex formation stability would have been totally confused [4,12,14]. An increased metal concentration would have changed the ionic strength, and the metal–126NNS complex ion pairs would not have been formed quantitatively because of the competition between the metals. Moreover, if a masking agent had been used, its absorbance might have been so strong as to cover the absorption of interest. The background absorption due to excess of the ligand was instead eliminated through careful stabilization of the system and zero setting of the detector.

The ion-pair former was not used in excess in the eluent because it disturbed the ion-pair equilibrium in the system and prevented the ion-pair elution, as observed with the unstable baseline on the monitor of the chromatograph and the split peaks in the chromatograms.

Gradient elution was the main method used.

However, under the conditions optimized for the formation and separation of the metal ion pairs the proportion of methanol had to be greater than 50%, otherwise, the peaks were broad and retention times long. The more water in the eluent, the less likely was the metal ion pair to elute as a single peak, and conversely, the more methanol the eluent contained, the shorter was the analysis time. A short analysis time is essential for routine methods.

Detection limits

For the purposes of this work, the detection limit was considered to be the minimum concentration at which the minimum abundance for the detector (1.0 mAU) was exceeded. Using the detector at 260 nm, the detection limit (signal-to-noise ratio 2) for the cobalt–126NNS ion-pair was 69 n*M*, for palladium 50 n*M*, for copper 43 n*M* and for iron 76 n*M*. The response was linear from the detection limit up to the maximum concentrations tested, *i.e.*, for copper, palladium, cobalt and iron ion pairs 43–870, 50–950, 69–980 and 76–1120 n*M*, respectively. The relative standard deviation at the detection limit was 4.3, 5.0, 6.9 and 7.6 n*M* for copper, palladium, cobalt and iron, respectively. The reproducibility was within 1–3%. The results of the method applied to simulated samples are summarized in Table I and show that the on-line derivatization is useful even when small concentrations are to be detected.

In addition to copper, cobalt, palladium and iron we studied nickel, mercury and zinc. As seen in Fig. 4, all three metals were eluted within 25 min under gradient elution conditions. All seven metals formed low-UV absorbing complexes with 126NNS, but with nickel coloured metal complexes with different metal to ligand molar ratios were formed, depending on the eluent content and its pH.

Applications

Our on-line complexation and ion-pairing system with optimized gradient elution was tested on health drinks and nutrient sticks. Before injection into the chromatograph, the organic materials were carefully acid hydrolysed to eliminate background absorbance. The chromatograms obtained are shown in Fig. 6A and B and standard addition plots are presented in Fig. 7. To study the usefulness of the method, four samples were prepared of each matrix and ten injections were made for each sample. Compared with the precolumn method described previously [14], the conditions for this study proved more difficult to optimize. The present method is nevertheless suitable for routine use and, once the chromatographic conditions have been optimized to produce stable metal ion pairs and to separate them, provides sufficient sensitivity for detection. The selectivity of the method can be exploited by modifying the detection wavelength according to the compound of interest. As the column pressure is low even in sequential runs, and elution occurs at pressures below 160 bar, the ion-pair compounds are eluted more slowly than in the precolumn system [14]. Accordingly, the peaks in the chromatograms tend to be broad.

TABLE I

THE RESULTS OF THE METHOD APPLIED TO SIMULATED SAMPLES

Metal	Metal concentration (μg/ml)	Metal-complex ion concentration (μg/ml)	Recovery (μg/ml) (mean ± S.D.)	Recovery (%)
Copper	2.73	42.3	36.3 ± 1.9	85.8
	553	857	852 ± 7.7	99.5
Palladium	5.32	54.1	48.8 ± 3.4	90.2
	101	1028	1022 ± 30	99.4
Cobalt	4.06	105	95.9 ± 5.8	91.3
	57.7	1492	1489 ± 29	99.8
Iron	4.24	116	97.7 ± 5.2	84.2
	62.6	1702	1695 ± 20	99.6

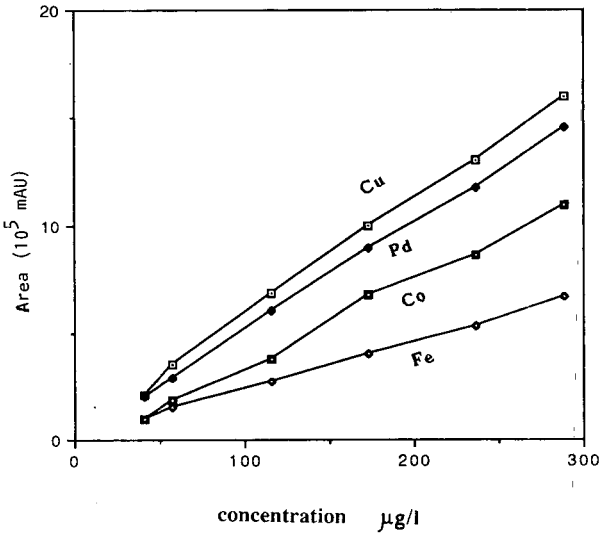

Fig. 7. Standard addition plots for copper, cobalt, iron and palladium.

CONCLUSIONS

The on-line method described here is useful for the determination of copper, cobalt, iron and palladium in mixtures. The equilibria of metal complex and ion-pair formations in the mobile phase governed the retention of the ion pairs. Therefore, the ion pairs were formed simultaneously and quantitatively only in the pH range 7–8. The selectivity of the method was enhanced by the reaction of the metal, the ligand and the ion-pair former in the mixer–reactor system. The detector response for copper, palladium, cobalt and iron was linear up to concentrations of 10 μM. In spiked water–methanol samples the detection limits for these metals ranged from $1 \cdot 10^{-3}$ mg/l to 1 mg/l. The method can also be applied to samples containing zinc, nickel and mercury. Our present and earlier [4,14] findings show the on-line complexation and ion-pairing techniques to be more useful than time-consuming liquid–liquid extraction of ion pairs and metal complex formation before injection. By optimizing the eluent flow-rate and the methanol content, band broadening in the on-line mixer–reactor system was minimized and the peak tailing of the ion pairs was avoided.

REFERENCES

1 A. Munder and K. Ballschmiter, *Fresenius' Z. Anal. Chem.*, 323 (1986) 869.
2 G. Schwedt and P. Schneider, *Fresenius' Z. Anal. Chem.*, 325 (1986) 116.
3 S. Ichinoki, N. Hongo and M. Yamazaki, *Anal. Chem.*, 60 (1988) 2099.
4 H. Siren and M.-L. Riekkola, *Mikrochim. Acta, Part II*, (1989) 77.
5 M. E. D. Rey and L. E. Vera-Avila, *J. Liq. Chromatogr.*, 11 (1988) 2885.
6 B. D. Karcher and I. S. Krull, *J. Chromatogr. Sci.*, 25 (1987) 472.
7 X. X. Zhang, M. S. Wang and J. K. Cheng, *Anal. Chem.*, 60 (1988) 1670.
8 X. X. Zhang, M. S. Wang and J. K. Cheng, *J. Chromatogr. Sci.*, 26 (1988) 517.
9 J. R. Poulsen, K. S. Birks, M. S. Gandelman, J. W. Birks, *Chromatographia*, 22 (1986) 231.
10 C. M. Selavka, K. S. Jiao and I. S. Krull, *Anal. Chem.*, 59 (1987) 2221.
11 H. M. M. Siren and M. M. Shapi, *Thermochim. Acta*, 102 (1986) 239.
12 H. Siren and M.-L. Riekkola, *Mikrochim. Acta, Part III*, (1986) 159.
13 H. Siren, R. Dammert and L. Huhanantti, *Fresenius' Z. Anal. Chem.*, 332 (1988) 245.
14 H. Siren, *Chromatographia*, 29 (1990) 144.
15 K. C. van Horne (Editor), *Sorbent Extraction Technology, Handbook*, Analytichem International, Harbor City, CA, 1985, Sect. 4.

Journal of Chromatography, 590 (1992) 271–288
Elsevier Science Publishers B.V., Amsterdam

CHROM. 23 760

Activity testing and surface characterization of pretreated fused-silica capillaries for gas chromatography

A new modification of existing intermediate column tests☆

Gerard Rutten and Jacques Rijks*

Eindhoven University of Technology, Laboratory of Instrumental Analysis, P.O. Box 513, 5600 MB Eindhoven (Netherlands)

(Received July 26th, 1991)

ABSTRACT

A new modification of existing intermediate capillary column tests for uncoated columns is presented. A short (1 m), thick film (2 μm) precolumn is coupled to the column to be tested. The use of a short precolumn results in a rapid test. This makes it attractive in terms of time to inject the test compounds separately, thus excluding mutual influences, in diluted solutions spiked with *n*-alkanes as references. Moreover, the short precolumn gives sharp Gaussian injection profiles on the second column. A simple versatile coupling device has been developed, which permits easy control and adjustment of pressures and carrier flows, monitoring of the effluents of the precolumn and introduction of sharp input bands on the second column. The monitor detector accurately shows the shape and time of introduction of the compounds on the second column. This permits the evaluation of peak distortion, peak shift and yield on the second column. Test compounds were selected on the basis of their physico-chemical properties (vapour pressure, acid–base properties, dipole moments, hydrogen bonding, complexation with metals, etc.). A number of differently pretreated capillaries were tested with these compounds under various external conditions. Accurate quantification and qualification of the activity of the capillary present difficulties. The test is a case of nearly ideal non-linear chromatography. When peaks of different sizes are superimposed, the tails lie on a common envelope. The k' of the end of the tail is fixed, irrespective of the amount injected, and forms an important parameter in the evaluation. Reconstruction of the chromatogram with a k' scale instead of a time scale eliminates the influence of carrier velocity and column length. The method is a sensitive tool for intermediate column testing and shows promises for surface characterization.

INTRODUCTION

For a number of years this laboratory has been studying the mechanisms of deactivation reactions for fused-silica capillary columns using fume silica as a model material and ^{29}Si magic angle spinning NMR [1–5]. The use of a model material is inevitable as hardly any spectroscopic or surface analysis method is available to study the interior of a capillary column. However carefully the situation inside a capillary column was imitated, the results were obtained under artificial conditions and the application of the NMR results to fused-silica columns remains conjectural. It is therefore important that this relationship is established more clearly.

Gas chromatography (GC) is an excellent method for studying the adsorptive properties of small surface areas [6], such as the internal surface of a capillary column. Present test methods for capillary columns, however, focus on the general analytical performance rather than on the surface activity and do not provide specific information. It is attractive to develop existing column tests further in this respect.

☆ Presented at the *18th International Symposium on Chromatography, Amsterdam, September 23–28, 1990*. The majority of the papers presented at this symposium have been published in *J. Chromatogr.*, Vols. 552 and 553 (1991).

0021-9673/92/$05.00

Column tests

Ideally, any compound that can be volatilized without decomposition should be amenable to GC analysis. In practice, however, the shape, area and position of a peak are often affected by adsorption (reversible physisorption or irreversible chemisorption) and by decomposition or transformation of the analyte. A column test should be able to reveal the exact nature and extent of this activity. For general use tests should be standardized and universal, and the results should be expressed in numerical form.

In tests for adsorption a number of polar compounds are injected, either separately or as a mixture. The Grob "comprehensive quality test" [7,8] is well documented and standardized and generally applicable to a wide range of columns. A severer test was introduced by Lee and co-workers [9,10]: two mixtures of test probes were used, one containing basic compounds and the other acidic compounds.

Tests for catalytic activity [11–15] are based on the decomposition of labile compounds. The choice of the probes seems fairly accidental: the various workers used compounds which happened to cause problems in their regular analytical work. Chromatographic determination of the decomposition rate constant of a labile compound [12–14] gives an very valuable, absolute measure of catalytic activity.

Testing an uncoated column is another attractive option: (i) the pretreatment can be studied without the interfering effects of the stationary phase, (ii) the test can be performed at lower temperatures and (iii) much time can be saved because the lengthy coating procedure can be omitted. It is therefore very suitable as an intermediate test between pretreatment and coating. The introduction of the test probes presents difficulties: because of the lack of a stationary phase one cannot inject a mixture of test probes or diluted solutions. Undiluted test probes can be injected at high splitting ratio [16] or headspace vapour of the test probe [17,18] at normal splitting ratios. Schomburg *et al.* [19] placed a coated column before the uncoated column. Thus, injection of diluted solutions or of full test mixtures [20–24] is possible.

Silica surface and choice of the test probes

In order to be informative, the behaviour of the test probes must reflect the state of the fused-silica surface. The surface of silica is characterized by two types of surface groups: siloxanes (≡Si–O–Si≡) and silanols [≡SiOH or $=Si(OH)_2$]. The silanols are relatively acidic and constitute the strongest adsorption sites. Their acidity, concentration and closeness may change their adsorptive properties considerably. On a fully hydroxylated silica the OH concentration is about 8.2 μmol/m^2 [25], a quarter of which form part of a $=Si(OH)_2$ [26]. About half of all hydroxyls are close enough (<3.1 Å) to form a mutual hydrogen bond. These "bonded" hydroxyl groups are less adsorptive [27,28] and on heating they easily split off water, forming strained, active siloxanes. Fused-silica columns, which are drawn at about 1900°C, are largely dehydroxylated and contain only 0.31 μmol OH/m^2 [29]. Rehydroxylation of a dehydroxylated silica surface is possible, but it is a slow process. Standard procedures have been published [30]. Rehydroxylation, *e.g.*, by hydrothermal treatment, is common in capillary column preparation [31].

The probes should therefore be sensitive to the hydroxylation, the acidity, the catalytic activity and the metal impurities of the surface. Monofunctional, sterically unhindered probes preclude ambiguous results. However, on a chemically modified surface, steric hindrance of the functional group may be useful to study the accessibility of remaining adsorptive sites.

To test the polarity of the surface, probes with a large permanent dipole moment can be used, such as amides, nitro compounds, nitriles and sulphoxides. Few or none of these have been used in capillary column tests. Polar interactions between molecules are now often formulated as donor–acceptor or Lewis acid–base interactions rather than dipole interactions [32], and this concept has been applied to glass and silica [33].

Aldehydes and ketones are useful probes for hydrogen bonding [22–24]. The hydrogen bond capacities of silanol groups can also be studied with alcohols. Alcohols are good probes for "free" silanols, but they adsorb less at "bonded" or at hydrated silanols. Alcohols also interact with siloxane bridges, especially strained ones. It was demonstrated [34] that this type of interaction, which may lead to chemisorption, is even the preferred one at low coverages. As the surface of a fused-silica capillary column is largely dehydroxylated, such (chemi)sorption of alcohols is probably important.

To probe the surface acidity, organic bases are commonly used: strong bases (using the pK_a value in water as an indication of basicity) such as primary alkylamines (10.5–10.8)[a], aromatic nitrogen compounds such as pyridine, picolines and lutidines (5.25–7.0) and aromatic amines such as aniline, toluidines and xylidines (3.9–5.2). Alkaloids (pK_a 8–9) can be used to fill the gap between pK_a 7 and 10, *e.g.*, nicotine (8.0), but alkaloids are usually not monofunctional and may not give unequivocal results. In a (Lewis) acid–base scheme of test probes ketones, esters, (cyclic) ethers, (cyclic) sulphides, amides, nitriles, aromatic hydrocarbons, etc., must also be considered as bases.

Basic sites on the surface (which are not likely to occur on fused silica) can be probed with organic acids. Carboxylic acids (pK_a 4.7–4.9) are often used. Lower pK_a values are met with α-chlorocarboxylic acids. Unfortunately, carboxylic acids readily cause overloading problems on the precolumn. Phenol, cresols and xylenols are only weak acids (pK_a 9.9–10.6). Chloro- and nitro-substituted phenols have lower pK_a values (7.1–9.2), but also high boiling points. In an acid–base scheme of test probes, aliphatic and aromatic nitro compounds, alcohols and chloroform must also be considered as acids.

In high-purity fused silica, the total metal oxide content is less than 1 ppm, but in less pure qualities it may mount to 100 ppm. Liquid chromatographic packings have been tested for transition metals using metal-complexing probes such as diketones, sulphides, 2,2′-bipyridine and thiols [36]. Such probes have not been used in capillary GC.

Choice of test conditions

Judicious choice of the GC conditions contributes to standardization. The most important variables are carrier velocity and temperature.

Carrier velocity cannot be varied as easily as temperature. As a rule, most GC analyses are executed at velocities near or above the optimum velocity and so are column tests. The use of the optimum velocity minimizes dispersion effects, so that peak broadening due to adsorption processes is clearly visible.

Temperature markedly influences column activity: at high temperatures reversible adsorption decreases whereas catalytic decomposition increases [37]. Most tests for adsorption use moderate temperatures of 60–100°C. Following the practice of static adsorption measurements, the saturated vapour pressure of a test probe could be used as an indicator of the temperature of the test or, conversely, having fixed a temperature, for the selection of the test probes. In the Grob comprehensive test the programming rate is carefully adjusted to the column length in order to maintain constant elution temperatures. The figures we found in a particular case (see Table I) suggest a standardization to a vapour pressure of 1–5 mmHg. In our experience, vapour pressures up to 10 mmHg can still be used in isothermal tests. Many familiar test probes such as decylamine, phenol, octanol, nonanal and 2,3-butanediol have vapour pressures of 5–10 mmHg at 60–100°C. Injection of the probes with a splitter presents no problems at this range of temperatures and vapour pressures.

We prefer isothermal test conditions to programmed temperature conditions. In isothermal operation parameters such as carrier flow, temperature and column dimensions are independent of each other, whereas in a programmed run they are intertwined with each other in a complicated manner. An isothermal test allows (i) easier adaptation of the conditions to a wide range of column dimensions, (ii) severer conditions matching the activity of

TABLE I

ELUTION TEMPERATURES OF A GROB TEST

Column: 7 m × 0.32 mm I.D., deactivated PS-122, 0.14 μm SE-54.

Test probe	Elution temperature (°C)	Corresponding vapour pressure (mmHg)
2,3-Butanediol	43.6	1.0
n-Decane	53.6	9.2
n-Octanol	60.5	1.8
n-Undecane	63.3	6.3
Nonanal	63.6[a]	5.1
2,6-Dimethylphenol	63.6[a]	2.1
2-Ethylhexanoic acid	68.7	0.6
2,6-Dimethylanaline	69.9	4.3
Methyl caprate	92.1	4.7
Dicyclohexylamine	101.0	4.9
Methyl laurate	117.6	4.9

[a] Co-elution.

[a] pK_a values taken from ref. 35.

the column, (iii) fundamental interpretation of surface–probe interactions and (iv) studies of chemisorption or catalytic activity.

Precolumn and coupling device

Isothermal conditions limit the choice of probes to those having about the same vapour pressure at the selected temperature of the test. This hampers the formulation of comprehensive mixtures, because probes with about the same vapour pressure will probably co-elute on apolar columns.

If one uses a short, thick-film precolumn, just long enough to separate the test probe from the solvent and a pair of *n*-alkane standards, a test run takes little time. A selected number of test probes can be injected separately in the same time otherwise required to chromatograph a comprehensive mixture. One may fix the vapour pressure and adjust the temperature for each, separately injected, probe. Moreover, a thick-film column usually shows good elution profiles and permits large amounts to be injected.

A straight connection of the precolumn and test column is not attractive: to obtain reference chromatogram of the precolumn it must be disconnected and fed directly into the detector. It is much more convenient to divert part of the effluent from the precolumn permanently to a monitor detector. This permits detailed study of the effect that the second column has on the peak shape, peak area and retention. Moreover, if the columns are connected directly to each other, the carrier flows in the columns cannot be adjusted independently. A coupling device should permit (i) independent control of carrier flows, (ii) monitoring of the precolumn and (iii) easy exchange of the columns to be tested.

A commercial two-dimensional double-oven chromatograph has been used to good purpose in the intermediate test [23,24]. The use of two ovens is especially advantageous. However, its coupling device has been designed for two-dimensional chromatography with quantitative transfer and "live" switching without monitoring. Consequently, it requires careful adjustment of carrier and purge flows. Therefore, we developed a simple, versatile coupling device, which allows easy adjustment of flows and easy and frequent exchange of a wide range of the test columns.

Evaluation

Standard column tests rarely offer procedures for accurate quantification of column activity. Chromatograms obtained from an "intermediate" test of an uncoated column usually show very pronounced effects of peak shift and skew, which have a strong visual impact. On closer examination, however, accurate quantitative and qualitative evaluation of the results presents difficulties: peak position, width and tailing vary considerably with the amount injected. A test of an uncoated capillary column is a case of nearly ideal, non-linear gas–solid chromatography: the dispersion by the capillary being negligible, peak shape and peak position are determined solely by the form of the adsorption isotherm. Methods are available, although not common practice in capillary GC, to determine the adsorption isotherm from the shape of the peak [6,38].

Extreme tailing of a peak is an indication of heterogeneity of the sites. Heterogeneity of the surface hampers the application of peak-shape parameters derived from simple adsorption models [39,40]. Surface heterogeneity can also be studied by GC, resulting in adsorption energy distribution functions of the sites [41,42]. This has been used in the definition of a surface selectivity triangle representing acidic, basic and dipolar interactions [43,44]. Another approach to determining heterogeneity of the sites is "gas-phase titration" in which the most active sites are blocked with a known amount of an amine [45].

Inverse gas chromatography (IGC) has also been used in the study of modified silicas [24,46]. IGC requiring symmetrical elution profiles uses probes at infinite dilution and studies mainly dispersion (London) or weak polar interactions at near-zero coverage.

In this paper, however, only simple parameters based on the shift, tailing and area of the peak will be considered in relation to chromatographic conditions such as temperature, carrier flow and column dimensions.

EXPERIMENTAL

Materials and equipment

The coupling device (Fig. 1a) consists of a quartz glass tube (5 cm × 2 mm I.D. × 4 mm O.D.) deactivated with PS 122 [a poly(methylhydrosilox-

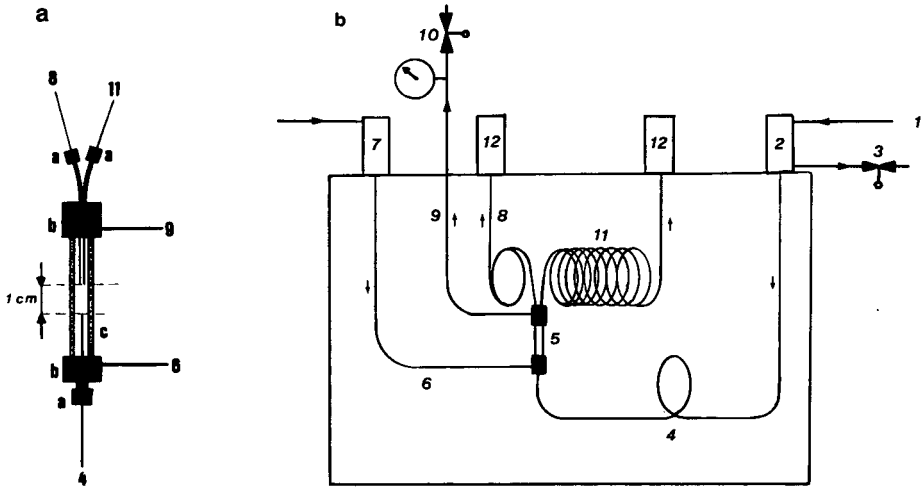

Fig. 1. (a) Coupling device and (b) arrangement for testing. Identification (for dimensions see text): 1 = carrier in (He); 2 = injector (splitter); 3 = split vent valve; 4 = precolumn; 5 = coupling device; 6 = purge gas line; 7 = second injector supplying purge gas; 8 = monitor line; 9 = vent line; 10 = needle valve and manometer; 11 = test column; 12 = flame ionization detector. a, 1/16-in. Swagelok connector; b, 4-mm coupling; c, quartz tube.

ane); Petrarch Systems, Bristol, PA, USA]. Couplings are fixed to the quartz tube with nuts and polyimide ferrules. One carries a soldered purge gas line and a 1/16-in. Swagelok connector for the precolumn, and the other one a soldered vent line and two soldered metal capillaries (2 cm × 1 mm O.D. × 0.5 mm I.D.) provided with 1/16-in. Swagelok connectors for monitor line and test column. These capillaries greatly facilitate alignment and exchange of the test column. Precolumn, monitor line and test column are positioned to a mutual distance of 1 cm. Control of carrier flow in the second column can be obtained by addition of purge gas and/or venting. This also allows the introduction of very small amounts on the second column (as a result of splitting in the device) and sharp input bands (by using high carrier velocities in the first column).

The coupling device was mounted in a Mega 5300 gas chromatograph (Carlo Erba, Milan, Italy) equipped with two flame ionization detectors and a conventional splitter injector (Fig. 1b). A second injector supplied the purge gas. The precolumn was 1.1 m × 0.31 mm I.D. with 2-μm chemically bonded 100% methylsilicone (CP-Sil 5 CB; Chrompack, Middelburg, Netherlands). The monitor line was 0.25 m × 84 μm I.D. fused-silica tubing (Siemens, Karlsruhe, Germany) deactivated with PS 122, following the same procedure as for column E (see *Columns*).

Chromatograms were evaluated and stored on disk with a PE-Nelson 2100 integration system in the dual-channel mode (PE-Nelson Systems, Cupertino, CA, USA).

Test probes

The probe substances were dissolved in carefully redistilled analytical-reagent grade cyclohexane (E. Merck, Darmstadt, Germany) at concentrations of about 20 and 2 mg/ml. For some polar substances dichloromethane or tetrahydrofuran had to be used as solvents. Each probe is accompanied by four *n*-alkanes, which surround the peak in the chromatogram. Table II gives an overview of the compounds and some physico-chemical properties pertaining to the test.

Columns

To explore the possibilities of the system, five fused-silica capillary columns were pretreated in different ways (see Table III).

Column A was used as received and not pretreated.

Column B was hydrothermally treated: at 100°C deionized water from a Milli-Q system (Millipore, Bedford, MA, USA) was forced through the column

TABLE II

TEST PROBES

Compound	Concentration, 2% solution (mg/ml)[a]	Alkanes added Carbon numbers				Temperature (°C)[b]				pK_a (25°C)[c]
						5 mmHg	10 mmHg	20 mmHg	760 mmHg	
Nonanal	20.40	9	10	12	13	58.4	71.6	85.0	185.0	
p-Tolualdehyde	(3.98)	9	10	12	13	67.6[d]	81.4	96.3	204–205	
Caprylonitrile	20.49	9	10	12	13	68.2[e]	81.8	96.5	206.9	
Pelargononitrile	20.77	10	11	13	14	83.2[e]	97.0	112.2	226.6	
p-Toluonitrile	19.84	9	10	12	13	71.3	85.8	101.7	217.6	
Phenol	20.44	8	9	11	12	62.5	73.8	86.0	181.9	9.89 (20°C)
Valeric acid	19.84	7	8	10	11	67.7	79.8	93.1	184.4	4.82
2-Chloropropionic acid	20.38	8	9	11	12	68.5[d]	80.3	93.3	184–187	2.83 (18°C)
p-Toluidine	20.13	8	9	11	12	68.2	81.8	95.8	200.4	5.08
Heptanol	20.32	8	9	11	12	64.3	74.7	85.8	175.8	
1,2-Propanediol	21.40[f]	6	7	9	10	70.8	83.2	96.4	188.2	
1,3-Propanediol	21.70[g]		7	9	10	87.1	100.6	115.5	214.2	
2,3-Butanediol	19.96[f]		7	9	10	68.4	80.3	93.4	182.8	
1,2-Pentanediol	19.36[f]	7	8	10	11	88.6[d]	101.0	114.4	206–210	
Octanethiol	20.21	9	10	12	13	63.3[d]	77.0	91.8	199.1	
p-Thiocresol	20.73	9	10	12	13	57.7[d]	71.5	86.5	194–195	8.03[h]
Nitrobenzene	19.86	9	10	12	13	71.6	84.9	99.3	210.6	3.98 (0°C)
3-Butylpyridine	20.54	10	11	13	14	72.4[d]	85.8	100.4	205–208	5.72–5.75[i]
Quinoline	19.76	11	12	14	15	89.6	103.8	119.8	237.7	4.90 (20°C)
Nonylamine	20.16	10	11	13	14	66.7[j]	97.0	112.1	220.5	10.64
Decylamine	20.21	11	12	14	15	83.0[j]	97.0	112.1	220.5	10.64
1,7-Diaminoheptane	20.61	10	11	13	14	85.0[d]	98.7	113.7	223–225	11.86, 10.76[k]

[a] 0.2% Solution made by tenfold dilution of a 2% solution.
[b] Data from ref. 47.
[c] pK_a values from ref. 35.
[d] Data from *Beilstein*, fitted according to Hass and Newton in ref. 35, p. D-186.
[e] Interpolated from ref. 48.
[f] Solvent dichloromethane.
[g] Solvent of 2% solution tetrahydrofuran is 0.2% solution dichloromethane.
[h] Data from ref. 49.
[i] Estimated from 3-methyl- and 3-ethylpyridine (*Beilstein*).
[j] Interpolated from ref. 50.
[k] $pK_{a,2}$ and $pK_{a,1}$ values, respectively, of 1,6-diaminohexane (*Beilstein*).

TABLE III

COLUMN TREATMENTS

Column	Supplier	Length (m)	I.D. (mm)	Treatment
A	Siemens	14	0.32	None
B	Siemens	14	0.32	Hydration: water (flow), 100°C, 5 h Drying: vacuum, 90°C, overnight
C	Polymicro	14	0.32	Acid leach: 10% HCl, 150°C, 1 h Drying: helium flow, 200°C, 2 h
D	Polymicro	14	0.32	Hydration: as for B Deactivation: D4, 390°C, 4 h + 405°C, 2 h
E	Polymicro	7	0.32	Half of column C (acid leached) Deactivation: PS 122, *ca.* 40 nm, 290°C, 2 h

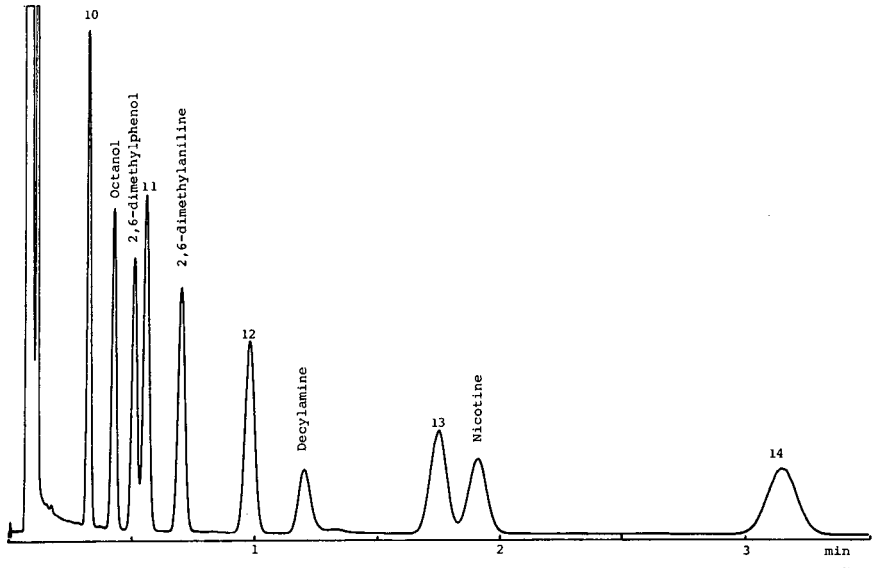

Fig. 2. Polarity mixture on the precolumn (recording of the monitor detector). Peak identification as in Fig. 3a.

at a rate of 0.2 ml/min for 5 h. Then the column was dried under vacuum at 90°C overnight.

Column C was treated with acid: 90% of the column was filled with 10% (w/w) hydrochloric acid (Merck Suprapur), flame sealed at both ends and heated at 150°C for 2 h. Then the column was opened, rinsed with deionized water and dried at 200°C for 2 h under a helium flow.

Column D was hydrothermally treated as described for B, and then deactivated with octamethylcyclotetrasiloxane (D4) (ABCR, Karlsruhe, Germany). The column was coated dynamically with pure D4 at a rate of 1 cm/s using nitrogen pressure. After coating, the column was purged for a few minutes with nitrogen, flame sealed and heated in a nitrogen atmosphere at 390°C for 4 h followed by 405°C for 2 h. Then, the column was rinsed with *n*-pentane and dried.

Column E was half of column C and was deactivated with polymethylhydrosiloxane (PMHS): the column was coated dynamically with a 2% (w/w) solution of PS 122 (Petrarch) in *n*-pentane at a rate of 1 cm/s. According to Bartle [51], this results in a film thickness of *ca.* 40 nm[a]. After coating, the column was flushed with nitrogen for 30 min, flame sealed and heated at 290°C for 2 h. Then the column was opened, rinsed copiously with *n*-pentane and dichloromethane and dried.

Performance of the system

Operation of the system and testing procedure. The inertness and performance of the system were checked by injection of a polarity mixture (Fig. 2). All critical compounds (octanol, decylamine, nicotine) show symmetrical peak shapes and correct peak areas.

As a rule, the following procedure was adopted: for each test probe two chromatograms were recorded, injecting 1 μl of the 2% and 0.2% solutions. Depending on the activity of the column, the oven was set to a temperature at which the saturated vapour pressure of the test probe was 5, 10 or 20 mmHg (in rare cases 1 or 40 mmHg). The temperature of the injector was set to the boiling point of the test probe. The mean carrier velocity of the test column was adjusted to about 40 cm/s and the carrier velocity of the precolumn was regulated in such a way that the last *n*-alkane eluted within 5–10 min. The splitting ratios of the precolumn injector and the coupling piece were both adjusted to about 1:40, resulting in an overall splitting ratio of about 1:1600. Injection of 1 μl of the 0.2% and 2% solutions then results in column loads of 2 and 20 ng,

[a] Assumed viscosity $1.8 \cdot 10^{-3}$ kg/ms, surface tension $2.5 \cdot 10^{-2}$ N/m.

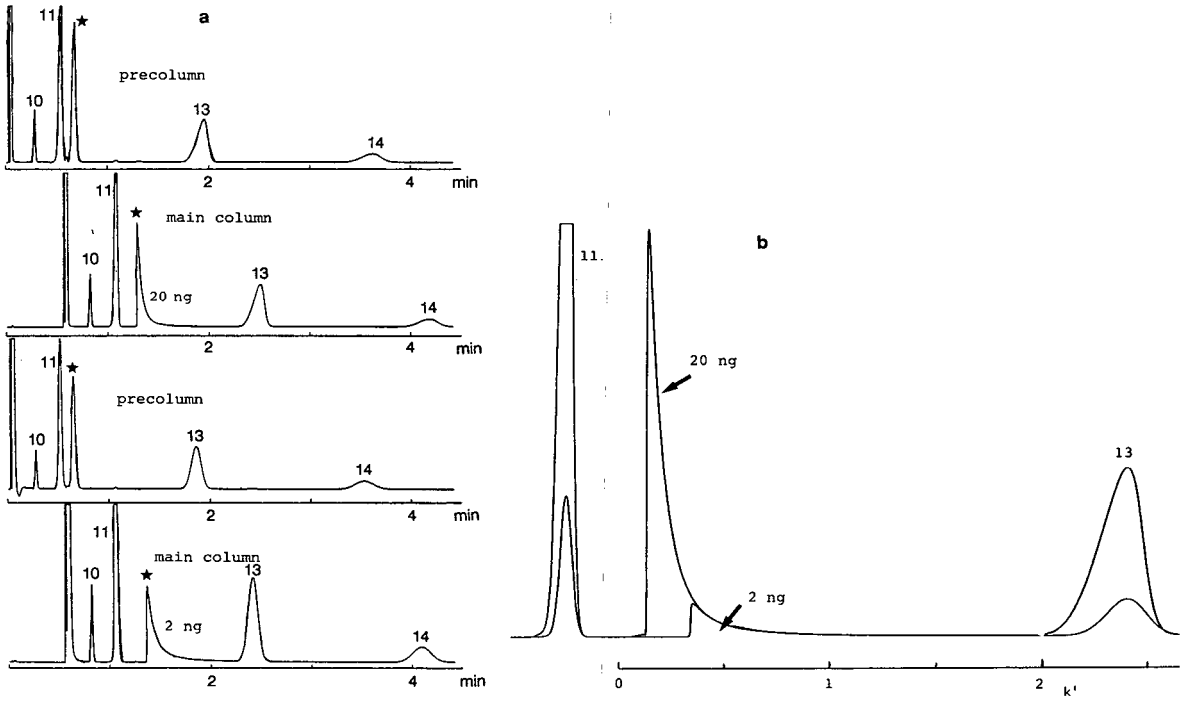

Fig. 3. (a) Operation of the system (nonylamine on column D, 94°C, 20 mmHg). Column load: upper pair of chromatograms, 720 ng (precolumn) and 20 ng (test column); lower pair of chromatograms, 72 ng (precolumn) and 2.0 ng (test column). Peak identification: the test probe is marked with an asterisk and *n*-alkanes are indicated with their number of carbon atoms. (b) Superimposed nonylamine peaks in (a) (capacity factor scale relates to nonylamine); peak identification as in (a).

respectively (accounting for evaporation of an additional 0.4 μl from the needle). Fig. 3a and Table IV give a typical example of the operation of the system,

TABLE IV

EXAMPLE OF FLOWS AND VENTS (SEE FIG. 3a)

Column D, 94°C, normalized flows (20°C, 1 atm). Numbers in parentheses refer to items in Fig. 1.

Parameter	Value
Precolumn inlet pressure (2)	54 kPa (gauge)
Split vent, injector (3)	133 ml/min
Precolumn flow (4)	3.4 ml/min
Splitting ratio, injector	1:39
Coupling piece pressure (5)	39 kPa (gauge)
Purge gas flow (6)	65 ml/min
Monitor line flow (8)	0.5 ml/min
Vent, coupling piece (9)	66 ml/min
Test column flow (11)	1.85 ml/min
Splitting ratio, coupling piece	1:36
Overall splitting ratio	1:1400

using column D and nonylamine as a test probe.

Selection of the amount to be injected. On comparison of the injections of the 0.2% and 2% solutions, notable differences in peak shift and peak shape are observed. Fig. 4a gives an example with toluonitrile on column B. However, if the chromatograms are superimposed, it turns out that the tails of the peaks coincide (Figs. 3b and 4b). It appears that this is a case of almost ideal non-linear gas–solid chromatography with a concave adsorption isotherm (towards the c_g axis) without inflection points. The capacity factor k'_f of the front edge depends on the loading factor L_f[a] [40]. Consequently, the retention time of the peak top or the front edge cannot be used as a parameter. However, it is advisable to inject several concentration levels of the test probe in order to obtain an idea of the loadability and the number of active sites of the test column. The end of the

[a] L_f is defined as the ratio of the sample amount to the amount of sample required to saturate the column.

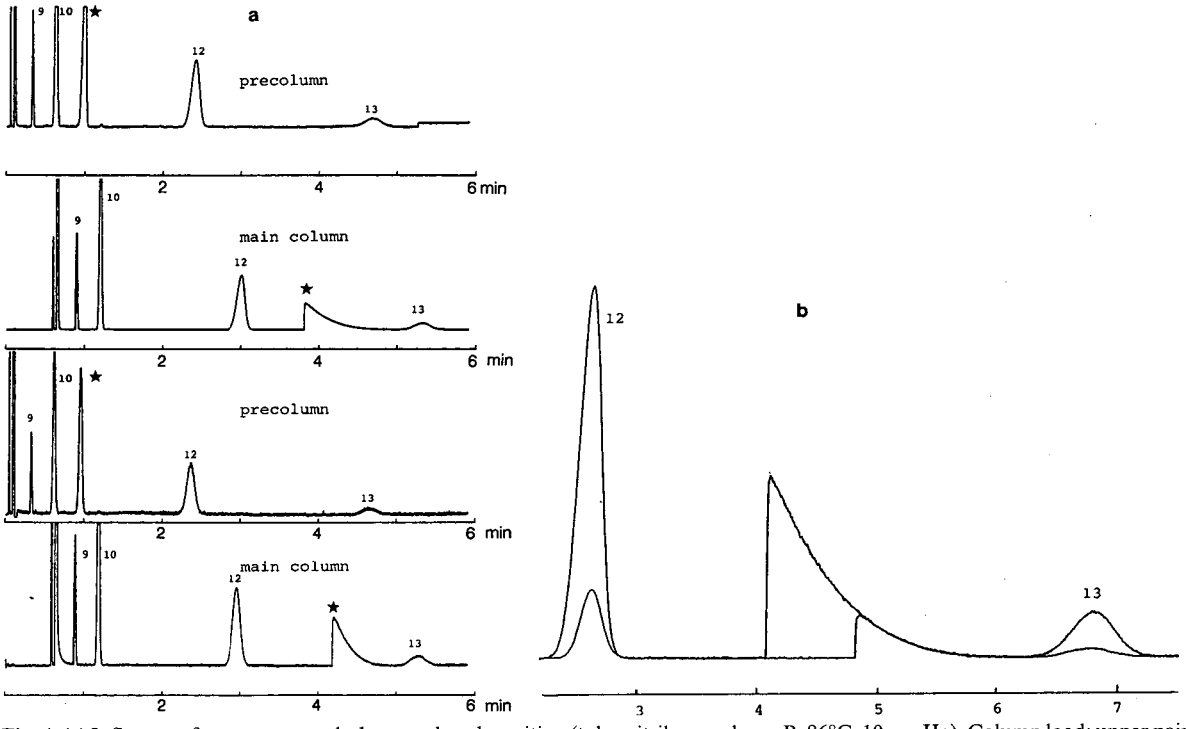

Fig. 4. (a) Influence of amount on peak shape and peak position (toluonitrile on column B, 86°C, 10 mmHg). Column load: upper pair of chromatograms, 660 ng (precolumn) and 14 ng (test column); lower pair of chromatograms, 77 ng (precolumn) and 1.6 ng (test column). Peak identification as in Fig. 3a. (b) Superimposed toluonitrile peaks in (a) (capacity factor scale relates to toluonitrile).

peak, in contrast, is fixed: its capacity factor k'_0 depends on the initial slope of the adsorption isotherm. The toluonitrile peaks (Fig. 4b), for instance, end at $k'_0 = 6.1$, but the ends of the nonylamine peaks (Fig. 3b) are lost in the elongated tail and cannot be determined exactly.

Appearance of the chromatogram and selection of carrier flows. The appearance of the chromatogram may be misleading: shift and tailing of a peak should not be judged at a glance. Especially the carrier flow of the precolumn affects the chromatogram strongly. Fig. 5a (caprylonitrile on column C) gives a typical example: when the carrier velocity was increased from 12.5 to 42 cm/s, the caprylonitrile peak shifted from a position between C_{10} and C_{12} to a position between C_{12} and C_{13} and the width of the tail was doubled relative to the widths of the *n*-alkane peaks. However, if we reconstruct these chromatograms with a k' axis instead of a real-time axis, the peaks almost coincide (Fig. 5b).

Quantitative aspects. The yield (Y_i) of a test probe can be defined as the ratio of the amount that enters the test column and the amount that elutes from it. Assuming that the coupling device splits all compounds in the same proportions between vent, monitor line and test column, Y_i can be calculated from the peak areas (A):

$$Y_i = (A_{i,p}/A_{i,t})/(A_{s,p}/A_{s,t})$$

where the subscript p refers to the precolumn, t to the test column, i to the test probe and s to a non-adsorbed standard, *e.g.*, an *n*-alkane. We found that for the four *n*-alkanes in the test chromatograms the ratio $A_{s,p}/A_{s,t}$ generally followed a smooth trend. Interpolating between these values to obtain a "local" value for $A_{s,p}/A_{s,t}$, it turned out that in the great majority of cases Y_i was within 90–110%. Deviations usually resulted from incorrect integration because of excessive tailing by which the last part of the peak was lost in the noise, drift and wander of the baseline. This lost area is a crude but not particularly accurate parameter for tailing.

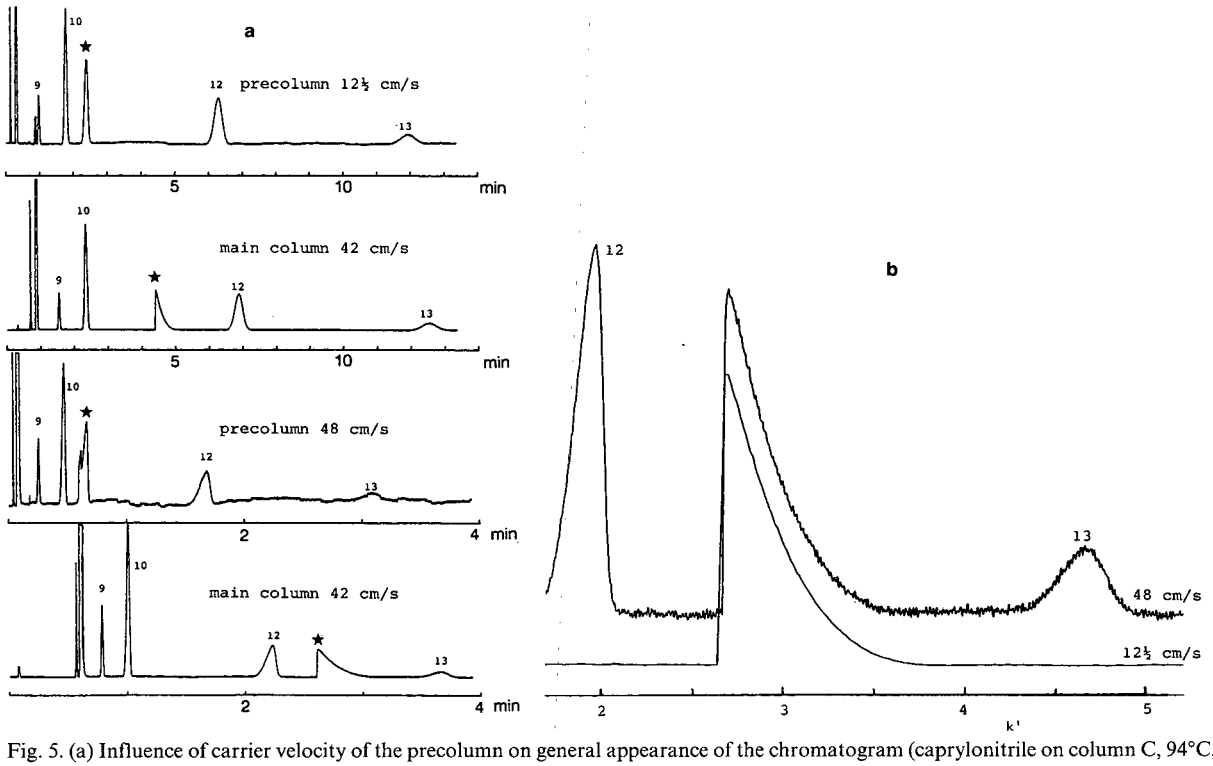

Fig. 5. (a) Influence of carrier velocity of the precolumn on general appearance of the chromatogram (caprylonitrile on column C, 94°C, 20 mmHg). Peak identification as in Fig. 3a. (b) Caprylonitrile peaks in (a) superimposed on a k' scale (scale relates to caprylonitrile).

Moreover, real losses by decomposition may remain unnoticed.

RESULTS AND DISCUSSION

The chromatograms produced by the system under various operating conditions vary greatly. Standardized chromatographic conditions are therefore necessary. However, this is not always feasible and therefore it is important to ascertain the consistency of the results obtained under various conditions of temperature, flow, length of the test column, etc.

Moreover, to achieve efficient use of time, only a limited number of test probes matching the (expected) activity of the column should be injected. To that end, the set of test probes should be ordered according to adsorptive properties, regarding vapour pressure, acidity–basicity, dipole moment, etc.

Influence of vapour pressure

The possible use of the saturated vapour pressure (p^0) as a selection criterion was considered. To investigate the influence of vapour pressure on peak shape, nonanal was injected on column A at temperatures of 57.4, 71.8, 85.4 and 100.2°C, corresponding to vapour pressures of 5, 10, 20 and 40 mmHg, respectively (Fig. 6). At vapour pressures of 5, 10 and 20 mmHg the nonanal peaks have sharp front edges and distinct ends. The k'_0 values are 10.68, 3.28 and 1.34, respectively. Linear regression of ln k'_0 *vs.* $1/T$ shows a correlation coefficient of 0.999. The peak widths from front edge to end of tail, expressed in k' units (w_b/t_m) decrease: 3.50, 0.91 and 0.28, respectively. At 40 mmHg, the nonanal peak has no sharp front edge, although the peak is still tailing.

We also checked whether members of a homologous series gave similar peak shapes when injected at the same vapour pressure. Caprylonitrile ($C_7H_{15}CN$) and pelargononitrile ($C_8H_{17}CN$) were injected on column A at vapour pressures of 5, 10 and 20 mmHg (Fig. 7). Table V lists the end times, $t_{R,0}$, and the widths, w_b, of the peaks. Linear regression of ln (k'_0) *vs.* $1/T$ gave correlation coeffi-

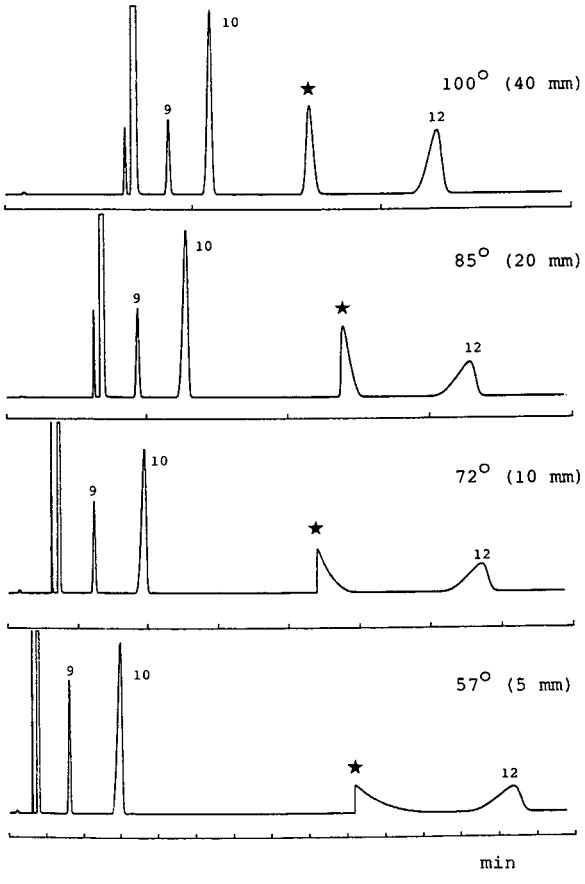

Fig. 6. Influence of vapour pressure on peak shape and peak position (nonanal on column A). Peak identification as in Fig. 3a.

cients of 0.99999. At corresponding vapour pressures, k'_0 and w_b/t_m of the peaks are of the same order of magnitude. It seems that within a limited range of temperatures and alkyl chain lengths, injection at corresponding vapour pressures gives roughly comparable results.

Influence of carrier velocity on peak shape

If the test is indeed a case of ideal non-linear chromatography, the velocity of the carrier gas should have no influence on peak shape and peak position, provided that the kinetics of adsorption and desorption are fast.

To check this, caprylonitrile was injected at 95°C (p^0 20 mmHg) on column C at mean linear velocities of 9.9, 20.7, 41.9, 81.3 and 119.0 cm/s (Fig. 8a). The chromatograms were stored on disk and reconstructed with a k' axis (Fig. 8b). At further enlargement the peaks showed distinct ends at nearly the same k' value (mean k'_0 3.71 $\pm$ 0.09). The tails have the same shape and almost coincide. The front edges, however, do not do so because the load on the test column was not strictly controlled.

The results obtained indicate that the linear velocity of the carrier gas has no influence on the position of the end and the shape of the tail of the peak over a wide range of values.

Influence of length of test column

Often, columns that have to be tested are of different length. To permit comparison of such columns with each other, the influence of column length on peak shape and peak position must be established. In a study on the necessary length of the test column [21], it was observed that reduction of the length resulted in gradually better and, ultimately, symmetrical peak shapes. However, such a gradual improvement is at variance with the theory of ideal non-linear GC. Therefore, we carried out a similar experiment under isothermal conditions and controlled carrier gas velocities.

Caprylonitrile was injected at 80°C (p^0 10 mmHg) on to pieces of 13.40, 6.85, 3.40 and 1.70 m lengths taken from column C. Inlet pressures were set so as to give for each piece (theoretically) the same linear outlet velocity (about 49 cm/s). The existing split vent settings resulted in column loads of about 0.6–1.1 ng. The chromatograms were recorded on disk and plotted with a k' axis (Fig. 9a). At further enlargement the peaks show distinct ends. At short lengths the determination of the retention time on the test column becomes inaccurate, because the travelling time through the monitor line can no longer be neglected. Calculations of k'_0 resulted in values varying from 12.3 to 13.9. To make visual comparison easier, the ends of the peaks in Fig. 9b were aligned by shifting the k' axes. The tails of the peaks have similar shapes, whereas the tops and fronts elute at different k' values. The elution profile of caprylonitrile on the 1.7-m column is different: its front edge is less sharp and it is rounded at the top. This column is of insufficient length to complete the transformation of the Gaussian input profile to the "adsorption GC profile". On the basis of these results, it can be concluded that column length

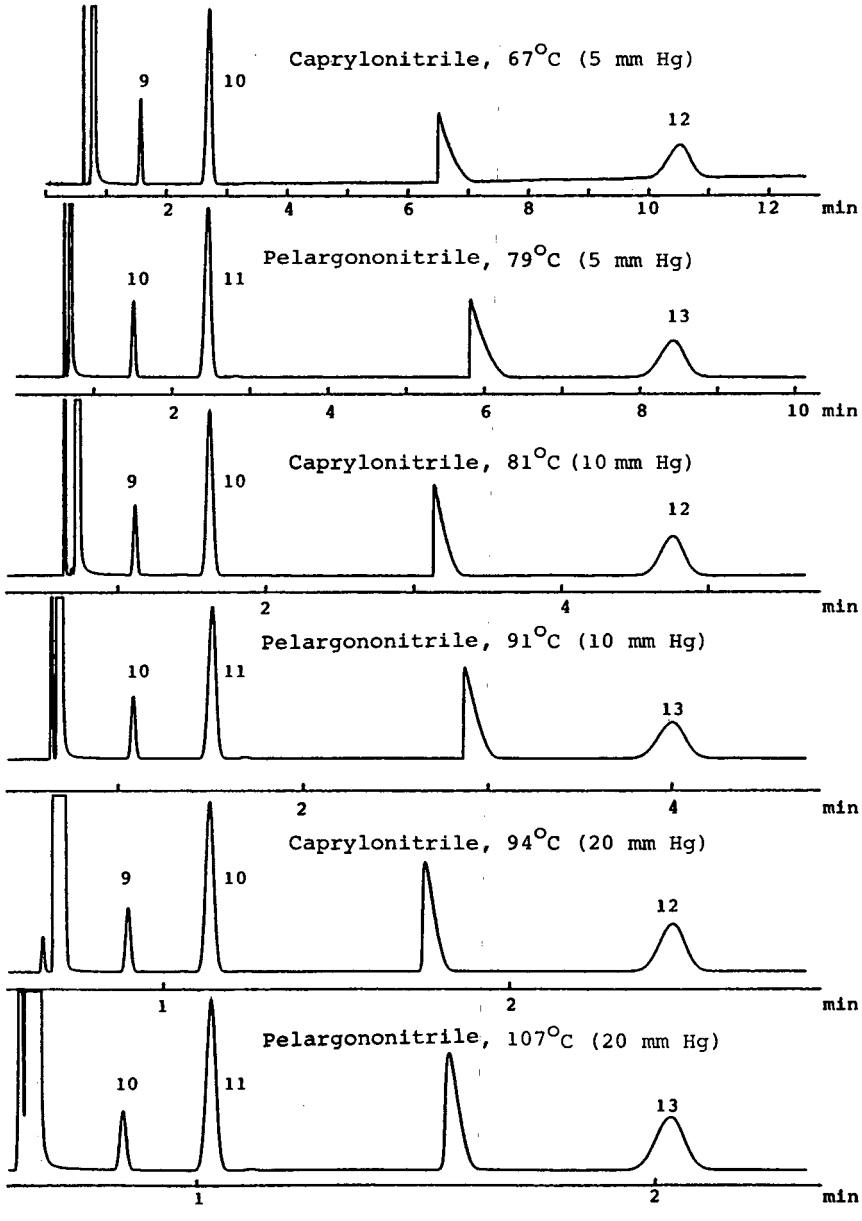

Fig. 7. Influence of vapour pressure and alkyl chain length on peak shape and peak position (column A). Peak identification as in Fig. 3a.

generally has no influence on peak shape and peak position. However, a certain length of column is required to produce the typical profile with its tail and front edge.

Some idea of the necessary length, L_{req}, can be obtained from the following approximation: at the front of the Gaussian input band, the low concentrations, travelling more slowly, are gradually overtaken by the high concentrations. Thus, a steep, self-sharpening front edge is formed. Finally, the top overtakes the front edge and the typical profile emerges. At the rear, the low concentrations lag

TABLE V

INFLUENCE OF SATURATED VAPOUR PRESSURE AND ALKYL CHAIN LENGTH ON PEAK END AND PEAK WIDTH

Caprylonitrile (7-CN) and pelargononitrile (8-CN), column A.

p^0 (mmHg)	Temperature (°C)	Test probe	$t_{R,0}$ (s)	k'_0	w_b (s)	w_b/t_M
5	67.3	7-CN	250	6.24	33.7	0.98
	79.2	8-CN	227	5.51	29.0	0.83
10	80.5	7-CN	118	2.32	11.7	0.33
	91.4	8-CN	113	2.08	10.5	0.29
20	94.3	7-CN	70.3	0.88	4.80	0.13
	106.9	8-CN	68.1	0.78	4.71	0.12

behind and the typical tail is formed. Let k'_0 now be the capacity factor for the zero concentration, k'_t that for the concentration at the top of the profile, $w_{in} = 4\sigma_{in}$ the width at the base of the input peak, $w_{out} = t_m(k'_0 - k'_t)$ the width at the base of the transformed peak and u_m the linear velocity of the carrier gas. Then, the base of the peak moves with a velocity $u_m/(1 + k'_0)$ and its top, lagging $0.5\ w_{in}$ behind at the entrance of the test column, with $u_m/(1 + k'_t)$. The top would then overtake the base at time $0.5\ w_{in}(1 + k'_0)/(k'_0 - k'_t)$. The corresponding distance, which is the necessary length L_{req}, is

$$L_{req} = 0.5\ w_{in}u_m/(k'_0 - k'_t) = 0.5\ L(w_{in}/w_{out})$$

The necessary length therefore depends on the ratio of inlet and outlet band width. The outlet band width is determined by the carrier velocity and the difference in capacity factor between the top and end of the peak, which in turn is correlated to the curvature of the adsorption isotherm, the number and activity of the adsorption sites and the surface area of column.

Summarizing, high carrier velocities, weak adsorption, little curvature of the adsorption isotherm and small-diameter columns increase the necessary

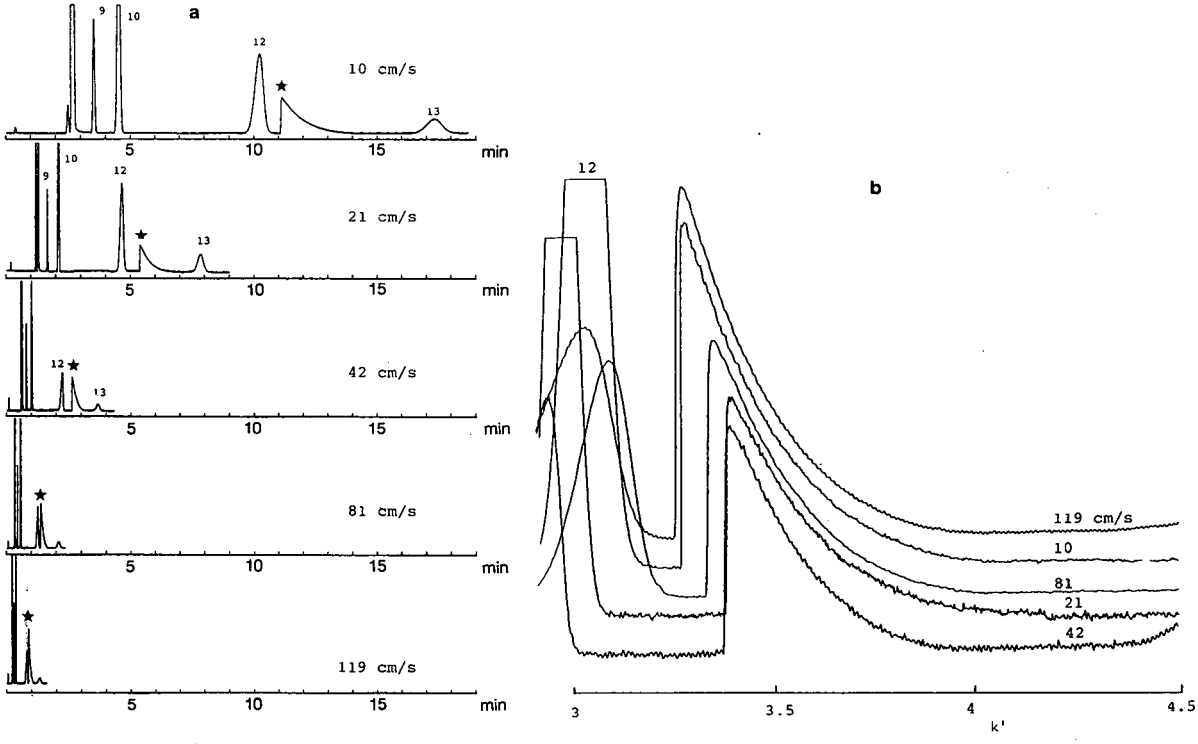

Fig. 8. (a) Influence of carrier velocity on peak shape and peak position (caprylonitrile on column C, 95°C, 20 mmHg). Peak identification as in Fig. 3a. (b) Caprylonitrile peaks in (a) superimposed on a k' scale (scale relates to caprylonitrile).

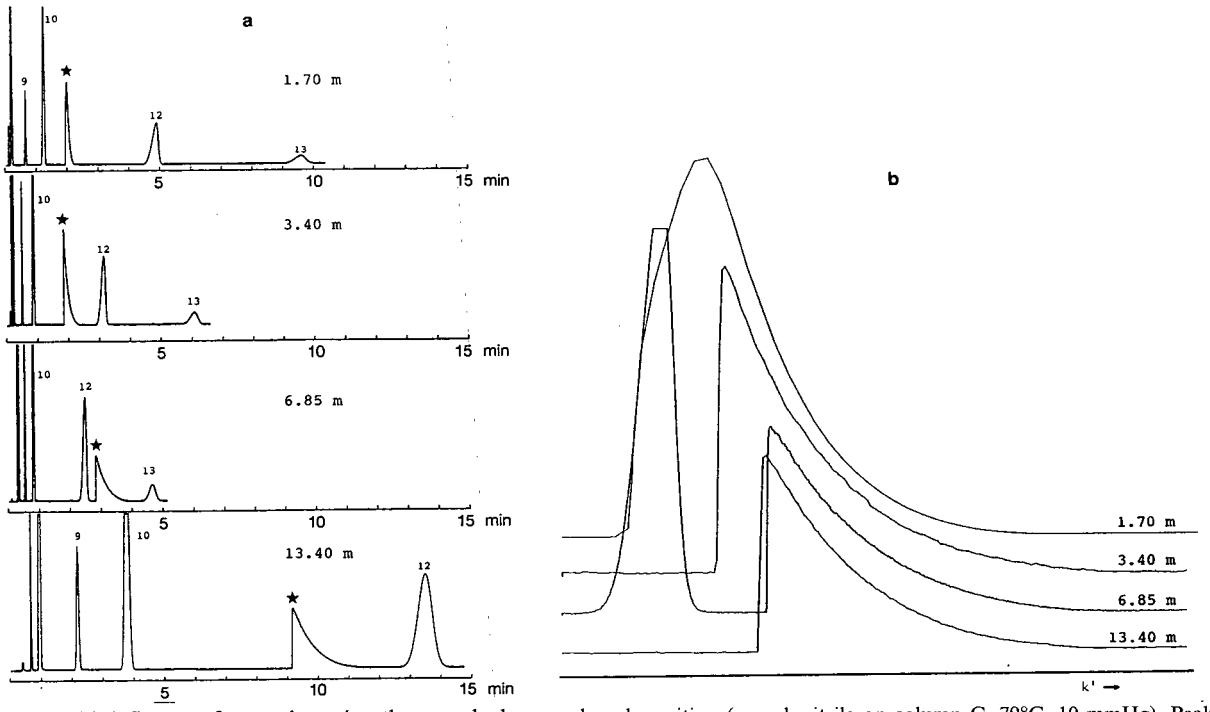

Fig. 9. (a) Influence of test column length on peak shape and peak position (caprylonitrile on column C, 79°C, 10 mmHg). Peak identification as in Fig. 3a. (b) Caprylonitrile peaks in (a) superimposed on a k' scale.

length of the test column. In an evaluation of column activity, these factors must be taken into consideration against the length of the column. Fortunately, the coupling device permits manipulation of the ratio w_{in}/w_{out} by varying the carrier flows in the precolumn and the test column.

Behaviour of test compounds

A broad variety of compounds were tried for use as test probes (Table II): aliphatic and aromatic nitriles, aldehydes, amines and thiols, aliphatic alcohols, diols, diamines and carboxylic acids, phenols and N-heterocyclics.

On the basis of their tailing behaviour, the probes were divisible into two main groups. One group consisted of alcohols, amines, phenols and carboxylic acids. These compounds are characterized by a hydrogen in their polar group. They showed a very curved tail which returned only asymptotically to the baseline. This is indicative of a very heterogeneous adsorption mechanism. Also, when small amounts were injected the peaks remained tailing and tended to be lost in the noise.

The other group consisted of nitriles, aldehydes and nitro compounds. These more weakly adsorbing compounds have no hydrogen atom in their polar group. They showed a more triangular peak shape with a distinct end of the tail. This is indicative of more homogeneous adsorption. When small amounts were injected the peaks became symmetrical and were not lost in the noise.

As a rule aromatic nitriles, aldehydes, amines and thiols adsorbed less than the corresponding aliphatic compounds. Probing the surface for metal ions with aliphatic or aromatic thiols was without result: a test with fused-silica can dispense with the use of thiols. Part of the test probes could be ordered according to strength of adsorption: nitrogen bases > aldehydes > nitriles > nitro compounds > thiols. Hydroxyl-containing probes could not be fitted in with this sequence. Within the group of nitrogen bases, ordering according to pK_a is possible (see next section).

The columns received treatments which are not likely to change the chemical nature of the surface considerably. It remains essentially acidic in nature,

only the concentration of silanol groups changes. Accordingly, the use of acidic test probes (carboxylic acids, phenols, alcohols, diols) was inconclusive. Moreover, carboxylic acids and diols were easily overloaded on the apolar precolumn. Alcohols are common probes for surface hydroxyl groups. In practice, their behaviour towards changes in the silanol concentration was not very pronounced. Possibly adsorbed water from the carrier plays a role here.

The use of bifunctional probes (diamines, diols) is questionable. The peak shifts and peak shapes of mono- and diamines were very similar when plotted with a k' axis (see next section). Lower diols (propanediol, butanediol) showed stronger adsorption than monofunctional alcohols. However, their vapour pressures, especially those of the α,ω-diols, are aberrant from those of monofunctional alcohols. Also, they showed very low retention on the apolar precolumn. For these compounds the saturated vapour pressure proved to be an incorrect selection criterion.

Organic N-bases as test probes

Basic test probes are appropriate indicators of the activity of the silica surface. As an example, the use of organic nitrogen compounds will be considered (Fig. 10). k'_0 cannot be given exactly here, as these test probes did not show a clearly marked end of the tail. Instead, the time where k' of the test probe is zero is marked with △, and a round figure of k' near the end of the tail is marked with ▽.

The behaviour of *p*-toluidine, quinoline and 3-butylpyridine on column A at temperatures corresponding to a vapour pressure of 10 mmHg is shown in Fig. 10a. Peak tailing and peak shift tend to increase with increasing pK_a value, but aromaticity also plays a role here.

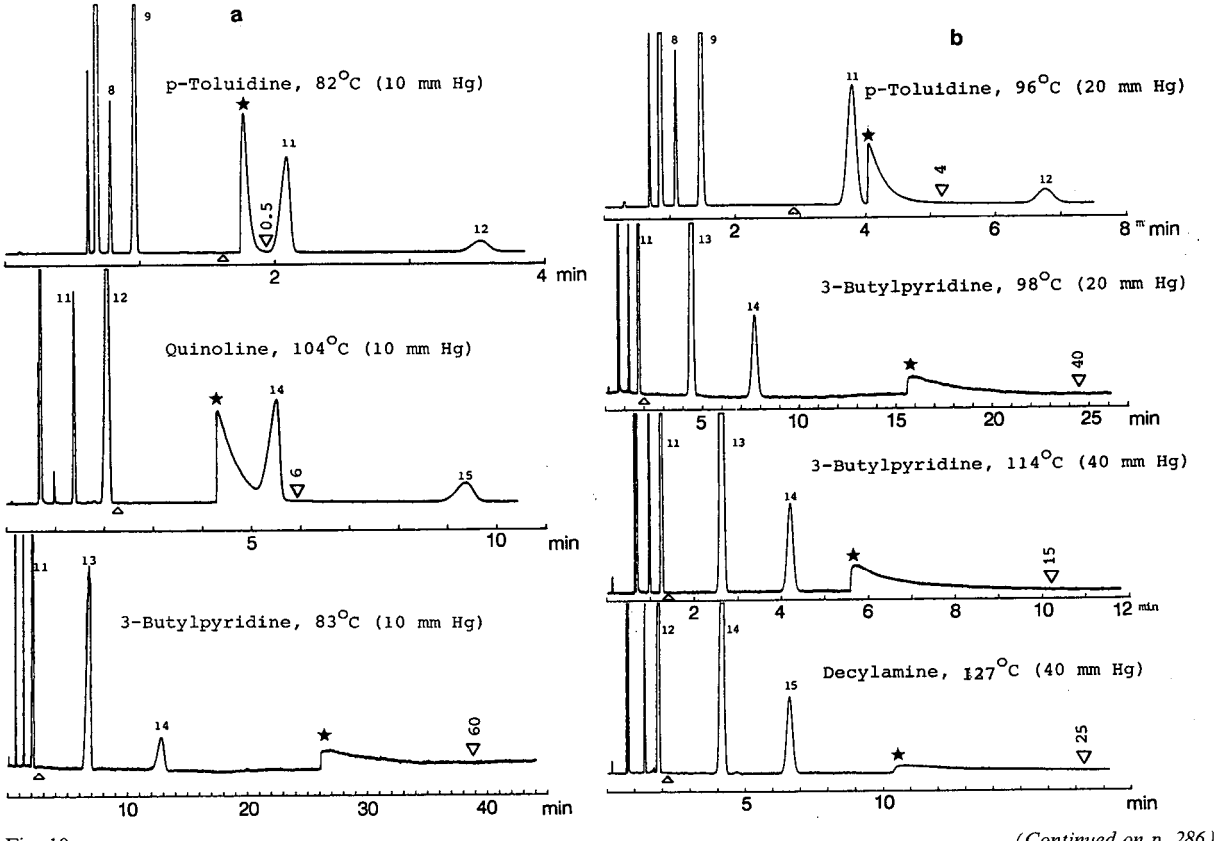

Fig. 10.

(Continued on p. 286)

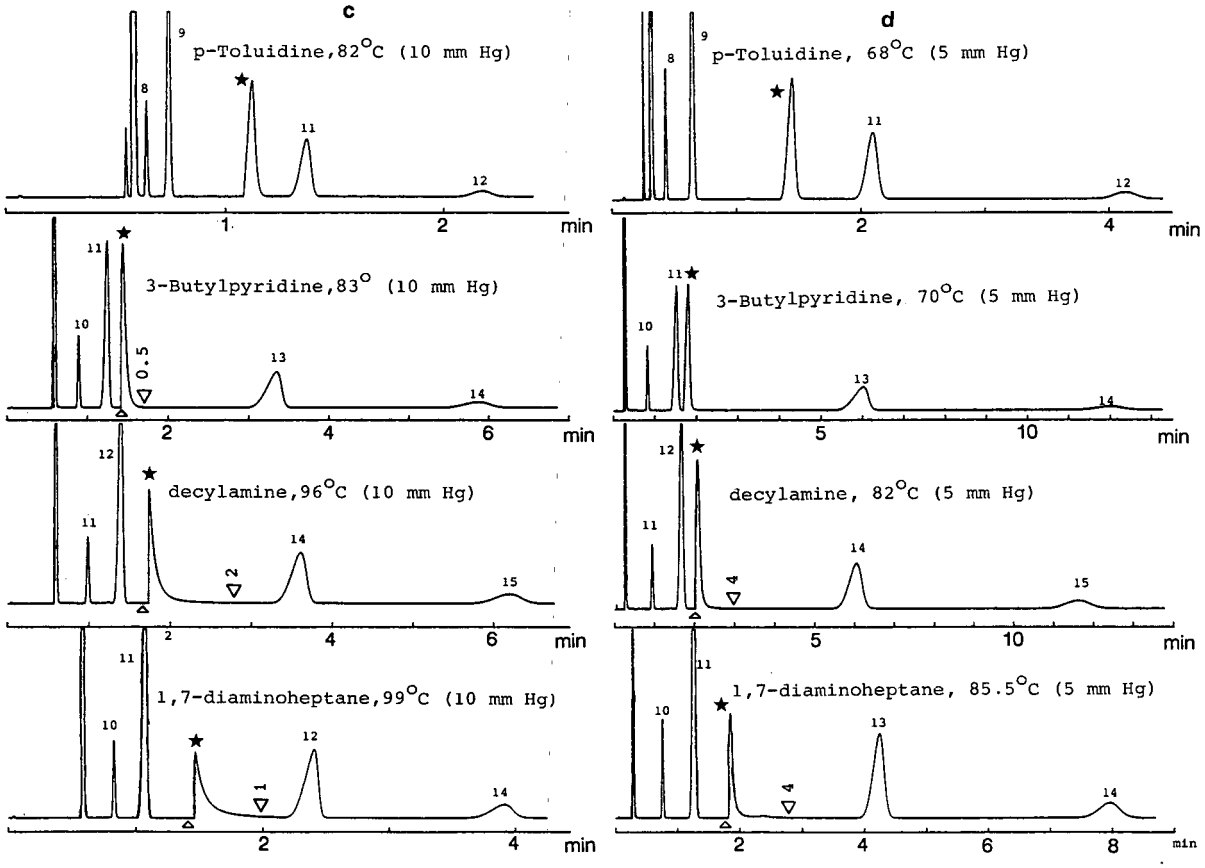

Fig. 10. Organic nitrogen bases as test probes. Peak identification as in Fig. 3a. △ indicates $k' = 0$; ▽ indicates an arbitrary k' value at the end of the tail. (a) Column A, load *p*-toluidine 8.5 ng, quinoline 9.4 ng and 3-butylpyridine 5.2 ng; (b) column C, load *p*-toluidine 7.6 ng, 3-butylpyridine 7.0 ng (20 mmHg) and 6.1 ng (40 mmHg) and decylamine 8.0 ng; (c) column D, load *p*-toluidine 7.0 ng, 3-butylpyridine 28 ng, decylamine 36 ng and 1,7-diaminoheptane 28 ng; (d) column E, load *p*-toluidine 7.2 ng, 3-butylpyridine 17 ng, decylamine 17 ng and 1,7-diaminoheptane 24 ng.

Column C received a more intense pretreatment with hydrochloric acid and was expected to have a higher activity. Therefore, *p*-toluidine was injected at 20 mmHg, 3-butylpyridine at 20 and 40 mmHg and decylamine at 40 mmHg (Fig. 10b). As compared with column A, the peak shift and peak tailing are much increased. Again, shift and tailing increase with increasing pK_a values.

On deactivated columns better peak shapes are expected. Therefore, we added 1,7-diaminoheptane to the test. At a vapour presure of 10 mmHg, *p*-toluidine, 3-butylpyridine, decylamine and 1,7-diaminoheptane were injected on column D (Fig. 10c). *p*-Toluidine is symmetrical and 3-butylpyridine is almost symmetrical. The amines still show tailing but, in comparison with column C, the shift and tailing are much less. The shift and tailing of 1,7-diaminoheptane are comparable to those of decylamine. This suggests that bifunctional compounds are not severer test probes than monofunctional compounds.

Fig. 10d shows the results on column E, which was deactivated with PMHS. As the best results were expected here, the probes were injected at 5 mmHg. *p*-Toluidine and 3-butylpyridine are symmetrical. Decylamine and 1,7-diaminoheptane are only slightly tailing. In spite of the higher symmetry, the k' values are higher than on column D. This is in

accordance with earlier conclusions [5,10] that deactivation with PS 122 creates a polymer layer on the surface of fused-silica.

The examples show that N-bases are good test probes for fused-silica columns. Their pK_a values in water are useful indicators of their adsorptive properties and can be used to select a probe matching the expected or observed activity of the column.

CONCLUSIONS

The coupling device is a simple yet valuable tool to study the activity of uncoated capillary columns. The device is versatile: it permits rapid and easy exchange of test columns, it allows wide variations of carrier flows and splitting ratios and flows and splitting ratios can easily be adjusted to columns of different dimensions. However, such variations also lead to very different appearances of the chromatograms. Either standardized chromatographic conditions have to be used or the chromatogram has to be reconstructed with a k' axis. The monitor line proved indispensable to numerical evaluation of the results. The short, thick-film precolumn gives fast, ample separations even at relatively high carrier flows and temperatures. This results in rapid tests and sharp Gaussian input profiles on the test column. The thick-film also permits the injection of fairly large amounts of the test probes (up to 0.5–1 μg), which largely precludes adsorption problems in the precolumn and monitor line.

The velocity of the carrier gas has no influence on peak shape and peak position expressed in k' units. Neither has column length, although a minimum length is necessary to produce the typical peak profile. This necessary length depends on the ratio of inlet and outlet peak widths.

Temperature strongly influences peak shape and peak position, especially of weakly adsorbing probes (aldehydes, nitriles, etc.). The vapour pressure of the test probe is a useful parameter in this respect. Vapour pressures of 5–10 mmHg give good results. The effect of alkyl chain length can in a limited range be counterbalanced by performing the test at a standardized vapour pressure.

The test is a case of nearly ideal non-linear GC. Peaks obtained with different amounts of the test probe can be superimposed and the tails then coincide. The typical peak shape with a sharp front edge and a tail was nearly always observed. The end of the tail is fixed and its capacity factor k'_0 forms an important quantity for evaluation, but the front edge and the peak top shift with the load. It is recommended to inject several concentration levels of a test probe, in order to obtain an impression of the column loadability. The yield of a probe on the test column is mostly 100% even for strongly adsorbing compounds, and seems not an effective parameter in this test based on reversible adsorption.

For active surfaces compounds with a large dipole moment such as nitriles, nitro compounds and aldehydes are good test probes. For deactivated surfaces more strongly adsorbing test probes are necessary, such as alcohols or amines. For fused-silica surfaces organic nitrogen bases have proved to be good test probes. They adsorb roughly according to their pK_a values in water and hence a selection can be made matching the observed or expected activities of the column. Acidic compounds, on the other hand, are not useful test probes for fused-silica.

REFERENCES

1 G. Rutten, A. van de Ven, J. de Haan, L. van de Ven and J. Rijks, *J. High Resolut. Chromatogr. Chromatogr. Commun.*, 7 (1984) 607.
2 G. Rutten, J. de Haan, L. van de Ven, A. van de Ven, H. van Cruchten and J. Rijks, *J. High Resolut. Chromatogr. Chromatogr. Commun.*, 8 (1985) 664.
3 L. J. M. van de Ven, G. Rutten, J. A. Rijks and J. W. de Haan, *J. High Resolut. Chromatogr. Chromatogr. Commun.*, 9 (1986) 741.
4 M. Hetem, G. Rutten, L. van de Ven, J. de Haan and C. Cramers, *J. High Resolut. Chromatogr. Chromatogr. Commun.*, 11 (1988) 510.
5 M. Hetem, G. Rutten, B. Vermeer, J. Rijks, L. van de Ven, J. de Haan and C. Cramers, *J. Chromatogr.*, 479 (1989) 3.
6 J. R. Condor and C. L. Young, *Physicochemical Measurement by Gas Chromatography*, Wiley, Chichester, 1979.
7 K. Grob, Jr., G. Grob and K. Grob, *J. Chromatogr.*, 156 (1978) 1.
8 K. Grob, G. Grob and K. Grob, Jr., *J. Chromatogr.*, 219 (1981) 13.
9 B. W. Wright, P. A. Peaden, M. L. Lee and T. Stark, *J. Chromatogr.*, 248 (1982) 17.
10 C. L. Woolley, K. E. Markides and M. L. Lee, *J. Chromatogr.*, 367 (1986) 23.
11 M. Donike, *Chromatographia*, 6 (1973) 190.
12 R. C. M. de Nijs, J. J. Franken, R. P. M. Dooper and J. A. Rijks, *J. Chromatogr.*, 167 (1978) 231.
13 M. Ahnhoff, M. Ervik and L. Johanssqn, in R. E. Kaiser (Editor), *Proceedings of the 4th International Symposium on*

Capillary Chromatography, Hindelang, GFR, May 3–7, 1981, Hüthig, Heidelberg, 1981, p. 487.
14 M. Ahnhoff and L. Johansson, *J. Chromatogr.*, 279 (1983) 75.
15 W. Blum, *J. High Resolut. Chromatogr. Chromatogr. Commun.*, 8 (1985) 718.
16 G. A. F. M. Rutten and J. A. Luyten, *J. Chromatogr.*, 74 (1972) 177.
17 R. C. M. de Nijs and R. P. M. Dooper, *J. High Resolut. Chromatogr. Chromatogr. Commun.*, 3 (1980) 583.
18 K. Grob, Jr. and H. P. Neukom, *J. Chromatogr.*, 323 (1985) 237.
19 G. Schomburg, H. Husmann and F. Weeke, *Chromatographia*, 10 (1977) 580.
20 K. Grob and G. Grob, *J. High Resolut. Chromatogr. Chromatogr. Commun.*, 1 (1978) 302.
21 W. Bertsch, V. Pretorius and K. Lawson, *J. High Resolut. Chromatogr. Chromatogr. Commun.*, 5 (1982) 568.
22 L. J. Anthony, R. A. Holland and S. A. Heffner, *J. High Resolut. Chromatogr. Chromatogr. Commun.*, 11 (1988) 167.
23 L. J. Anthony and R. A. Holland, *J. Chromatogr.*, 477 (1989) 291.
24 L. J. Anthony and R. A. Holland *J. Non-Cryst. Solids*, 120 (1990) 82.
25 L. T. Zhuravlev, *Langmuir*, 3 (1987) 316.
26 A. Tuel, H. Hommel, A. P. Legrand and E. Sz. Kováts, *Langmuir*, 6 (1990) 770.
27 M. L. Hair and W. Hertl, *J. Phys. Chem.*, 73 (1969) 4269.
28 C. Clark-Monks and B. Ellis, *J. Colloid Interface Sci.*, 44 (1973) 37.
29 B. W. Wright, P. A. Peaden, M. L. Lee and G. M. Booth, *Chromatographia*, 15 (1982) 584.
30 J. Gobet and E. Sz. Kováts, *Adsorpt. Sci. Technol.*, 1 (1984) 77.
31 M. W. Ogden and H. M. McNair, *J. High Resolut. Chromatogr. Chromatogr. Commun.*, 8 (1985) 326.
32 R. S. Drago, L. B. Parr and C. S. Chamberlain, *J. Am. Chem. Soc.*, 99 (1977) 3203.
33 F. M. Fowkes, D. W. Dwight, D. A. Cole and T. C. Huang, *J. Non-Cryst. Solids*, 120 (1990) 47.
34 H. Knözinger and W. Stählin, *Prog. Colloid Polym. Sci.*, 67 (1980) 33.
35 R. C. Weast (Editor), *Handbook of Chemistry and Physics*, CRC Press, Boca Raton, FL, 69th ed., 1988.
36 D. C. Sadek, C. J. Koester and L. D. Bowers, *J. Chromatogr. Sci.*, 25 (1987) 489.
37 K. Grob, *J. High Resolut. Chromatogr. Chromatogr. Commun.*, 7 (1980) 585.
38 J. F. K. Huber and R. G. Gerritse, *J. Chromatogr.*, 58 (1971) 137.
39 R. P. W. Scott and P. Kucera, *J. Chromatogr.*, 149 (1978) 93.
40 S. Golshan-Shirazi and G. Guiochon, *J. Phys. Chem.*, 94 (1990) 495.
41 W. Rudziński, A. Waksmundzki, R. Leboda, Z. Suprynowicz and M. Lasoń, *J. Chromatogr.*, 92 (1974) 25.
42 J. Roles and G. Guiochon, poster presented at the *18th International Symposium on Chromatography, Amsterdam, September 23–28, 1990.*
43 S. P. Boudreau and C. T. Cooper, *Anal. Chem.*, 59 (1987) 353.
44 S. P. Boudreau and C. T. Cooper, *Anal. Chem.*, 61 (1989) 41.
45 J. Nawrocki, *Chromatographia*, 23 (1987) 722.
46 E. Papirer, H. Balard and A. Vidal, *Eur. Polym. J.*, 24 (1988) 783.
47 D. R. Stull, *Ind. Eng. Chem.*, 39 (1947) 517.
48 A. W. Ralston, W. M. Selby and W. O. Pool, *Ind. Eng. Chem.*, 33 (1941) 682.
49 H. A. Stober (Editor), *CRC Handbook of Biochemistry: Selected Data for Molecular Biochemistry*, Chemical Rubber Co., Cleveland, OH, 2nd ed., 1970.
50 A. W. Ralston, W. M. Selby, W. O. Pool and R. H. Potts, *Ind. Eng. Chem.*, 32 (1940) 1093.
51 K. D. Bartle, *Anal. Chem.*, 45 (1973) 1831.

Journal of Chromatography, 590 (1992) 289–296
Elsevier Science Publishers B.V., Amsterdam

CHROM. 23 754

High-temperature continuous counter-current gas–liquid chromatography

Katsunori Watabe

Central Research Laboratory, Shimadzu Corporation, Kyoto (Japan)

Hisashi Kanda

Laboratory of Industrial Analytical Chemistry, Faculty of Technology, Tokyo Metropolitan University, Tokyo (Japan)

Katsuya Sato

Central Research Laboratory, Shimadzu Corporation, Kyoto (Japan)

Toshiyuki Hobo*

Laboratory of Industrial Analytical Chemistry, Faculty of Technology, Tokyo Metropolitan University, 1-1 Minamiohsawa, Hachiohji-shi, Tokyo 192-03 (Japan)

(First received July 4th, 1991; revised manuscript received September 17th, 1991)

ABSTRACT

In continuous counter-current gas–liquid chromatography, which has a high resolving power and is suitable for the large-scale purification of organic solvents, it is very important that the samples that can be applied extend from easily separable to more difficult to separate, such as azeotropes, low-volatility compounds and stereoisomers. A system was designed and constructed for high-temperature operation up to 200°C, and was applied to the separation of dimethyl and diethyl phthalate, *trans*- and *cis*-decahydronaphthalene and *cis*-decahydronaphthalene and tetrahydronaphthalene. It was confirmed that over 99% of purity could be achieved for dimethyl and diethyl phthalate, *trans*-decahydronaphthalene, and tetrahydronaphthalene.

INTRODUCTION

Many attempts have been made to develop preparative-scale chromatography on account of its excellent separation capability. In conventional chromatography, however, samples cannot be introduced continuously, because it is a sequential method and the amount of sample applied each time is limited. Therefore, counter-current chromatography has been considered as an effective method for preparative separations. In counter-current chromatography, the difference in the partition coefficients of samples between two phases moving counter-currently to each other is utilized for separation and purification.

Several methods have been proposed in order to realize the counter-current flow of two phases; (1) moving bed, to gravitate packing material coated with a liquid phase and to flow a carrier gas in the opposite direction of the flow of the packing material [1,2]; (2) rotation of a special type of column, to rotate doughnut-type tubing packed with absorbent [3,4]; and (3) circulation of liquid phase, to gravitate the stationary phase over the surface of the packing in the column against a gas stream [5–7]. Considering desirable attributes such as a simple scheme,

0021-9673/92/$05.00

having little mechanical movement and direct control of liquid phase flow-rate, we chose the last method, and carried out studies on continuous counter-current gas–liquid chromatography (CCGLC). Despite its good resolving power, it has not become popular as a large-scale preparative separation method as it seems to have narrow range of application. The recent needs for the highly efficient separation and purification of large molecules with similar structures in the fields of fine chemistry and biochemistry encouraged us to develop further the capability of continuous counter-current chromatography.

However, the system reported previously [5–7] could be applied only up to 60°C and was used to separate volatile solvents with boiling points up to *ca.* 130°C. To extend the applicability of this method in practice, it is necessary that the system can be used above 150°C and be applicable to the separation of samples with the boiling points of more than 250°C.

In this work, we designed a high-temperature continuous CCGLC system, and applied it to the separation of high-boiling sample mixtures with close boiling points and to azeotropic systems.

THEORETICAL

In previous papers we have discussed the separation conditions, the theoretical plate number and the maximum sample feed rate [5–7]. The basic consideration required for the separating condition is as follows.

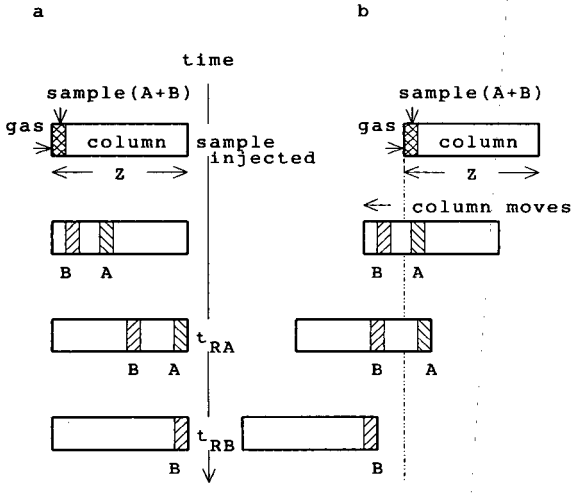

Fig. 1. Schematic comparison between (a) conventional gas chromatography and (b) continuous counter-current gas–liquid chromatography.

The separation of components depends on the difference in partition coefficients between two phases. In Fig. 1, schematic comparison between conventional gas chromatography (GC) and CCGLC is shown to clarify the difference between these two methods. In a column of length Z the retention times of component A and B are t_{RA} and t_{RB}, so that the velocities of the components in the column are Z/t_{RA} and Z/t_{RB}, respectively. When the column moves in the opposite direction to the gas flow and its velocity is between Z/t_{RA} and Z/t_{RB}, component A with a lower partition coefficient moves in the direction of the gas flow and component B with a higher partition coefficient moves in the direction of the column movement; components A and B move in different directions from the place of introduction. In order to determine the operational parameters, the principle of this method is expressed by using physico-chemical constants.

The partition coefficient $K_{(n)}$ is defined as follows:

$K_{(n)}$ = (weight of component n in unit volume of liquid phase)/(weight of component n in unit of gas phase) (1)

This equation is also expressed as follows:

$$K_a = \frac{\frac{W_l}{L}}{\frac{W_g}{G}} = \frac{W_l}{W_g} \cdot \frac{G}{L} \tag{2}$$

where K_a = partition coefficient of component A, W_l = weight of component A contained in l ml of liquid phase (g), W_g = weight of component A contained in g ml of gas phase (g), L = flow-rate of liquid phase (ml/min) and G = flow-rate of gas phase (ml/min).

For component A, it is necessary that the amount of A in the gas phase is larger than that in the liquid phase in order to drive component A in the direction of the gas flow. That is,

$$\frac{W_l}{W_g} < 1 \tag{3}$$

Substituting eqn. 3 by eqn. 2,

$$\frac{G}{L} > K_a \tag{4}$$

Under the condition

$$\frac{G}{L} < K_b \tag{5}$$

component B moves in the direction of liquid flow in the same manner. From the eqns. 4 and 5, it is necessary that G/L is between K_a and K_b in order to separate components A and B:

$$K_a < \frac{G}{L} < K_b \tag{6}$$

The optimum separating conditions are defined by

$$(G/L)^{-1} = (1/K_a + 1/K_b)/2 \tag{7}$$

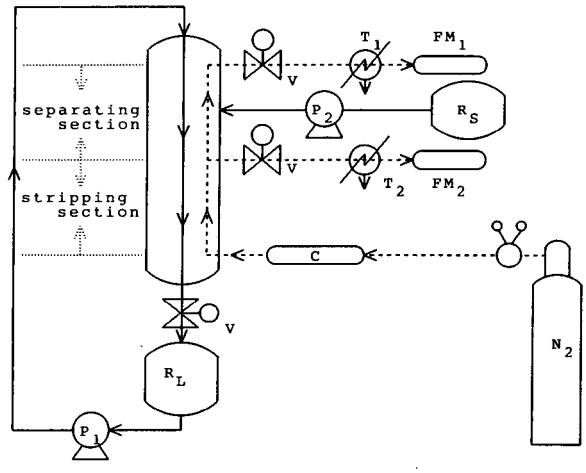

Fig. 2. Continuous counter-current gas–liquid chromatographic system, P_1, P_2 = Pumps; T_1, T_2 = traps; v = valve; FM_1, FM_2 = flow meters; R_L = liquid-phase tank; R_s = sample tank; C = purifier.

EXPERIMENTAL

Instrumentation

The basic scheme of the CCGLC system is shown in Fig. 2.

Gas and liquid flows and sample introduction. Liquid phase is fed from the tank R_L to the top of the column by a plunger-type constant-flow pump, P_1. The liquid phase as a thin film on the surface of packing materials gravitates in the column from the top to the bottom. The liquid phase is recycled through the tank R_L. A inert gas from a high-pressure cylinder, after removing trace amounts of oxygen by passing through a purifier C, is supplied to the system from the bottom of the column and moves towards the top of the column. In the middle of the column, the gas stream is separated into two streams. One leaves the column and vents through a cold trap and a flow meter. The other goes to the top of the column and out through a trap and a flow meter. Sample is injected continuously through the septum in the middle of the separating section into the column from tank R_S by pump P_2.

Column. A Pyrex glass tube (3 m × 17 mm I.D.) was used as a column. It consists of two sections, the separating section and the stripping section (both 1.5 m in length). The temperature of the separating section could be raised to 200°C and that of the stripping section to 260°C. Stainless-steel helical packing (NANIWAPAC No. 1, 0.9 × 1.8 × 1.8 mm) was filled into the column. The surface area and density of the packing were 3.743 m^2/m^3 and 1500 kg/m^3, respectively.

In the stripping section, component B, which is moved from the separating section into the stripping section, is removed from the liquid phase at a higher temperature than that in the separating section, and is carried out from the middle of the column through a cold trap and a flow meter. To strip the component completely from the liquid phase in the stripping section, the following condition must be valid.

$$(G_s/L) > K_b^s \tag{8}$$

where G_s = flow-rate of the gas phase in the stripping section (ml/min), L = flow-rate of the liquid phase (ml/min) and K_b^s = partition coefficient of the component at the temperature of the stripping section.

Trap. A glass tube of (0.3 m × 17 mm I.D.) was used as a trap. The trap was set in a liquid nitrogen coolant vessel as shown in Fig. 3. The efficiency of the trap was about 80%, which was not sufficiently satisfactory, and further study of the trapping system is needed.

Heating system. The structure of the heating system is shown in Fig. 4. There were two layers of heater around the column and connecting tubings. As the first heating layer, glass tape was wrapped

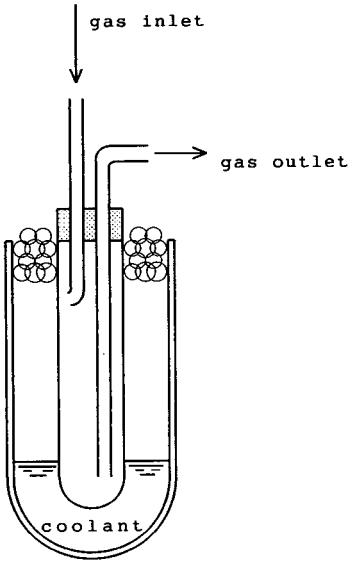

Fig. 3. Trap.

directly on the column and tubing and Nichrome wire and asbestos tape were wrapped over the glass tape. The second heating layer, overlapping the first, utilized the same structure as the first heating layer. The first layer was used for fine temperature control. Copper–constantan thermocouples were located at several positions, such as the separating section, stripping section and connectors, to measure the respective temperatures.

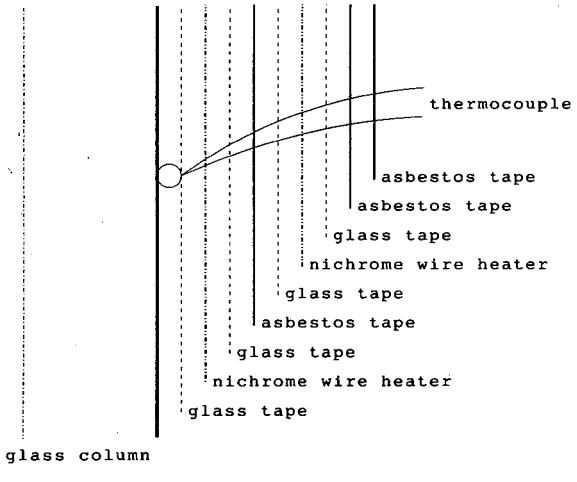

Fig. 4. Heating system.

Mobile phases. As thermally stable liquid mobile phases, silicone KF-54 (methylphenylsilicone; Shinetsu Kagaku) and poly(diethylene glycol succinate) were tested. For subsequent experiments KF-54 was selected for reasons given later.

Carrier gas. Nitrogen (B grade; Nippon Sanso) from a high-pressure cylinder was used after passing it through a purifier (0.3 m × 6 mm I.D. stainless-steel tube packed with reduced copper beads (1–2 mm diameter) in order to remove trace amounts of oxygen.

Samples. As test samples, three mixtures (50:50, w/w) of dimethyl phthalate (b.p. 283.7°C)–diethyl phthalate (b.p. 294.0°C), *trans*- (b.p. 187.2°C)–*cis*-decahydronaphthalene (b.p. 195.7°C) and *cis*-decahydronaphthalene–tetrahydronaphthalene (b.p. 207.2°C) were prepared by mixing the pure compounds purchased from Tokyo Kasei Kogyo (Tokyo, Japan). All sample systems are azeotropic and the components have close boiling points, and therefore they are very difficult to purify by distillation and other industrial methods.

Procedure

Preparation of the system. NANIWAPAC No. 1 helical wire packing was packed in the column by tapping the column gently. The column was washed with acetone and dried by passing nitrogen. The flow system, including tanks and traps, was connected with the column. The liquid phase was filled in the tank and allowed to circulate through the column to make a liquid film on the packing. To remove the highly volatile components present in the liquid phase, the whole system was heated gradually to 200°C with gas- and liquid-phase flows.

Operating conditions. Although the G/L values will be determined by eqn. 6, the maximum gas and liquid flow-rates are limited by the structure of the system. When silicone KF-54 was used as the liquid phase, the maximum liquid flow-rate with this system was found to be less than 1.7 ml/min to maintain a laminar flow as a thin film stream over the packing. At G/L values >500, the gas flow became unstable and carried liquid phase out of the top of the column. Owing to the maximum G/L value, the range of the partition coefficients of the samples was limited. The operating temperature was determined from the partition coefficients and the vapour pressure of the samples. Considering the

amount of sample feed, the vapour pressure of the sample will be in the range 200–400 mmHg at the operating temperature. Partition coefficients were calculated from the gas chromatographic retention data by the equation

$$K = jF_c(t_R - t_0)/V_L \quad (9)$$

where

$$j = [3(P_i/P_o)^2 - 1]/[2(P_i/P_o)^3 - 1]$$

P_i = inlet pressure of carrier gas (kg/cm^2), P_o = outlet pressure of carrier gas (kg/cm^2), F_c = flow-rate of carrier gas (ml/min), t_R = retention time of component (min), t_0 = retention time of air (min) and V_L = volume of liquid phase (ml).

A Shimadzu Model 3A gas chromatograph equipped with a thermal conductivity detector and with a stainless-steel column (3 m × 3 mm I.D.) of Chromosorb W AW (60–80 mesh) coated with 21.8% silicone KF-54 was used to measure partition coefficients.

Fig. 5 illustrates the plot of the logarithm of partition coefficients *versus* the inverse of the column temperature.

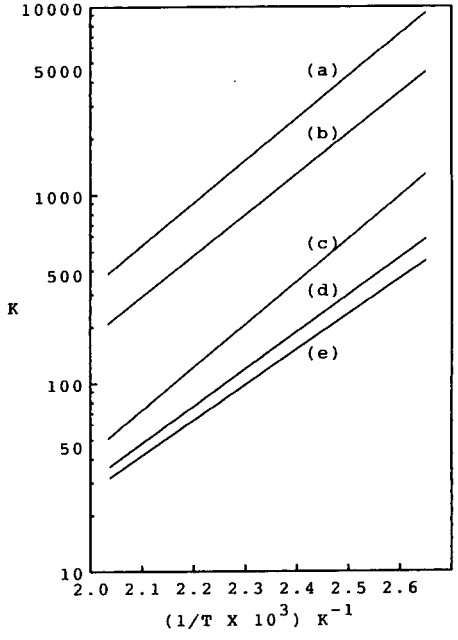

Fig. 5. Partition coefficients (K) (measured on silicone KF-54) of (a) diethyl phthalate, (b) dimethyl phthalate, (c) tetrahydronaphthalene, (d) *cis*-decahydronaphthalene and (e) *trans*-decahydronaphthalene plotted against the reciprocal of the column temperature ($1/T$).

System setting and warm-up. According to eqn. 6, the ratio of the flow-rates of the gas phase and liquid phase (G/L) was set at a value between the partition coefficients of the two components. The total flow-rate of the gas phase was set at double that required for separation, *i.e.*, the flow-rate at the bottom of the column was double that at the top of the column. The temperature of the stripping section was 30–40°C higher than the temperature of the separating section, which was sufficient to satisfy eqn. (8).

The temperature of the system was kept at the set value by controlling the heater voltage with a variable transformer. The gas flow was controlled by a pressure regulator and liquid was circulated by a constant-flow pump. After about 2 h, the conditions became steady. Then, a sample mixture of two components was introduced continuously by a constant-flow pump.

Retention time. The retention time, t_{RA}, of component A, which is the travelling time of component A from the point of introduction to the top of the column, can be calculated with the equation [8]

$$t_{RA} = (K_A \cdot L_0/G \cdot 1/j)/[1 - (K_A \cdot L/G \cdot 1/j)] \quad (10)$$

and the retention time, t_{RB}, of component B, which is the travelling time of the component B from the point of introduction to the bottom of the separating section, can be calculated with the equation

$$t_{RB} = (K_B \cdot L_0/G \cdot 1/j)/[(K_B \cdot L/G \cdot 1/j) - 1] \quad (11)$$

where

$$j = [3(P_i/P_o)^2 - 1]/[2(P_i/P_o)^3 - 1]$$

P_i = inlet pressure of carrier gas (kg/cm^2), P_o = outlet pressure of carrier gas (kg/cm^2) and L_0 = volume of liquid phase in the upper half of the separating section of the column (ml).

It is important to calculate the retention time to establish whether the operating conditions are adequate. For example, the calculated retention times of dimethyl and diethyl phthalate were about 140 and 250 min, respectively, at 200°C with a G/L value of 430, a gas flow-rate of 250 ml/min and a volume of liquid phase of 34 ml.

Sample feed rate. If the feed rate of component A with a small partition coefficient is larger than the

maximum feed rate in an equilibrium state, an excess amount of component A flows down and leaves the bottom of the separating section with the other component. Therefore, the maximum sample feed rate is determined by the maximum feed rate of component A, which is equal to the eluting rate of the same component at the top of the column, without disturbing its partition equilibrium between the gas and liquid in the column. In this experiment, the sample feed rates were decided to be about half of the maximum sample feed rates calculated by the equation described in a previous paper [6], considering that the system was laboratory built.

Analysis of eluates. Eluates from the top and bottom of the column were collected by the traps. As the separation of the two components was the aim, GC was used to determine the ratios of the two components in the eluates. A Shimadzu Model 3A gas chromatograph equipped with a thermal conductivity detector was used with a stainless-steel column (3 m × 3 mm I.D.) packed with 21.8% silicone KF-54 on Chromosorb W AW (60–80 mesh).

RESULTS AND DISCUSSION

Separation of dimethyl and diethyl phthalate

The partition coefficients of dimethyl and diethyl phthalate with the KF54 column at 200°C were 300 and 560, respectively. As the difference between these two partition coefficients was large, their mixture was assumed to be a typical sample for CCGLC. A mixture of dimethyl and diethylphthalate (50:50, w/w) was introduced continuously into the column at 200°C. G/L values were adjusted in the range 256–512 by controlling the gas flow-rates. The highest purity of dimethyl phthalate obtained at the top of the column was 99.96% at $G/L = 453$. For diethyl phthalate, 99.69% purity was achieved at $G/L = 329$. In Fig. 6, the content of diethyl phthalate is plotted against G/L, and indicates that the best separation would be obtained at a G/L value of about 430.

Separation of trans- and cis-decahydronaphthalenes

CCGLC is considered to be effective for the separation of these isomers. According to the partition coefficients (162 and 208) of the isomers on KF-54 at 140°C, the G/L values were adjusted in the range 173–212. A mixture of *trans*- and *cis*-decahydronaphthalene (50:50, w/w) was introduced at 140°C. The content of *cis*-decahydronaphthalene is plotted against G/L in Fig. 7. For small G/L values, the separation at the top of the column was better than that at the bottom, whereas for large G/L values this relationship was reversed.

Separation of cis-decahydronaphthalene and tetrahydronaphthalene

cis-Decahydronaphthalene and tetrahydronaphthalene form an azeotropic mixture so that an effective separation cannot be achieved by conven-

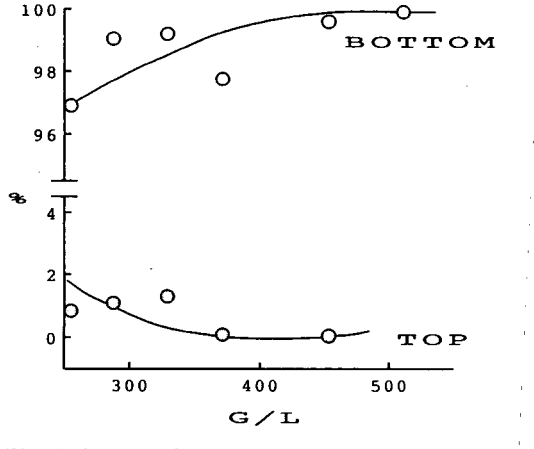

Fig. 6. Content of diethyl phthalate (%).

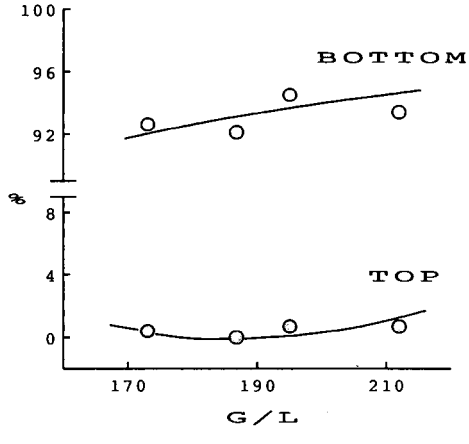

Fig. 7. Content of *cis*-decahydronaphthalene (%).

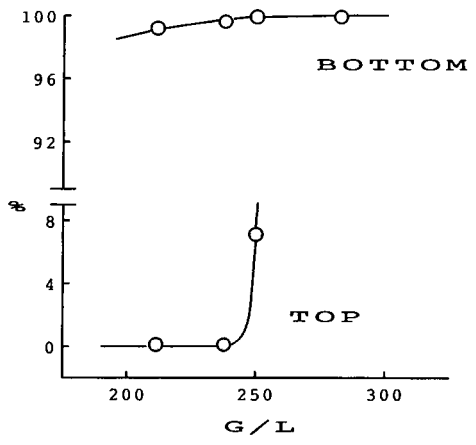

Fig. 8. Content of tetrahydronaphthalene (%).

tional distillation. They were separated by CCGLC at 140°C. The range of G/L values was set from 212 to 282. Over 99% purity of both components was obtained at $G/L = 235$. Fig. 8 shows the content of tetrahydronaphthalene *vs.* G/L. The relationship between G/L value and the purity of the eluate is similar to that for the separation of decahydronaphthalene stereoisomers.

Optimum G/L value for the separation of a two-component mixture

Figs. 6 and 7 indicate that the best separation of the two-component mixture was obtained when the G/L values are set at the mid-point of the partition coefficients, *i.e.*, the optimum G/L value measured for the dimethyl–diethyl phthalate sample was 430, the partition coefficients of dimethyl and diethyl phthalate being 300 and 560, respectively, at 200°C. The optimum G/L value for the *trans-* –*cis*-decahydronaphthalene sample at 140°C was about 185, the partition coefficients of these isomers being 162 and 208, respectively. This conclusion was also confirmed by the plot of the calculated theoretical plate numbers against G/L based on the equation in a previous paper [5]. For example, the maximum theoretical plate number for the dimethyl–diethyl phthalate separation was about 30 at $G/L = 440$, and that for the decahydronaphthalene stereoisomer separation was 62 at $G/L = 185$. For the *cis*-decahydronaphthalene–tetrahydronaphthalene sample, the optimum G/L value measured at 140°C was 235, which was about 45 lower than the calculated value. As there was no observed change in the operating conditions except for prolonged use of the liquid phase, the partition coefficients of the components might be decreased owing to the partial deterioration of the liquid phase [9].

Optimum G/L value for purifying one particular component

From Figs. 5–7, it is suggested that the larger the G/L value, the better is the resolution at the bottom of the column and the less is the separation at the top. Figs. 6 and 7 also indicate that with decreasing G/L value the resolution efficiency became higher at the top and lower at the bottom of the column. This means that if one particular component is required to be purified, the G/L value should be set close to the partition coefficient of the other component.

Liquid phases

The requirements for the liquid phase in CCGLC include not only high selectivity but also low viscosity. The liquid phase should flow by gravity as a thin film over the packing in the column. Durability and cost are also important factors. Poly(diethylene glycol succinate) and silicone KF-54 (methylphenylsilicone) were studied with respect to these requirements. Poly(diethylene glycol succinate), a highly polar liquid phase for GC, was denatured quickly from a transparent brown liquid to a dark brown paste even during the warm-up period. Silicone KF-54, a slightly polar liquid phase, remained as a smooth liquid with long-term operation at 200°C. Using KF-54, over 99% purities of the samples of dimethyl–diethyl phthalate and *cis*-decahydronaphthalene–tetrahydronaphthalene were obtained. For the separation of decahydronaphthalene stereoisomers, about 94.5% purity of *cis*-decahydronaphthalene was obtained. It is necessary for more polar and stable liquid phases to be developed in order to extend the applicable range of this method. Precise temperature control system would also improve the separation, as the system used was made in the laboratory, and might have some temperature deviation.

CONCLUSION

The separation of test samples with high boiling points could have been achieved by using the

TABLE I

COMPARISON OF THE SYSTEMS

Parameter	Previous system	Present system
Sample applicable	B.p. up to 130°C, *e.g.*, *n*-hexane, isooctane, benzene, toluene, ethanol	B.p. up to 300°C, *e.g.*, dimethyl phthalate, diethyl phthalate, decahydronaphthalene, tetrahydronaphthalene
Temperature of separating section	Up to 60°C	Up to 200°C
Temperature of stripping section	Up to 85°C	Up to 260°C
Liquid phase	PEG 400, squalane	Silicone KF-54

proposed system. The characteristics of the system are given in the Table I in comparison with the previous system.

REFERENCES

1 P. E. Barker and D. Critcher, *Chem. Eng. Sci.*, 13 (1960) 82.
2 P. E. Barker and D. H. Huntington, *J. Gas Chromatogr.*, (1966) 59.
3 P. E. Barker and D. H. Huntington, in A. B. Littlewood (Editor), *Gas Chromatography*, Elsevier, New York, 1967, p. 135.
4 D. Glasser, in A. B. Littlewood (Editor), *Gas Chromatography*, Elsevier, New York, 1967, p. 119.
5 S. Araki, S. Suzuki and Y. Takahata, *Kogyo Kagaku Zasshi*, 73 (1970) 923.
6 S. Araki, S. Suzuki, H. Iwahara and Y. Takahata, *Kogyo Kagaku Zasshi*, 74 (1971) 647.
7 K. Watabe, T. Sengoku, S. Suzuki and S. Araki, *Nippon Kagaku Kaishi*, (1975) 88.
8 K. Watabe, *Master Thesis*, Tokyo Metropolitan University (1972).
9 S. Araki, S. Suzuki, K. Watabe and Y. Takahata, *Bunseki Kagaku*, 20 (1971) 1200.

Journal of Chromatography, 590 (1992) 297–303
Elsevier Science Publishers B.V., Amsterdam

CHROM. 23 747

Gas chromatographic retention behaviour of dibenzothiophene derivatives on a smectic liquid crystalline polysiloxane stationary phase

H. Budzinski, P. Garrigues* and J. Bellocq

Groupe d'Océanographie Physico-Chimique, UA 348 CNRS, Université de Bordeaux I, F-33405 Talence, Cédex (France)

(First received June 11th, 1991; revised manuscript received September 19th, 1991)

ABSTRACT

The gas chromatographic retention behaviour, on a smectic liquid crystalline polysiloxane stationary phase, of methyldibenzothiophenes and eighteen C_2-dibenzothiophenes (sixteen dimethyldibenzothiophenes and two ethyldibenzothiophenes), out of twenty possible compounds, was investigated. The retention, in addition to vapour pressure and polarity, was greatly influenced by the molecular geometry of the solutes. The major factor affecting this behaviour was the length to breadth ratio (L/B). The elution order of the dimethyldibenzothiophenes was fairly well correlated with L/B values: Roughly, the lower the L/B values, the earlier the dimethyldibenzothiophenes were eluted. However, the solute molecular shape, although of less importance, was also a significant retention-affecting factor, having the contrary effect to L/B values on the elution order. Arc-like molecules (dibenzothiophenes) with groups attached to the outer curved side (*i.e.*, in positions 3 and 4) were retained longer than predicted by L/B values. In contrast, isomers conforming to the arc-like arrangement (*i.e.*, with substituents in positions 1 and 2) were less retained than predicted. The application of these identifications to a crude oil sample is described.

INTRODUCTION

Complex mixtures of alkylated polycyclic aromatic sulphur heterocyclic (PASHs) present in natural matrices contain numerous isomeric structures. Increasing attention has been paid to the separation and determination of individual alkylated PASHs both in organic geochemistry [1–3] (the distribution of methylated dibenzothiophenes may be typical of the origin or of the maturation of crude oils [4–6]) and in environmental chemistry [7] (isomeric forms often have different carcinogenic or mutagenic activities). Even if little is known about these properties of alkylated PASHs, the example of the ability of monomethyl derivatives of benzo[*a*]pyrene (BaP) to initiate mouse skin tumours may illustrate this well [8].

Much systematic work has been carried out on the analysis of polycyclic aromatic hydrocarbons (PAHs), with systematic studies of the C_1, C_2, C_3 and C_4 derivatives of compounds such as naphthalene [9–11] and phenanthrene [12–14], often for geochemical reasons, but no corresponding systematic work is known for dibenzothiophenes. The detection of these compounds represents a real challenge because of the large number of isomers to be separated. Moreover, in most instances the dibenzothiophenes are minor constituents compared with the more abundant phenanthrenes. In order to obtain a good gas chromatographic separation, we chose a liquid crystalline stationary phase for the analysis of dibenzothiophene derivatives.

Liquid crystalline stationary phases have temperature-dependent ordered structures. The solute interacts with this ordered structure [15]. While compounds on non-polar stationary phases elute

0021-9673/92/$05.00

according to their increasing boiling points, on liquid crystalline stationary phases retention is also governed by solute geometry. In liquid chromatography the length-to-breadth ratio (L/B) had appeared as a reliable descriptor for polymeric C_{18} phases [16]. Nishioka *et al.* [17] also related gas chromatographic retention behaviour, on liquid crystalline phases, to this ratio and to the space molecular shape. In this work, retention data for C_1- and C_2-dibenzothiophenes (DBTs) on a liquid crystalline stationary phase were determined with a view to geochemical applications, and we also correlated these data with the L/B values for each molecule studied. Liquid crystals can demonstrate nematic, cholesteric or smectic properties within a certain temperature range. It has been generally accepted that nematic phases produced a better chromatographic resolution than did smectic phases [18]. However, Nishioka *et al.* [17] have developed smectic liquid crystalline stationary phases which demonstrated very good resolution for isomeric polycyclic aromatic compounds (PACs). These considerations led us to choose a smectic liquid crystalline phase for the separation of the C_1- and C_2-benzothiophenes.

EXPERIMENTAL

Materials

The methyldibenzothiophenes (MDBTs) and the C_2-dibenzothiophenes [dimethyldibenzothiophenes (DMDBTs) and ethyldibenzothiophenes (EtDBTs)] were synthesized at Brigham Young University (Provo, UT, USA) [19] and were kindly provided by M. L. Lee. The positions of substitution on the aromatic nucleus were numbered according to the numbering system currently in use (Fig. 1) with the sulphur atom at position 5.

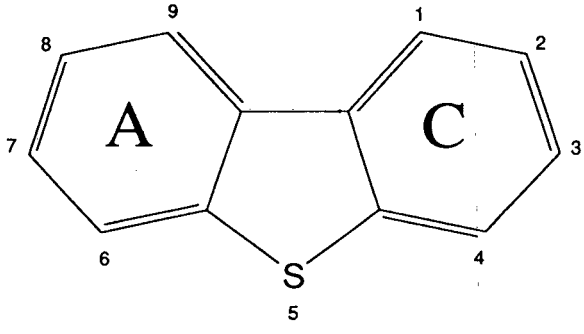

Fig. 1. Numbering of the dibenzothiophene molecule.

The crude oil sample came from a Tunisian oil field. Sample preparation and aromatic compound separation by high-performance liquid chromatography (HPLC) have been described elsewhere [20].

Retention indices

Retention data are expressed in the form of retention indices (*RI*). They are based on comparison of the retention times of the compounds of interest with those of calibration products. In the original Kováts retention index scale, they are the homologous *n*-alkanes. However, for the analysis of PAHs, Lee *et al.* [21] introduced a calibration scale specifically based on aromatic standards, benzene, naphthalene, phenanthrene, chrysene and picene, denoted in this work as *RIN* (retention indices for neutral aromatic compounds). According to this approach, Andersson [22] also defined a scale for the analysis of benzothiophenes based on the following PASHs: thiophene, benzothiophene, dibenzothiophene, benzonaphtho[2,1-*d*]thiophene and benzophenanthro[2,1-*d*]thiophene. These compounds were assigned *RI* values of 100, 200, 300, 400 and 500, respectively. The *RI* values based on this scale are denoted *RIS* (retention indices for sulphur aromatic compounds) and were calculated according to the equation [21]

$$RIS = 100 \cdot \frac{t_{r_x} - t_{r_z}}{t_{r_{z+1}} - t_{r_z}} \quad (1)$$

where t_r is retention time, x the compound of interest (in this study the DBT derivatives) and z and $z + 1$ are the number of aromatic rings in the standard thiophenes eluting prior to and after the studied compounds (here $z = 3$).

Chromatographic and detection conditions

The DBT derivative standards and the collected HPLC fractions were analysed by gas chromatography–mass spectrometry, using an HP 5890 Series II gas chromatograph equipped with a splitless injector (purge delay 30 s, purge flow 60 ml/min) and a 50 m × 0.22 mm I.D. SB-Smectic phase column (Dionex, Lee Scientific Divison), film thickness 0.1 μm. Helium was used as the carrier gas with a column head pressure of 3.5 bar. The detector was an HP 5970 mass-selective detector [electron impact,

70 eV; selected ion monitoring (SIM) mode, *m/z* 184 for DBT, *m/z* 198 for the MDBTs, *m/z* 212 for the C_2-DBTs; 2 scans/s; voltage, 2200 V]. The temperature programme consisted of an initial isothermal period of 2 min at 50°C, then programming at 10°C/min to 140°C, followed by an isothermal period of 2 min at 140°C, then programming at 2°C/min to 250°C with an isothermal period of 30 min at 250°C. The injector and detector were kept at 250°C.

The DBT derivatives were dissolved in cyclohexane at a concentration of 40 μg/ml. The retention time of each compound was determined three to five times; all the compounds showed a standard deviation below 0.20 *RIS*.

Length to breadth ratio (L/B) calculations

The calculations were carried out on a desk-top microcomputer (TANDY 3000 NL) for the C_1- and C_2-DBT isomers using the MMX software (Serena Software, Bloomington, GA, USA), derived from the original MM2MP2 empirical force field method [23,24]. The calculations provided an estimate of the steric energy and the heat of formation (ΔH_f^0) at 298 K in the gas phase of the compounds; they also yielded the geometry of the molecule [bond lengths, angles and particularly the dihedral angle between rings A and C (see Fig. 1)]. In-house software also provided the length (*L*) and the breadth (*B*) of the molecule, which correspond to the dimensions of a minimized rectangle for each molecule studied.

RESULTS AND DISCUSSION

Retention indices and molecular shape

A SIM gas chromatogram of DMDBT and MDBT standards used in the determination of retention indices is shown in Fig. 2.

The *RIS* and *RIN* values determined on the smectic liquid crystalline stationary phase for all C_1- and C_2-dibenzothiophenes (except for 1- and 3-EtDBT, which were not available) are given in Table I. One unit of *RIS* correspond to 30 s. Compounds differing by 0.60 *RIS* units were baseline resolved.

All the methyldibenzothiophenes are separated on the smectic phase and there are only three severe co-elutions, between 1,4- and 1,8-DMDBT, 2,7- and 3,6-DMDBT and 1,2-, 1,7- and 1,9-DMDBT, for the eighteen studied C_2-DBT isomers. These results demonstrate once again the selectivity of liquid crystal phases, as shown previously for methylphenanthrenes [17].

The DMDBT isomers differ significantly in length, breadth and *L/B* values (see Table I). The elution order of DBT derivatives follows roughly increasing *L/B* values (see Fig. 3). For instance, 3,7- and 2,3-DMDBT, which exhibit high *L/B* values (1.81 and 1.48, respectively) are eluted latter whereas 4,6- and 2,4-DMDBT with low values of *L/B* (1.11 and 1.04, respectively) are eluted first (see also Fig. 3).

The correlation equation obtained for the fifteen DMDBTs is

$$RIS = 281.75 + 32.23L/B \quad (2)$$

with a correlation coefficient $r = 0.74$. Predicted *RIS* values (RIS_c) were calculated from eqn. 2 and compared with measured values. The average deviation was *ca.* 1%. Higher deviations of *ca.* 4% were obtained for 3,4- and 2,8-DMDBT. The correlation coefficient (*r*) increases to 0.93 when 2,8- and 3,4-DMDBT are omitted and reaches 0.98 when, in addition, 1,8- and 1,9-DMDBT (deviation higher than 1%) are not considered. This means that the retention behaviour of the compounds is not exactly and entirely dependent only on the *L/B* values. The spatial molecular shape (as discussed previously by Nishioka *et al.* [17]) and dihedral angles or, more precisely, the distorsion of the molecules (as mentioned and shown more precisely for dimethylphenanthrene isomers in the case of liquid chromatography [16]) are also important factors affecting retention.

A correlation coefficient of 0.57 is obtained when the retention indices (*RIS*) of all sixteen DMDBTs are plotted as a function of the molecular length (*L*) and 0.72 for the molecular breadth (*B*) (Table I). This indicates that the retention behaviour of DMDBT isomers is mainly controlled by the breadth of the molecules. When 3,4-, 2,8-, 1,8- and 1,9-DMDBT are not considered in the DMDBT set, the latter correlation coefficient reaches 0.96.

The relatively anomalous behaviour of 3,4-, 2,8- and 1,8-DMDBT is dependent on the molecular shape of the solutes. As can be seen in Table I, by comparison of the *RIS* and RIS_c values, 3,4-DMDBT is more retained and 2,8- and 1,8-DMDBT are eluted earlier than predicted from their *L/B* values.

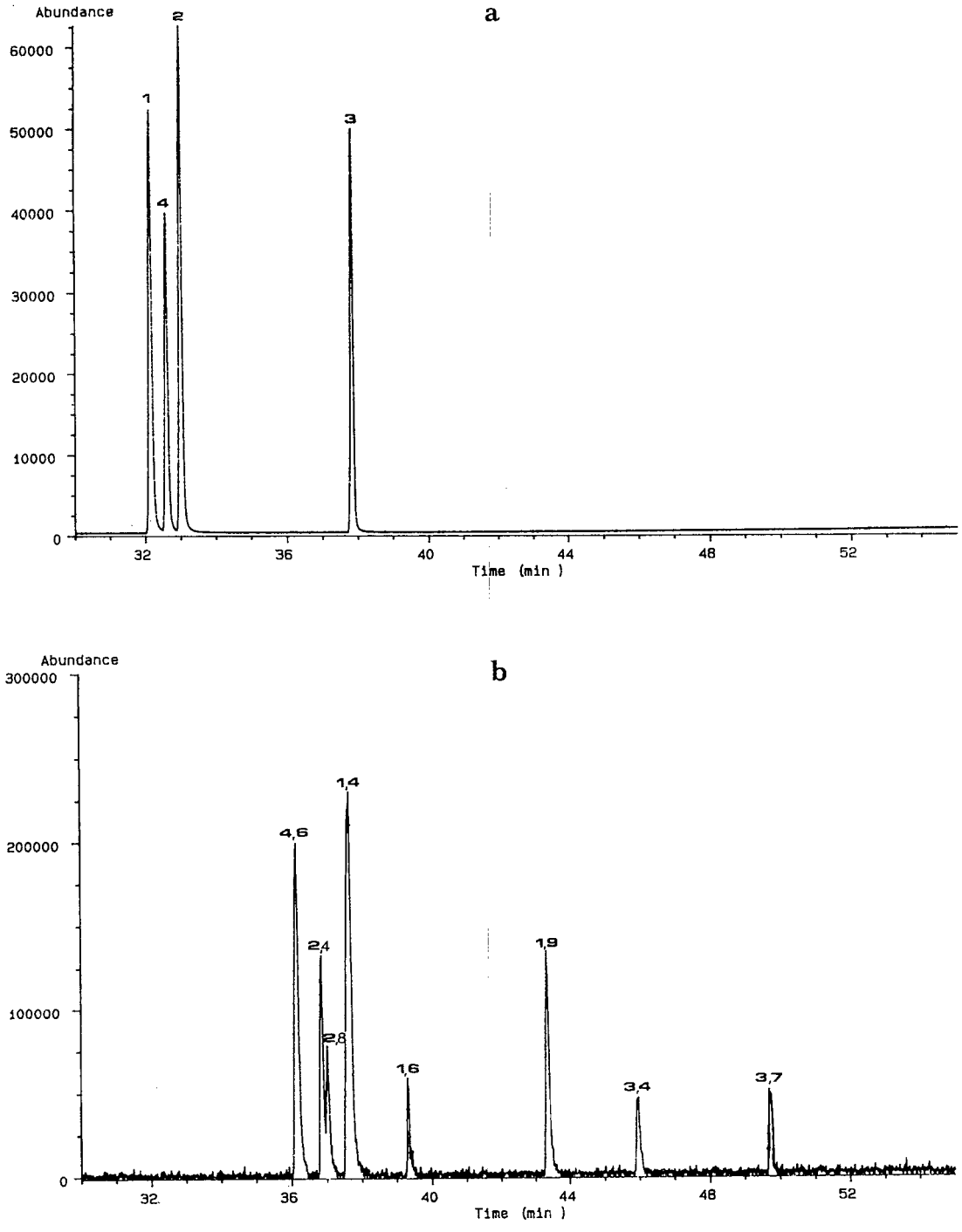

Fig. 2. Partial SIM gas chromatograms of DBT derivative standards used in the determination of gas chromatographic retention indices (see text for experimental conditions). (a) MDBT, *m/z* 198; (b) C_2-DBT, *m/z* 212.

TABLE I

RETENTION INDICES AND SHAPE PARAMETERS FOR METHYL-, ETHYL- AND DIMETHYLDIBENZOTHIOPHENE ISOMERS

RIS and *RIN* were determined by experiments whereas RIS_c were calculated through the correlation eqns. 2 and 3 (see text).

Compound	*RIN*	*RIS*	RIS_c	Deviation (%)	Length (*L*) (Å)	Breadth (*B*) (Å)	*L*/*B*	Dihedral angle (°)[a]
1-MDBT	302.41	308.53	310.33	+0.6	11.40	8.30	1.37	n.d.
2-MDBT	303.85	310.30	314.24	+1.2	11.95	7.95	1.50	n.d.
3-MDBT	312.08	320.35	316.85	−1.1	12.55	7.90	1.59	n.d.
4-MDBT	303.08	309.34	307.08	−0.7	11.40	8.90	1.28	n.d.
1,2-DMDBT	319.75	329.73	327.19	−0.8	12.10	8.55	1.41	8.4
1,3-DMDBT	316.28	325.31	328.81	+1.1	12.60	8.60	1.46	5.6
1,4-DMDBT	309.81	317.40	319.78	+0.7	11.65	9.90	1.18	5.8
1,6-DMDBT	312.63	320.85	321.07	+0.1	11.70	9.55	1.22	6.5
1,7-DMDBT	319.53	329.28	329.77	+0.1	12.50	8.40	1.49	5.9
1,8-DMDBT	309.81	317.40	323.33	+1.9	12.30	9.50	1.29	5.4
1,9-DMDBT	319.53	329.28	323.33	−1.8	11.40	8.85	1.29	20.0
2,3-DMDBT	322.40	332.97	329.77	−1.0	12.50	8.40	1.49	0.1
2,4-DMDBT	308.51	315.80	316.88	+0.3	11.50	10.55	1.09	0.1
2,6-DMDBT	314.87	323.59	323.33	+0.1	12.60	9.75	1.29	0.4
2,7-DMDBT	321.50	331.70	331.38	−0.1	13.00	8.45	1.54	0.1
2,8-DMDBT	308.81	316.17	328.16	+3.8	12.05	8.35	1.44	0.1
3,4-DMDBT	323.87	334.60	321.07	−4.0	11.65	9.55	1.22	0.1
3,6-DMDBT	321.58	331.79	331.06	−0.2	12.80	8.35	1.22	0.6
3,7-DMDBT	330.21	342.34	340.09	+0.7	13.50	7.45	1.81	0.1
4,6-DMDBT	307.30	314.33	317.52	+1.0	11.65	10.50	1.11	0.1
2-EtDBT[b]	305.55	312.19	n.d.[c]	n.d.	n.d.	n.d.	1.32	n.d.
4-EtDBT	306.54	313.39	n.d.	n.d.	n.d.	n.d.	1.37	n.d.

[a] Angles between rings A and C (see Fig. 1).
[b] Et = Ethyl.
[c] n.d. = Not determined.

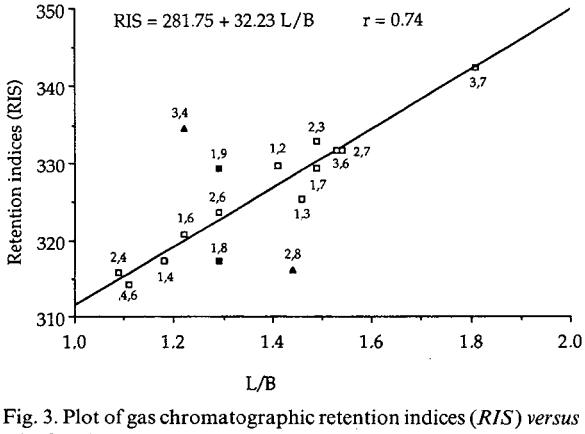

Fig. 3. Plot of gas chromatographic retention indices (*RIS*) *versus* *L*/*B* for the sixteen studied DMDBT isomers. ▲ = Deviation >3%; ■ = deviation >1%; □ = deviation <1%.

The same features can be observed for the MDBTs. The correlation equation obtained for the four MDBTs (see Fig. 4) is

$$RIS = 265.86 + 32.24L/B \quad (3)$$

with a correlation coefficient $r = 0.80$. RIS_c values were calculated from eqn. 3 and compared with the measured values (*RIS*). Despite a good agreement between the *RIS* and RIS_c values (see Table I; the highest deviations were near 1%), the 1- and 2-MDBTs are eluted earlier than predicted by their *L*/*B* values, with the largest difference for 2-MDBT (see Table I). In comparison, the 3- and 4-MDBTs are more strongly retained, with the greatest deviation for 3-MDBT (see Table I).

As previously reported by Nishioka *et al.* [17], arc-like molecules (such as DBT or DBT with methyl groups in position 1 or 2; see Fig. 1) seem to

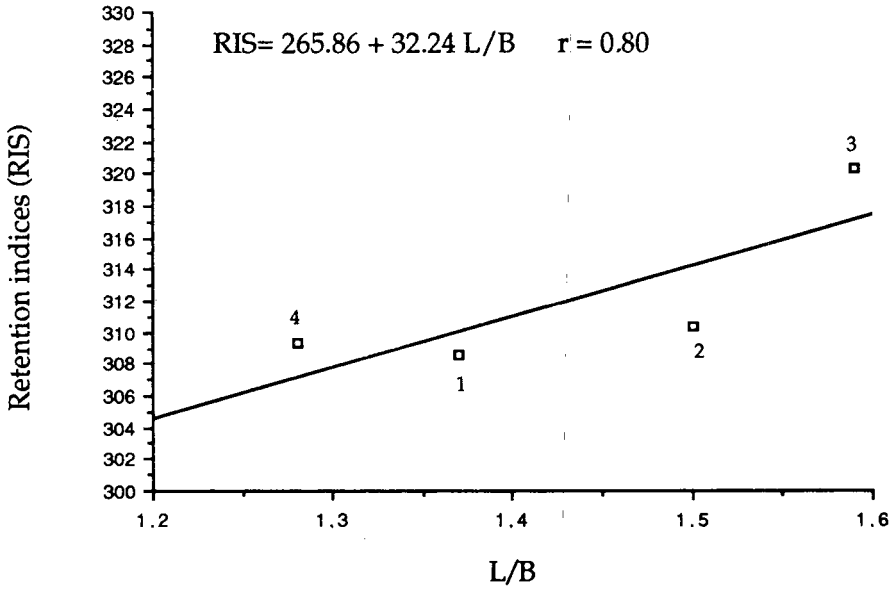

Fig. 4. Plot of gas chromatographic retention indices (*RIS*) *versus* *L/B* for the 4 MDBT isomers.

be eluted earlier than predicted by the *L/B* ratios. In contrast, molecules with substituents attached to the outer curved side (*i.e.*, DBT with methyl groups in positions 3 and 4; see Fig. 1) seem to be retained longer than expected. The apparently anomalous behaviour of 3,4-, 2,8- and 1,8-DBT fits these observations, but no retention mechanism has yet been proposed.

Analytical applications

Fig. 5 shows the identification of the C_1- and C_2-DBTs in a crude oil. True identifications were

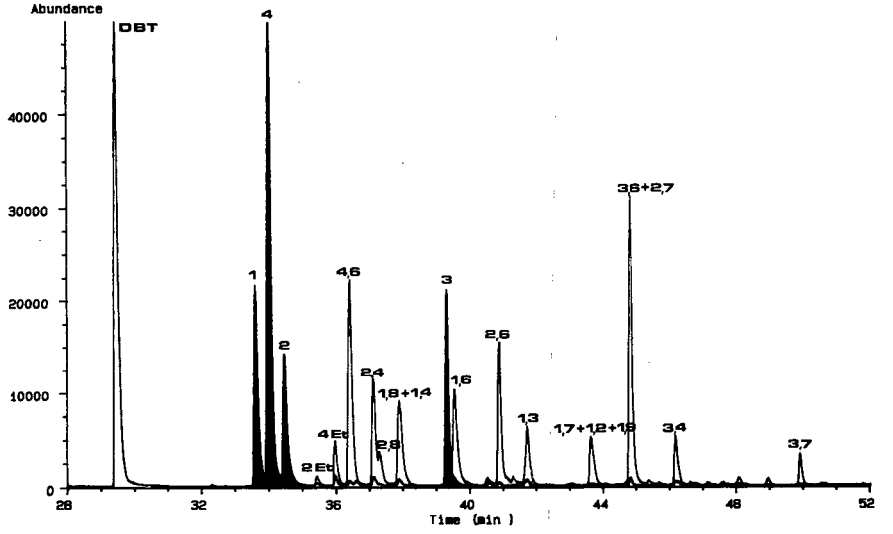

Fig. 5. SIM gas chromatogram (*m/z* 184 for DBTs; *m/z* 198 for the MDBTs; *m/z* 212 for C_2-DBTs) of a dibenzothiophenic fraction from a crude oil (see text for experimental conditions). DBT = Dibenzothiophene; 1, 2, 3 and 4 = 1-, 2-, 3- and 4-methyldibenzothiophene, respectively; 2-Et and 4-Et = 2- and 4-ethyldibenzothiophene, respectively; 4,6, etc. = 4,6-dimethyldibenzothiophene, etc.

achieved by capillary gas chromatography–mass spectrometry and co-injections with pure standards. It can be seen that even though the resolution is not complete between 2,4- and 2,8-DMDBT (they differ by 0.37 *RIS* unit), it is more than 50%, which is sufficient to identify and determine them correctly in natural samples.

Although all the MDBTs and C_2-DBTs studied were present in natural samples, the more abundant isomers were those with a methyl group in position 4 or 6, as predicted by molecular mechanics calculations. Such trends illustrate well the opportunity to obtain theoretical information in order to predict retention behaviour and abundance of alkylated PASHs in natural samples. This will be of a great interest for future geochemical applications.

CONCLUSIONS

This study illustrates well the great selectivity of smectic liquid crystalline phases for analyses of PAHs (in this instance DBT derivatives). Twelve out of eighteen C_2-DBTs available in this study could be baseline resolved. There were only two severe co-elutions, between the 3,6- and 2,7-DMDBT and between 1,2-, 1,9- and 1,7-DMDBTs. The 2,8- and 2,4-DMDBTs were not baseline resolved but the separation was sufficient to determine each independently. The very good separation obtained for the MDBTs and C_2-DBTs will be very useful for further geochemical studies based on DBT isomers. Further, this study provides a good illustration of the applicability of theoretical calculations to predict elution order or at least to obtain an idea of the general retention behaviour of DBT derivatives on smectic liquid crystalline stationary phases. Parameters such as the arc-like arrangement and the distorsion angles of the molecules have not been taken into account, and further investigations are needed to develop descriptors which include these two molecular parameters.

ACKNOWLEDGEMENTS

M. L. Lee (Brigham Young University, Provo, UT, USA) is acknowledged for the gift of dimethyldibenzothiophene isomers. Thanks are also due to J. Connan and J. L. Oudin for discussions. SNEA(P) and TOTAL-CFP are acknowledged for financial support in these studies.

REFERENCES

1 J. S. Sinnighe Damste, *Thesis*, University of Delft, Delft, 1988.
2 D. Leythaeuser, M. Radke and H. Willsch, *Geochim. Cosmochim. Acta*, 52 (1988) 2879.
3 M. Radke, D. Welte and H. Willsch, *Org. Geochem.*, 10 (1986) 51.
4 W. B. Hughes, *Bull. Am. Assoc. Pet. Geol.*, (1986) 181.
5 L. Schou and M. B. Myhr, *Org. Geochem.*, 13 (1988) 61.
6 I. C. Burkow, E. Jorgensen, T. Meyer, O. Rekdal and L. K. Sydnes, *Org. Geochem.*, 15 (1990) 101.
7 M. L. Lee, C. Willey, R. N. Castle and C. M. White, in A. G. Dennis and M. Cooke (Editors), *Polynuclear Aromatic Hydrocarbons: Analysis, Chemistry and Biology*, Batelle Press, Columbus, OH, 1980, p. 54.
8 R. I. Iger, J. W. Lyga, G. H. Daub and T. Slaga, *J. Cancer Res.*, 40 (1980) 1073.
9 R. Alexander, R. I. Kagi and P. N. Sheppard, *J. Chromatogr.*, 267 (1983) 367.
10 R. Alexander, R. I. Kagi, S. J. Rowland, P. N. Sheppard and T. V. Chirila, *Geochim. Cosmochim. Acta*, 49 (1985) 385.
11 P. G. Forster, R. Alexander and R. I. Kagi, *J. Chromatogr.*, 483 (1989) 384.
12 P. Garrigues, E. Parlenti, M. Radke, J. Bellocq, H. Willsch and M. Ewald, *J. Chromatogr.*, 395 (1987) 217.
13 M. Radke, D. H. Welte and H. Willsch, *Geochim. Cosmochim. Acta*, 46 (1982) 1.
14 M. Radke, P. Garrigues and H. Willsch, *Org. Geochem.*, 15 (1990) 17.
15 Z. Witkiewicz, *J. Chromatogr.*, 251 (1982) 311.
16 P. Garrigues, M. Radke, O. Druez, H. Willsch and J. Bellocq, *J. Chromatogr.*, 473 (1989) 207.
17 M. Nishioka, B. A. Jones, B. J. Tarbet, J. S. Bradshaw and M. L. Lee, *J. Chromatogr.*, 357 (1986) 79.
18 G. M. Janini, K. Johnston and W. L. Zielinski, Jr., *Anal. Chem.*, 47 (1975) 670.
19 Y. Tominaga, M. L. Lee and R. J. Castle, *J. Heterocycl. Chem.*, 18 (1981) 967.
20 P. Garrigues, R. de Sury, M. L. Angelin, J. Bellocq, J. L. Oudin and M. Ewald, *Geochim. Cosmochim. Acta*, 52 (1988) 375.
21 M. L. Lee, D. L. Vassilaros, C. M. White and M. Novotny, *Anal. Chem.*, 51 (1979) 768.
22 J. T. Andersson, *J. Chromatogr.*, 354 (1986) 83.
23 N. L. Allinger, J. T. Sprague and T. J. Liljefors, *J. Am. Chem. Soc.*, 96 (1974) 5100.
24 J. Kao and N. L. Allinger, *J. Am. Chem. Soc.*, 99 (1977) 975.

Journal of Chromatography, 590 (1992) 305–312
Elsevier Science Publishers B.V., Amsterdam

CHROM. 23 761

Deuteration as an aid to the high-temperature gas chromatography–mass spectrometry of steryl fatty acyl esters

Richard P. Evershed*, Mark C. Prescott and L. John Goad

Department of Biochemistry, University of Liverpool, P.O. Box 147, Liverpool L69 3BX (UK)

(Received July 29th, 1991)

ABSTRACT

A method is presented for reducing degradative losses of steryl fatty acyl esters bearing polyunsaturated fatty acyl moieties during high-temperature gas chromatography (GC) and combined high-temperature GC–mass spectrometry (MS). The method employs selective deuteration of the double bonds in the fatty acyl moiety using a homogeneous catalyst (Wilkinson's catalyst). The Δ^5 double bond, which occurs in the most commonly occurring plant and animal sterols, is not deuterated under the conditions described. In addition to improving GC behaviour, the method has the advantage of preserving structure information by labelling each double bond present in the original unsaturated fatty acyl moiety. The carbon number and degree of unsaturation of the labelled fatty acyl moiety are readily revealed by combined GC–MS employing negative-ion ammonia chemical ionisation. Two applications of the method are demonstrated in the analysis of steryl fatty acyl esters isolated from a rape seed oil and ovary tissue of the marine prawn *Penaeus monodon*.

INTRODUCTION

Flexible fused-silica capillary columns coated with various high-temperature stable stationary phases are finding increasing use in the separation of high-molecular-weight acyl lipids, such as triacylglycerols, steryl esters and wax esters [1]. Although many impressive separations have been demonstrated, a number of workers have observed poor recoveries of certain high-molecular-weight and polyunsaturated compounds during gas chromatographic (GC) analyses [1–5]. Losses of apolar high-molecular-weight triacylglycerols have been attributed to their reversible saturation in the apolar immobilised dimethyl polysiloxane stationary phase employed for analysis [2]. Although this effect may also account for losses of polyunsaturated components, thermal decomposition or polymerisation may be a more important factor [1].

When performing high-temperature GC analyses of plasma steryl esters using a polar SP 2330 capillary column Kuksis *et al.* [3] observed a reduced abundance of steryl esters bearing an arachidonate (C20:4) moiety. Mareš [1] has also reported substantial losses of cholesteryl arachidonate and other polyenoic cholesteryl esters on capillary columns coated with a polarisable stationary phase. In our own work with authentic compounds, chromatographed on an immobilised dimethyl polysiloxane stationary phase, we observed only 40% recovery of cholesteryl arachidonate relative to cholesteryl palmitate [5]. Catalytic hydrogenation of this mixture, resulting in conversion of the cholesteryl arachidonate to cholesteryl arachidate, followed by GC, showed the similar recoveries of the palmitate and arachidate esters. Thus, the selective loss of ester that was occurring was due to the presence of the polyunsaturated arachidonate moiety. The wide oc-

0021-9673/92/$05.00

currence of highly unsaturated acyl moieties, particularly in marine organisms, would appear to limit the usefulness of high-temperature GC and GC–mass spectrometry (MS) in accurate steryl ester analyses.

In this paper we describe a technique for improving recoveries of steryl esters bearing polyunsaturated fatty acyl moieties during high-temperature GC and GC–MS analyses. The technique involves selective catalytic reduction of double bonds in unsaturated fatty acyl moieties using deuterium gas and Wilkinson's catalyst [tris(triphenylphosphine)–rhodium(I) chloride]. The resulting steryl esters display enhanced recoveries in GC analyses, with structure information (carbon number and degree of unsaturation) preserved through stable isotope labelling at the positions of the original double bonds in the fatty acyl moieties.

EXPERIMENTAL

Samples

The authentic compounds listed in Table I were purchased from Sigma. Rapeseed oil steryl fatty acyl esters were isolated by column chromatography (Al_2O_3; Brockmann, Grade III) of the whole oil eluting with hexane, followed by 2% diethyl ether in hexane [6]. The latter fraction containing the steryl fatty acyl esters was further purified by preparative thin-layer chromatography (TLC; 20 × 20 cm; 0.5 mm silica gel layer). Elution with 2% (v/v) diethyl ether in cyclohexane and visualisation under UV light after spraying with berberine (0.005% in ethanol) revealed a band eluting adjacent to authentic cholesteryl oleate (R_F 0.35). Steryl fatty acyl esters of the ovaries of the marine prawn, *Penaeus monodon*, were obtained as above by preparative TLC of the hexane extract of freeze-dried ovary tissue [7].

Catalytic reductions

Heterogeneous catalyst. Deuterium reduction was carried out by adding catalytic amounts of platinum on activated carbon (Aldrich) to 100 μg–1 mg amounts of steryl fatty acyl esters dissolved in ethyl acetate (100 μl) in screw-capped vials (5 ml). Each of the vials was purged with deuterium gas (99.95%; Air Products) tightly capped, and allowed to stand at room temperature (2 h).

Homogeneous catalyst. Catalytic reductions using Wilkinson's catalyst (Aldrich Chemical) were based on the method used by Dickens *et al.* [8] to deuterate diacylglycerols released enzymatically from phospholipids. Reactions were again performed in screw-capped vials (5 ml) by heating (60°C, 2 h) steryl fatty acyl esters (100 μl to 1 mg), dissolved in 1,4-dioxane (300 μl) in the presence of Wilkinson's catalyst (0.5 mg) in the presence of deuterium gas.

Sample purification. The products of reductions using both heterogeneous and homogeneous catalysts were purified by TLC (SiO_2, 2% (v/v) diethyl ether in cyclohexane; R_F 0.35) prior to GC–MS analysis. Visualisation was by UV illumination following spraying with berberine as described above.

High-temperature GC–MS

The GC–MS instrumentation comprised a Pye 204 GC linked to a VG7070H double-focussing magnetic sector mass spectrometer *via* an interface oven modified for high-temperature operation (> 300°C) [9,10]. Samples were dissolved in hexane for injection *via* an SGE OCI III on-column injector at a GC oven temperature of 50°C. A 0.5-m "retention gap" was used to protect the analytical column and eliminate undesirable injection phenomena [11]. The analytical column was an SGE 12 m × 0.22 mm I.D. aluminium clad BP-1 coated capillary (immobilised dimethyl polysiloxane; 0.1 μm film thickness) connected directly into the MS ion source [12]. Temperature programming of the GC oven temperature was from 50 to 330°C at 8°C min^{-1}.

The mass spectrometer was operated in the full scan mode at an accelerating voltage of 4 kV. In analyses employing electron ionisation (EI; 70 eV) the m/z range was scanned from 40 to 700 in a total cycle time of 3.25 s. When conducting negative ion chemical ionisation (NICI) using ammonia as reagent gas [9,10,13] the m/z range was scanned from 150 to 450 in a total cycle time of 2.75 s. Instrument operation, data acquisition and processing were under the control of a Finnigan INCOS 2300 data system.

RESULTS AND DISCUSSION

The aim of this work was to develop a technique for improving the GC behaviour of intact steryl fat-

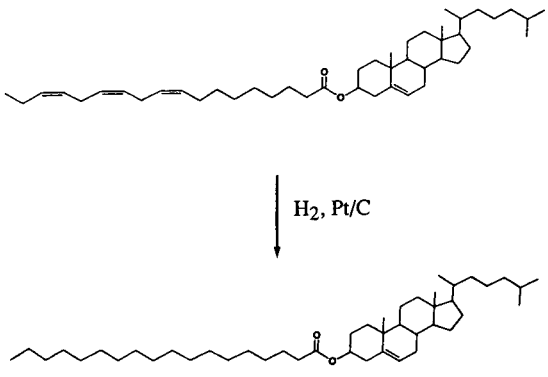

Scheme 1.

ty acyl esters bearing polyunsaturated acyl moieties that would also allow structure investigations to be performed by mass spectrometry. The approach which was investigated involved: (i) Catalytic reduction of the double bonds in the fatty acyl moieties in order to enhance thermal stability of the intact steryl esters in high-temperature GC–MS analyses. (ii) Labelling the double bond with deuterium in order that the carbon number and degree of unsaturation of the original polyunsaturated fatty acyl moiety could be deduced by GC–MS employing NICI using ammonia as reagent gas [9,10,13].

Heterogeneous catalyst

Hydrogenation, using heterogeneous catalysts, has been used previously to enhance recoveries of

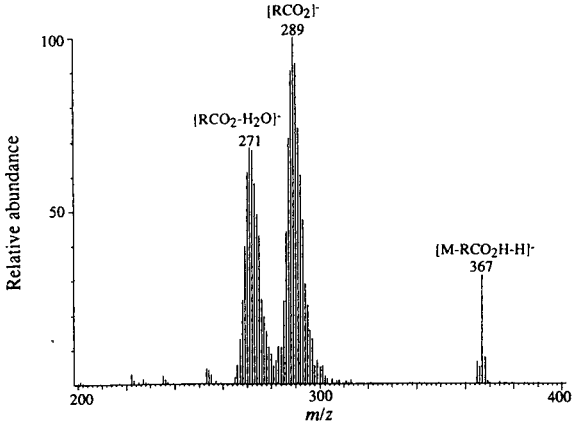

Fig. 1. NICI mass spectrum of cholesteryl linolenate reduced with deuterium gas in the presence of platinum on activated charcoal.

polyunsaturated lipids in GC and GC–MS analyses. The recovery of steryl ester in GC analyses is greatly improved in the case of cholesteryl linolenate, following its catalytic reduction to cholesteryl arachidate using hydrogen and a heterogeneous catalyst, such as platinum on activated carbon. Although this latter technique is useful for revealing the presence of polyunsaturated lipid species which display poor GC performance, all structural information concerning the degree of unsaturation of the original unsaturated fatty acyl moiety is lost (Scheme 1). Simply replacing hydrogen with deuterium gas in the catalytic reduction when using a heterogeneous catalyst is ineffective, as the addition of deuterium atoms to the double bonds in alkyl compounds, in the presence of this type of catalyst is not discrete but rather non-specific with hydrogen exchange for deuterium at other methylene groups. This lack of specificity in the catalytic reduction is clearly revealled by the ammonia NICI mass spectrum shown in Fig. 1 recorded for cholesteryl linolenate reduced with $^2H_2$ over Pt/C. The mass spectrum shows two complex envelopes of fragment ion peaks centering on *m/z* 289 and 271, respectively. The former envelope represents a cluster of ions corresponding to the $[RCO_2]^-$ moiety while the group at *m/z* arise from $[RCO_2-H_2O]^-$ and $[RCO_2-H_2O-H]^-$ ions bearing varying numbers of deuterium atoms in the fatty acyl moiety. This lack of specificity in the labelling precludes any deductions concerning the degree of unsaturation in an unknown compound, particularly if a mixture of compounds is present. The ion at *m/z* 367 corresponds to $[M-RCO_2H-H]^-$, (*i.e.* the steryl moiety) and the lack of deuterium and consequent mass change shows that the Δ^5 double bond in the sterol moiety was not catalytically reduced under the reaction conditions employed.

Homogeneous catalyst

Homogeneous catalysts are preferred for more specific labelling of double bonds by catalytic deuterium reduction. Among the catalysts that were considered, bis(triphenylphosphine)rhodium(I) chloride (Wilkinson's catalyst) was favoured on account of its ease of use and previously demonstrated ability to catalyse the deuteration of unsaturated diacylglycerols with a high degree of specificity [8].

The somewhat simplified approach adopted in

TABLE I

MASS SPECTRA OF AUTHENTIC CHOLESTERYL FATTY ACYL ESTERS OBTAINED BY GC–MS WITH NICI BEFORE AND AFTER TREATMENT WITH DEUTERIUM GAS IN THE PRESENCE OF WILKINSON'S CATALYST

Compounds	Characteristic fragment ions *m/z* (relative abundance)	
	Before	After
Saturated		
Cholesteryl myristate (14:0)[a]	367(10), 227(65), 209(100)	367(10), 227(60), 209(100)
Cholesteryl palmitate (16:0)	367(9), 255(65), 237(100)	367(13), 255(63), 237(100)
Cholesteryl stearate (18:0)	367(15), 283(71), 263(100)	367(11), 283(58), 263(100)
Unsaturated		
Cholesteryl palmitoleate (16:1)	367(23), 253(59) 235(100)	367(15), 257(60), 239(100)
Cholesteryl oleate (18:1)	367(27), 281(58), 263(100)	367(14), 285(54), 267(100)
Cholesteryl linoleate (18:2)	367(21), 279(38), 261(100)	367(31) 287(48), 269(100)
Cholesteryl linolenate (18:3)	367(28), 277(47), 259(100)	367(21), 289(43), 271(100)

[a] (Carbon number/number of double bonds) in the fatty acyl moiety.

this investigation was very economical in terms of the amounts of deuterium gas required for each reaction. Preliminary investigations with the commercially available authentic cholesteryl esters showed a high degree of specificity was attainable in deuterium reductions performed using Wilkinson's catalyst according to the conditions described in the Experimental. Table I summarises the results obtained for the range of authentic compounds tested. Fig. 2 shows the NICI spectrum for cholesteryl linolenate reduced with deuterium gas in the presence of Wilkinson's catalyst. The absence of excessive clustering in the $[RCO_2]^-$, and $[RCO_2-H_2O]^-$ and $[RCO_2-H_2O-H]^-$ ion regions confirms that a high degree of specificity was attained in the reduction. It can be assumed from this that each double bond in the fatty acyl moiety has been labelled with two deuterium atoms and minimal exchange has occurred between deuterium and hydrogen atoms at other sites in the molecule (Scheme 2). The *m/z* val-

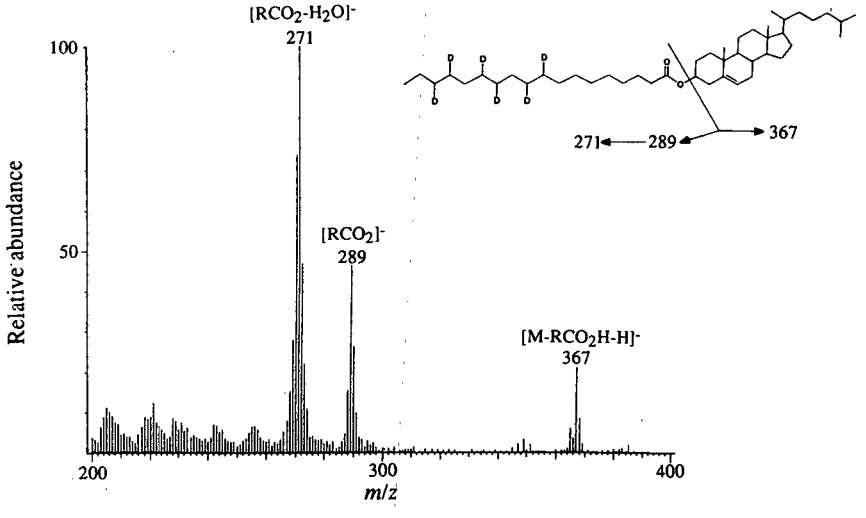

Fig. 2. NICI mass spectrum of cholesteryl linolenate reduced with deuterium gas in the presence of Wilkinson's catalyst.

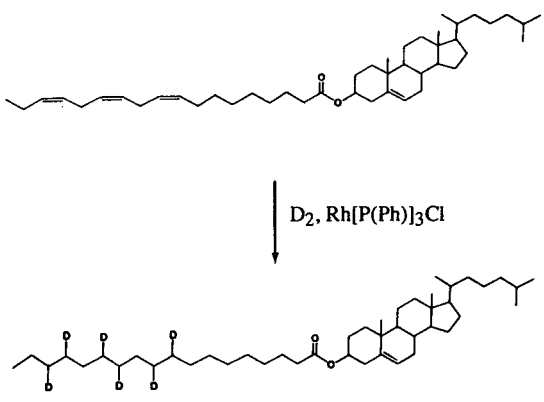

Scheme 2.

ues of the $[RCO_2]^-$ and $[RCO_2 - H_2O]^-$ ions, 289 and 271, respectively, determined from the NICI spectrum allow confident assignment of the carbon number and degree of unsaturation of the fatty acyl moiety in the case of an unknown compound. The ion at *m/z* 367 corresponds to $[M - RCO_2H - H]^-$ and shows that the Δ^5 double bond in the sterol moiety is not reduced under the reaction conditions employed; this is confirmed by the EI spectrum shown in Fig. 3. The EI spectrum shown in Fig. 3 is typical for this class of compounds and shows the paucity of ions containing information concerning the fatty acyl moiety [13–15]. Table I also shows NICI data for cholesteryl esters bearing saturated fatty acyl moieties, which again confirms that deuterium exchange does not occur at other sites in the steryl ester molecule in the presence of Wilkinson's catalyst.

Analysis of biological extracts

Rape seed oil steryl esters. Application of the deuteration technique is demonstrated first through the analysis of steryl fatty acyl esters from rape seed oil. Previous work in this laboratory [6] has shown that the steryl fatty acyl esters of this sample of rape seed oil are composed principally of sitosteryl esters of oleate (C18:1), linoleate (C18:2) and linolenate (C18:3). A partial total ion current (TIC) chromatogram resulting from the GC–MS analysis using NICI of rape seed oil steryl esters, following deuterium reduction is shown in Fig. 4. The mass spectrum for the major peak in the chromatogram is shown in Fig. 5. The mass spectrum confirmed that the reduction had proceeded to completion. The $[RCO_2]^-$ ions at *m/z* 285, 287 and 289, separated by 2 a.m.u. increments, (see inset partial mass spectrum in Fig. 5) corresponds to the fully deuterium-reduced oleate, linoleate, and linolenate, respectively. The presence of an ion at *m/z* 395 corresponds to $[M - RCO_2H - H]^-$ and confirms that sitosterol is the major sterol moiety associated with each of these acyl groups and it has not been reduced. The oleate, linoleate and linolenate content of these sitosteryl esters deduced from the deuterated products is in accord with the amounts observed in our

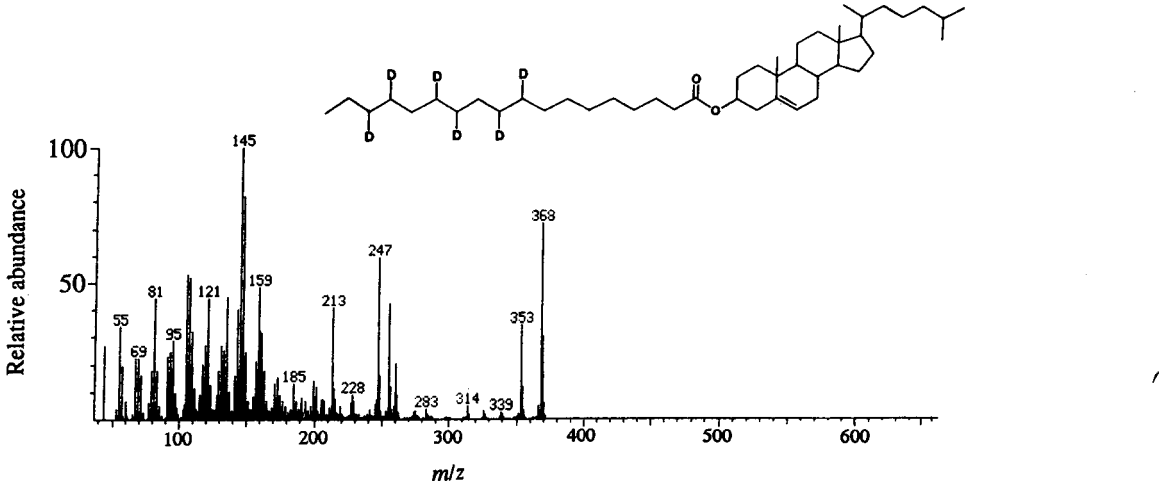

Fig. 3. EI (70 eV) mass spectrum of cholesteryl linolenate reduced with deuterium gas in the presence of Wilkinson's catalyst.

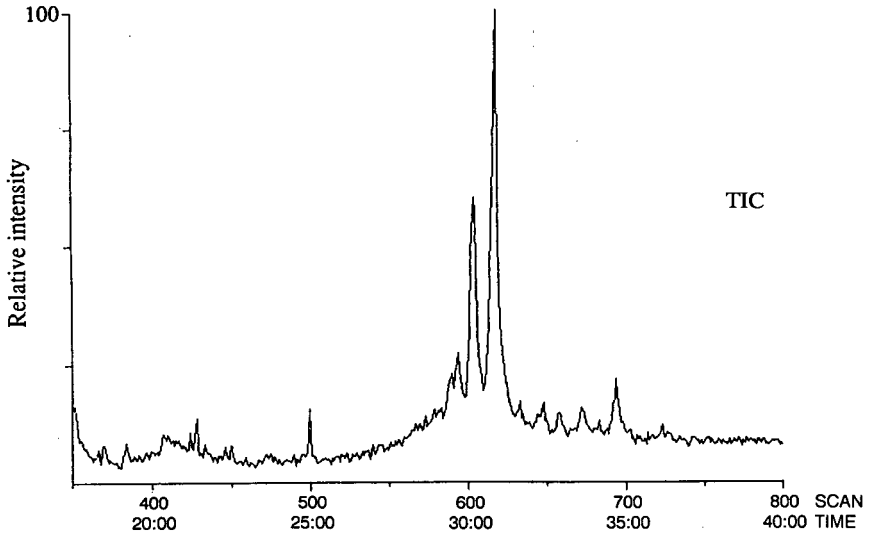

Fig. 4. TIC chromatogram for rape seed oil steryl fatty acyl esters reduced with deuterium gas using Wilkinson's catalyst determined by capillary GC–MS using NICI.

earlier studies [6]. Interpretation of the relative proportions of the fatty acyl moieties from the $[RCO_2-H_2O]^-$ ions is complicated by the clustering that results from the attendant $[RCO_2-H_2O-H]^-$ ions.

Penaeus monodon ovary steryl fatty acyl esters. Application of this technique to the analysis of the steryl fatty acyl ester mixture from the ovary of the marine prawn, *P. monodon* provides an example of the examination of a sample in which poor recov-

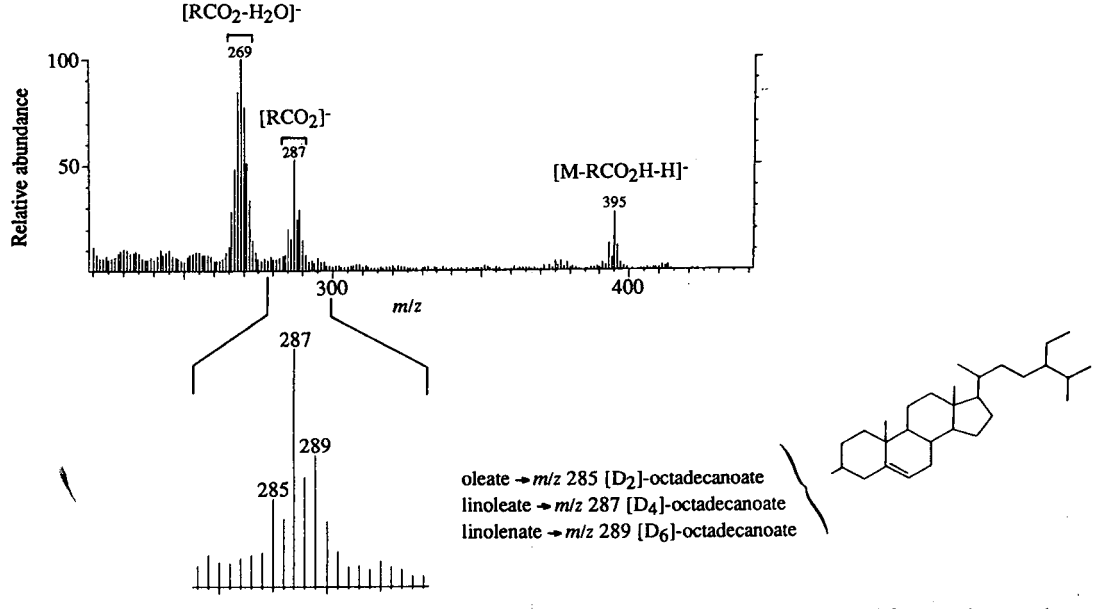

Fig. 5. NICI mass spectrum of the major peak in the TIC of the deuterated rape seed oil steryl fatty acyl esters shown in Fig. 4.

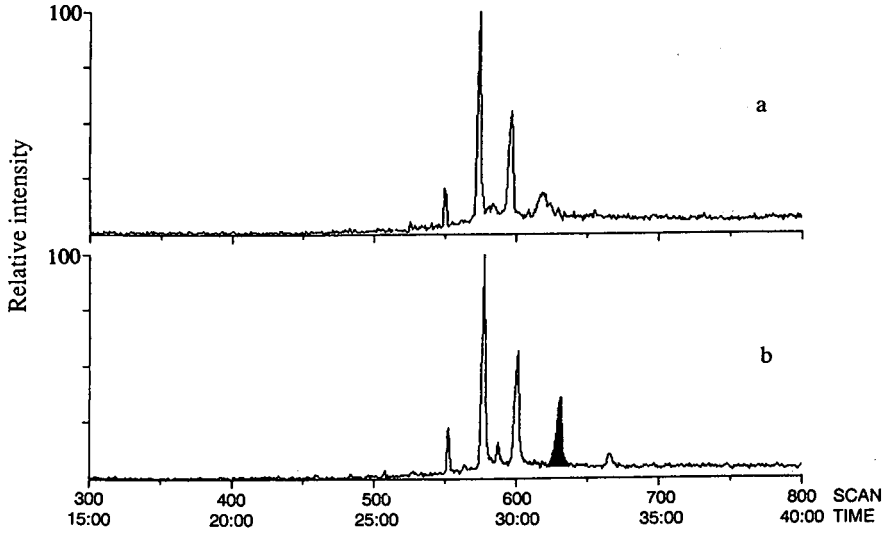

Fig. 6. TIC chromatograms obtained by GC–MS with NICI of the steryl fatty acyl esters from prawn ovaries (a) before and (b) after deuterium reduction using Wilkinson's catalyst.

eries were observed in high-temperature GC and GC–MS analyses. The partial TIC chromatogram for the intact steryl esters recorded before catalytic reduction, is shown in Fig. 6a. The chromatogram shows 3 well-shaped peaks eluting between scans 550 and 600, and a single much broader peak eluting at *ca.* scan 615. The TIC chromatogram shown in Fig. 6b was recorded after deuterium reduction using Wilkinson's catalyst. In addition to the three well-shaped peaks eluting between scans 550 and 600 two further later eluting peaks became clearly evident in the chromatogram. The inference was that these new peaks corresponded to steryl esters bearing polyunsaturated fatty acids that were being

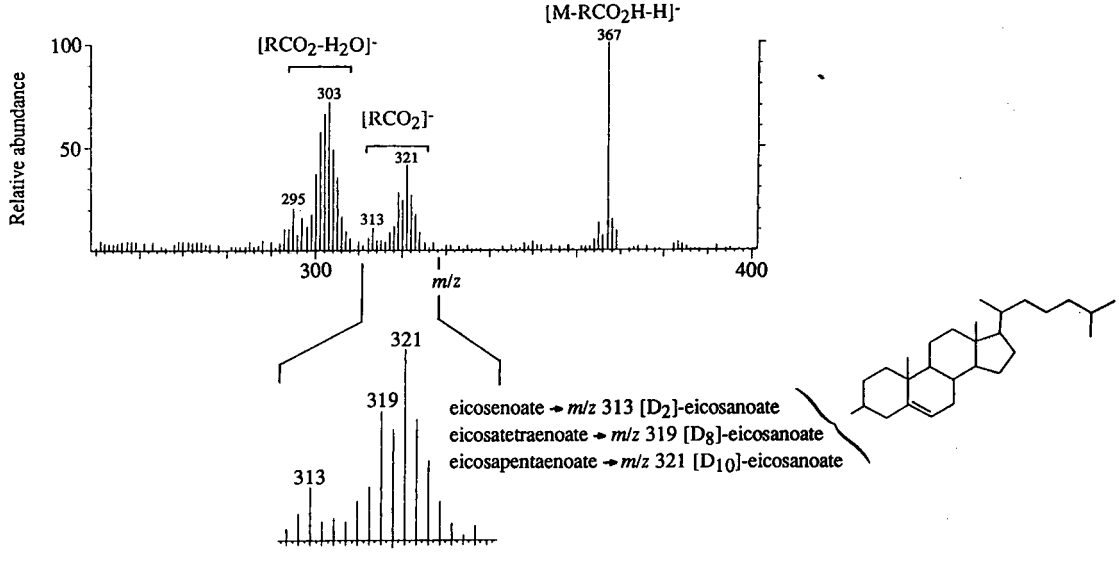

Fig. 7. NICI mass spectrum of the highlighted peak in the TIC shown in Fig. 6b.

lost through thermolysis during the analysis represented by the chromatogram shown in Fig. 6a. Subsequent deuterium reduction gave steryl esters bearing fully saturated fatty acyl moieties which exhibit the greatly improved GC behaviour, as shown in Fig. 6b. Examination of the NICI mass spectra of these later eluting peaks confirmed this interpretation. For example, the NICI mass spectrum of the highlighted peak in Fig. 6b is shown in Fig. 7. The complex cluster of the $[RCO_2]^-$ ion can be readily interpreted to reveal the nature of the original fatty acyl moieties present. The ion at *m/z* 367 corresponds to $[M-RCO_2H-H_2O]^-$, and confirmed that cholesteryl esters predominated. The cluster of $[RCO_2]^-$ ions indicates that this peak contains principally cholesteryl esters bearing twenty carbon fatty acyl moieties. As shown in Fig. 7 the fragment ions at *m/z* 313, 319 and 321 correspond respectively to $[RCO_2]^-$ ions resulting from the deuterium reduction of eicosenoate, eicosatetraenoate and eicosapentaenoate moieties in cholesteryl esters. The more complex clustering at lower mass is the result of overlap of the $[RCO_2-H_2O]^-$ and $[RCO_2-H_2O-H]^-$ ions resulting from these compounds. However, the ions present do corroborate the deductions made on the basis of the $[RCO_2]^-$ ions. The greatly improved chromatographic behaviour of the steryl esters bearing deuterated fatty acyl moieties, compared to that of their polyunsaturated precursors, clearly illustrates the usefulness of this technique in high temperature GC–MS analyses of steryl ester mixtures.

CONCLUSIONS

In summary, we have shown that deuterium reduction, using a homogeneous catalyst (Wilkinson's catalyst), of the widely occurring Δ^5-steryl esters bearing polyunsaturated fatty acyl moieties affords: (i) improved GC recovery through reduction of only those double bonds associated with the fatty acyl moiety; (ii) retention of structure information content in NICI spectra owing to the specificity of the reduction achieved using Wilkinson's catalyst. In addition to improving GC behaviour, the reduction and labelling provides a convenient means of preserving compounds that are particularly sensitive to autoxidation for structure investigation at a later date.

ACKNOWLEDGEMENTS

Ms. Lynne Dyas is thanked for valuable discussions, and Dr. Nicola J. Young for providing the prawn ovary tissue.

REFERENCES

1 P. Mareš, *Prog. Lipid Res.*, 27 (1988) 107.
2 P. Mareš and P. Hušek, *J. Chromatogr.*, 350 (1985) 87.
3 A. Kuksis, J. J. Myher, L. Marai, J. A. Little, R. G. McAuthur and D. A. K. Roncari, *Lipids*, 21 (1986) 371.
4 A. Kuksis, J. J. Meyher and P. Sandra, *J. Chromatogr.*, 500 (1990) 427.
5 R. P. Evershed, N. J. Fairs and L. J. Goad, unpublished results.
6 R. P. Evershed, V. L. Male and L. J. Goad, *J. Chromatogr.*, 400 (1987) 187.
7 N. J. Fairs, *Ph.D. Thesis*, University of Liverpool, Liverpool, 1989.
8 B. F. Dickens, C. S. Ramesha and G. A. Thompson, *Anal. Biochem.*, 127 (1982) 37.
9 R. P. Evershed, M. C. Prescott, L. J. Goad and H. H. Rees, *Biochem. Soc. Trans.*, 15 (1987) 175.
10 R. P. Evershed and L. J. Goad, *Biomed. Environ. Mass Spectrom.*, 14 (1987) 131.
11 K. Grob, *J. Chromatogr.*, 237 (1982) 15.
12 R. P. Evershed and M. C. Prescott, *Biomed. Environ. Mass Spectrom.*, 18 (1989) 503.
13 R. P. Evershed, M. C. Prescott, N. Spooner and L. J. Goad, *Steroids*, 53 (1989) 285.
14 S. G. Wakeham and N. M. Frew, *Lipids*, 17 (1982) 831.
15 W. R. Lusby, M. J. Thompson and J. Kochansky, *Lipids*, 19 (1984) 888.

Journal of Chromatography, 590 (1992) 313–328
Elsevier Science Publishers B.V., Amsterdam

CHROM. 23 762

Analytical methods for monoterpene glycosides in grape and wine

I. XAD-2 extraction and gas chromatographic–mass spectrometric determination of synthetic glycosides☆

Stéphane G. Voirin☆☆, Raymond L. Baumes*, Ziya Y. Gunata, Sylvaine M. Bitteur and Claude L. Bayonove

INRA, Institut des Produits de la Vigne, Laboratoire des Arômes et des Substances Naturelles, 2 Place Viala, 34060 Montpellier Cedex 01 (France)

Claude Tapiero

USTL, Laboratoire de Chimie Bioorganique, Place Eugène Bataillon, 34095 Montpellier Cedex 5 (France)

(Received July 29th, 1991)

ABSTRACT

Synthetic monoterpene and aromatic β-D-glucopyranosides, β-rutinosides and 6-O-(α-L-arabinofuranosyl)-β-D-glucopyranosides and their corresponding alcohols, diluted in a synthetic solution imitating wine, were isolated and separated by selective retention on Amberlite XAD-2. The corresponding recoveries and the conditions for the direct determination of these glycosides by gas chromatography and gas chromatography–mass spectrometry after derivatization were determined. Trifluoroacetylation gave the best results but trimethylsilylation provided complementary results. The separation of some diastereoisomeric monoterpene glycosides was also examined.

INTRODUCTION

Several methods for the extraction and determination of free and glycosidically bound volatile components of grape and wine have been described [1]. Although techniques for the extraction and isolation of these compounds and for the determination of free and enzymatically released volatiles have proved satisfactory [2,3], the bound forms have proved difficult to determine directly, using either gas chromatography (GC) or high-performance liquid chromatography (HPLC) [2,4,5]. Accordingly, no quantitative data are yet available for individual components of these precursors. Recently we synthesized many of the main glycosides of grape volatiles [6]; this has allowed further progress in their analysis. In this paper we report the GC–mass spectrometric (GC–MS) analysis of these representative glycosides. This was carried out to establish satisfactory conditions for their separation and identification, to facilitate detection of new glycosides through identification of characteristic fragmentation patterns and to determine individual gly-

☆ Part of a Doctoral Thesis presented to the University of Montpellier by S. Voirin [1].

☆☆ Present address: Domreco, B.P. 47, Aubigny, 80800 Corbie, France.

0021-9673/92/$05.00

cosides and their aglycones extracted by a method we developed earlier [7].

EXPERIMENTAL

Reagents and reference samples

Analytical-reagent grade solvents were further purified by redistillation before use. Amberlite XAD-2 resin from Rohm and Haas was purified according to the procedure of Günata *et al.* [7]. The trimethylsilylating (TMS) reagent [N,O-bis(trimethylsilyl)trifluoroacetamide–chlorotrimethylsilane, (99:1)] and the trifluoracetylating (TFA) reagent [N-methylbis(trifluoroacetamide)] were purchased from Touzart et Matignon and Sigma, respectively. Geraniol, nerol, (*RS*)-linalool, (*RS*)-α-terpineol, benzyl alcohol, 2-phenylethanol, (*RS*)-4-nonanol and (*RS*)-2-octanol were purchased from Fluka. Phenyl and 4-nitrophenyl β-D-glucopyranosides were obtained from Sigma and 4-nitrophenyl β-rutinoside from Sarsynthese. (*S*)-2,6-dimethyl-3,7-octadien-2,6-diol and (3*RS*,6*S*)-2,6-dimethyl-1,7-octadien-3,6-diol were synthesized according to Matsuura and Butsagan [8] by photooxidation of (*S*)-linalool [containing 15% of (*R*)-linalool] obtained from coriander oil. Syntheses of the glycosides used have been described in detail elsewhere [6].

Trimethylsilylation of glycosides

According to the method described by Sweeley *et al.* [9], an ethanolic mixture of the synthetic glycosides mentioned in Fig. 1 (about 5 μg of each compound) was concentrated to dryness in a small screw-capped vial at 60°C under nitrogen. After addition of 20 μl of anhydrous pyridine and 20 μl of the TMS reagent, the vial was tightly closed, stirred, stored for 20 min at 60°C, then allowed to cool at room temperature.

Trifluoroacetylation of glycosides

According to the method described by Sullivan and Schewe [10], a mixture of the synthetic glycosides (about 10 μg of each compound) was treated as above but using 20 μl of the TFA reagent instead of the TMS reagent.

Methylation of 4-nitrophenyl-β-rutinoside

According to the method described by Hakomori [11], 330 μl of a 2 *M* solution of sodium methylsulphinylmethide in dimethyl sulphoxide (DMSO) was added to a solution of 0.11 mmol of 4-nitrophenyl β-rutinoside in 1 ml of DMSO under nitrogen. The mixture was stirred at room temperature for 15 min and, after cooling to 0°C, 3.2 mmol of methyl iodide were added and the mixture was stirred for another 2 h at room temperature. Water (1 ml) was added and the aqueous solution was extracted with 1 ml of dichloromethane. The organic layer was dried (Na_2SO_4) and concentrated. The crude residue was subjected to column chromatography (silica gel 60, 63–200 μm) with diethyl ether to give 0.033 mmol of permethylated 4-nitrophenyl β-rutinoside (30%), syrup; R_F 0.35 (diethyl ether, Kieselgel 60); ^1H NMR, δ (ppm) 1.22 (d, 3H, $J_{5',6'}$ 6.2 Hz, H-6'), 3.39 (s, 3H, OCH_3), 3.50 (s, 3H, OCH_3), 3.55 (s, 6H,

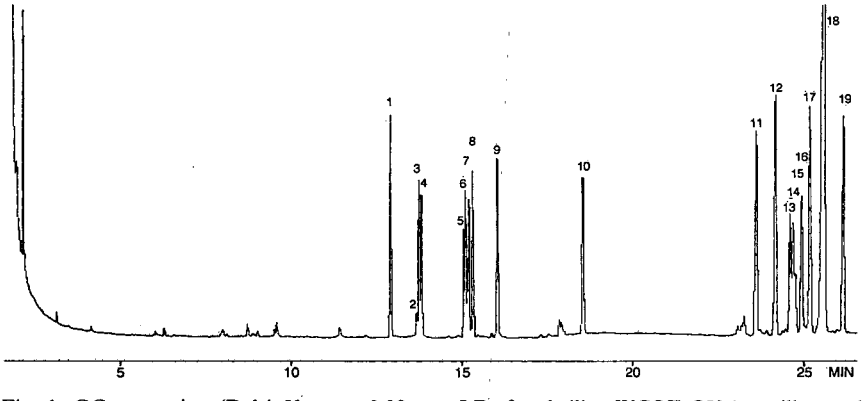

Fig. 1. GC separation (Delsi 50 m × 0.32 mm I.D. fused-silica WCOT OV-1 capillary column, film thickness 0.2 μm) of TMS derivatives of glycosides. For conditions, see Experimental. Peak numbers correspond to those in Tables I–III.

$2OCH_3$), 3.65 (s, 3H, OCH3), 3.67 (s, 3H, OCH_3), 4.79 (d, 1H, $J_{1',2'}$ 1.7 Hz, H-1'), 4.93 (d, 1H, $J_{1,2}$ 7.3 Hz, H-1), 7.09 (m, 2H, arom), 8.21 (m, 2H, arom); see below for GC.

According to the method described by Arnarp *et al.* [12], 12 mmol of 2,6-di-*tert.*-butylpyridine (Aldrich) and 6 mmol of methyl trifluoromethanesulphonate were added to a solution of 0.2 mmol of 4-nitrophenyl β-rutinoside in 9 ml of anhydrous chloroform. The mixture was stirred at room temperature for 20 h, then concentrated *in vacuo* at 40°C. The crude residue was subjected to column chromatography (silica gel 60, 63–200 μm) with diethyl ether to give 0.093 mmol of permethylated 4-nitrophenyl β-rutinoside (47%) as described above.

Gas chromatographic analysis of TMS derivatives of glycosides

TMS derivatives were analysed using an OV-1 fused-silica capillary column (Delsi Instruments) (50 m × 0.32 mm I.D.; 0.2-μm bonded phase). Injections of about 0.5 μl were made on-column; the injector temperature was programmed at 60°C min^{-1} from 90 to 150°C and then at 10°C min^{-1} to 310°C. The column temperature was programmed at 10°C min^{-1} from 125 to 220°C and then at 4°C min^{-1} to 310°C, with hydrogen as the carrier gas at 2 ml min^{-1} and a flame ionization detector temperature of 320°C.

Gas chromatographic analysis of TMS derivatives of linalyl diglycosides

TMS derivatives of linalyl diglycosides were analysed on a DB-17 fused-silica capillary column (J & W) (15 m × 0.32 mm I.D.; 0.25-μm bonded phase). Injections of about 0.5 μl were made on-column; the injector temperature was programmed at 60°C min^{-1} from 90 to 280°C. The column temperature was programmed at 3°C min^{-1} from 125 to 280°C with helium as the carrier gas at 1.8 ml min^{-1}. The GC instrument was coupled to a Finnigan MAT ITD 700 (see conditions below).

Gas chromatographic analysis of TFA derivatives of glycosides

TFA derivatives were analysed on a CP-Sil 8 CB fused-silica capillary column (Chrompack) (25 m × 0.32 mm I.D.; 1.2-μm bonded phase). Injections of about 0.5 μl were made on-column; the injector temperature was programmed at 60°C min^{-1} from 90 to 150°C and then at 10°C min^{-1} to 300°C. The column temperature was programmed at 4°C min^{-1} from 125 to 280°C, with hydrogen as the carrier gas at 1.3 ml min^{-1} and a flame ionization detector temperature of 300°C.

Gas chromatographic analysis of permethylated 4-nitrophenyl-β-rutinoside

This compound was analysed using the same CP-Sil 8 CB column as above under the same conditions except that the injector temperature was programmed at 60°C min^{-1} from 165 to 300°C and the column temperature at 2°C min^{-1} from 165 to 280°C. One peak was detected at an elution temperature of 268°C.

Gas chromatographic analysis of alcohols

The alcohols were analysed on a CP WAX 52 CB fused-silica capillary column (Chrompack) (25 m × 0.32 mm I.D.; 1.2-μm bonded phase). Injections of about 4 μl were made on-column; the injector temperature was programmed at 180°C min^{-1} from 10 to 250°C. The column temperature was programmed at 2°C min^{-1} from 60°C (3 min isothermal) to 220°C (10 min isothermal) with hydrogen as the carrier gas at 2.5 ml min^{-1} and a flame ionization detector temperature at 250°C.

Gas chromatography–mass spectrometry of glycoside derivatives (TMS or TFA)

Electron impact mass spectrometry (EI-MS) was applied to the TMS and TFA derivatives by coupling a Girdel 31 gas chromatograph equipped with the fused-silica capillary columns described above to a Nermag R 10-10 mass spectrometer. The transfer line consisted of a platinum capillary tube heated at 260°C. The source temperature was 200°C. Mass spectra were scanned at 70 eV in the range m/z 60–1050 at 2.87-s intervals.

The chromatographic conditions were as follows: 2 μl of glycoside derivatives were injected with a 10:1 splitting ratio into an injector held at 320°C. The helium carrier gas head pressure was 90 kPa for TMS derivatives and 10 kPa for TFA derivatives. For TMS derivatives the column was programmed at 3°C min^{-1} from 130 to 300°C and for TFA derivatives at 4°C min^{-1} from 120 to 280°C.

TABLE I

MASS SPECTRA OF TMS DERIVATIVES OF β-D-GLUCOPYRANOSIDES

Aglycone residue	Peak No. in Fig. 1	Relative retention time[a]	EI-MS: characteristic fragment ions[b] of			Mol. wt.[c] (MW_s)	Mol. wt.[d] of aglycone (MW_a)
			Sugar moiety	Aglycone moiety	Sugar and aglycone moieties		
Phenyl	1	0.698	361(74), 217(28), 271(10), 243(9.5), 204(5.9), 319(5.2), 191(5.1), 331(3.4), 233(2.4), 305(1.6), 451(0.5)	166(3.3), 151(1.7), 77(1.4), 208(0.7)	195(1.2)	544	94
(*R*)-Linalyl	2	0.739	331(52), 217(41), 233(27), 263(23), 204(19), 361(9.7), 191(6.2), 243(3), 271(1.9), 305(1.9), 319(1.9)	69(46), 81(20), 93(7.3), 80(6.2), 137(4.6)		604	154
(*S*)-Linalyl	3	0.742	217(42), 331(35), 233(28), 204(22), 263(20), 361(8.4), 191(6.1), 305(2.1), 271(1.2), 319(0.8)	69(50), 81(25), 93(11), 80(6.6), 137(6.2)		604	154
Benzyl	4	0.746	204(100), 217(25), 233(4.4), 191(3.8), 331(2.2), 305(1.9), 243(1.8), 263(1.3), 361(0.9), 319(0.8), 271(0.7), 451(0.03)	91(56), 107(0.4)	209(24)	558	108
(*S*)-α-Terpinyl	5	0.815	217(100), 204(32), 331(27), 361(20), 233(19), 263(13), 191(6.7), 243(3.5), 271(2.3), 305(1.8), 319(1.5), 451(0.5)	81(37), 136(15), 69(12), 137(9.9), 95(8.5)		604	154
(*R*)-α-Terpinyl	6	0.818	217(100), 204(34.5), 331(30), 361(24), 233(20), 263(16), 191(10.5), 243(7), 271(6), 305(5)	81(37), 136(20), 69(14), 137(6), 121(3)		604	154
2-Phenylethyl	6	0.818	204(100), 217(17), 191(3.5), 305(1.1), 243(0.7), 233(0.5), 331(0.5), 319(0.4), 361(0.4), 271(0.2)	105(34), 91(0.5)	223(23)	572	122

Neryl	7	0.823	217(74), 204(39), 331(35), 233(31), 263(19), 361(14), 191(7.7), 243(3.7), 305(2.4), 271(2.2), 319(1.5), 451(0.08)	69(49), 81(37), 137(13), 95(8.5), 136(5.5)		604	154
Unknown 1[e]	7	0.821	331(100), 233(47), 217(44), 263(44), 191(36), 204(35), 219(4.3), 243(3.9), 305(3.4), 271(3)	135(30), 225(24), 93(22), 107(21), 143(13), 81(5.1), 241(1.7)		692	170
Unknown 2[e]	7	0.823	331(100), 191(37), 263(36), 217(32), 233(32), 204(25), 305(3.4), 319(2.3), 243(2.2), 271(1.8)	107(30), 93(28), 135(26), 225(24), 143(17), 81(8.3), 241(1.4)		692	170
Diol-3,6[f] (3*RS*,6*S*)	8	0.827	331(92), 217(45), 263(45), 204(42), 233(41), 191(40), 361(25), 243(4.7), 305(4.3), 271(2.3), 319(1.4)	135(30), 225(28), 93(26), 107(24), 143(17), 81(5.5), 241(2.6)		692	170
(*S*)-Citronellyl	8	0.827	204(100), 217(15), 361(10), 191(3.9), 243(1.9), 305(1.8), 271(1.6), 319(1.2), 233(1.1), 331(0.9), 263(0.7), 451(0.6)	69(16), 83(5.7), 95(1.8), 139(1.3), 97(1.3), 109(0.8) 155(0.6), 140(0.5)	257(8.1)	606	156
Geranyl	9	0.866	331(65), 217(59), 233(27), 204(35), 263(29), 361(13), 191(8.1), 243(4), 305(3.5), 271(2.1), 319(1.8), 451(1.7)	69(70), 81(21), 137(6.7), 95(5.2), 93(3.5), 136(2.2)		604	154
4-Nitrophenyl	10	1	361(70), 217(26), 204(16), 271(8.5), 243(7.3), 191(5.8), 319(4.3), 331(2.8), 305(1.4), 233(0.4), 451(0.2)	196(1.8), 76(0.5)	240(2.8)	589	139

[a] Retention time relative to 4-nitrophenyl β-D-glucopyranoside (for TMS and GC conditions, see Experimental).
[b] *m/z*, with relative intensity (%) in parentheses.
[c] From CI-MS with ammonia as reactant gas.
[d] Obtained as $MW_a = MW_s - 451$ (molecular weight of the sugar moiety) + 1, except for the diol-3,6: $MW_a = MW_s - 451 - 73$ (TMS) + 2.
[e] Unknowns 1 and 2 were impurities of β-D-glucopyranoside of diol-3,6 (3*RS*,6*S*) and could be glucosides of diol-3,6 (3*RS*,6*R*) as their synthesis started from (*S*)-linalool containing 15% (*R*)-linalool.
[f] Diol-3,6 = 2,6-dimethyl-3-hydroxy-1,7-octadien-6-yl.

TABLE II

MASS SPECTRA OF TMS DERIVATIVES OF 6-O-(α-L-RHAMNOPYRANOSYL)-β-D-GLUCOPYRANOSIDES

Aglycone residue	Peak No. in Fig. 1.	Relative retention time[a]	EI-MS: characteristic fragment ions[b] of			Mol.wt.[c] (MW_s)	Mol.wt.[d] (MW_a)
			Sugar moiety	Aglycone moiety	Sugar and aglycone moieties		
Benzyl	12	1.304	204(100), 217(14.5), 191(3.1), 363(2.7), 319(1.9), 273(1.7), 305(1.6), 243(1), 245(0.9), 333(0.8), 361(0.4)	91(22)	209(7.6), 469(1.6)	848	108
Neryl	17	1.359	204(100), 217(53), 363(34), 273(12), 191(9), 319(8.4), 245(3.7), 305(3.4), 243(3), 333(1.5), 361(1.3), 271(1.2)	81(26), 69(24), 137(8.8), 95(5.9), 136(4.1)	515(0.3)	894	154
(*S*)-α-Terpinyl	18	1.377	204(100), 217(75), 363(55), 273(16), 319(9.6), 191(8.5), 245(5.3), 243(4.1), 305(3.8), 244(2.7), 361(1.7), 271(1.4), 333(1.4)	81(25), 136(15), 137(6.9), 69(6.5), 95(5.7)	515(0.4)	894	154
(*R*)-α-Terpinyl	18	1.381	204(100), 217(59), 363(31), 273(11), 191(8.5), 319(6.3), 245(4.1), 243(3.2), 244(2), 361(1.1)	81(32), 136(19.5), 69(14), 137(9), 95(6.4)		894	154
2-Phenylethyl	18	1.381	204(100), 217(71), 243(6), 191(4.8), 363(2.9), 305(2.5), 319(2.2), 244(1.9), 245(1.7), 273(1.6), 361(1), 333(1), 271(0.8), 331(0.4)	105(24), 91(4.5), 77(0.5)	223(8.2), 483(1.6)	862	122
Geranyl	19	1.412	204(100), 217(43), 363(41), 273(14), 319(9.3), 191(9.1), 245(3.9), 305(3.5), 243(2.7), 333(1.6), 244(1.3), 361(1.2), 271(1.2)	69(42), 81(17), 137(4.5), 95(3.4), 136(1.9)	515(0.7)	894	154
(*R*)-Linalyl[e]		1.149	204(42), 217(28), 273(28), 363(18), 191(11), 319(11), 245(4.4), 305(3.3)	69(30), 81(23), 155(4.4)			
(*S*)-Linalyl[e]		1.159	204(50), 273(38), 217(38), 363(23), 191(13), 319(13), 245(5.5), 305(1.1)	69(42), 81(33), 155(6.6)			

[a-d] See footnotes in Table I.

[e] Recorded by coupling a DB-17 fused-silica capillary column with a Finnigan MAT ITD 700 (See Experimental).

TABLE III

MASS SPECTRA OF TMS DERIVATIVES OF 6-O-(α-L-ARABINOFURANOSYL)-β-D-GLUCOPYRANOSIDES

Aglycone residue	Peak No. in Fig. 1.	Relative retention time[a]	EI-MS: characteristic fragment ions[b] of			Mol.wt.[c] (MW_s)	Mol.wt.[d] (MW_a)
			Sugar moiety	Aglycone moiety	Sugar and aglycone moieties		
Benzyl	11	1.273	217(100), 204(97), 259(14), 230(5.8), 231(3.2), 191(3.8), 243(3.6), 305(1.5), 349(1.4), 320(1.2), 319(1), 361(0.5)	91(35), 77(0.1)	209(5.8), 469(0.5)	834	108
Neryl	13	1.327	217(100), 259(62), 204(11), 243(7.8), 349(7), 230(4.4), 231(3.2), 191(3), 305(1.5), 361(1.2), 319(0.8), 320(0.7), 271(0.7)	81(12), 69(11), 137(3.9), 95(2.4), 136(1.7)	515(0.05)	880	154
(*S*)-α-Terpinyl	14	1.332	217(100), 259(40), 204(9), 243(6.1), 349(5.5), 230(3.9), 231(2.3), 191(1.6), 361(1.1), 305(1), 271(0.6)	136(20), 81(12), 137(6.2), 95(5.2), 69(3.7)		880	154
(*R*)-α-Terpinyl	15	1.335	217(100), 259(31), 204(10), 243(6), 349(3.7), 230(3.4), 231(2.3), 191(2.5), 305(1.3)	81(20.5), 136(10.5), 69(6), 95(4), 137(4), 121(1.6)		880	154
2-Phenylethyl	16	1.346	204(100), 217(92), 259(11), 230(5.9), 231(2.8), 191(2.7), 243(2.5), 349(1.1), 320(1), 305(0.9), 319(0.7), 361(0.3)	105(26), 77(0.4)	223(8.5), 483(0.5)	848	122
Geranyl	18	1.381	217(100), 259(67), 204(62), 243(8.7), 349(8.1), 230(4.3), 191(4.3), 231(3.8), 305(2.2), 319(1.6), 361(1.1), 320(1.1), 271(0.8)	69(18), 81(5.5), 137(2), 95(1.4), 136(0.9)	515(0.06)	880	154
(*R*)-Linalyl[e]		1.127	259(100), 217(68), 243(10), 191(1.1)	69(36), 81(21), 93(3.3)			
(*S*)-Linalyl[e]		1.136	259(100), 217(56), 243(8.9), 191(4.2), 231(1.8)	69(30), 81(20), 93(2.7)			

[a-e]See footnotes in Table II.

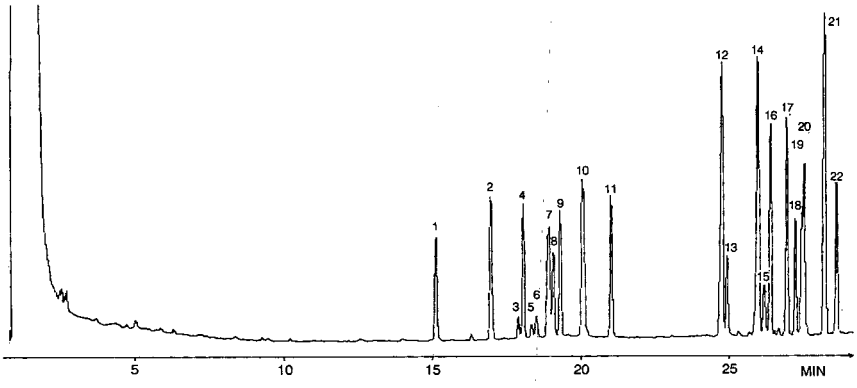

Fig. 2. GC separation (Chrompack 25 m × 0.32 mm I.D. fused-silica WCOT CP-Sil-8CB capillary column, film thickness 1.2 μm) of TFA derivatives of glycosides. For conditions, see Experimental. Peak numbers correspond to those in Tables IV–VI.

Chemical ionization mass spectrometry (CI-MS) was applied using the GC and transfer line conditions as for EI-MS. The source temperature was 90°C and ammonia was used as the reactant gas. Mass spectra were scanned at 70 eV in the range m/z 60–1050 at 2.87-s intervals.

MS monitoring of TMS derivatives of linalyl diglycosides was achieved by coupling the DB-17 fused-silica capillary column (see conditions above) to a Finnigan MAT ITD 700 mass spectrometer. The transfer line, heated at 280°C, consisted of an open-split GC–ITD interface at atmospheric pressure and, as a flow restrictor, a DB-5 fused-silica capillary column (1.2 m × 0.18 mm I.D.; bonded phase). The source temperature was 220°C. Mass spectra were scanned between 50 and 80 eV in the range m/z 61–650 at 2-s intervals.

Isolation of alcohols and glycosides from synthetic solutions of wine

To avoid co-elution in the GC analysis of the TFA derivatives of the glycosides, three different synthetic solutions were prepared. Each contained six or seven non-co-eluting glycosides from those reported in Table VIII (phenyl β-D-glucopyranoside as internal standard) and the corresponding terpenic and aromatic alcohols reported in Table VII [(*R*,*S*)-4-nonanol as internal standard] diluted in 50 ml of a synthetic solution to imitate wine. The amounts used for each component are given in Tables VII and VIII; the synthetic solution consisted of 20 g of tartaric acid, 15 g of malic acid, 0.5 g of acetic acid, 0.125 g of magnesium sulphate, 0.5 g of potassium sulphate, 0.6 kg of ethanol, diluted to 5 l with purified water and adjusted to pH 3.23 with 1 *M* NaOH. Each solution was diluted with 100 ml of purified water, then extracted on Amberlite XAD-2 resin according to the procedure previously described [7]. However, elution of the alcohols (free fraction) was carried out with either 50 ml of pentane or 50 ml of pentane–dichloromethane (2:1) and that of the glycosides (bound fractions) with either 50 ml of ethyl acetate or 50 ml of methanol.

The free fractions were dried with anhydrous sodium sulphate, filtered and concentrated to a final volume of about 1 ml, then 60.4 μg of (*R*,*S*)-2-octanol were added as external standards. These fractions were analysed by GC as described above. After analysis, the presence of glycosides was checked by GC after trifluoroacetylation according to the procedure described above.

A 10-μg amount of geranyl β-D-glucopyranoside was added as external standard to 0.5 ml of the bound fractions. These fractions were then concentrated to dryness at 60°C under nitrogen then analysed by GC after trifluoroacetylation according to the procedure described above.

Each experiment was performed in triplicate to test the reproducibility of the method.

RESULTS AND DISCUSSION

The various glycosides used (Table I) were available from syntheses reported previously [1,6,13] and have already been described as aroma precursors in grapes [13,14]. Phenyl β-D-glucopyranoside, 4-ni-

trophenyl β-D-glucopyranoside and 4-nitrophenyl β-rutinoside were also commercially available and could be used as chromatographic standards. These glycosides needed to be derivatized prior to their GC analysis in order to increase their volatility and thermal stability.

Simply and versatile methods have been described for the separation and determination of carbohydrates and related polyhydroxy compounds by GC: methylation, acetylation, silylation and trifluoroacetylation were the most frequently used for their derivatization.

Methylation was reported by Khoda *et al.* [15] and Konoshima and Sawada [16] for derivatization of terpene glycosides and by Schwab and Schreier [17] for derivatization of glycosidic conjugates of aliphatic alcohols. However, this required relatively long reaction times and drastic basic conditions. Further, an attempt to methylate 4-nitrophenyl β-rutinoside, either under standard conditions [11] or under mild conditions using methyl trifluoromethanesulphonate and 2,6-di-*tert.*-butylpyridine [12], gave unsatisfactory results as it yielded only 30% and 47% of the permethylated derivative.

Acetylation has been used extensively as a purification step for many natural glycosidic extracts [1]. It was used by Williams *et al.* [13,14] to identify the main grape glycosides. However, although acetyl derivatives give valuable structural information, these were not suited to analysis by GC owing to their limited volatility, especially in the case of terpenyl diglycosides [2]. Moreover, both acetylation and methylation sometimes resulted in incomplete reaction, giving rise to partially derivatized products [17,18].

We therefore focused on TMS ethers and TFA esters, which appeared to have more favourable properties for GC–MS analysis.

Gas chromatographic behaviour of glycoside TMS ethers

Trimethylsilylation, the most commonly used method for the derivatization of sugars and their derivatives, was first extensively studied by Sweeley *et al.* [9]. Later applications of this method to the investigation of plant glycosides, and investigations of silylating reagents used, were reviewed by Martinelli [18] and Voirin [1]. Among the silylating reagents commercially available, we chose N,O-bis-(trimethylsilyl)trifluoroacetamide (BSTFA) containing 1% of trimethylchlorosilane as a catalyst. This reagent, which exhibits a high silylating potential towards a wide variety of functional groups, rapidly produced the TMS derivatives of the synthetic glycosides in this study, without noticeable side reactions and under mild conditions. Their GC analysis requirements, discussed earlier [18], were easily met using capillary columns with bonded apolar stationary phases and cold on-column injection with temperature-programmed vaporization to minimize possible thermal degradation during the injection [19]. Owing to the low volatility and high hydrophobicity of the TMS derivatives of monoterpenyl diglycosides (resulting in high distribution constants in apolar phases), columns with high phase ratio were chosen [1]. Under our best conditions (see Experimental), most of the synthetic compounds tested were separated but many were insufficiently resolved (Fig. 1). Elution temperatures of the monoglucosides were between 234 and 246°C and those of the diglycosides between 276°C and 287°C. However, the (*R,S*)-linalyl diglycosides, in contrast to the corresponding glucosides, were not detected under the given experimental conditions, owing to their decomposition in the column at *ca.* 250°C [1], resulting in a baseline rise before the diglycoside range. Using a shorter and more polar capillary column (DB-17) and adjusting the carrier gas flow-rate and temperature programming to allow an elution temperature lower than 250°C allowed their analysis, but the resolution obtained for the diglycosides was unacceptable [1].

Moreover, Martinelli [18] showed that 1-O-acylglycosides were deglycosylated by some silylating reagents, which therefore appear unsuited to analysis of the glycosides of neric and geranic acids found in grapes [1].

Hence silylation appeared to have limitations when applied to the study of complex mixtures of terpenyl diglycosides, such as those in grapes. This method could be used, however, to obtain information complementary to other methods, although other natural diglycosides might behave as the linalyl diglycosides.

Phenyl β-D-glucopyranoside and 4-nitrophenyl β-D-glucopyranoside, both commercial products, were well separated from the glycosides studied and could be used as internal standards in quantitative studies.

TABLE IV

MASS SPECTRA OF TFA DERIVATIVES OF β-D-GLUCOPYRANOSIDES

Aglycone residue	Peak No. in Fig. 2	Relative retention time[a]	EI-MS: characteristic fragment ions[b] of		CI-MS: characteristic fragment ions[d]
			Sugar moiety	Aglycone moiety[c]	
Phenyl	1	1	319(15), 177(3.7), 205(2.5), 193(1.8), 291(0.5), 265(0.3), 547(0.02)	94(100), 97(8), 95(1.7)	432(6.5), 648(1.4)
Benzyl	2	1.122	193(1.7), 319(0.6), 265(0.2), 177(0.1), 205(0.08)	91(100), 92(17), 107(2.4), 108(2.1)	672(47), 446(17), 654(1.1)
(*R*)-Linalyl	3	1.182	319(26), 193(6.2), 205(3), 177(2.8), 265(1.9)	93(100), 69(96), 81(73), 80(50), 121(33), 136(31)	605(2), 492(1.2)
(*S*)-Linalyl	4	1.193	319(21), 193(5.8), 205(2.7), 177(2.7), 265(1.7), 291(0.4), 547(0.3)	93(100), 69(99), 81(56), 80(49), 121(33), 136(19)	605(2), 492(1.2)
Unknown 1[e]	5	1.210	319(100), 193(7.9), 205(6.8), 177(6.1), 547(4.8), 265(1.3)	71(83), 93(39), 69(32), 81(30), 107(23), 109(21), 135(18), 79(13)	
Unknown 2[e]	6	1.221	319(99), 193(16), 177(7.9), 205(7.7)	71(100), 93(95), 135(65), 69(63), 81(58), 107(56), 109(34), 79(29)	
Diol-3,6 (3*RS*,6*S*)[f]	7	1.250	319(100), 193(12), 205(9.2), 177(7.4), 547(4.8), 265(2.8), 291(0.9)	93(100), 71(61), 135(56), 69(52), 107(45), 81(43), 68(31), 109(30), 67(28), 79(21), 97(13), 119(12)	716(12.6), 603(1.6), 490(1)
2-Phenylethyl	8	1.259	319(5.3), 177(1), 193(0.9), 265(0.2), 291(0.1)	105(100), 104(40), 91(35), 106(19)	686(100), 460(32), 668(1)
Neryl	9	1.274	319(3.2), 193(1), 205(0.5), 177(0.5), 265(0.3), 291(0.06)	69(100), 81(22), 93(7.9), 68(7.2), 95(6.4)	718(11), 492(9.8), 604(6.3)
(*S*)-Citronellyl	10	1.324	319(70), 193(1.4), 177(1.4)	69(100), 81(44), 83(26), 95(18), 82(17), 70(16), 97(7.6), 123(7.5), 109(7.4)	494(4.7), 720(2.3), 608(1.4)
Geranyl	10	1.327	319(3.6), 193(1), 177(0.5), 205(0.4), 265(0.3), 547(0.07), 291(0.06)	69(100), 81(13), 123(8.2), 68(6.6), 93(5.6)	718(100), 492(7.9),
(*R,S*)-α-Terpinyl	11	1.387	319(21), 193(4.7), 265(2.7), 177(2.7), 205(2.4), 547(0.6), 291(0.5)	136(100), 81(69), 93(59), 121(49), 137(41), 69(40)	492(4.3)
4-Nitrophenyl	12	1.634	319(100), 177(13), 205(12), 547(9.6), 193(5.3), 291(1.9), 265(1.6)	139(16), 76(3.8), 122(2.6)	

[a] Retention time relative to phenyl β-D-glucopyranoside (for TFA and GC conditions, see Experimental).
[b] See footnote *b* in Table I.
[c] A small portion of *m/z* 69 can be accounted for by CF_3^+.
[d] From CI-MS with ammonia as reactant gas.
[e,f] See footnotes *e* and *f* in Table I.

TABLE V

MASS SPECTRA OF TFA DERIVATIVES OF 6-O-(α-L-RHAMNOPYRANOSYL)-β-D-GLUCOPYRANOSIDES

Aglycone residue	Peak No. in Fig. 2	Relative retention time[a]	EI-MS: characteristic fragment ions[b] of	
			Sugar moiety	Aglycone moiety[c]
Benzyl	12	1.634	193(9.4), 207(4.6), 278(1.9), 179(1.2), 265(0.7), 292(0.7), 435(0.6), 177(03), 319(0.2)	91(100), 107(23), 92(13), 108(6.4)
(*R*)-Linalyl	12	1.634	207(30), 435(4.8), 179(4), 265(2.6), 193(1.9), 177(1.4), 292(0.9), 319(0.6), 278(0.5)	69(100), 81(77), 93(77), 136(68), 80(55), 137(29), 92(24)
(*S*)-Linalyl	13	1.643	207(25), 193(5.3), 179(3.7), 435(3.4), 265(2.4), 177(1.3), 292(0.8), 319(0.5), 278(0.4)	69(100), 93(84), 81(79), 80(59), 136(37), 92(25), 127(23)
Neryl	14	1.713	207(11), 435(2.6), 179(1.7), 193(1.2), 265(0.8), 292(0.5), 177(0.4), 319(0.3), 278(0.2)	69(100), 81(24), 68(15), 93(13), 137(12), 123(11)
2-Phenylethyl	16	1.742	207(12), 179(2), 435(1.6), 193(1.1), 265(0.9), 292(0.8), 319(0.4), 177(0.4), 278(0.2)	105(100), 104(60), 106(23), 91(12)
Geranyl	17	1.778	207(6.8), 435(2), 193(1.2), 179(1.1), 265(0.6), 177(0.4), 292(0.4), 278(0.2), 319(0.2)	69(100), 81(24), 68(13), 123(11), 93(9.2), 95(8.6)
(*R,S*)-α-Terpinyl	19	1.810	207(14), 435(3.6), 193(2.7), 179(2.4), 265(1.4), 177(0.7), 292(0.7), 319(0.4), 278(0.3)	136(100), 81(47), 137(43), 93(30), 121(23), 69(22)

[a-c] See footnotes in Table IV.

TABLE VI

MASS SPECTRA OF TFA DERIVATIVES OF 6-O-(α-L-ARABINOFURANOSYL)-β-D-GLUCOPYRANOSIDES

Aglycone residue	Peak No. in Fig. 2	Relative retention time[a]	EI-MS: characteristic fragment ions[b] of		CI-MS: characteristic fragment ions[d]
			Sugar moiety	Aglycone moiety[c]	
Benzyl	14	1.713	193(21), 278(0.9), 265(0.9), 279(0.3), 177(0.3), 165(0.3), 421(0.2)	91(100), 107(26), 92(12), 108(5.2)	770(1.1)
(*R*)-Linalyl	14	1.713	193(28), 265(2.8), 177(1.2), 421(1), 165(0.9), 278(0.9), 319(0.35), 279(0.1)	136(100), 69(89), 81(79), 93(63), 137(51), 80(31)	
(*S*)-Linalyl	15	1.726	193(31), 265(2.3), 421(1.6), 165(1.3), 278(0.8), 177(0.7), 319(0.1)	69(100), 93(58), 81(54), 80(35), 136(20), 137(14)	
Neryl	18	1.796	193(22), 421(1.9), 265(1.7), 278(0.8), 165(0.7), 177(0.3), 279(0.25), 319(0.2), 307(0.03)	69(100), 81(35), 68(16), 93(16), 95(14)	
2-Phenylethyl	20	1.818	193(17), 265(1.5), 278(1), 421(0.9), 165(0.4), 279(0.4), 177(0.2), 319(0.07)	105(100), 104(55), 106(21), 91(12)	784(28), 1010(20)
Geranyl	21	1.863	193(17), 421(1.7), 265(0.9), 278(0.6), 165(0.5), 177(0.2), 279(0.1), 319(0.1)	69(100), 81(20), 68(14), 123(12), 93(9.3), 95(8)	
(*R,S*)-α-Terpinyl	22	1.889	193(31), 265(1.9), 421(1.4), 165(1.2), 278(0.9), 177(0.6), 279(0.2), 319(0.1)	136(100), 81(60), 137(49), 93(38), 121(26)	

[a-d] See footnotes in Table IV.

With regard to diastereoisomers, β-D-glucopyranosides of (*R,S*)-linalool and glycosides of (*R,S*)-α-terpineol were well or partially resolved (Tables I–III). The elution order of the glycosides of (*R,S*)-linalool was determined using synthetic (*S*)-linalyl glycosides. Each diastereoisomer of the glycosides of (*R,S*)-α-terpineol was easily identified from the significantly different relative concentrations (1:2) for each pair [6].

Gas chromatographic behaviour of glycosides TFA-esters

Trifluoroacetylation has been widely used to derivatize many functional groups [18]. Sullivan and Schewe [10] showed that N-methylbis(trifluoroacetamide) (MBTFA) cleanly produced the trifluoroacetates of some mono-, di-, tri- and tetrasaccharides, with high volatility, enabling single-run analyses of sugar mixtures to be performed. This reagent produced cleanly, rapidly and under mild conditions the TFA derivatives of the synthetic glycosides studied (Fig. 2). These TFA derivatives were more polar and far more volatile than the corresponding TMS derivatives. Consequently, the best separation was achieved when using a more polar capillary column than with the TMS derivatives [1]. Further, their distribution constants are probably low in moderately polar phases, as shown by the peak distortion when large amounts were injected. Thus good results were achieved when using a capillary column with a low phase ratio, a situation that was possible owing to the greater volatility of the TFA derivatives compared with the TMS derivatives.

Under these conditions, all the glycosides injected (injection mode as above) were detected and their separation was satisfactory except in a few instances (Fig. 2). The elution temperatures of the monoglucosides were between 185 and 209°C and those of the diglycosides between 224 and 240°C. The diastereoisomers of the glycosides of (*R,S*)-linalool were better resolved than their TMS derivatives, in contrast to those of (*R,S*)-α-terpineol (Tables IV–VI). Indeed, only a slight separation was observed for the (*R,S*)-α-terpineyl β-rutinosides and for the (3*RS*,6*S*)-2,6-dimethyl-3-hydroxy-1,7-octadien-6-yl β-D-glucopyranosides. The elution order of the glycosides of (*R,S*)-linalool was determined using synthetic (*S*)-linalyl glycosides and those of the glycosides of (*R,S*)-α-terpineol were determined as described above for the TMS derivatives.

Improvement of this method might be achieved with electron-capture detection, allowing detection on a submicrogram scale for these fluorinated derivatives [20], but difficulties such as an unstable baseline in the chromatogram of the natural glycoside extract at high ECD sensitivity need to be overcome.

As regards internal standards, phenyl β-D-glucopyranoside was well separated from the glycosides of interest, as it was eluted before the β-D-glucopyranosides. In contrast, 4-nitrophenyl β-D-glucopyranoside was co-eluted with (*R*)-linalyl β-rutinoside and benzyl β-rutinoside and could not be used for this purpose.

General mass spectrometric behaviour of glycosides of TMS and TFA derivatives

EI mass spectra of the TMS (Tables I–III) and TFA (Tables IV–VI) derivatives of the glycosides were complex, consisting of peaks resulting from the aglycone and from the sugar moieties; the molecular ion was never detected. However, as the peaks assignable to a given sugar moiety or to a given aglycone moiety were obtained from every compound containing that sugar or that aglycone, it was relatively easy to distinguish between them. Interestingly, sugar moieties gave characteristic fragment ions, of medium to strong intensities, in the range $m/z > 190$. In this mass range there were few, if any, fragment ions derived from the aglycones studied. Fragment ions resulting from the sugar moiety were only assignable to osidic units, even in the case of the diglycosides studied for which no fragment ion assignable to the disaccharide moiety was detected. In addition to fragment ions derived from the aglycone, the mass spectra of the TMS derivatives indicated fragment ions due to the aglycone bound to a fragment of the sugar moiety: these were very useful for characterization.

CI mass spectra of the TMS derivatives with ammonia as reactant gas allowed determination of their molecular mass from the medium or strong intensity pseudo-molecular ion peak (M + 18). Further, they often indicated fragment ions due to the cleavage of the interosidic linkage in addition to the ion due to the breakage of the bond between the oxygen atom O-1 and the aglycone carbon atom C-1″.

With the TFA derivatives, GC–CI-MS (with ammonia as reactant gas) gave unsatisfactory results (owing to weak peaks against a strong background), except for some terpenyl monoglucosides and for benzyl and 2-phenylethyl 6-O-(α-L-arabinofuranosyl)-β-D-glucopyranosides: the pseudomolecular ion, if any, was weak, replaced with or accompanied by weak fragment ions at m/z = M − 208 (M + NH_4^+ − 2TFAO) or at m/z = M − 95 or 96 (M + NH_4^+ − TFAO or TFAOH).

EI-MS of TMS derivatives: aglycone moiety (Tables I–III)

The fragment ions of a given aglycone were very similar, regardless of the structure of the sugar moiety. Indeed, they were similar, although with different abundance, to those observed for the corresponding acetates (NBS Library), making their identification easy. However, some unspecific fragment ions resulting from the sugar part (m/z 169, 147, 129, 117, 103, 89, 73; see below) were observed in the mass range of the fragment ions given by the aglycones, and showed intensities generally higher than those obtained for the latter moieties; this could make the identification of some natural aglycones difficult.

EI-MS of TMS derivatives: sugar moiety

β-D-glucopyranosides (Table I). The glucose moiety gave characteristic fragment ions at m/z 361, 331, 271 and 243. These have also been reported for the EI-MS of penta-O-(trimethylsilyl)-α-D-glucopyranoside [21] and TMS derivatives of glycosides of flavonoids, terpenoids and saponin [18]. Other significant peaks correspond to a fragment of the reducing sugar bound to aglycones such as benzyl, 2-phenylethyl, phenyl, 4-nitrophenyl and (*R,S*)-citronellyl (aglycone-O-CH^+-OTMS). These fragment ions were not obtained with the other terpenyl aglycones which gave fragment ions at m/z 233 and 263 with a higher abundance than that observed for the former compounds [1].

Along with these characteristic peaks, numerous other peaks at m/z 305, 217, 204, 191, 169, 147, 129, 117, 103, 89 and 73 were found in the mass spectra of the glucosides and of rutinosides and 6-O-(α-L-arabinofuranosyl)-β-D-glucopyranosides [1,21].

β-Rutinosides (Table II) and 6-O-(α-L-arabinofuranosyl)-β-D-glucopyranosides (Table III). The only fragment ions characteristic of the disaccharide moiety were those arising from each osidic unit, *i.e.*, ions at m/z 361, 331, 271 and 243 for the glucose unit, at m/z 363, 333, 273 and 244 for the rhamnose unit and at m/z 349, 259 and 230 for the arabinose unit. In addition, the fragment ions at m/z 217, 204 and 73 were the most abundant of the unspecific ions resulting from the disaccharide moiety. The other significant but very weak peaks observed in the mass spectra of both classes of diglycosides were due to breakage of the interosidic bond, at m/z 515, 483 and 469 depending on the aglycone, and due to a fragment of the reducing sugar unit bound to the aglycone moiety (aglycone-O-CH^+-OTMS), observed only for the benzyl and 2-phenylethyl derivatives (m/z 209 and 223).

EI-MS of TFA derivatives: aglycone moiety (Tables IV–VI)

It was interesting that fragment ions resulting from the sugar moiety were far less numerous and abundant than those from the aglycone moiety. This made assignment to the peaks of the aglycone easier than with the TMS derivatives. Further, as no peak resulting from the aglycone moiety was present in the mass range of the characteristic fragment ions of the sugar moiety, identification of the sugar moiety was as easy as for the TMS derivatives. However, part of the ion at m/z 69, which is abundant in the terpenyl glycosides (pentenyl ion, $C_5H_9^+$), could be accounted for by CF_3^+, found in all mass spectra of TFA derivatives (note the weakness of this peak for TFA derivatives of the phenyl, 4-nitrophenyl, benzyl and 2-phenylethyl glycosides). As with the TMS derivatives, fragment ions from a given aglycone were very similar, regardless of the structure of the sugar moiety, and were also similar, although with different abundance, to those observed for the corresponding acetates.

EI-MS of TFA derivatives: sugar moiety

β-D-glucopyranosides (Table IV). The glucose moiety gave characteristic fragment ions at m/z 547, 319, 291, 205, 193 and 177 and fragment ions at m/z 265, 157, 127, 113, 97 and 69 not specific to a hexose unit, similar to those reported earlier [22] for glucopyranoside TFA derivatives. The latter peaks were far weaker than the aglycone peaks, found mostly in the same mass range, making identification of the aglycones easier than for the TMS derivatives.

TABLE VII

MEAN EXTRACTION COEFFICIENTS, CALIBRATION FACTORS (INCLUDING XAD-2 EXTRACTION AND GC) AND REPRODUCIBILITY FOR ALCOHOLS FROM WINE MODEL MIXTURE WITH PENTANE AND AZEOTROPE PENTANE–DICHLOROMETHANE AS ELUTION SOLVENTS

Compound	Starting amount (mg)[a]	Pentane			Pentane–Dichloromethane (2:1)		
		Mean extraction coefficient (%)	Mean calibration factor	Reproducibility[b] (%)	Mean extraction coefficient (%)	Mean calibration factor	Reproducibility (%)
4-Nonanol[c]	6.66	70.4	1	0	81.5	1	0
Geraniol	0.49	65.5	1.1	7.4	79.8	1.1	1.2
Nerol	0.44	69.8	1.1	6.6	81.2	1.1	1.2
(*R,S*)-Linalol	0.47	74.8	0.9	2.7	82.3	1	0.4
(*R,S*)-α-Terpineo	0.53	75.9	1.1	5.5	82.7	1.1	0.7
Benzyl alcohol	0.48	49.8	1.3	4.7	84.9	0.9	0.7
2-Phenylethanol	0.42	56.4	1.2	6.8	87.9	0.9	0.4
Diol-3,6[d]	0.46	0.2	374	–	60.6	1.4	5.2
Diol-3,7[e]	0.48	0.1	712	–	33.7	2.6	10.6

[a] Amount used (mg) in 50 ml of synthetic wine for each repetition.
[b] Calculated as relative standard deviation ($n = 3$) for the calibration factor.
[c] Internal standard.
[d] Diol-3,6 = 2,6-dimethyl-1,7-octadien-3,6-diol.
[e] Diol-3,7 = 2,6-dimethyl-3,7-octadien-2,6-diol.

β-Rutinosides (Table V) and 6-O-(α-L-arabinofuranosyl)-β-D-glucopyranosides (Table VI). As observed for the TMS derivatives, the only fragment ions characteristic of the disaccharide residue were those arising from each osidic unit, *i.e.*, ions at *m/z* 319, 193 and 177 for the glucose unit, at *m/z* 435, 292, 207 and 179 for the rhamnose unit and at *m/z* 421, 193 and 165 for the arabinose unit. These fragment ions are similar to those reported earlier for glucopyranose, rhamnopyranose and aldopentofuranose TFA derivatives [22]. The fragment ion at *m/z* 193, although in the mass spectra of both classes of diglycosides, had a higher relative abundance with the 6-O-(α-L-arabinofuranosyl)-β-D-glucopyranosides. In addition to these fragment ions, the unspecific ions mentioned above were also detected, with weak relative abundance, in addition to fragment ions at *m/z* 279, 278 (di-TFA-butenyl) and 265 (di-TFA-propenyl), which were used to distinguish the 6-O-(α-L-arabinosyl)-β-D-glucopyranosides from the 6-O-(β-D-apiofuranosyl)-β-D-glucopyranosides, another class of diglycosides recently found in grapes [1,23].

Quantitative analysis of a synthetic mixture of wine: extraction yields, calibration and reproducibility

The procedure described here complements the technique published earlier [7] to determine the free and glycosidically bound fractions of grapes and wine. The earlier technique used XAD-2 resin to extract free terpenes and their glycosides from an aqueous or aqueous–alcoholic solution and allowed the recovery of the free and bound monoterpenes by successive elution of the resin with pentane and ethyl acetate, respectively.

The free fraction was analysed directly by GC and the bound fraction was analysed indirectly through enzymic hydrolysis. Now we can concomitantly directly analyse the bound fraction by GC and thus determine the extraction yields of a mixture of the available synthetic glycosides, in addition to the influence of the elution solvents (see Experimental) and the reproducibility of the whole method.

For this experiment we used a synthetic solution imitating wine, *i.e.*, an aqueous–alcoholic solution, to provide the least favourable conditions expected to be required for retention of the solutes by the

TABLE VIII

MEAN EXTRACTION COEFFICIENTS, CALIBRATION FACTORS (INCLUDING XAD-2 EXTRACTION, DERIVATIZATION AND GC) AND REPRODUCIBILITY FOR GLYCOSIDES FROM WINE MODEL MIXTURE

Compound[a]	Starting amount (mg)[b]	Mean extraction coefficient (%)	Mean calibration factor	Reproducibility[c] (%)
Phenyl GLU[d]	1	31	1	0
Neryl GLU	0.4	71.4	0.3	7.8
(*S*)-(+)-Linalyl GLU	0.65	88.1	0.4	9
(*R,S*)-α-Terpineyl GLU	0.8	97.6	0.5	9.3
(*R,S*)-Citronellyl GLU	0.5	76.3	0.4	8.5
Benzyl GLU	0.55	40	0.7	7.2
2-Phenylethyl GLU	0.5	65	0.4	8.1
Geranyl RG	0.75	84.5	0.4	6.8
Neryl RG	0.7	71.1	0.5	14.3
(*R,S*)-Linalyl RG	0.65	87.3	0.6	6.5
(*R,S*)-α-Terpinyl RG	0.85	99.7	0.7	10.4
Benzyl RG	0.4	15	2.1	8.2
2-Phenylethyl RG	0.8	13	1.9	9.6
Geranyl AG	0.7	80.5	0.6	7.5
Neryl AG	0.6	72.3	0.7	8.8
(*R,S*)-Linalyl AG	0.75	77.2	1.1	7.6
(*R,S*)-α-Terpinyl AG	0.85	98	0.8	13.5
Benzyl AG	0.6	15.3	2.7	7.9
2-Phenylethyl AG	0.75	10.8	2.4	12.1

[a] GLU = β-D-glucopyranoside; RG = 6-O-(α-L-rhamnopyranosyl)-β-D-glucopyranoside; AG = 6-O-(α-L-arabinofuranosyl)-β-D-glucopyranoside.
[b] Amount used (mg) in 50 ml of synthetic wine for each repetition.
[c] Calculated as relative standard deviation (n = 3) for the calibration factor.
[d] Internal standard.

resin. The compounds analysed for (Tables VII and VIII) were the glycosides studied above (except for the glucoside of the monoterpendiol, owing to an insufficient amount) together with their corresponding alcohols and two monoterpenediols that occur naturally in grapes; synthesized by previously reported methods [8].

The results are summarized in Table VII for the alcohols and in Table VIII for the glycosides. The azeotrope pentane–dichloromethane (2:1) provided better elution of alcohols than pentane, particularly for the more polar monoterpenediols (as previously reported [24]) and the aromatic alcohols, without partial elution of the glycosides. On the other hand, ethyl acetate allowed a good recovery of monoterpenylglycosides but only a low recovery of the glycosides of aromatic alcohols; elution with methanol increased the extraction yields (*ca.* 55%) but, owing to its low selectivity, it proved unsatisfactory for natural extracts [1]. Phenyl β-D-glucopyranoside, chosen as an internal standard, exhibited an extraction yield intermediate between those of the glycosides of the aromatic alcohols and those of the monoterpenyl glycosides. Finally, the reproducibility of the whole method (XAD-2 extraction, concentration, TFA derivatization and GC analysis) was tested by calculating the relative standard deviations of the calibration factors, *i.e.*, response relative to the internal standards. This showed fairly good results for both free and bound compounds (Tables VII and VIII).

CONCLUSION

Synthetic glycosides were used to demonstrate the potential of XAD-2 extraction [7] and GC–MS analysis in investigation of naturally occurring mono- and diglycosides of volatile compounds.

TFA derivatization proved more suitable for the qualitative and quantitative analysis of monoterpenyl diglycosides but TMS derivatization, as well as recent HPLC methods [4,5], could provide complementary information. The XAD-2 extraction/GC–MS analysis method has been successfully applied to extraction and determination of glycosides in some grape cultivars; these results will be reported in a future paper.

ACKNOWLEDGEMENTS

We thank Dr. J. L. Le Quere and E. Semon, Laboratoire des Arômes, Dijon, France, for recording the mass spectra.

REFERENCES

1 S. Voirin, *Doctoral Thesis*, Montpellier University, 1990, and references cited therein.
2 C. R. Strauss, B. Wilson, P. R. Gooley and P. J. Williams, in T. H. Parliment and R. Croteau (Editors), *Biogeneration of Aromas* (*ACS Symposium Series*, No. 317), American Chemical Society, Washington, DC, 1985, p. 222; and references cited therein.
3 W. Schwab and P. Schreier, *J. Agric. Food Chem.*, 36 (1988) 1238.
4 S. Bitteur, Z. Günata, J. M. Brillouet, C. Bayonove and R. Cordonnier, *J. Sci. Food Agric.*, 47 (1989) 341.
5 C. Salles, *Doctoral Thesis*, Montpellier University, 1989.
6 S. Voirin, R. Baumes, C. Bayonove, O. M'Bairaroua, C. Tapiero, *Carbohydr. Res.*, 207 (1990) 39.
7 Y. Z. Günata, C. L. Bayonove, R. L. Baumes and R. E. Cordonnier, *J. Chromatogr.*, 331 (1985) 83.
8 T. Matsuura and Y. Butsagan, *Nippon Kagaku Zasshi*, 89 (1968) 513.
9 C. C. Sweeley, R. Bentley, M. Makita and W. W. Wells, *J. Am. Chem. Soc.*, 85 (1963) 2497.
10 J. E. Sullivan and L. R. Schewe, *J. Chromatogr. Sci.*, 15 (1977) 196.
11 S. Hakomori, *J. Biochem.*, 55 (1966) 205.
12 J. Arnarp, L. Kenne, B. Lindberg and J. Lönngren, *Carbohydr. Res.*, 44 (1975) C5.
13 P. J. Williams, C. R. Strauss, B. Wilson and R. Massy-Westropp, *Phytochemistry*, 21 (1982) 2013.
14 P. J. Williams, C. R. Strauss, B. Wilson and R. Massy-Westropp, *Phytochemistry*, 22 (1983) 2039.
15 H. Khoda, R. Kasai, K. Yamsaki, K. Murakami and O. Tanaka, *Phytochemistry*, 15 (1976) 981.
16 T. Konoshima and T. Sawada, *Chem. Pharm. Bull.*, 30 (1982) 4082.
17 W. Schwab and P. Schreier, *J. Agric. Food Chem.*, 38 (1990) 757.
18 E. M. Martinelli, *Eur. J. Mass Spectrom., Biochem. Med. Environ. Res.*, 1 (1980) 33.
19 F. Pierrisnard, *Diplôme d'Etudes Approfondies*, Montpellier University, 1986.
20 J. Drozd, *J. Chromatogr.*, 113 (1975) 303.
21 D. C. De Jongh, T. Radford, J. D. Hribar, S. Hanessian, M. Bieber, G. Dawson and C. C. Sweeley, *J. Am. Chem. Soc.*, 91 (1969) 1728.
22 W. A. Konig, H. Bauer, W. Voelter and E. Bayer, *Chem. Ber.*, 106 (1973) 1905.
23 S. G. Voirin, R. L. Baumes, S. M. Bitteur, Z. Y. Günata and C. L. Bayonove, *J. Agric. Food Chem.*, 38 (1990) 1373.
24 G. Versini, personal communication.

Journal of Chromatography, 590 (1992) 329–339
Elsevier Science Publishers B.V., Amsterdam

CHROM. 23 757

Complex mixture analysis based on gas chromatography–mass spectrometry with time array detection using a beam deflection time-of-flight mass spectrometer

G. A. Schultz

Department of Chemistry, Michigan State University, East Lansing, MI 48824 (USA)

B. A. Chamberlin and C. C. Sweeley

Department of Biochemistry, Michigan State University, East Lansing, MI 48824 (USA)

J. T. Watson

Departments of Chemistry and Biochemistry, Michigan State University, East Lansing, MI 48824 (USA)

J. Allison*

Department of Chemistry, Michigan State University, East Lansing, MI 48824 (USA)

(First received July 1st, 1991; revised manuscript received September 3rd, 1991)

ABSTRACT

A beam deflection time-of-flight mass spectrometer was developed in conjunction with an integrating transient recorder to provide time array detection, permitting high mass spectral scan file acquisition rates for complex mixture analysis by capillary gas chromatography–mass spectrometry (GC–MS). Results are presented for the analysis of a urinary organic acid mixture by GC–MS at a scan file acquisition rate of 10 scan files per second (sf/s), showing the advantages of such data collection in the deconvolution of partially resolved components. The reconstructed total ion current (RTIC) chromatogram available from data acquired at this scan file generation rate is shown to be comparable to the profile obtained from a flame ionization detector in representing the chromatography performed under identical experimental parameters. The RTIC chromatogram available from the database obtained at 10 sf/s is compared with that available from a database obtained at 1 sf/s, the latter representing that scan rate typically used with most GC–MS instruments. The advantages of the higher scan file acquisition rate in representing the chromatographic profile and in allowing mass spectral data to be obtained for components in the complex mixture that are unresolved chromatographically are discussed.

INTRODUCTION

This paper focuses on problems associated with complex mixture analysis by gas chromatography–mass spectrometry (GC–MS), in the context of capillary GC. A solution to problems with this technology is discussed by presenting time-of-flight mass spectrometry (TOF-MS) as the mass spectrometric detection technique of choice for this work. With such instrumentation, in which mass spectra can be recorded at exceeding high rates when required, high-quality mass spectra can be obtained for all components in the mixture, and these data can be used to improve the results of GC beyond those preivously reported in the context of conventional GC–MS.

Advances in high-resolution GC in the past decade are manifested in the development of narrow-

0021-9673/92/$05.00

bore chromatographic columns, which, with their tens of thousands of theoretical plates, provide chromatographic peaks of the order of 2 s or less in duration. Extremely high-efficiency capillary columns have seen limited use in GC–MS applications owing to limitations in the scan rates available with the quadrupole and magnetic sector mass spectrometers commonly used in GC–MS instrumentation [1]. Scan rates of a quadrupole instrument are limited by the transit time of the ions through the mass filter. In order to obtain unit mass resolving power, the radio frequency (r.f.) and dc potentials applied to the quadrupole must be held at fixed values for a sufficient length of time (milliseconds) to allow ions of a given mass-to-charge ratio (m/z) to pass through the device. Magnetic sector instrument scan rates are limited by the rate at which the magnetic field can be swept.

Another problem in capillary GC–MS experiments that employ quadrupole or magnetic sector devices is that the mass spectra obtained from these scanning mass spectrometers can be distorted by the changes in the partial pressure of an analyte as it elutes from the capillary column; the distortion manifests itself as a skewing of the relative mass spectral peak intensities. The degree of this skewing is dependent on the time necessary to acquire a mass spectrum and the rate at which the partial pressure of the analyte changes in the ion source (sharpness of the GC peak).

We have proposed the use of TOF-MS for GC–MS instrumentation [1,2] to overcome the limitations of scanning mass spectrometers. Time-of-flight mass spectrometers produce as many as 10 000 mass spectra every second, which, if ion currents at all m/z values were collected for each of these transient mass spectra, permits an increase in the data acquisition rate for GC–MS. Importantly, time-of-flight mass spectrometers operated in this way are not "scanning" instruments such as a quadrupole or magnetic sector instrument. The mass spectra produced by TOF-MS result from the sampling of ions produced in the ion source at a given time interval. This process produces mass spectral transients (100-μs duration), in which the relative peak intensities are unskewed regardless of changes in analyte partial pressure (on any time scale) in the ion source [1].

We have developed time array detection (TAD) for TOF-MS by using an integrating transient recorder (ITR) [3]. The ITR is a data system that can continuously collect up to 10 000 transient mass spectra per second, as produced by TOF-MS. Each transient mass spectrum is digitized at 200 MHz (one data point every 5 ns). Many transient mass spectra are summed by the ITR (typically 500–1000), creating a scan file that contains the resultant (summed) mass spectrum. The number of transient mass spectra summed into each scan file determines the scan file generation rate. For example, if 5000 transient mass spectra are produced every second in TOF-MS and a scan file generation rate of 10 scan files per second (sf/s) is desired, 500 consecutive mass spectral transients are summed and stored as a single mass spectrum in each scan file. The scan file generation rate can be adjusted easily to meet the needs of the chromatographic analysis. Ideally, at least ten scan files should be generated in a time period corresponding to the temporal width of the sharpest chromatographic peaks. If 50 sf/s are necessary to represent the chromatography accurately, the ITR data system can easily accommodate this.

An instrument for beam deflection time-of-flight mass spectrometry (BDTOF-MS) has been developed that provides transient mass spectra to the ITR with a mass-resolving power sufficient for GC–MS applications [4,5]. The advantages of the BDTOF-MS over conventional (pulsed-source) TOF-MS instruments have been described [6]. In BDTOF-MS, a continuous ion beam is focused into the flight tube where it passes between two parallel plates. Each of the parallel plates in the beam deflection assembly has a time-dependent voltage applied to it, producing an electric field between the plates. Most of the time, the continuous ion beam is deflected away from the center axis of the flight tube by the electric field between the parallel plates; under these conditions, no ions reach the detector at the end of the flight tube. Reversing the sign of the electric field between the parallel plates sweeps the continuous ion beam from one side of the flight tube to the other, allowing a portion of the continuous ion beam, containing all m/z values, to strike the detector in a time-dependent manner. BDTOF-MS has produced a mass-resolving power ($m/\Delta m$) of 1400, which, when coupled with the performance of the ITR, provides a powerful system for GC–MS applications.

This paper describes the results of analyses using the GC–BDTOF-MS–ITR system in the context of metabolic profiling of urinary organic acids. Metabolic profiling is a method for the quantitative and qualitative analysis of metabolites in complex mixtures extracted from physiological fluids such as urine or plasma [7]. The coupling of GC and MS has played a crucial role in the development of methodologies for such analyses. The metabolic profile of urinary organic acids reflects metabolic status and allows for the identification of genetic disorders that perturb homeostasis. The metabolic profile, which is a chromatogram of the components of the mixture, portrays the relative amounts of these metabolites as derived from intermediary metabolism of carbohydrates, amino acids and lipids in the individual. Improvements in metabolic profiling have been limited in the same way as have analyses of other complex mixtures. Even with capillary column technology, chromatographic resolution is not sufficient to separate every component in the mixture and some components in these complex mixtures may therefore go undetected.

This paper compares the results of the GC-only analysis of a urinary organic acid mixture using flame ionization detection (FID) with those obtained with the GC–BDTOF-MS–ITR system at data acquisition rates of 1 and 10 sf/s. The advantages of the higher scan file acquisition rate are demonstrated, both in terms of accurately representing the chromatographic profile and in providing a database from which mass spectra can be obtained for closely eluting components.

Two points should be made clear. First, there are quadrupole and magnetic sector instruments available today that can obtain several mass spectra per second. However, these faster scanning speeds cannot be used without sacrificing sensitivity. The TOF instrument as described also has a sensitivity *versus* scan file generation rate trade-off, although all TOF mass spectra are unskewed. The second point is that the scan file generation rate of 10 sf/s is not the limit of this instrument, but the optimum for the chromatography used in the application. If the chromatography was improved to generate chromatographic peaks with temporal dimensions of 0.2 s, the instrument could generate 50 sf/s, giving ten scan files across each chromatographic peak. Such mass spectral generation rates are unavailable when scanning instruments are used. At a scan file generation rate of 50 sf/s, each scan file represents the sum of 100 mass spectral transients; thus, a scan file generation rate greater than 50 sf/s is possible, but with a sacrifice in sensitivity.

EXPERIMENTAL

The BDTOF-MS instrument in these laboratories is a highly modified Bendix 12-101 TOF-MS instrument. A schematic diagram of the basic components is shown in Fig. 1. The ion source has been adapted from a JEOL DM303 mass spectrometer. The pulsing circuitry for the beam deflection assembly was designed and built in-house. The beam deflection plates are constructed from two copper-coated PTFE circuit boards. The detector is a Galileo FTD-2003 (Galileo Electro-Optics, Sturbridge, MA, USA) in which the standard multi-channel plates (MCP) were replaced with high-output (HOT) MCPs. The preamplifier was made in-house. The GC and BDTOF-MS instruments are connected via a modified JEOL HX110 aluminum block interface, heated to 260°C. The gas chromatograph is a Hewlett-Packard Model 5790. The urinary organic acid mixture was separated using a short DB-5 capillary column (6 m × 0.2 mm I.D.) (J&W Scientific), 0.4-μm film thickness, using a column head pressure of 13 p.s.i.g. with helium as the carrier gas, splitless injection with an injector temperature of 275°C and temperature programming from 50 to 325°C at 20°C/min. The combination of the

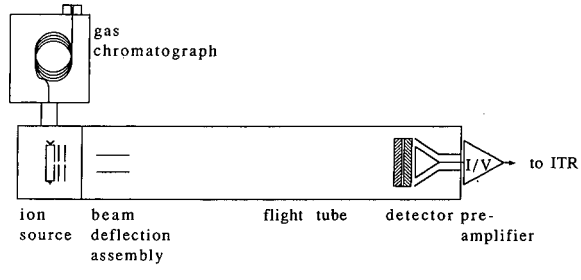

Fig. 1. Schematic diagram of beam deflection time-of-flight mass spectrometer interfaced to a gas chromatograph. Shown are ion source, beam deflection assembly, flight tube and detector. The flight tube is 2 m in length. The current output from the detector is amplified and converted to a voltage that is digitized by the integrating transient recorder (ITR).

short column with the fast temperature program reduces the normal analysis time by a factor of four.

The urinary organic acid mixture also was analyzed on a Hewlett-Packard Model 5890 gas chromatograph with a flame ionization detector. The FID output was digitized by an HP 3392A printing integrator, with the peak width response set to 0.01 min, which digitizes the data at a 20-Hz sampling rate.

The number of theoretical plates for the capillary column used for these analyses was determined on the GC–FID instrument. A two-component hydrocarbon mixture containing nonane and decane was analysed isothermally at 120°C. The average value for the number of plates as determined by measurements on each of the two peaks was 51 000.

The method of urinary organic acid extraction has been reported previously [8]. The acidic metabolites, isolated from 1 ml of a control urine sample, were derivatized by mixing 25 ml of pyridine and 100 ml of bis(trimethylsilyl)trifluoroacetamide–trimethylchlorosilane and heating at 80°C for 1 h. A 1.0-μl aliquot of the trimethylsilylated (TMS) urinary organic acids was analyzed by GC–MS with data acquisition rates of 1 and 10 sf/s, with the same column and GC conditions.

RESULTS AND DISCUSSION

Comparison of chromatographic profiles from GC–FID and GC–BDTOF-MS–ITR

A comparison of the chromatograms obtained from analysis of a urinary organic acid mixture by GC–FID and by GC–MS with reconstruction of the total ion current (RTIC) is shown in Fig. 2. The RTIC chromatograms represent the analysis of the same amount of this mixture and were generated from data obtained at 1 and 10 sf/s on the GC–BDTOF-MS–ITR system. A 3 min delay between injection of the mixture and initiation of data collection was used. The database obtained at 1 sf/s (providing only one RTIC point per second with which to reconstruct the chromatogram) was generated by summing 5000 consecutive mass spectral transients into each scan file, producing 600 scan files during the 10-min analysis. This database, obtained at 1 sf/s, represents that typically obtained with commercially available GC–MS instruments, which produce one spectrum per second. Another database, obtained at 10 sf/s, was generated by summing 500 consecutive mass spectral transients into each scan file, producing 6000 scan files during the 10-min analysis. Table I lists several of the TMS-derivatized organic acids identified from data collected at 10 sf/s, with their retention times and relative amounts for each component. The components in the mixture were identified by comparison of retention times and mass spectra of each component to those in a reference library previously compiled in our laboratory using another GC–MS instrument. Components that are yet to be identified have been labeled as unknowns. Quantification was achieved based on the area in the RTIC represented by 36 ng of the TMS derivative of tropic acid (peak marked with an asterisk in Fig. 2c) used as the internal standard.

The goal of any GC–MS analysis is to obtain useful information for all of the components in a mixture represented by the RTIC chromatogram. Ideally, the RTIC chromatogram provides an accurate representation of the chromatographic profile for retention times and quantification of the components in the mixture. The database from which the RTIC chromatogram is generated should provide information to distinguish those components that are not fully resolved chromatographically. In capillary GC–MS, it is difficult to meet these criteria when scan files are generated at 1 sf/s or less. Scan file acquisition rates of 10 sf/s or greater are necessary to generate RTIC chromatograms that accurately represent the resolution achieved by the capillary GC column used in this analysis [9]. The RTIC chromatogram in Fig. 2c accurately represents the chromatographic peak shapes and areas as verified by comparison with the chromatogram obtained by GC–FID in Fig. 2a.

Selected segments of the complete RTIC chromatograms (shown in Fig. 2) are shown in more detail in Fig. 3. The RTIC chromatogram from the database collected at 1 sf/s (Fig. 3a), typical of GC–MS analyses using scanning mass spectrometers, clearly does not accurately represent the chromatographic profile when compared with either the GC–FID or the GC–BDTOF-MS–ITR RTIC traces generated from the database collected at 10 sf/s (Fig. 3b). Regions where there are two or more closely eluting components are represented by a single peak in the RTIC chromatogram in Fig. 3a ow-

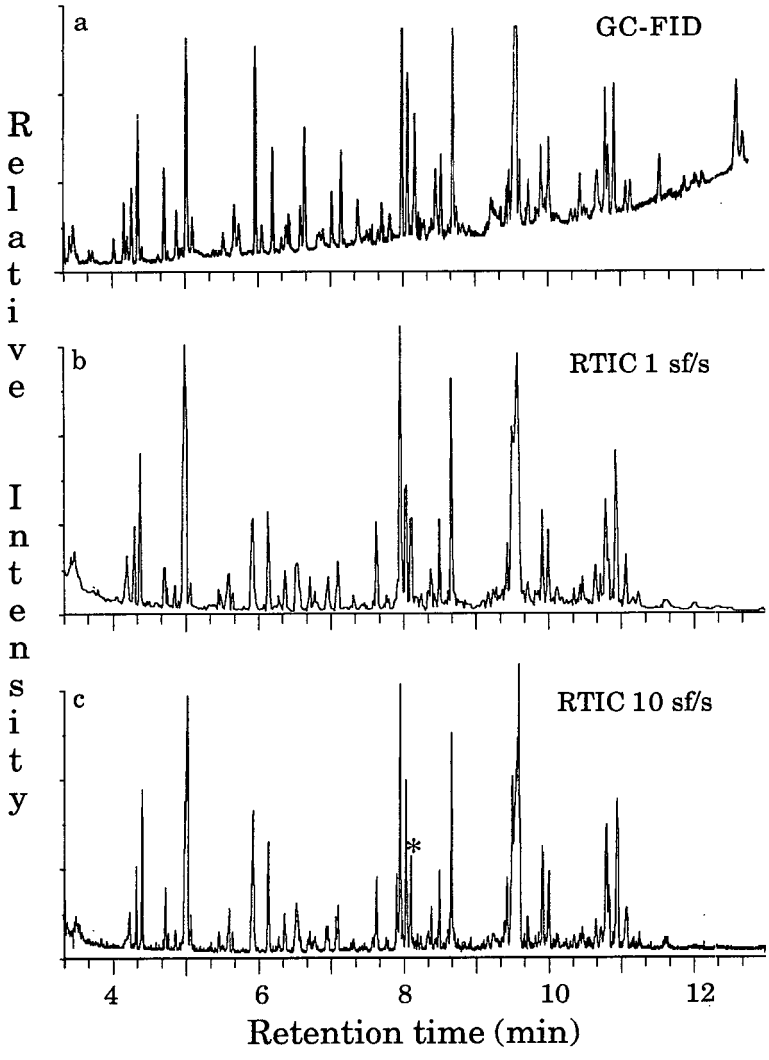

Fig. 2. (a) Gas chromatogram obtained using FID. (b) Reconstructed total ion current (RTIC) chromatogram generated from the GC–MS database collected at 1 sf/s. (c) RTIC chromatogram generated from the GC–MS database collected at 10 sf/s. The peak marked with the asterisk represents 36 ng of tropic acid (injected) as the internal standard.

ing to the small number of data points available with which to reconstruct the chromatographic peak profiles. For example, the segment marked A in Fig. 3a suggests the presence of three components, whereas the data in Fig. 3b clearly show that at least five components are eluting in this time period. Region B in Fig. 3a may represent baseline noise; however, the data in Fig. 3b show a chromatographic peak in that time window (see arrow). Similarly, region C becomes a chromatographic doublet (or possibly a triplet) when the mass spectra database allows for adequate reconstruction of the chromatographic resolution (Fig. 3b). If the RTIC chromatogram in Fig. 3a were the only one available, an analyst would incorrectly interpret apparent "single peaks" as representing single components. However, the mass spectrum obtained by averaging the scan files across the peak, as is common-

TABLE I

URINARY ORGANIC ACIDS IN MIXTURE

Quantitative results assuming identical ionization efficiencies for all compounds. The table contains information on compounds present at greater than 2.0 μg/mg of creatinine.

Retention time (min) (± 0.002 min)	Scan file number	Acid (or other compound)	Relative response (μg/mg creatinine)
4.328	798	Lactic	27.0
4.412	848	Glycolic	59.7
4.728	1038	Oxalic	25.9
4.767	1061	Glyoxylic oxime	7.1
4.863	1119	Unknown	8.8
4.928	1157	Unknown	3.6
4.988	1194	*p*-Cresol	17.6
5.035	1222	Sulfuric	182
5.080	1249	4-Hydroxybutyric	14.4
5.460	1477	3-OH-isovaleric	6.6
5.573	1545	Urea	9.4
5.605	1564	Unknown amino acid	18.8
5.653	1593	Benzoic	7.2
5.937	1763	Phosphoric	91.1
5.958	1776	Unknown amino acid	7.4
6.143	1887	Succinic	31.7
6.155	1894	Tri-TMS-glycine	28.2
6.285	1972	Pyrocatechol	6.4
6.365	2020	Glyceric	13.4
6.507	2105	4-Deoxyerythronic	8.7
6.542	2125	Unknown amino acid	22.1
6.560	2137	4-Deoxythreonic	10.8
6.708	2225	Unknown	12.8
6.958	2375	3-Deoxytetronic	30.2
7.092	2455	2-Deoxytetronic	42.7
7.432	2594	Unknown	6.2
7.642	2786	Pyroglutamic	39.6
7.768	2862	5-Hydroxymethyl-2-furoic	8.5
7.915	2950	Erythronic (isomer)	46.6
7.967	2981	Erythronic	147
7.998	3000	Threonic (isomer)	11.8
8.048	3030	Threonic	89.2
8.117	3071	Internal standard, tropic (36 ng)	55.6
8.208	3125	3-Hydroxyphenylacetic	3.5
8.358	3215	Furan-2,5-dicarboxylic	6.4
8.393	3237	4-Hydroxyphenylacetic	15.1
8.445	3267	2-Aminoadipic	4.2
8.502	3302	Tartaric	37.6
8.672	3404	2-Deoxyribonic	116
9.403	3843	Arabinonic	32.6
9.435	3862	Ribonic	58.4
9.565	3940	Hippuric	297
9.615	3970	Citric	39.6
9.720	4032	Methylhydroxyphenylhydracrylic	17.0
9.922	4153	Deoxyhexonic lactone	49.9
9.843	4106	Gluconolactone	40.3
10.357	4415	Ascorbic	9.8
10.657	4594	Glucuronic	23.2
10.803	4683	Gluconic	81.0
10.837	4703	Gluconic	31.5
10.953	4773	Glucaric	111
11.073	4845	Galacturonic	39.3

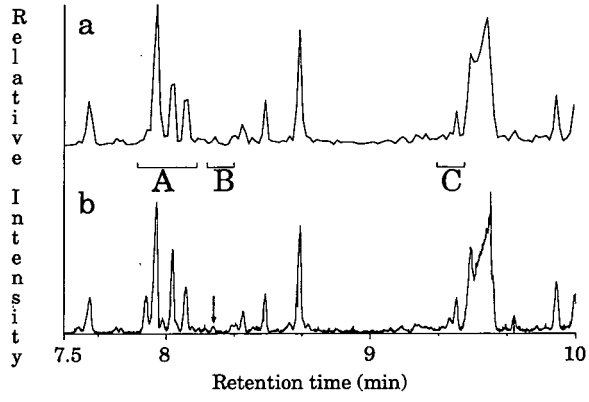

Fig. 3. (a,b) Selected segments of the complete RTIC chromatograms generated at 1 and 10 sf/s as shown in Fig. 2b and c, respectively. The region marked A in (a) suggests the presence of three components, whereas the data in (b) clearly show that at least five components are eluting during this time period. Region B in (a) may represent baseline noise, but the data in (b) show a chromatographic peak (arrow). Similarly, region C becomes a chromatographic doublet when the mass spectral database (acquired at 10 sf/s) allows for adequate reconstruction of the chromatographic resolution.

ly done for data presumed to represent a single component, would be the sum of mass spectra from two or more components, thus making mass spectral interpretation difficult, if not impossible. Minor components in the mixture are also difficult to distinguish from the baseline in Fig. 3a, again owing to the insufficient number of data points (scan files) with which to reconstruct the chromatographic peak profiles.

Mass spectral deconvolution: improving "chromatographic resolution" and compound identification from the mass spectral database

An important difference between the RTIC chromatogram in Fig. 2c and the GC–FID trace (Fig. 2a) is that with the RTIC chromatogram, additional dimensions of information are available in the mass spectra database. The mass spectral database can be used in two ways. Deconvolution of chromatographically unresolved components is possible by plotting the ion current at specified m/z values *versus* scan file number, generating a mass chromatogram. Mass chromatograms suggest which scan files should contain mass spectral information for particular components, allowing qualitative and quantitative information to be obtained, even for overlapping components. The success of this approach depends on the scan file generation rate of the mass spectrometer. For example, a sufficient number of scan files must be generated during a chromatographic doublet for the mass spectral database to be adequately time-resolved for identifying and deconvoluting overlapping components. The result of mass spectral interpretation is only as good as the quality of the mass spectra, which can be compromised owing to skewing of peak intensities by scanning mass spctrometers, or to spectral interferences from co-eluting components. Because the BDTOF-MS–ITR system can generate many unskewed mass spectra each second, mass spectral quality is outstanding and interferences are relatively easy to identify and remove.

One of the advantages of generating a mass spectral database at 10 sf/s, rather than at 1 sf/s, is demonstrated in Fig. 4. A portion of the RTIC chromatogram generated from the database collected at 1 sf/s shown in Fig. 4a has one "peak" in the vicinity of scan file 125 that appears to result from a single component in the mixture. The 5-s peak width might be interpreted as resulting from overloading the column, and the scan files 123–128 of the RTIC chromatogram would be averaged and the resulting mass spectrum (mis)interpreted. In comparing Fig. 4a with Fig. 4b (reconstructed from the database collected at 10 sf/s), it is apparent that more than one component is eluting during this time period, with very different elution profiles.

Differential comparison of adjacent mass spectra collected for a GC peak may help to discern the number of components present. For example, Fig. 5a and b show the mass spectra in scan files 1197 and 1220, respectively, from the region of the RTIC chromatogram in Fig. 4b. The mass spectrum in Fig. 5a has a number of peaks not observed in Fig. 5b; the most obvious are at m/z 165 and 180. Other peaks, such as those at m/z 73, 147 and 227 are found in both scan files. Because there are peaks that are not found in both scan files, one can assume that there is more than one component represented by the "peak" in the RTIC chromatogram in Fig. 4b. The ratio of relative intensities at m/z 147 and 227 in Fig. 5a and b remains constant, which indicates that both mass spectral peaks represent the

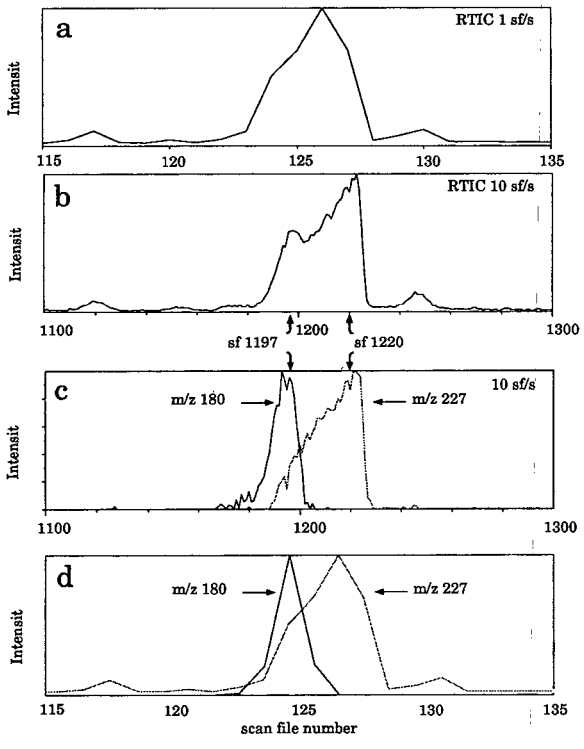

Fig. 4. (a,b) Comparison of a 20-s region of the RTIC chromatograms generated from databases collected at 1 and 10 sf/s. Mass chromatograms at *m/z* 180 (solid lines) and *m/z* 227 (broken lines).

same component. Also, the mass chromatograms at each of these *m/z* values correlate with each other. By plotting the signal intensities at *m/z* 180 and 227 *versus* scan file number, the elution profiles of the two components can be resolved, and these individual profiles realized as shown in Fig. 4c. Clearly, the second component exhibits considerable fronting on this particular column.

For further comparison, the mass chromatograms at *m/z* 180 and 227 from the database generated at 1 sf/s are shown in Fig. 4d. There are only three scan files in this database that contain mass spectral data at *m/z* 180. The partial pressure of the component represented at *m/z* 180 changes by 80% from scan file 123 to 124. With a scanning mass spectrometer, this would result in significant skewing of the relative ion intensities in the mass spectrum as well as making mass spectral subtraction difficult.

Mass spectra can be obtained after identification of a unique ion for each component. Ion current at *m/z* 180 is observed in scan files 1180 to 1203. Hence the data in Fig. 4c show that the mass spectrum in scan file 1220 is representative of the second component with no mass spectral interferences from the first, and can be interpreted as such. The mass spectrum in scan file 1197 contains mass spectral data from both of the components. A mass spectrum representative of the first component can be obtained by mass spectral subtraction. By subtracting the peak intensities at *m/z* values representative of the second component found in scan file 1220 from those in scan file 1197, a mass spectrum for the first component will result. The base peak in scan files 1197 and 1220 is at *m/z* 147, which represents only the second component. The ion current at *m/z* 147 in scan file 1220 is 34 384 arbitrary units (AU) and 14 704 AU in scan file 1197. Subtracting 43% [(14 704/34 384 AU) × 100] of the ion current at all of the peaks in scan file 1220 from those for corresponding peaks in scan file 1197 will remove all of the ion current indicative of the second component, leaving only ion currents indicative of the first component. The mass spectrum resulting from this mass spectral subtraction is shown in Fig. 5c. This simple, but powerful, operation is possible only when unskewed mass spectra, such as those obtained by TOF-MS as described here, are processed.

The first component represented in the RTIC segment in Fig. 4 has been identified as the TMS derivative of *p*-cresol. The molecular ion, $M^{+}\cdot$, is represented by the peak at *m/z* 180; the characteristic ion, $[M-15]^{+}$, due to the loss of a methyl group from the trimethylsilyl group, is represented by the peak at *m/z* 165. The second component has been identified as the bis-TMS derivative of sulfuric acid. The molecular weight of this compound is 242 u, and the mass spectrum shows a peak at *m/z* 227 for the characteristic ion corresponding to $[M-15]^{+}$.

A more dramatic example of a reconstructed chromatographic peak profile, suggesting, incorrectly, the elution of a single component, is shown in Fig. 6a. The peak shape and width are consistent with the elution of a single component at this retention time. The mass spectral data in scan files 1883, 1890 and 1899 are shown in Fig. 7a, b and c, respectively. The most obvious differences are the changes in relative intensities at *m/z* 147, 174 and 247 in the three mass spectra, suggesting the elution of at least

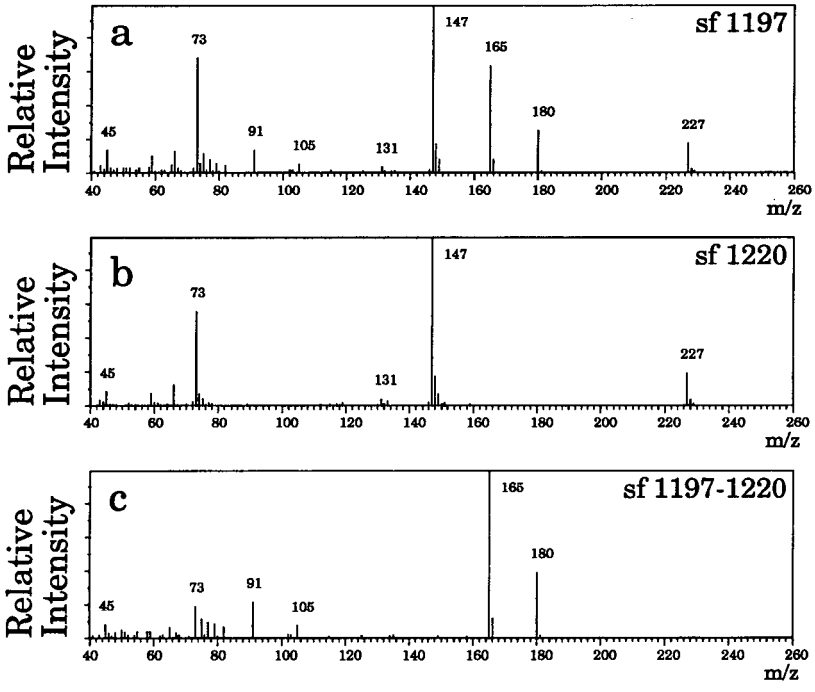

Fig. 5. (a) Mass spectrum in scan file 1197 that has mass spectral information for both of the components eluting over the peak profile shown in Fig. 4c. (b) Mass spectrum in scan file 1220. The mass spectrum shown in (c) is the result of subtracting 43% of the ion currents in scan file 1220 from the corresponding ones in scan file 1197.

two different components. Mass chromatograms at *m/z* 174 and 247 are shown in Fig. 6b. Again, the mass chromatograms do not overlap completely, indicating the presence of two components. By identifying a unique mass spectral peak for each of the components in the chromatographic peak profile, a mass spectrum for each component can be obtained. A comparison of the mass spectra in Fig. 7a–c shows that scan file 1883 only has ion currents indicative of one of the components. Similarly, scan file 1899 only has ion currents indicative of the other component. Selection of these scan files is clearer on examination of the overlapping mass chromatograms shown in Fig. 6b. Note that at the maximum intensities at *m/z* 174 and 247, the retention times, shown in Fig. 6b, only differ by 0.8 s, but one can still obtain a mass spectrum for each of the components directly from the database generated at a rate of 10 sf/s.

The two components represented in Fig. 6 have been identified as bis-TMS-succinic acid and tri-TMS-glycine, respectively. The TMS ester of succinic acid has a molecular weight of 262 u and its mass spectrum shows a peak for the characteristic

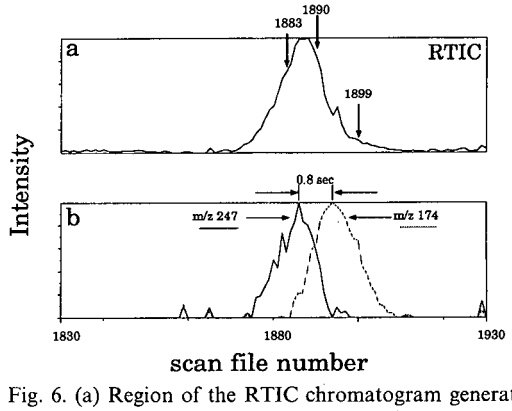

Fig. 6. (a) Region of the RTIC chromatogram generated from the database acquired at 10 sf/s. (b) Mass chromatograms at *m/z* 174 (broken line) and *m/z* 247 (solid line). The difference in the maxima of the two mass chromatograms indicates the presence of two components.

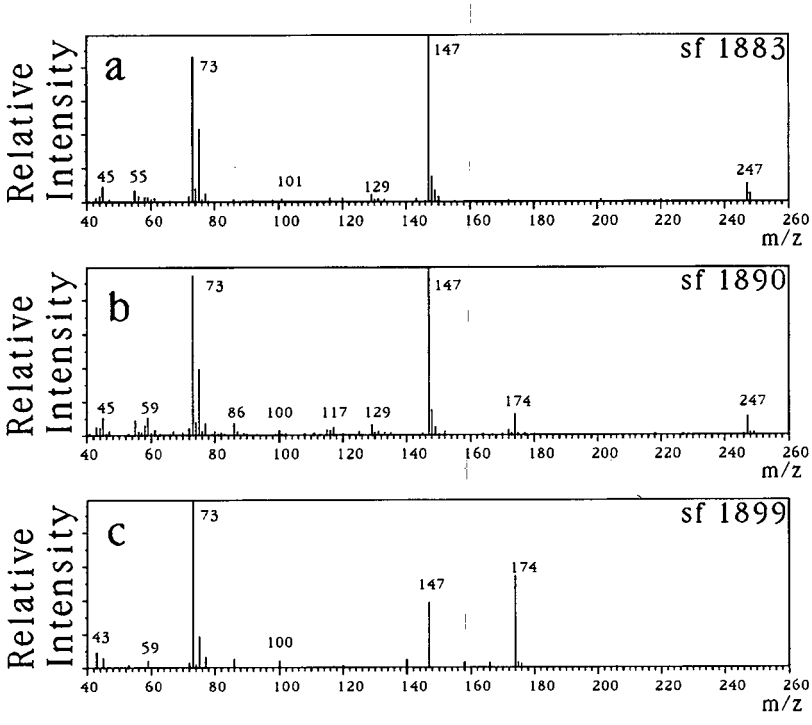

Fig. 7. Comparison of mass spectral data in scan files (a) 1883, (b) 1890 and (c) 1899 over the peak profile in Fig. 6. Comparison of the mass spectral data in each of the scan files shown, indicates that (a) (scan file 1883) represents the first component in the peak profile, (b) (scan file 1890) contains mass spectra data for both components and (c) (scan file 1899) is the mass spectrum of the second component represented by the poorly resolved doublet in Fig. 6b.

$[M-15]^+$ ion at *m/z* 247. Other peaks indicative of the TMS derivative of succinic acid are located at *m/z* 73, 129, 147, 172 and 218.

Three-dimensional data presentation

Three-dimensional (3-D) plots of mass spectra *versus* scan file number are another useful means of displaying data consisting of a large number of scan files per chromatographic peak [10]. These 3-D plots are constructed by plotting mass chromatograms for all *m/z* values in a given region of the RTIC chromatogram. This allows the temporal profiles of each mass chromatogram to be compared to indicate which chromatographic peaks result from more than one component. An example of a 3-D plot is shown in Fig. 8 for the chromatographic peak in the metabolic profile represented in Fig. 6. The 3-D plot clearly shows evidence for the two components over this region of the RTIC. The two components have peaks in common at *m/z* 73 and 147, but there are a number of peaks that are unique to one or the other components. The two major peaks that are unique to each of the components occur at *m/z* 174 and 247 (as in Fig. 6b). Chromatographic profiles for the two components can be recognized by plotting mass chromatograms at *m/z* 174 and 247. The mass spectrum of each

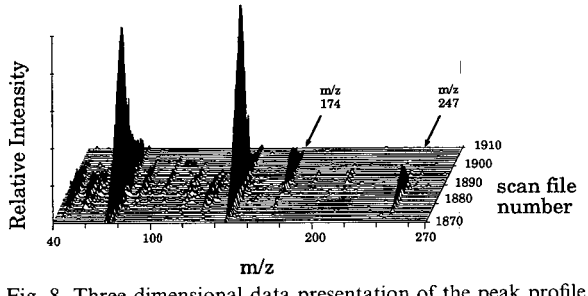

Fig. 8. Three-dimensional data presentation of the peak profile in Fig. 6. The 3-D plot shows ion current at all of the *m/z* values for direct comparison of individual mass chromatograms.

component can be obtained by examining the mass chromatograms as shown previously.

CONCLUSIONS

A GC–MS instrument based on BDTOF-MS can perform complex mixture analyses by generating complete mass spectra at a rate appropriate for specific chromatographic conditions. The scan file generation rate for an analysis is dictated by requirements to represent the chromatography accurately and provide data with good signal-to-noise ratios. The utility of this unique system has been demonstrated in the context of realistic problems encountered in the analysis of the complex mixture of organic acids extracted from human urine. The problems in such analyses frequently manifest themselves as components that are chromatographically unresolved. It is further demonstrated that long capillary columns, with high numbers of theoretical plates and peak separation, are not necessary with this technology. Rather, an analysis can be performed on a short capillary column giving the same analytical information, but with a reduced analysis time. The typical analysis time for this metabolic profile was reduced from 1 h to 15 min (this particular analysis time was limited by the rate at which the GC temperature could be increased). The success of these analyses is due to the nature of the BDTOF-MS instrument combined with the ITR. In this application, each of the ten scan files generated each second is the sum of 5000 transient mass spectra. The high scan file generation rate provides a database that can be used to represent accurately the chromatographic information, which facilitates the identification of each of the components in a complex mixture. Quantification of each of the components is facilitated owing to the greater number of points available with which to determine peak shape, width and area. The "unskewed" nature of the mass spectrum in each of the scan files facilitates the preparation of "pure" mass spectra by deconvolution of nearly co-eluting components using mass spectral subtraction. For the data presented here, compounds with retention times differing by 0.1 s can be analyzed. The three-dimensional presentation of the data allows the user to identify peaks that are representative of poorly resolved components, display the corresponding mass chromatograms and then choose scan files and background scan files for subtraction to obtain mass spectra for closely eluting components.

In closing, we note that the concepts discussed here, including the use of mass chromatograms, RTIC chromatograms and mass spectral subtraction, in the context of GC–MS are more than 20 years old. However, their utility can be a source of frustation for chromatographers because the low spectral acquisition rates of scanning mass spectrometers yield reconstructed chromatograms that have much less detail than those acquired by GC only. With the capabilities of the instrument described here, these established methods become much more useful to the chromatographer who is using a mass spectrometer as the chromatographic detector. Scan rate limitations no longer degrade chromatographic information available in databases obtained by GC–MS.

ACKNOWLEDGEMENTS

This work was supported by a grant from the Biotechnology Research Program of the National Institutes of Health, Division of Research Resources (DRR-00480-22). The authors thank M. Rabb for his assistance and Galileo Electro-Optics (Sturbridge, MA, USA) for their donation of the high-output multi-channel plates.

REFERENCES

1 J. F. Holland, J. Allison, C. G. Enke, J. T. Stults, J. D. Pinkston, B. Newcome and J. T. Watson, *Anal. Chem.*, 55 (1983) 997A.
2 J. Allison, J. F. Holland, C. G. Enke and J. T. Watson, *Anal. Instrumen.*, 16 (1987) 207.
3 J. F. Holland, B. Newcome, R. E. Tecklenburg, Jr., M. Davenport, J. Allison, J. T. Watson and C. G. Enke, *Rev. Sci. Instrum.*, 61 (1990) 69.
4 J. D. Pinkston, M. Rabb, J. T. Watson and J. Allison, *Rev. Sci. Instrum.*, 57 (1986) 583.
5 G. E. Yefchak, G. A. Schultz, J. Allison, J. F. Holland and C. G. Enke, *J. Am. Soc. Mass Spectrom.*, 1 (1990) 440.
6 J. T. Watson, G. A. Schultz, R. E. Tecklenburg, Jr. and J. Allison, *J. Chromatogr.*, 518 (1990) 283.
7 J. F. Holland, J. J. Leary and C. C. Sweeley, *J. Chromatogr.*, 379 (1986) 3.
8 B. A. Chamberlin and C. C. Sweeley, *Clin. Chem.*, 33/4 (1987) 572.
9 S. N. Chesler and S. P. Cram, *Anal. Chem.*, 43 (1971) 1922.
10 R. Reimendal and J. Sjovall, *Anal. Chem.*, 44 (1972) 21.

Journal of Chromatography, 590 (1992) 341–353
Elsevier Science Publishers B.V., Amsterdam

CHROM. 23 744

Comparison of isotachophoresis, capillary zone electrophoresis and high-performance liquid chromatography for the determination of salbutamol, terbutaline sulphate and fenoterol hydrobromide in pharmaceutical dosage forms

M. T. Ackermans, J. L. Beckers*, F. M. Everaerts and I. G. J. A. Seelen

Laboratory of Instrumental Analysis, Eindhoven University of Technology, P.O. Box 513, 5600 MB Eindhoven (Netherlands)

(First received June 11th, 1991; revised manuscript received September 16th, 1991)

ABSTRACT

Reversed-phase high-performance liquid chromatography (RP-HPLC), isotachophoresis (ITP) and capillary zone electrophoresis (CZE) were applied to the determination of salbutamol, terbutaline sulphate and fenoterol hydrobromide in commercially available pharmaceutical dosage forms. The comparison showed that especially with the use of ITP, high concentrations of other charged sample components can disturb the separation process. If special attention is paid to ensure a complete separation, all methods give comparable results. For the regression lines of the calibration graphs, regression coefficients of at least *ca.* 0.999 and nearly zero intercepts are obtained with relative standard deviations of *ca.* 1–2% for peak area or zone lengths. By applying the different techniques, often different components of the sample matrix can be detected, *i.e.*, a more complete impression of the sample composition can be obtained by using all the three techniques.

INTRODUCTION

With the development of capillary zone electrophoresis (CZE), the analyst now has available several separation techniques, isotachophoresis (ITP), CZE and high-performance liquid chromatography (HPLC), with an overlap of application areas. Although ITP can be applied for the separation of uncharged components, *e.g.*, by complexation with charged additives in the electrolyte system, ITP is most suitable for the separation of charged components and the separation principle is based on differences in the effective mobilities of the components. The effective mobilities can be affected, *e.g.*, by changing the pH of the electrolyte system and the addition of complexing agents.

HPLC can be applied to both uncharged and charged components and the separation principle is based on partitioning between a stationary and a mobile phase. The capacity factors, k', can be affected by changing, *e.g.*, the polarity and pH of the mobile phase and the addition of complexing agents.

In CZE, the separation principle is based on differences in effective mobilities although the application of a second mobile phase leads to a hybrid technique by which the separation principle depends on both differences in effective mobilities and partitioning over two mobile phases (micellar electrokinetic capillary chromatography). In the latter instance uncharged components can also be separated.

Altogether, it is clear that the overlap in the application areas of ITP, CZE and HPLC lies in the separation of charged components.

Although HPLC is often used for analyses of drugs [1–6], less attention has been paid to the use of

0021-9673/92/$05.00

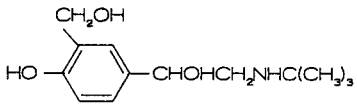

Salbutamol

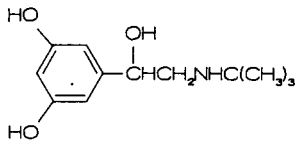

Terbutaline

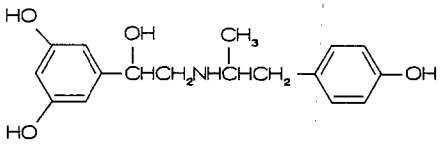

Fenoterol

Fig. 1. Structural formulae of salbutamol, terbutaline and fenoterol.

ITP and CZE and to compare these methods concerning reproducibility and accuracy. Particularly for CZE, few quantitative applications have been published.

In this paper, the abilities of ITP, CZE and HPLC are compared for the determination of some drugs in pharmaceutical dosage forms. As the UV detector of the Beckman CZE apparatus has standard wavelengths of 214, 254 and 280 nm, we selected for the quantitative comparison salbutamol, fenoterol and terbutaline because they have optimum UV absorbance at a wavelength of about 214 nm. For ITP the choice of the wavelength is of less importance because the sample zone concentration is high compared with CZE and HPLC. The structural formulae of the drugs are given in Fig. 1.

EXPERIMENTAL

Instrumentation

The HPLC equipment (Pharmacia–LKB, Bromma, Sweden) consisted of a Model 2150 pump, a Model 2152 controller, a low-pressure mixer, a Model 2156 solvent conditioner and a VWM 2141 dual-wavelength UV detector. Chromatographic separation was obtained with a LiChrospher 100 RP-18 end-capped column (125 × 4 mm, 5 μm) from E. Merck (Darmstadt, Germany). Injections were made with a Model 7125 universal loop injector (20 μl) (Rheodyne, Berkeley, CA, USA).

For all CZE experiments the P/ACE System 2000 HPCE (Beckman, Palo Alto, CA, USA) was used. The capillary was an original Beckman capillary cartridge (capillary length 57 cm, distance between injection and detection 50 cm and 75 μm I.D.). The wavelength of the UV detector was 214 nm in all experiments and the operating temperature was 25°C. All experiments were carried out in the cationic mode (anode placed at the inlet and cathode at the outlet), applying a constant voltage of 12.5 kV. The sample introduction was achieved by pressure injection for 5 s (about 100 nl).

For all ITP experiments, a laboratory-built apparatus [7] with conductivity and UV detectors (254 nm) was used. In this apparatus, a closed system is obtained by shielding the separation capillary from the open electrode compartments with semipermeable membranes. A PTFE capillary tube (0.2 mm I.D.) was used, in contrast to the fused-silica capillary in the Beckman apparatus. The sample was introduced with a syringe and the sample volume was 3 μl, unless stated otherwise.

All data obtained from the chromatograms and electropherograms were handled using the laboratory-written program CAESAR.

Chemicals

Salbutamol sulphate, terbutaline sulphate and fenoterol hydrobromide were kindly donated by the State Institute of Quality Control for Agricultural

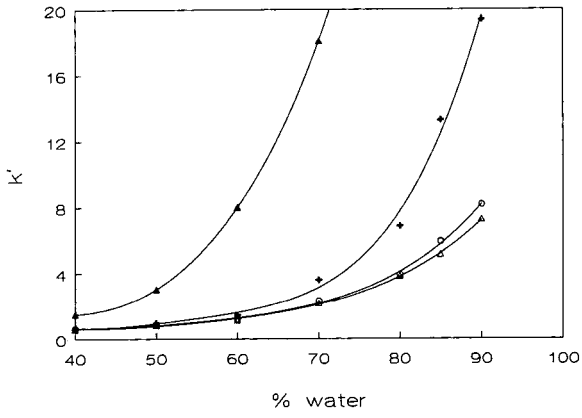

Fig. 2. Relationship between capacity factor, k', and percentage of water in the water–methanol mobile phase containing 0.002 *M* KOH and 0.01 *M* hexanoic acid for (△) terbutaline sulphate, (○) salbutamol sulphate, (+) fenoterol hydrobromide and (▲) the analogue antibiotic clenbuterol hydrochloride.

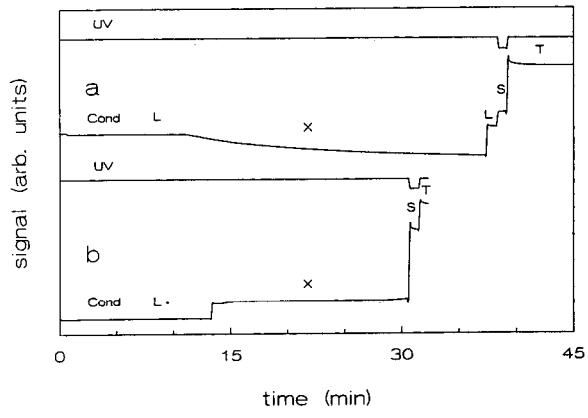

Fig. 3. Isotachopherograms for the analysis of Ventolin syrup by ITP applying (a) electrolyte system A and (b) electrolyte system B. The zone of salbutamol is indicated by S. The unknown sample component X migrates isotachophoretically in system B and zone electrophoretically in the leading zone histidine in system A. L = leading electrolyte, T = terminator.

Products (RIKILT, Wageningen, Netherlands). All salbutamol pharmaceuticals are Ventolin products from Glaxo (Nieuwegein, Netherlands), the terbutaline pharmaceuticals are Bricanyl products from Astra Pharmaceutica (Rijswijk, Netherlands) and the fenoterol pharmaceuticals are Berotec products from Boehringer Ingelheim (Alkmaar, Netherlands).

Standard solutions

Standard solutions of 1 mg/ml of salbutamol, terbutaline sulphate and fenoterol hydrobromide were prepared by weighing accurately 50.0 mg of the standards and dissolving them in 50.0 ml of distilled water. From these solutions appropriate dilutions were made so that the concentration of each sample solution approached the concentration of that in the middle of the standard solution range.

Sample preparation

All tablets and the capsules were mixed with 10 ml of water and, after ultrasonication for about 30 min, the sample solution was centrifuged. The clear supernatant solution was used for the analysis after dilution with distilled water to the desired concentration. All liquid pharmaceuticals were diluted to the desired concentration with distilled water.

Separation conditions for HPLC

Reversed-phase HPLC was performed at ambient temperature. Several experiments were carried out to select a suitable mobile phase and water–methanol (60:40, v/v) containing 0.002 *M* KOH and 0.01 *M* hexanoic acid as an ion-pair reagent was found suitable for the analysis of the pharmaceuticals. In Fig. 2 the capacity factor, k', is given as a function of the percentage of water in the water–methanol mixture for salbutamol sulphate, fenoterol hydrobromide, clenbuterol hydrochloride and terbutaline sulphate. The mobile phase was degassed by vacuum filtration through a 0.22-μm filter and sparging with helium. The column was equilibrated with mobile phase at a flow-rate of 0.4 ml/min for about 1 h.

Separation conditions for ITP

For the ITP experiments, two electrolyte systems were used. System A consisted of a leading electrolyte of 0.01 *M* histidine adjusted to pH 4.75 by adding acetic acid with the terminator acetic acid at pH 3.5. System B consisted of a leading electrolyte of 0.01 *M* KOH adjusted to pH 4.75 by adding acetic acid with the terminator acetic acid at pH 3.5.

With electrolyte system A, ionic species present in the sample solutions with high effective mobilities (such as sodium) will migrate in a zone electrophoretic manner through the leading zone of histidine.

TABLE I

AVERAGE VALUES (AV) AND RELATIVE STANDARD DEVIATIONS (R.S.D.) OF THE RELATIVE STEP HEIGHTS *RSH* (AS % OF THE STEP HEIGHT OF PYRAZOLE-3,5-DICARBOXYLIC ACID) AND ZONE LENGTHS *ZL* WITH ITP

Component	*RSH* (AV)	R.S.D. (%)	*ZL* (s) (AV)	R.S.D. (%)
Chloric acid	63.6	1.35	13.23	1.18
Malonic acid	83.6	0.54	24.23	0.90
Pyrazole-3,5-dicarboxylic acid	100.0	–	27.02	0.65
Acetic acid	141.6	0.71	15.93	1.57
Glutamic acid	237.1	1.31	19.58	0.62

The drugs migrate in an ITP manner between the leading ions histidine and the terminating hydrogen ions. Applying electrolyte system B, the drugs migrate behind a large zone of the sample ions with a high effective mobility. Nevertheless, identical results were obtained for test samples with both systems A and B. As an example, the isotachopherograms (both the UV and conductivity detector signals) of Ventolin syrup are given in Fig. 3, applying both (a) system A and (b) system B. It can clearly be seen that in system B, salbutamol migrates behind a large amount of a sample cation with high mobility, whereas in system A that sample cation migrates in the leading zone of histidine. For the determination of the drugs in the pharmaceuticals we applied system B.

Separation conditions for CZE

All CZE experiments were carried out with the background electrolyte 0.01 *M* tris(hydroxymethyl) aminomethane (Tris) adjusted to pH 5.0 by adding acetic acid.

RESULTS AND DISCUSSION

In the comparison of the efficiency of ITP, HPLC and CZE for the determination of components in different samples, validation of the methods is an important task. The validation requires a demonstration of the specificity, sensitivity, calibration linearity, precision and accuracy of the methods. For this reason we shall first consider the within-day precision (repeatability) and between-day precision (reproducibility) and compare the calibration graphs obtained with the different methods.

Within-day precision

In order to obtain an impression of the within-day precision of the methods, replicate separations ($n = 10$) were made of sample mixtures of five components with the apparatus for ITP, HPLC and CZE.

With the ITP apparatus we performed separations of a mixture of chloric, malonic, pyrazole-3,5-dicarboxylic, acetic and glutamic acids (all at a concentration of $8 \cdot 10^{-4}$ *M*) applying a leading electrolyte of 0.01 *M* HCl adjusted to pH 6.0 by adding histidine and a terminating electrolyte of 0.01 *M* 2-(N-morpholino)ethanesulphonic acid (MES). The current was 25 μA. In Table I the average values and relative standard deviations are given for the relative step heights as a percentage of

TABLE II

AVERAGE VALUES (AV) AND RELATIVE STANDARD DEVIATIONS (R.S.D.) OF THE RETENTION TIMES t_R AND PEAK AREA *A* WITH HPLC

Component	t_R (min) (AV)	R.S.D. (%)	*A* (AUs) (AV)	R.S.D. (%)
Toluene	3.58	0.11	5.47	0.92
Ethylbenzene	4.43	0.15	5.36	1.00
Propylbenzene	5.91	0.25	4.18	0.90
Butylbenzene	8.19	0.26	6.52	1.01
Pentylbenzene	11.66	0.34	7.15	1.42

TABLE III

AVERAGE VALUES (AV) AND RELATIVE STANDARD DEVIATIONS (R.S.D.) OF THE MIGRATION TIMES t_m, EFFECTIVE MOBILITIES m_{eff} AND PEAK AREA A WITH CZE

Component	t_m (min) (AV)	R.S.D. (%)	$m_{eff} \times 10^5$ ($cm^2/V \cdot s$) (AV)	R.S.D. (%)	A (mAUs) (AV)	R.S.D. (%)
Salbutamol	5.54	1.01	19.07	0.72	12.29	1.51
Creatinine	6.12	1.02	12.61	0.90	6.72	2.08
Aniline	6.43	1.05	9.56	1.15	26.37	1.21
m-Aminobenzoic acid	12.96	1.71	−20.20	0.95	21.29	0.88
Benzoic acid	17.19	2.19	−27.42	0.80	22.63	0.93

TABLE IV

BETWEEN-DAY PRECISION: AVERAGE VALUES OF PEAK AREA (A) MEASURED WITH HPLC AND CZE AND ZONE LENGTHS (ZL) MEASURED WITH ITP AND THE RELATIVE STANDARD DEVIATIONS (R.S.D.) FOR SEVERAL CONCENTRATIONS (c) OF SALBUTAMOL SULPHATE, WITH REGRESSION PARAMETERS r (REGRESSION COEFFICIENT), b (SLOPE) AND a (INTERCEPT)

c (mg/ml)	HPLC (n = 5)				CZE (n = 5)			
	Day 1		Day 2		Day 1		Day 2	
	A	R.S.D. (%)	A	R.S.D. (%)	A	R.S.D. (%)	A	R.S.D. (%)
0.100	24.08	0.46	24.89	0.19	59.43	0.18	58.36	6.21
0.075	18.75	0.09	18.58	0.08	45.78	0.58	44.15	0.54
0.066	16.51	0.13	16.44	0.11	39.44	0.20	39.06	1.14
0.050	12.39	0.14	12.28	0.13	29.38	1.09	30.16	1.55
0.033	8.24	0.14	8.23	0.06	19.33	0.17	19.90	0.29
0.025	6.13	0.04	6.16	0.09	14.27	0.28	14.48	0.20
0.010	2.51	0.02	2.51	0.01	5.72	0.04	5.60	0.15
r	0.99943		0.99996		0.99967		0.99976	
b	242.92		248.70		604.85		586.10	
a	0.20		−0.027		−0.54		0.11	
c (mg/ml)	ITP (conductivity) (n = 3)				ITP (UV) (n = 3)			
	Day 1		Day 2		Day 1		Day 2	
	ZL	R.S.D. (%)	ZL	R.S.D. (%)	ZL	R.S.D. (%)	ZL	R.S.D. (%)
1.000	124.93	0.66	126.37	0.34	124.60	1.00	126.60	0.47
0.750	94.15	0.97	95.42	1.05	94.00	0.98	95.80	1.30
0.625	76.43	0.69	77.52	1.10	76.20	0.79	78.20	1.17
0.500	64.22	0.72	64.55	0.60	64.60	1.07	63.63	0.95
0.375	46.95	0.32	46.62	0.54	46.20	1.30	46.60	1.49
0.250	31.33	0.24	31.40	0.55	31.60	1.10	31.40	1.10
0.100	12.65	0.40	12.85	1.56	12.38	1.22	12.37	0.71
r	0.99967		0.99970		0.99950		0.99988	
b	124.57		126.44		124.42		127.31	
a	0.32		−0.065		0.24		−0.53	

the step height of pyrazole-3,5-dicarboxylic acid and the zone lengths measured with the conductivity detector.

With the HPLC apparatus we analysed a mixture of toluene ($5.9 \cdot 10^{-5}$ *M*) and ethyl- ($5.1 \cdot 10^{-5}$ *M*), propyl- ($4.5 \cdot 10^{-5}$ *M*), butyl- ($8 \cdot 10^{-5}$ *M*) and pentylbenzene ($7.3 \cdot 10^{-5}$ *M*) in methanol, applying methanol–water (80:20) as eluent. The flow-rate was 1.0 ml/min. The UV detector wavelength was 209 nm. In Table II the average values and relative standard deviations (R.S.D.s) for the retention times and peak area are given.

With the CZE apparatus we analysed a mixture of salbutamol ($1.75 \cdot 10^{-5}$ *M*), creatinine ($2 \cdot 10^{-5}$ *M*), aniline ($1 \cdot 10^{-4}$ *M*), benzoic acid ($1 \cdot 10^{-5}$ *M*) and *m*-aminobenzoic acid ($2 \cdot 10^{-5}$ *M*), applying a background electrolyte of 0.01 *M* Tris at pH 5.0 adjusted by adding acetic acid. In Table III the average values and R.S.D.s are given for the migration times, calculated effective mobilities [8] and peak area.

The within-day precision for the techniques is about 1–2%.

Between-day precision

To establish the between-day precision we measured the peak area ($n = 5$) for CZE and HPLC and zone lengths ($n = 3$) for ITP (with both the conductivity and UV detectors) of salbutamol sulphate and calculated the average values and R.S.D.s for several different concentrations of the solute. This series was repeated with freshly prepared electrolyte solutions after 1 week. The results are given in Table IV. It can be concluded that the reproducibility of the HPLC experiments is by far the best. The high R.S.D. of 6.21% in the second series of CZE experiments is due to one bad value, which could not be considered statistically as an outlier, however. The ITP experiments were carried out only three times in order to be able to measure the complete calibration graph in 1 day.

Quantification and limit of detection

For the "limit of quantification" or "limit of determination", which can be regarded as the lower limit for precise quantitative measurements, we used the value $y_B + 3\,s_B$, whereby the calculated intercept of the regression line can be used as an estimate of y_B and s_B is the standard deviation in the *y*-direction of the regression line [9].

The standard deviation in the concentration of unknown samples, determined with a calibration graph, is calculated according to the equation [9]

$$s = \frac{s_B}{b}\sqrt{\frac{1}{m} + \frac{1}{n} + \frac{(y - \bar{y})^2}{b^2 \sum_i (x_i - \bar{x})^2}} \qquad (1)$$

where m is the number of measurements of the unknown sample, n is the number of points of the calibration graph, b is the slope of the calibration graph, $\bar{x}$ and $\bar{y}$ are the average values of the x and y values of the calibration points, x_i is the x value of the calibration points and y is the average value of the m measurements of the unknown sample.

Although in most papers the R.S.D. values of the results obtained with calibration graphs are calculated with the equation

$$s = \sqrt{\frac{\sum_i (x_i - \bar{x})^2}{n - 1}} \qquad (2)$$

where x_i is the determined sample concentration and n is the number of measurements of the unknown sample, we prefer to use eqn. 1 because the "quality" of the calibration graph is included in the R.S.D. values. For techniques with a high precision, eqn. 2 leads to very low R.S.D. values, often unjustly indicating a high accuracy. The disadvantage of the use of eqn. 1 is that high R.S.D. values result if the sample concentration does not lie near the centroid of the regression line. For all quantitative determinations we applied the unweighted regression lines with seven concentrations per decade, taking care that the sample concentration lay near the centroid of the regression line.

Comparison of ITP, HPLC and CZE

For a first comparison of the separation methods we measured the peak area and zone lengths for samples of salbutamol sulphate from 1 to 0.001 mg/ml for HPLC and CZE and to 0.01 mg/ml for ITP and compared the linear regression lines. All zone lengths and peak area were recalculated as percentages of the highest values for each method. In Fig. 4A, B, C and D the values are presented graphically (logarithmic scale) for HPLC *versus* ITP (conductivity), CZE *versus* ITP (conductivity), CZE *versus* HPLC and conductivity *versus* UV detector

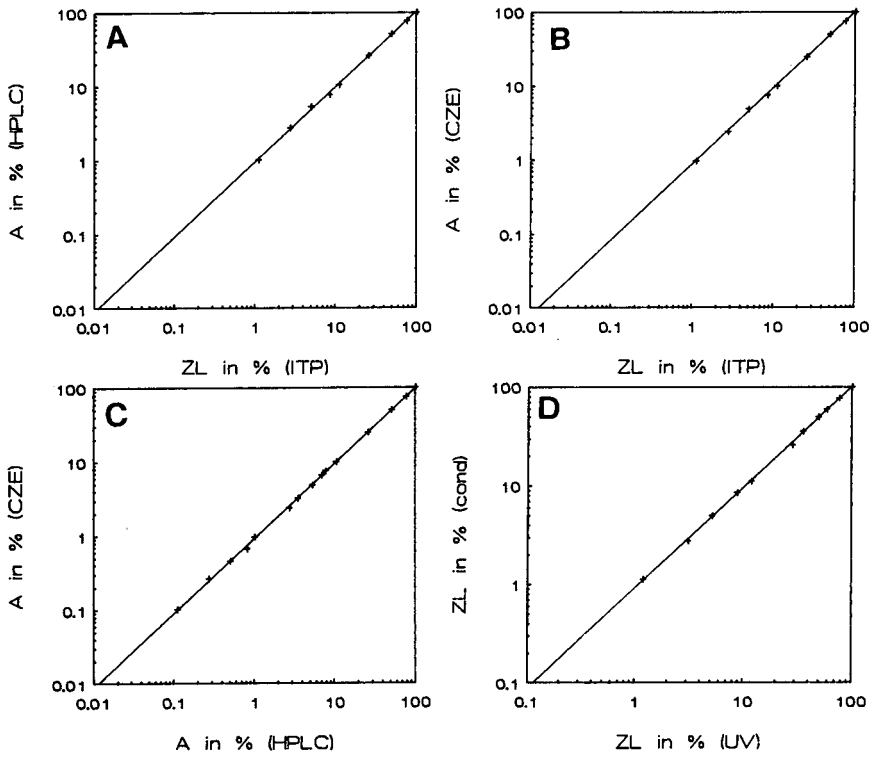

Fig. 4. Regression lines for the measured peak area *A* and zone lengths *ZL* as percentages of the maximum values for (A) HPLC *versus* ITP (conductivity signal), (B) CZE *versus* ITP (conductivity signal), (C) CZE *versus* HPLC and (D) conductivity *versus* UV signal for ITP.

signal for ITP, respectively. In Table V the slope, intercept, regression coefficient and limit of detection calculated for the regression lines (non-logarithmic scale) are given. The obtained linear relationships, with a slope nearly 1 and a nearly zero intercept, validate the techniques.

TABLE V

SLOPE, INTERCEPT, REGRESSION COEFFICIENT AND LIMIT OF DETECTION FOR THE INDIVIDUAL REGRESSION LINES OF PEAK AREA AND ZONE LENGTHS FOR SALBUTAMOL SULPHATE MEASURED WITH ITP, HPLC AND CZE AND CORRELATIONS BETWEEN THEM

Regression line of	Slope	Intercept	Regression coefficient	Detection limit (μg/ml)
ITP (conductivity)	139.21	0.1298	0.998929	41.20
ITP (UV)	115.45	0.8537	0.998508	58.38
CZE	744.97	−0.8805	0.999972	6.05
HPLC	283.72	0.3685	0.999960	7.17
HPLC–ITP (conductivity)	1.004	−0.096	0.999872	
CZE–ITP (conductivity)	0.999	−0.592	0.999804	
CZE–HPLC	0.991	−0.296	0.999871	
ITP (conductivity)–ITP (UV)	1.005	−0.604	0.999759	

Matrix effects

The composition of the sample can strongly influence the quality of the separation. Especially sample components with high effective mobilities present at a high concentration in a sample will affect the migration behaviour in electrophoresis. In CZE this can create an ITP system with two leading ions [10,11], leading to very sharp peaks and high plate numbers (this effect must be distinguished from stacking effects due to the injection of very dilute samples).

A typical difference between electrophoretic and chromatographic techniques is that in electrophoresis at any point the situation is determined by the initial conditions, as Kohlrausch formulated with his "regulation function" in 1897. This means that in electrophoresis the concentration of the injected sample adapts to the initial concentration of the background electrolyte migrating in the separation capillary. If one of the sample components is present at a high concentration, the length of the injected sample zone elongates during this adaptation process and the separation capacity of the system can be insufficient to separate all sample components. A way to solve this problem is to inject smaller amounts of the sample. However, the amount of the sample component of interest must be sufficient in order to detect and quantify that component. This is often a disadvantage in ITP, because the sample components migrate in consecutive zones, after the separation process, at a concentration adapted to that of the leading ions, which generally means at a concentration of about 0.005–0.01 *M*. Very small amounts of a sample component lead to very short, undetectable zones.

In ITP, the response factor, *RF* [12], defined as the slope of the calibration graph of the product $ZL \cdot I$ (A s) *versus* the amount of the sample Q (mol), can be utilized for quantitative determinations:

$$RF = \frac{ZL \cdot I}{Q} \qquad (3)$$

where ZL is the zone length (s) and I the electric current (A). This *RF* value is a constant (about $2 \cdot 10^5$ C/mol for monovalent ions) and indicates that the minimum detectable amount can be decreased by applying lower values of the electric current, assuming that a minimum zone length is required. Of course, this results in longer analysis times. This principle was applied in the determination of salbutamol, fenoterol hydrobromide and terbutaline sulphate with ITP (see Tables VI–VIII). In first instance, deviating values were obtained. After diluting the sample solutions tenfold, injecting 1 μl of sample solution and applying 7 μA instead of 25 μA, good results were obtained for the previously too low values. Another way to solve this problem is to use a column-coupling system with a higher separation capacity.

Determination of drugs in pharmaceuticals

In Tables VI–VIII all results for the determination of salbutamol, terbutaline sulphate and fenoterol hydrobromide are given. For the calibration graphs, the concentration decade (CD), indicated with its highest concentration, the regression coefficient (r) and calculated limit of detection (LOD, μg/ml) are given. For all pharmaceuticals the number of measurements (m), the determined amount of the drugs (Q) and the calculated R.S.D. according to eqn. 1 are given.

For HPLC and CZE we used standard solutions in the decade 0.01–0.1 mg/ml, determined the calibration graph twice at a wavelength of 214 nm and applied each calibration graph for the quantification of all sample solutions ($m = 3$).

For ITP we worked in the first instance with standard solutions with concentrations in the concentration decade 0.1–1 mg/ml and applied a current of 25 μA. With the calibration graph, both using the conductivity and UV detector signals (injection volume 3 μl) we determined the amount of the drugs in all sample solutions and observed too low values for the liquid samples containing a very large amount of a sample component with a high effective mobility (probably sodium). After diluting these samples tenfold and working in the concentration decade 0.01–0.1 mg/ml (current 7 μA), the results covered the labelled values. In some instances (marked with asterisks in the tables) even 1 μl had to be injected in order to obtain a complete separation and in these instances we calculated the R.S.D. with the three lowest points ($n = 3$) of the concentration decade in order to obtain the measured zone length in the centroid of the regression line.

For the peak area in CZE we determined the temporal and not the spatial peak area because the

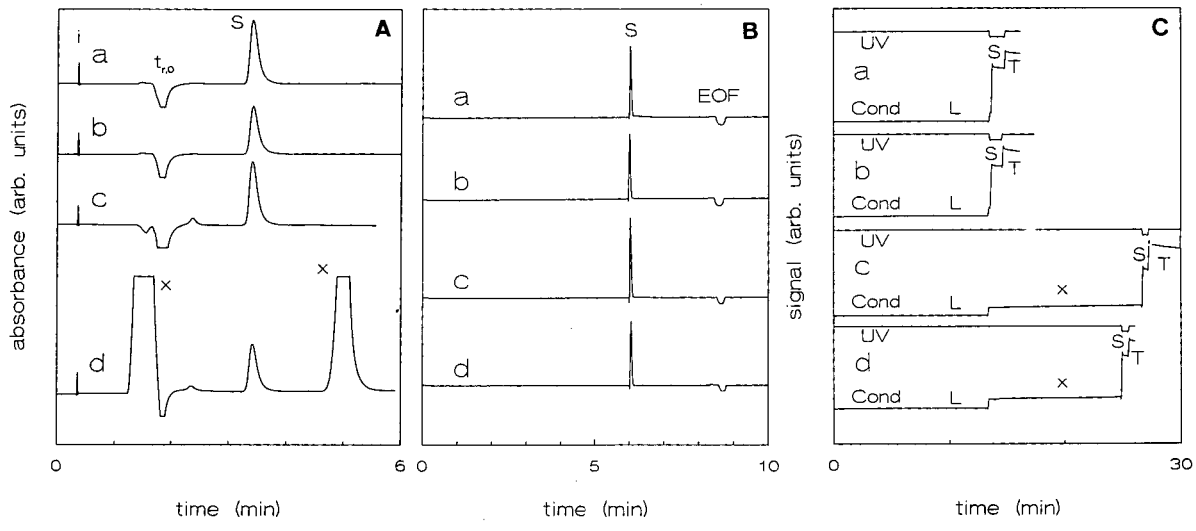

Fig. 5. (A) High-performance liquid chromatograms, (B) zone electropherograms and (C) isotachopherograms of (a) a standard solution of salbutamol, (b) the sample solution of Ventolin tablet, (c) the sample solution of the Ventolin solution for intervenous infusion and (d) the sample solution of Ventolin syrup. Salbutamol is indicated with S and all unknown components with X. In the isotachopherograms c and d the electric current is decreased to 7 μA at the time of detection of the zone X.

migration time in all experiments was fairly constant.

Determination of salbutamol

We studied the determination of salbutamol in Ventolin tablets (labelled value 4 mg per tablet), Ventolin solution for intravenous infusion (labelled value 1 mg/ml) and Ventolin syrup (labelled value 0.4 mg/ml). All the results are given in Table VI.

In Fig. 5, examples are given of the results of (A) HPLC, (B) CZE and (C) ITP experiments on (a) a standard solution of salbutamol, (b) a sample solution prepared from the Ventolin tablet, (c) the Ventolin solution for intravenous infusion and (d) the Ventolin syrup. For the HPLC and CZE experiments the UV signal and for the ITP experiments both the conductivity and UV signals are given. The salbutamol zones are marked with S. All other unknown sample components are indicated by X.

Comparing the chromatograms and electropherograms in Fig. 5A, B and C, some comments can be made. In all instances the salbutamol could be easily separated from other sample components without any pretreatment and the values obtained cover the labelled values, although for ITP a low current density had to be applied to obtain a complete separation from the matrix with sufficiently large zone lengths of salbutamol. For the Ventolin tablet, all the techniques show only the salbutamol component. For the Ventolin solution for intravenous infusion there is present at least one extra non-UV-absorbing sample component with a high effective mobility (probably sodium; see Fig. 5C), which could be present at about $t_{R,0}$ in the HPLC trace and is invisible in CZE. For the Ventolin syrup CZE shows only the salbutamol peak, ITP shows one non-UV-absorbing component and HPLC two extra UV-absorbing components. The time of analysis for HPLC and CZE is about 6 and 9 min [until electroosmotic flow (EOF) marker], respectively, and increases to about 30 min for the ITP analyses with samples containing a large amount of an unknown component X with a high effective mobility. An advantage of the electrophoretic methods is that the analysis can be stopped after the detection of the desired sample component, after which a new experiment can be started. A disadvantage of the HPLC method is the long equilibration time of the system and the fact that all components, including those not of interest, must pass the detector before a new run can be started.

In order to obtain more information about the

TABLE VI

AMOUNTS OF SALBUTAMOL (Q) IN VENTOLIN TABLETS, VENTOLIN SOLUTION FOR INTRAVENOUS INFUSION AND VENTOLIN SYRUP AND CALCULATED RELATIVE STANDARD DEVIATIONS (R.S.D.) DETERMINED WITH HPLC, CZE AND ITP

Method	Calibration graph			Tablet (4 mg per tablet)			Infusion (1 mg/ml)			Syrup (0.4 mg/ml)		
	CD	r	LOD	m	Q (mg per tablet)	R.S.D. (%)	m	Q (mg/ml)	R.S.D. (%)	m	Q (mg/ml)	R.S.D. (%)
HPLC												
214 nm	0.1	0.99985	1.76	3	4.05	1.02	3	1.04	0.81	3	0.40	1.03
214 nm	0.1	0.99977	1.80	3	4.00	1.04	3	1.02	0.83	3	0.40	1.03
CZE												
214 nm	0.1	0.99945	2.23	3	3.94	1.35	3	0.99	1.16	3	0.41	1.31
214 nm	0.1	0.99947	2.73	3	3.72	1.70	3	1.00	1.31	3	0.39	1.61
ITP												
UV	1	0.99933	37.0	3	3.96	2.20	3	0.90	3.06	3	0.34	2.62
Conductivity	1	0.99939	35.1	3	3.95	2.10	3	0.89	2.94	3	0.35	2.47
Conductivity	0.1	0.99931	3.12	3	4.07	1.77	3	1.00	1.91*	3	0.40	2.52*

TABLE VII

AMOUNTS OF TERBUTALINE SULPHATE (Q) IN BRICANYL TABLETS, BRICANYL AMPOULES FOR INJECTION AND BRICANYL SYRUP AND CALCULATED RELATIVE STANDARD DEVIATIONS (R.S.D.) DETERMINED WITH HPLC, CZE AND ITP

Method	Calibration graph			Tablet (5 mg per tablet)			Ampoules (0.5 mg/ml)			Syrup (0.3 mg/ml)		
	CD	r	LOD	m	Q (mg per tablet)	R.S.D. (%)	m	Q (mg/ml)	R.S.D. (%)	m	Q (mg/ml)	R.S.D. (%)
HPLC												
214 nm	0.1	0.99995	1.03	3	4.92	0.48	3	0.51	0.46	3	0.31	0.83
214 nm	0.1	0.99974	2.32	3	4.89	1.09	3	0.51	1.05	3	0.30	1.91
CZE												
214 nm	0.1	0.99895	4.62	3	4.68	2.28	3	0.52	2.05	3	0.30	3.89
214 nm	0.1	0.99952	3.11	3	4.67	1.54	3	0.50	1.43	3	0.30	2.62
ITP												
UV	1	0.99985	17.31	3	4.84	0.82	3	0.41	2.26	3	0.27	1.63
Conductivity	1	0.99990	14.01	3	4.87	0.66	3	0.42	1.78	3	0.27	1.32
Conductivity	0.1	0.99952	3.12	3	4.95	1.45	3	0.50	2.80*	3	0.31	2.55

TABLE VIII

AMOUNTS OF FENOTEROL HYDROBROMIDE (Q) IN BEROTEC TABLETS, BEROTEC ROTACAPS AND BEROTEC RESPIRATOR SOLUTION AND CALCULATED RELATIVE STANDARD DEVIATIONS (R.S.D.) DETERMINED WITH HPLC, CZE AND ITP

Method	Calibration graph			Tablet (2.5 mg per tablet)			Rotacaps (0.2 mg per capsule)			Respirator (5 mg/ml)		
	CD	r	LOD	m	Q (mg fenoterol per tablet)	R.S.D. (%)	m	Q (mg fenoterol hydrobromide per capsule)	R.S.D. (%)	m	Q (mg/ml fenoterol hydrobromide)	R.S.D. (%)
HPLC												
214 nm	0.1	0.99983	1.54	3	1.84	0.76	3	0.123	2.27	3	4.98	0.71
214 nm	0.1	0.99982	1.92	3	1.86	0.94	3	0.125	2.78	3	4.99	0.89
CZE												
214 nm	0.1	0.99986	1.70	3	1.88	0.82	3	0.121	2.57	3	4.89	0.80
214 nm	0.1	0.99935	3.64	3	1.97	1.68	3	0.117	5.73	3	4.91	1.71
ITP												
UV	1	0.99985	17.53	3	1.91	0.84	3	0.133	1.68	3	4.14	0.99
Conductivity	1	0.99994	10.94	3	1.89	0.53	3	0.136	1.02	3	4.24	0.60
Conductivity	0.1	0.99995	1.05	3	1.83	0.52	3	0.154	1.19	3	4.96	0.49

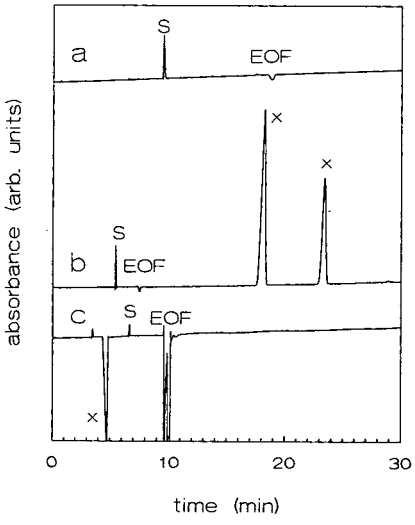

Fig. 6. Zone electropherograms of Ventolin syrup applying as background electrolyte (a) Tris–acetate (pH 5.0), (b) Tris–acetate (pH 5.0) after rinsing the capillary tube with 0.1 *M* KOH to obtain a higher velocity of the EOF and (c) histidine–acetate (pH 5.0). For further explanation, see text.

sample composition of Ventolin syrup, we performed an experiment with the background Tris–acetate at pH 5.0 (see Fig. 6a, where only one sample component salbutamol could be observed). After carefully rinsing the capillary tube with 0.1 *M* KOH, in order to obtain a higher velocity of the EOF, we repeated this separation (see Fig. 6b). With the high EOF also negative ions can be detected and two UV-absorbing negative ions are present in the electropherogram. We repeated this separation with the background electrolyte 0.01 *M* histidine adjusted to pH 5.0 by adding acetic acid. Non-UV-absorbing positive ions can now be made visible by indirect UV detection and in Fig. 6c it can clearly be seen that also a non-UV-absorbing positive ion with a high effective mobility is present in the sample solution.

Applying a background electrolyte with UV-absorbing ions affects the UV signal of salbutamol [13], as can be observed in Fig. 6c. Summarizing, the results indicate that the sample of Ventolin syrup contains at least four components, *viz.*, salbutamol, a non-UV-absorbing positively charged component and two UV-absorbing negatively charged components. We repeated the CZE experiments with several different background electrolytes at pH values from 4 to 8 and obtained good separations, showing that the choice of the background electrolyte is not critical.

Determination of terbutaline sulphate

For the determination of terbutaline sulphate we used Bricanyl tablets (labelled value 5 mg per tablet), Bricanyl ampoules for injection (labelled value 0.5 mg/ml) and Bricanyl syrup (labelled value 0.3 mg/ml). All results for terbutaline sulphate are given in Table VII.

As for salbutamol, terbutaline could easily be separated from all other sample components without any pretreatment. The values obtained for the Bricanyl tablet with CZE are slightly lower than those for the other methods. The liquid Bricanyl samples also contain some other components, visible with HPLC and ITP.

Determination of fenoterol hydrobromide

Fenoterol hydrobromide was determined in Berotec tablets (labelled value 2.5 mg of fenoterol per tablet; all measured values were recalculated to fenoterol per tablet), Berotec Rotacaps (labelled value 200 μg of fenoterol hydrobromide per capsule) and Berotec respirator solution (labelled value 5 mg of fenoterol hydrobromide/ml). All results are given in Table VIII.

The results of the respirator solution covered the labelled values. All methods show comparable values for the amount of fenoterol per tablet, although much lower than the labelled value. In the sample preparation, much of the tablet did not dissolve and probably fenoterol partially adsorbs on the insoluble components. In the comparison of the techniques we did not seek a sample preparation with 100% recovery.

A similar problem occurred with Berotec Rotacaps. In the isotachopherograms a slow UV-absorbing component could be observed migrating between fenoterol and the terminating hydrogen zone, probably in an enforced way [14,15]. This component is partially mixed with fenoterol. For this reason, the determined values are higher than those of HPLC and CZE. On diluting the sample solution, the determined amount of fenoterol increases because fenoterol is completely separated from the unknown sample component with high effective mobility and the zone is enlarged owing to

the presence of the unknown UV-absorbing sample component with low effective mobility.

CONCLUSIONS

In the analyses with ITP, CZE and HPLC for all components, a linear relationship between measured peak area or zone length and concentration of the components is obtained with regression coefficients better than about 0.999 and R.S.D. values up to about 2%. ITP and CZE seem to be more sensitive to irreproducibilities in, amongst others, the injected amounts, through which the repeatability of the HPLC values seem to be slightly better than those of ITP and CZE, although a disadvantage of the HPLC technique is the decreasing column quality.

In the comparison of the measured peak areas and zone lengths for the different techniques, regression lines were obtained with slopes of about 1 and nearly zero intercepts, validating these techniques. Application of the techniques to the determination of salbutamol, terbutaline sulphate and fenoterol hydrobromide in several pharmaceutical dosage forms gave comparable results covering the labelled values although, especially in the electrophoretic techniques, other sample components, present at high concentrations, can affect the separation. In CZE with high EOF, both anions and cations can be observed, in contrast to ITP. For most pharmaceuticals a very simple pretreatment is sufficient to obtain sample solutions. This procedure is, however, not adequate to desorb fenoterol from the Berotec tablets and Rotacaps. Because the aim of this investigation was to compare ITP, CZE and HPLC we did not seek a procedure to desorb the fenoterol completely. The combined application of these techniques provides more information about the sample composition.

In conclusion, it can be stated that CZE can compete with well established techniques such as HPLC and ITP for the determination of drugs in fairly simple matrices with regard to time of analysis and quantification, whereas the choice of the background electrolyte is not critical.

REFERENCES

1 M. J. Hutchings, J. D. Paull and D. J. Morgan, *J. Chromatogr.*, 277 (1983) 423.
2 N. Kurosawa, S. Morishima, E. Owada and K. Ito, *J. Chromatogr.*, 305 (1984) 485.
3 V. Das Gupta, *J. Liq. Chromatogr.*, 9 (1986) 1065.
4 S. Ray and A. Bandyopadhyay, *Indian Drugs*, 27 (1990) 313.
5 J. E. Kountourellis and C. Markopoulou, *J. Liq. Chromatogr.*, 12 (1989) 3279.
6 D. A. Williams, E. Y. Y. Fung and D. W. Newton, *J. Pharm. Sci.*, 78 (1982) 956.
7 F. M. Everaerts, J. L. Beckers and Th. P. E. M. Verheggen, *Isotachophoresis, Theory, Instrumentation and Applications*, Elsevier, Amsterdam, 1976.
8 J. L. Beckers, F. M. Everaerts and M. T. Ackermans, *J. Chromatogr.*, 537 (1991) 407.
9 J. C. Miller and J. N. Miller, *Statistics for Analytical Chemistry*, Ellis Horwood, Chichester, 1984.
10 J. L. Beckers and F. M. Everaerts, *J. Chromatogr.*, 508 (1990) 3.
11 J. L. Beckers and F. M. Everaerts, *J. Chromatogr.*, 508 (1990) 19.
12 J. L. Beckers and F. M. Everaerts, *J. Chromatogr.*, 470 (1989) 277.
13 M. T. Ackermans, F. M. Everaerts and J. L. Beckers, *J. Chromatogr.*, 549 (1991) 345.
14 P. Gebauer and P. Boček, *J. Chromatogr.*, 267 (1983) 49.
15 P. Boček and P. Gebauer, *Electrophoresis*, 5 (1984) 338.

Journal of Chromatography, 590 (1992) 354–358
Elsevier Science Publishers B.V., Amsterdam

CHROM. 23 832

Short Communication

Determination of the enantiomeric composition of samples of cocaine by normal-phase high-performance liquid chromatography with UV detection

Robert R. MacGregor*, Joanna S. Fowler and Alfred P. Wolf

Department of Chemistry, Brookhaven National Laboratory, Upton, NY 11973 (USA)

(First received September 19th, 1991; revised manuscript received October 29th, 1991)

ABSTRACT

A high-performance liquid chromatographic method has been developed for the quantitation of the enantiomers of cocaine. Mixtures of the naturally occurring (−)-cocaine and synthetically produced (+)-cocaïne were hydrolyzed in water to (+) and (−)-benzoyl ecgonine. Esterification with an optically pure 2-octanol resulted in diastereoisomers that could be separated on bare silica gel using an acetonitrile–aqueous ammonium phosphate mobile phase.

INTRODUCTION

(−)-Cocaine is the naturally occurring alkaloid produced by the coca plant (erythroxylon coca). In 1923 a method for the synthesis of (±)-cocaine was published [1]. The racemic mixture was resolved into the pure (+) and (−) isomers by crystallizations with tartaric acid. Modifications [2,3] of this method and a new synthetic sequence [4] have been reported.

Since recent studies [5–8] indicate that the pharmacology and metabolism of the (+)-isomer may be very different from the natural (−)-cocaine, it would be useful to have a convenient method for the quantitative determination of the enantiomeric composition of small samples of cocaine. A high-performance liquid chromatographic (HPLC) separation of (±)-cocaine on two 25-cm β-cyclodextrin columns in series requiring a 90-min elution has been reported [9].

Eskes [10] developed a thin-layer chromatographic (TLC) method for the detection of each enantiomer of cocaine. Samples of cocaine were hydrolyzed with 2 *M* hydrochloric acid to ecgonine which was then esterified with (+)- or (−)-2-octanol by the action of benzenesulfonyl chloride in pyridine [11]. The resulting diastereomers could be separated on silica gel TLC.

It was felt that a similar procedure which cleaved only the methyl ester and left the benzoyl ester intact would allow convenient detection with a UV monitor at 254 nm. Since it is known that cocaine is hydrolyzed by neutral water to benzoyl ecgonine [12], this seemed feasible. As the use of bare silica gel with aqueous eluents for the separation of basic lipophilic amines is well known [13,14], we investigated the use of such a system.

0021-9673/92/$05.00

MATERIALS AND METHODS

Instrumentation

HPLC was performed with a Perkin-Elmer (Norwalk, CT, USA) series 3B pump, a Rheodyne (Cotati, CA, USA) 7125 injection valve fitted with a 2.0-ml loop, a Phenomenex (Rancho Palos Verdes, CA, USA) Spherisorb 5 silica column (250 × 4.6 mm I.D.) and a Knauer (Dusseldorf, Germany) variable-wavelength UV detector operated at 254 nm. Integrations were performed by a Hewlett-Packard (Palo Alto, CA, USA) 3390A integrator at an attenuation of 1 or 2. The solvent system was acetonitrile–0.001 *M* ammonium phosphate, dibasic (pH 7.4) (75:25) with a flow-rate of 2 ml/min.

Materials

(−)-Benzoyl ecgonine (BE), and (+)- and (−)-cocaine (COC) were kindly provided by Research Triangle Institute (Research Triangle Park, NC, USA). Benzenesulfonyl chloride and *S*-(+)- and *R*-(−)-2-octanol (99% optical purity) were obtained from Aldrich (Milwaukee, WI, USA). Pyridine was distilled from BaO and stored over KOH pellets. Reactions were carried out in 1-ml V-vials with PTFE-faced screwcaps (Wheaton, Millville, NJ, USA).

Procedure

COC (0.5–1 mg; 0.0015–0.003 mmol) and 200 μl of water in a tightly capped reaction vial were heated in an oil bath at 130°C for 20 to 30 min. The cap was removed and heating continued under a stream of nitrogen. When the water had evaporated, two 200-μl portions of acetonitrile were added and blown dry.

After the vial had cooled to room temperature, 50 μl of pyridine, 5 μl (0.032 mmol) of the appropriate 2-octanol and 3 μl (0.023 mmol) of benzenesulfonyl chloride were added. After 15 min at ambient temperature, the pyridine was evaporated under a stream of nitrogen with gentle warming. To the residue were added 200 μl of acetonitrile and 1 μl of this solution was chromatographed. In the event of incomplete esterification, the acetonitrile was evaporated and the derivatization procedure repeated with the residue.

When the progress of the esterification was monitored, 5-μl aliquots of the pyridine solution were removed and diluted with 200 μl of acetonitrile. These solutions were evaporated and the residue redissolved in 100 μl of acetonitrile and chromatographed.

To analyze mixtures of (+)- and (−)-COC of known composition, standard solutions of each were prepared in acetonitrile and appropriate volumes of each were added to the reaction vial and blown to dryness before the hydrolysis step.

The relative rates of reaction of the enantiomers of BE with the enantiomers of 2-octanol were determined by reacting each pure COC isomer with an excess of racemic alcohol. The relative amounts of the two diastereomeric esters formed is proportional to relative rates of reaction of each of the alcohols with the isomerically pure COC.

RESULTS AND DISCUSSION

Under the conditions described 75–85% of the COC was hydrolyzed to BE. As this step is not enantioselective, there was no need to take the hydrolysis to completion. If heating was continued much after the evaporation of water, decomposition or sublimation resulted in a significant loss of mass.

The esterification of BE using the method of Eskes [9] was rapid and quantitative. In cases where the reaction was incomplete, it was probably the result of the presence of moisture rather than insufficient reaction time. As would be expected, the enantiomers of BE reacted with the enantiomers of 2-octanol at different rates. The esterification of (−)-BE with (−)-2-octanol was 1.4 times as fast as with (+)-2-octanol. With (+)-BE the ratio of (+/+) to (+/−) was also 1.4. Thus for an accurate determination of the enantiomeric composition of the BE produced by the hydrolysis of COC samples, it is necessary of react all of the BE with enantiomerically pure alcohol, otherwise the faster reacting enantiomer will appear in erroneously high proportion.

The diastereometric esters from BE and 2-octanol had nearly baseline separation with the (+)-BE-(−)-2-octyl ester (+/−), or its enantiomer (−/+), eluting 1 min before (+)-BE-(+)-2-octyl ester (+/+) or its enantiomer (−/−) (Fig. 1 shows the relevant portion of the chromatogram). The resolution (the distance between the peak centers divided by

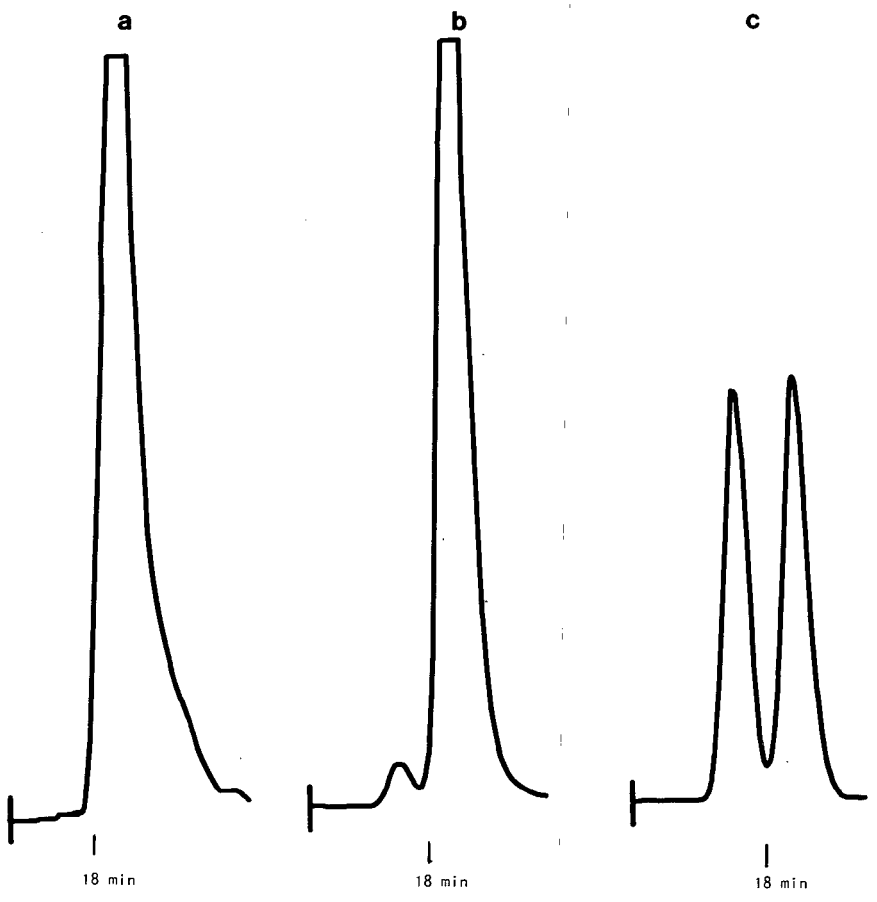

Fig. 1. (−)-2-Octyl esters from reaction with benzoyl ecgonine mixtures resulting from the hydrolysis of (a) (−)-COC, (b) 95% (−)-COC, 5% (+)-COC and (c) 50% (−)-COC, 50% (+)-COC.

the average peak width) of the diastereometric esters was 1.1 and the separation factor was 1.06. The relationships between the actual composition of mixtures of (+)- and (−)-COC and the integrated peak areas of their 2-octyl ester derivatives are given in Fig. 2. As can be seen from Fig. 2, a calibration curve should be obtained in each case as the integrator processes the leading peak (○) slightly differently than it does the trailing peak (●). Even without taking this systematic variation into account the correlation coefficient for the data in Fig. 2 was 0.997. Multiple injections of a solution showed a standard deviation of 1%.

Fig. 3 shows a typical chromatogram with retention times.

The commercial availability of both *S*-(+)- and *R*-(−)-2-octanol allows the enantiomeric analysis to be tailored to cause the minor component to elute first for greater sensitivity. Analyzing for contamination by (−)-COC in a preparation of (+)-COC by derivatization with (+)-2-octanol results in the elution of the minor component before that of the major one, making it easier to more accurately determine optical purities when small amounts of the minor isomer are present. While no attempt was made to optimize the sensitivity of this assay, it was capable of quantitating a 5% enantiomeric contamination in a 500 μg sample of cocaine.

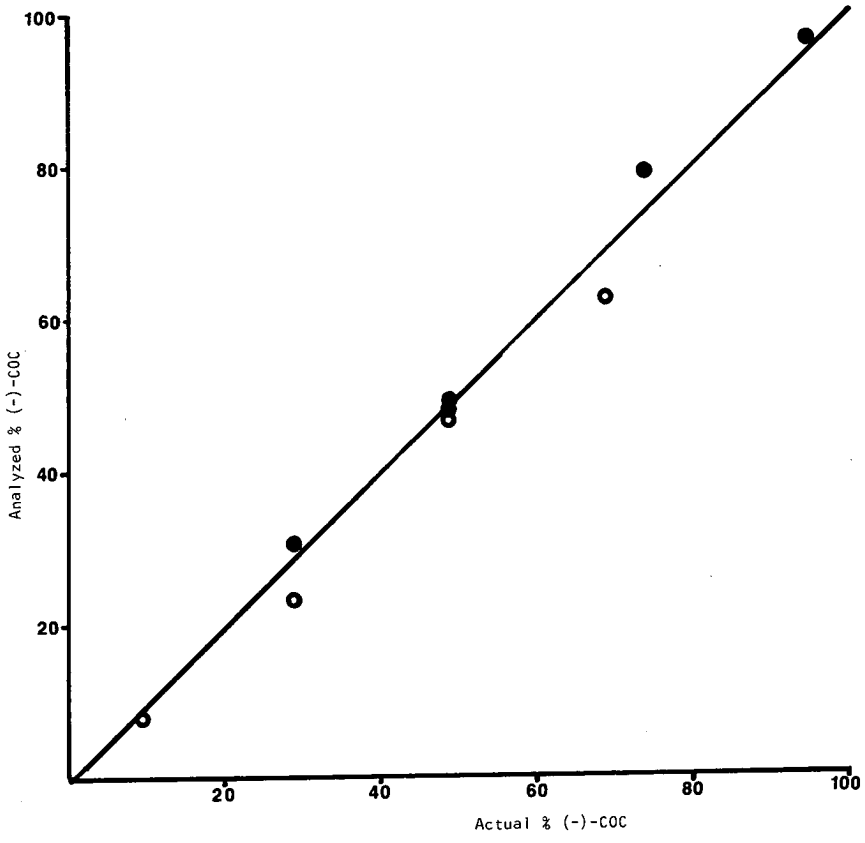

Fig. 2. Comparison of the analysis of enantiomeric purity of (−)-COC versus the actual composition of (±) mixtures. Reaction with (●) (−)-2-octanol and (○) (+)-2-octanol.

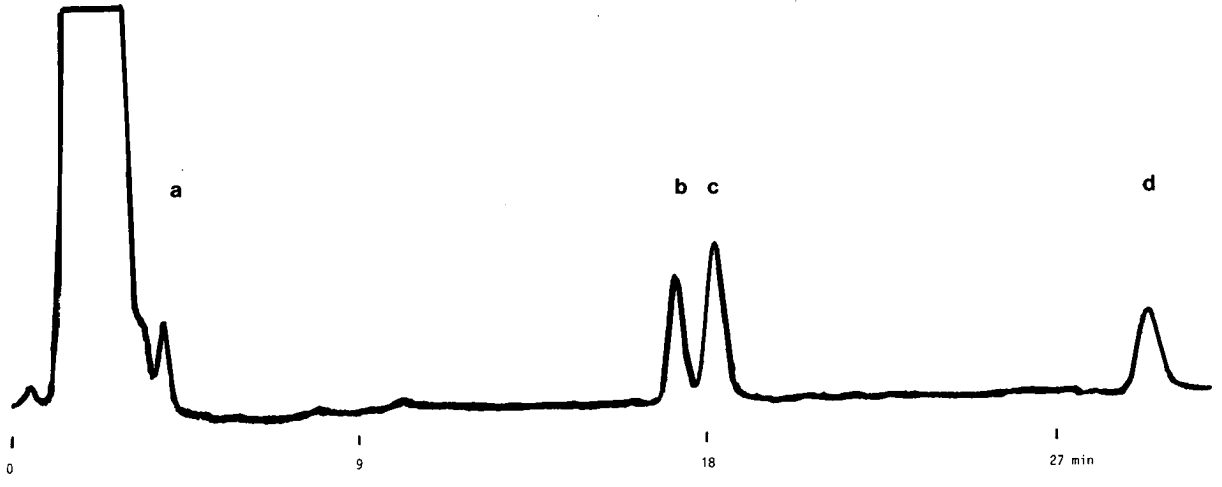

Fig. 3. Chromatogram of the reaction mixture of benzoyl ecgonine, from the hydrolysis of (−)-cocaine, and racemic 2-octanol after 5 min reaction. Peaks: a = (−)-Benzoyl ecgonine (3.8 min); b = (−)-benzoyl ecgonine-(+)-2-octyl ester (17.6 min); c = (−)-benzoyl ecgonine-(−)-2-octyl ester (18.6 min); d = (−)-cocaine (30.2 min).

ACKNOWLEDGEMENTS

This research was carried out at Brookhaven National Laboratory under contract with the US Department of Energy and supported by its Office of Health and Environmental Research and also supported by National Institute of Drug Abuse Grant DA06278. We thank the Research Triangle Institute for providing samples of (+)- and (−)-cocaine and of benzoyl ecgonine.

REFERENCES

1 R. Willstatter, O. Wolfes and H. Mader, *Ann.*, 434 (1923) 111.
2 A. H. Lewin, T. Naseree and F. I. Carroll, *J. Heterocyclic Chem.*, 24 (1987) 19.
3 J. F. Casale, *Forensic Sci. Int.*, 33 (1987) 275.
4 J. J. Tufariello, G. B. Mullen, J. J. Tegeler, E. J. Trybulski, S. C. Wong and S. A. Ali, *J. Am. Chem. Soc.*, 101 (1979) 2435.
5 R. D. Spealman, R. T. Kelleher and S. R. Goldberg, *J. Pharmacol. Exp. Ther.*, 225 (1983) 509.
6 M. C. Ritz, R. J. Lamb, S. R. Goldberg and M. J. Kuhar, *Science, (Washington, D.C.)*, 237 (1987) 1219.
7 J. Sharkey, M. C. Ritz, J. A. Schenden, R. C. Hanson and M. J. Kuhar, *J. Pharmacol. Exp. Ther.*, 246 (1988) 1048.
8 S. J. Gatley, R. R. MacGregor, J. S. Fowler, A. P. Wolf, S. J. Dewey and D. J. Schlyer, *J. Neurochem.*, 54 (1990) 720.
9 D. W. Armstrong, S. H. Han and Y. I. Han, *Anal. Biochem.*, 167 (1987) 261.
10 D. Eskes, *J. Chromatogr.*, 152 (1978) 589.
11 J. H. Brewster and C. J. Ciotti, Jr., *J. Am. Chem. Soc.*, 77 (1955) 6214.
12 S. P. Findlay, *J. Am. Chem. Soc.*, 76 (1954) 2855.
13 B. A. Bidlingmeyer, J. K. Del Rios and J. Korpi, *Anal. Chem.*, 54 (1982) 442.
14 R. J. Flanagan and I. Jane, *J. Chromatogr.*, 323 (1985) 173.

Journal of Chromatography, 590 (1992) 359–363
Elsevier Science Publishers B.V., Amsterdam

CHROM. 23 804

Short Communication

Ultramicrodetermination of cyanocobalamin in elemental diet by solid-phase extraction and high-performance liquid chromatography with visible detection

Hiroshi Iwase

Ajinomoto Co., Inc., Kawasaki Factory, 1–1 Suzuki-cho, Kawasaki-ku, Kawasaki (Japan)

(First received May 31st, 1991; revised manuscript received October 15th, 1991)

ABSTRACT

The ultramicrodetermination of cyanocobalamin (9 ng/g) in elemental diet containing 46 kinds of compounds, with concentrations at least $50–10^6$ times higher than that of cyanocobalamin, was performed by Sep-Pak C_{18} purification and concentration of cyanocobalamin followed by HPLC with detection at 550 nm. The method is simple, rapid, sensitive and reproducible. The calibration graph was linear in the range of 0–0.2 μg. The recovery of cyanocobalamin was over 95% by the standard addition method. There was good agreement between the cyanocobalamin concentrations indicated and found.

INTRODUCTION

Cyanocobalamin (vitamin B_{12}) is widely distributed and plays an important role in animal and plant metabolisms. Ultramicro amouns of cyanocobalamin are contained in foods, foodstuffs and drugs. It is necessary to monitor the intermediates and finished products of drugs for process control and quality control purposes for good manufacturing practice, hence simple, rapid, sensitive and reproducible analytical methods are required.

Cyanocobalamin has been determined by spectrophotometry [1,2], microbiological method [3] and high-performance liquid chromatography (HPLC) [4–10]. Spectrophotometry is not suitable for complex sample matrices. Microbiological methods have generally been used for the routine determination of vitamins. Ujiue *et al.* [3] reported the analysis of samples of foods, foodstuffs and drugs for the content of cyanocobalamin by a microbiological method. However, this method requires culture of the tissue and preservation of its strain. Further, the procedure of sample preparation is tedious and the incubation is time consuming.

Analyses for many kinds of vitamins have been investigated by HPLC [4–15]. The separation of cyanocobalamin and its analogues has been reported by many workers [4–10]. However, HPLC could not be used for the routine ultramicrodetermination of cyanocobalamin, because experimental conditions for the sample preparation such as the concentration of ultramicro amounts of cyanocobalamin and removal of interferences caused by the complex sample matrix were not investigated in detail.

This paper deals with the routine ultramicrodetermination of cyanocobalamin (9 ng/g) in elemental diet (commercial name Elental, Ajinomoto, Kawasaki, Japan) by HPLC. Elental drug is in powder form to be dissolved prior to use, and it contains 46

0021-9673/92/$05.00

kinds of compounds (*e.g.*, amino acids, vitamins, organic acids, soybean oil, dextrin, minerals), the concentration of which is at least $50–10^6$ times higher than that of cyanocobalamin [16]. A simple sample preparation was carried out, using a Sep-Pak C_{18} cartridge to concentrate the ultramicro amount of cyanocobalamin. Routine ultramicrodetermination of cyanocobalamin was performed by using a Sep-Pak C_{18} cartridge followed by HPLC with visible detection at 550 nm, which is specific to cyanocobalamin. This paper also describes the ultramicrodetermination of cyanocobalamin of further two elemental diets, Elental P for paediatrics and Hepan ED for hepatic failure.

EXPERIMENTAL

Reagents and materials

Cyanocobalamin was of Japanese Pharmacopoeia Standard. Sep-Pak C_{18} cartridges were purchased from Waters Assoc. (Milford, MA, USA). Other reagents were all of analytical-reagent or HPLC grade.

Apparatus and conditions

A Model 655 A-11 high-performance liquid chromatograph (Hitachi, Tokyo, Japan) equipped with a Uvidec 100-IV detector (JASCO, Tokyo, Japan) set at 550 nm was used. The samples were applied with a Rheodyne Model 7125 sample loop injector with an effective volume of 2 ml. A 25 × 0.46 cm I.D. Column of Capcellpak C_{18} (5 μm) (Shiseido, Tokyo, Japan) was used under ambient conditions. Water–acetonitrile (87:13) was used as the mobile phase at a flow-rate was 0.6 ml/min. A Model UV-2100 variable-wavelength UV recording spectrophotometer (Shimadzu, Kyoto, Japan) was used for the absorption spectra.

Sample preparation

The Sep-Pak C_{18} cartridge was washed with 5 ml of acetonitrile and then with 10 ml of deionized water prior to use.

To a solution of Elental (20 g) dissolved completely in deionized water (60 ml) on a water-bath at 50°C was added sodium chloride (10 g). After this solution had been allowed to stand at room temperature for 30 min, it was diluted accurately to 100 ml with deionized water and then this solution was extracted with hexane (10 ml) for 3 min to remove oils. This aqueous layer was passed through a Sep-Pak C_{18} cartridge and then the cartridge was washed with 50% acetonitrile (8 ml). The eluate was concentrated to dryness in a water-bath at 50°C *in vacuo*. Concentrates were dissolved accurately in deionized water (4 ml) and an aliquot (2 ml) was injected into the chromatograph.

Elental P and Hepan ED were also prepared in the same manner as described for Elental.

RESULTS AND DISCUSSION

Stability of cyanocobalamin in aqueous solution at 50°C

As a preliminary test, the stability of cyanocobalamin in aqueous solution was examined periodically, because the sample was heated at 50°C for complete dissolution. Cyanocobalamin was stable in aqueous solution at 50°C for 1 h. Thus it was found

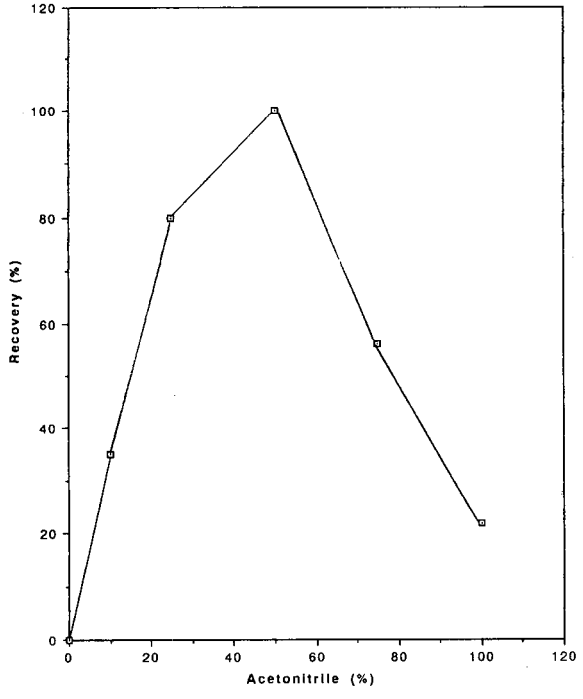

Fig. 1. Variation of recovery with acetonitrile content in acetonitrile–water eluent. A 100-ml volume of deionized water containing cyanocobalamin (1.8 ng/ml) was passed through a Sep-Pak C_{18} cartridge and cyanocobalamin was eluted with 8 ml of acetonitrile solution.

that cyanocobalamin was stable in this sample preparation.

Effect of acetonitrile concentration of elution of cyanocobalamin using a Sep-Pak C_{18} cartridge

Using a Sep-Pak C_{18} cartridge, optimum elution and retention characteristics of a cyanocobalamin standard were determined. An acetonitrile–water mobile phase was examined for the complete elution of cyanocobalamin on a Sep-Pak C_{18} cartridge. The optimum elution of cyanocobalamin achieved with acetonitrile–water (50:50) (Fig. 1). Cyanocobalamin in the aqueous fraction (unbound) was examined for the complete retention of cyanocobalamin on a Sep-Pak C_{18} cartridge. Cyanocobalamin was not detected in the aqueous fraction. From the above result, cyanocobalamin in aqueous solution was completely retentioned on one Sep-Pak C_{18} cartridge and eluted with acetonitrile–water (50:50).

Chromatography

Not only cyanocobalamin but also other vitamins, amino acids and organic acids absorb in the UV region. Cyanocobalamin shows UV absorbance at 260 and 360 nm and visible absorbance at 550 nm, that at 550 nm being specific to cyanocobalamin. Thiamine, riboflavin, ascorbic acid, nicotinamide, pyridoxine, folic acid, tyrosine, phenylalanine and tryptophan have absorbance at 260 nm and several compounds, such as folic acid and riboflavin, have absorbance at 360 nm.

Many overloading peaks were observed on the chromatograms at 260 and 360 nm, and cyanocobalamin could not be identified at 260 and 360 nm. Large amounts of co-existing compounds such as other vitamins and amino acids, with concentrations at least 50–10^6 times higher than that of cyanocobalamin, were observed after the retention time of cyanocobalamin, and it took about 50–60 min to obtain a stable baseline. Hence, monitoring at 260 or 360 nm was not suitable for the ultramicrodetermination of cyanocobalamin. On the other hand, a sharp and reproducible peak [relative standard deviation (R.S.D.) 1.5%] of cyanocobalamin in the sample treated with a Sep-Pak C_{18} cartridge and monitoring at 550 nm was observed with sufficient intensity (Fig. 2, *ca.* 9 ng/g), the baseline was stable and the retention time was about 20 min, irrespective of the large injection volume (2 ml). It was necessary to inject 2 ml of sample solution because cyanocobalamin was present in the sample in ultramicro amounts. As a possible mechanism of this method, sample enrichment at the top of column might be considered. A similar technique has been used in ion chromatography.

However, cyanocobalamin in an untreated sample was not detected (Fig. 3), owing to the presence of unknown peaks and a lack of sensitivity for cyanocobalamin. Hence, for the ultramicrodetermination of cyanocobalamin in complex mixtures, the procedure used here, involving Sep-Pak C_{18} purification and concentration of cyanocobalamin in Elental followed by HPLC with detection at 550 nm, seems appropriate.

From the above results, it seems that ultramicro amounts of cyanocobalamin were completely re-

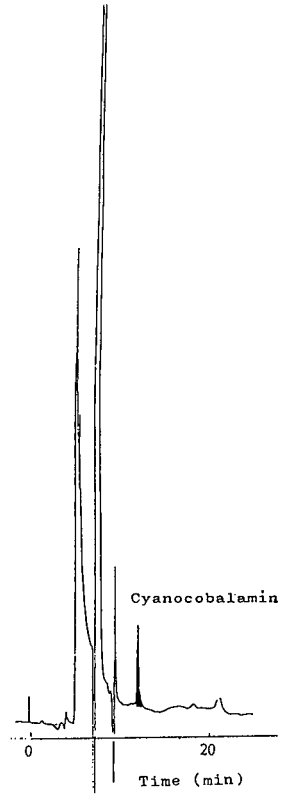

Fig. 2. Chromatogram of cyanocobalamin (treated wth a Sep-Pak C_{18} cartridge) with detection at 550 nm. Amount of cyanocobalamin injected, 0.09 μg in 2 ml.

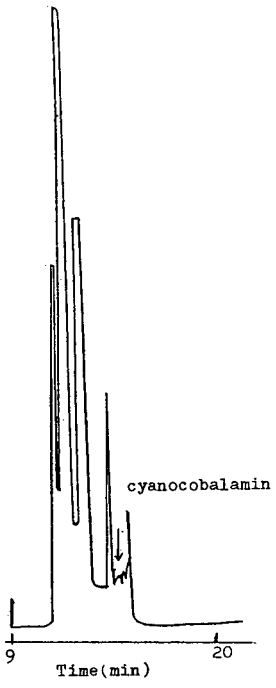

Fig. 3. Chromatogram of cyanocobalamin (not treated with Sep-Pak C_{18}) with detection at 550 nm. Amount of cyanocobalamin injected, 3.6 ng in 2 ml.

tained and concentrated on the Sep-Pak C_{18} cartridge, despite the large injection volume (100 ml) without interference from other compounds. Despite the large injection volume (2 ml), cyanocobalamin was concentrated on a Capcellpak C_{18} column, separated and detected at 550 nm without interference from any other compounds.

TABLE I

RECOVERIES OF CYANOCOBALAMIN ADDED TO ELENTAL

According to the label Elental contains 0.9 μg of cyanocobalamin per 100 g.

Cyanocobalamin (μg per 100 g)		Recovery (%)
Added	Found	
0	0.86[a]	–
0.22	1.07	95.5
0.45	1.29	95.6
0.90	1.75	98.9
1.80	2.63	97.8

[a] R.S.D. = 1.5% (n = 7) with no addition of cyanocobalamin.

Determination of cyanocobalamin

The calibration graph was linear ($y = 7.7x$) in the range 0–0.2 μg. The results in Table I show that recovery of cyanocobalamin was over 95% by the standard addition method.

The results in Table II show that the analytical data for cyanocobalamin in Elental, Elental P and Hepan ED were excellent without an internal standard. Jansen and De Kleijn [10] reported the assay of cyanocobalamin in pharmaceutical preparations using an internal standard, Co-α-(5-hydroxybenzimidazoyl)-Co-β-cyanocobamide, which was not commercialy available. If such an an internal standard were available, it would be better to use it in routine analyses.

TABLE II

ANALYTICAL DATA FOR CYANOCOBALAMIN IN THREE ELEMENTAL DIETS

Diet	Concentration indicated (μg per 100 g)	Analytical data result (μg per 100 g)	Recovery (%)
Elental	0.9	0.86	95.6
		0.86	95.6
		0.87	96.7
Elental P	1.5	1.45	96.7
		1.44	96.0
		1.43	95.3
Hepan ED	2.7	2.61	96.7
		2.59	95.9
		2.57	95.2

There was good agreement between the cyanocobalamin concentrations indicated and found. This method was suitable for the routine ultramicrodetermination of cyanocobalamin in Elental, Elental P and Hepan ED because it is simple, rapid (retention time 20 min), sensitive, reproducible (R.S.D. 1.5%) and the recovery was over 95%. This method may be suitable for the ultramicrodetermination of cyanocobalamin in body fluids such as human plasma or serum, and this is currently under investigation.

REFERENCES

1 *The United States Pharmacopeia, XXII Revision*, US Pharmacopeial Convention, Rockville, MD, 1990, p. 363.
2 *The Pharmacopoeia of Japan*, Hirokawa Publishing, Tokyo, 11th ed., 1986, p. C-847.
3 T. Ujiue, M. Mori, T. Ito, Y. Iida, M. Mabuchi and K. Okamura, *Vitamins*, 63 (1989) 87.
4 E. P. Frenkel, R. L. Kitchen and R. Prough, *J. Chromatogr.*, 174 (1979) 393.
5 T. Hattori, N. Asakawa, M. Ueyama, A. Shinoda and Y. Miyake, *Yakugaku Zasshi*, 100 (1980) 386.
6 D. W. Jacobsen, R. Green, E. V. Quadros and Y. D. Montejano, *Anal. Biochem.*, 120 (1982) 394.
7 M. Binder, J. F. Kolhouse, K. C. VanHorne and R. H. Allen, *Anal. Biochem.*, 125 (1982) 253.
8 W. B. Whitman and R. S. Wolfe, *Anal. Biochem.*, 137 (1984) 261.
9 S. H. Ford, J. Gallery, A. Nichols and M. Shambee, *J. Chromatogr.*, 537 (1991) 2356.
10 C. C. Jansen and J. P. de Kleijn, *J. Chromatogr. Sci.*, 28 (1990) 42.
11 R. M. Kothari and M. W. Taylor, *J. Chromatogr.*, 247 (1982) 187.
12 P. Wimalasiri and R. B. H. Wills, *J. Chromatogr.*, 318 (1985) 412.
13 M. Yoshida and K. Iriyama, *J. Liq. Chromatogr.*, 9 (1985) 177.
14 K. Hayakawa and J. Oizumi, *J. Chromatogr.*, 413 (1987) 247.
15 T. Yoshida, A. Uetake, C. Nakai, N. Nimura and T. Kinoshita, *J. Chromatogr.*, 456 (1988) 421.
16 S. Ogoshi (Editor), *Elental Diet*, Nankodo, Tokyo, 1983.

Journal of Chromatography, 590 (1992) 364–368
Elsevier Science Publishers B.V., Amsterdam

CHROM. 23 802

Short Communication

Determination of cefixime and its metabolites by high-performance capillary electrophoresis

Susumu Honda*

Faculty of Pharmaceutical Sciences and Pharmaceutical Research and Technology Institute, Kinki University, Kowakae, Higashi-osaka (Japan)

Atsushi Taga and Kazuaki Kakehi

Faculty of Pharmaceutical Sciences, Kinki University, Kowakae, Higashi-osaka (Japan)

Shigetaka Koda and Yoshihiko Okamoto

Research Laboratories, Fujisawa Pharmaceutical Company, Kashima, Yodogawa-ku, Osaka (Japan)

(First received July 4th, 1991; revised manuscript received October 14th, 1991)

ABSTRACT

Cefixime (CX), an oral cephalosporin antibiotic, and its metabolites in human digestive organs were separated by various modes of high-performance capillary electrophoresis. The zone electrophoresis mode in phosphate buffer (pH 6.8) containing 3-[(3-cholamidopropyl)dimethylammonio]-1-propanesulphonate gave the best separation, permitting the complete resolution of CX and all of five metabolites. On the other hand, the plain zone electrophoresis mode in phosphate buffer (pH 6.8) offered a simple procedure for the direct determination of urinary CX concentration using intact urine samples.

INTRODUCTION

High-performance capillary electrophoresis (HPCE) is now widely applied in analyses of biological substances, especially oligo- and polynucleotides (*e.g.*, [1]), and applications in other fields, including drugs and metabolites, are developing.

Cefixime, (6*R*,7*R*)-7-[(*Z*)-2-(2-amino-4-thiazolyl)-2-(carboxymethoxyimino)acetamido]-8-oxo-3-vinyl-5-thia-1-azabicyclo[4.2.0]oct-2-ene-2-carboxylic acid, is a cephalosporin antibiotic for oral administration, having a broad spectrum for Gram-negative bacteria. It is known to be metabolized in human digestive organs to give compounds as shown in Fig. 1, by the action of bacterial enzymes.

CX and its metabolites, M1–M5, have a common characteristic feature that they all have carboxyl groups(s), and hence are hydrophilic. For this reason, they cannot be extracted from biological fluids by solvent extraction. From an analytical viewpoint, the strong hydrophilicity also hampers their separation by liquid chromatography in the direct partitioning mode. Separation was barely achieved by reversed-phase partitioning with ion pairing to the tetrabutylammonium ion in the mobile phase [2]. In this paper, we propose an alternative method

0021-9673/92/$05.00

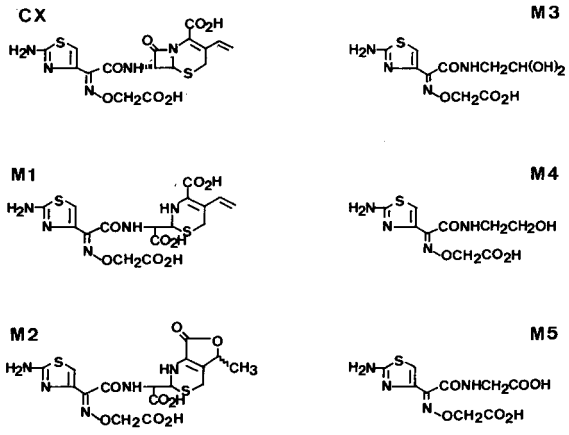

Fig. 1. Structures of cefixime (CX) and its metabolites (M1–M5).

based on high-performance capillary electrophoresis (HPCE).

EXPERIMENTAL

Chemicals

CX and its metabolites were prepared by Fujisawa Pharmaceutical (Osaka, Japan) and used as received. 3-[(3-Cholamidopropyl)dimethylammonio]-1-propanesulphonate (CPDAPS) and 1,5-dimethyl-1,5-diazaundecamethylene polymethobromide (polybrene or hexadimethrine bromide) were obtained from Sigma (St. Louis, MO, USA) and Aldrich (Milwaukee, WI, USA), respectively. All other chemicals were purchased from Wako (Osaka, Japan).

HPCE

HPCE was performed by using a Model 270 A capillary electrophoresis system (Applied Biosystems, San Jose, CA, USA), equipped with an automated vacuum injector, a UV detector, a thermostated bath and a data processor. A capillary tube of fused silica (50 μm I.D., 375 μm O.D.) was used for all modes of HPCE, and detection was carried out in the on-column mode at the 22-cm position from the outlet. At this position of the tube the polyimide coating was removed and the transparent portion was fixed on the detector block. The compositions and pH values of the carriers are given in the figure captions. The electric current was *ca.* 30 μA in all systems. Sample solutions were introduced into the tube by suction under a weak vacuum for 1.5 s.

RESULTS AND DISCUSSION

Separation modes

The basic mode of separation in HPCE is zone electrophoresis, but other modes can be realized simply by dissolving additives in the carrier. In this work the separation of CX and its metabolites was examined using the zone electrophoresis and electrokinetic modes under various conditions.

Zone electrophoresis mode. In the zone electrophoresis mode separation is based on the difference in electric charge relative to molecular size among the sample components. The magnitude of the electric charge is dependent on the number of carboxyl groups. It also depends on the pH of the carrier, because the dissociation of the carboxyl group is controlled by pH. Therefore, separations at various pH values were compared using 50 m*M* phosphate buffer. The best separation was achieved at pH 6.8. Fig. 2 shows the electropherogram obtained under these conditions utilizing a capillary tube of fused silica.

A mixture of CX and its metabolites was introduced from the anodic end of the tube. Electroosmotic flow was toward the cathode and the electrophoretic attraction of the sample components to the anode was at lower velocities than that of electroosmosis. The metabolites except M3 and M4 were completely separated from each other; the peaks of M3 and M4 partially overlapped, because their structures are only slightly different from each other (in the side-chain at the 5-position of the thiazole ring). Metabolite M2 was unfortunately unresolved from CX. CA denotes cinnamic acid added as an internal standard, which was well separated from CX and the metabolites.

Suppression of electroosmotic flow by addition of hydroxypropylcellulose at a concentration of 0.02% and introduction of the sample from the cathodic end of the tube resulted in the appearance of peaks in the reverse order, but the separations of the M3–M4 and M2–CX pairs were not improved (Fig. 3).

Addition of CPDAPS to 20 m*M* phosphate buffer (pH 6.8) at a low concentration of 0.15% (w/v)

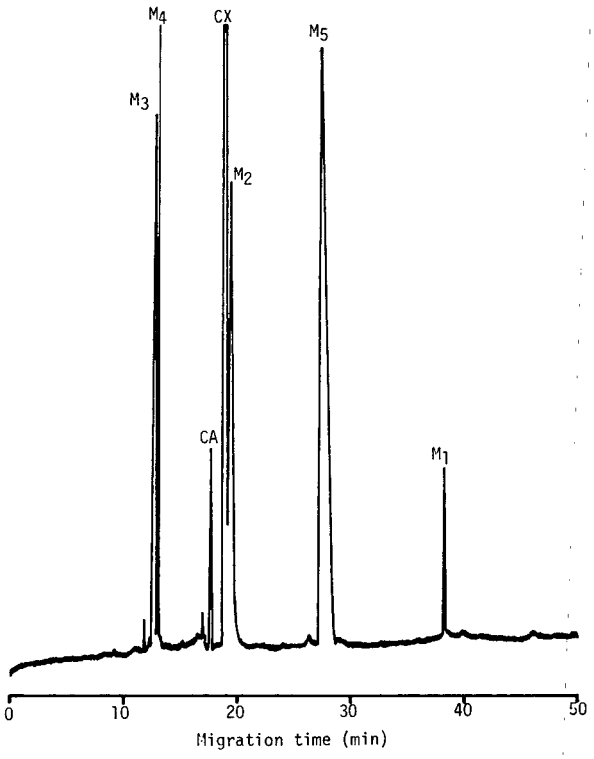

Fig. 2. Separation of CX and its metabolites by plain zone electrophoresis with electroosmotic flow. Capillary, fused silica (72 cm × 50 μm I.D.); carrier, 50 m*M* phosphate buffer (pH 6.8); applied voltage, 15 kV; detection, UV absorption at 280 nm; sample solution, aqueous solution containing CX, M1, M2, M3, M4, M5 and cinnamic acid (CA) (internal standard); sample concentration, $1.0 \cdot 10^{-3}$ *M* (CX, M1, M2, M3, and M4), $1.0 \cdot 10^{-4}$ *M* (M5) and $5.0 \cdot 10^{-4}$ *M* (CA). The sample solution was introduced from the anodic end of the tube.

caused a drastic change in the electropherogram; all components gave their peaks in 15 min and separations of the M3–M4 and M2–CX pairs were not so good. In addition, the migration time of M1 became especially shorter, and as a result the peaks of M1 and M5 partially overlapped (electropherogram not shown). However, addition of methanol to this system at a concentration of 20% (v/v) resulted in retardation of the peaks and an improvement in the separation of the M3–M4, M2–CX and M1–M5 pairs compared with those in the carrier not containing methanol (Fig. 4).

In the zone electrophoresis mode, addition of methanol generally causes retardation and improved separation of peaks, because the degree of hydration of the component ions is reduced and accordingly the effective sizes of the ions are decreased (*e.g.*, ref. 5). The phenomenon observed in Fig. 4 is

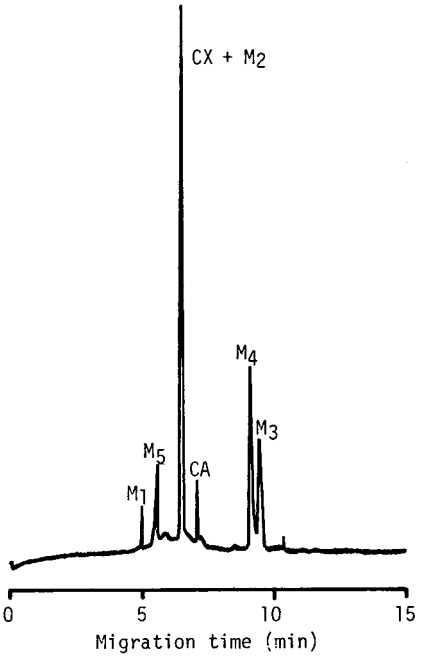

Fig. 3. Separation of CX and its metabolites by plain zone electrophoresis without electroosmotic flow. Capillary, fused silica (68 cm × 50 μm I.D.); carrier, 20 m*M* phosphate buffer (pH 6.8) containing hydroxypropylcellulose (0.02%, w/v); applied voltage, 20 kV. Other conditions as in Fig. 2. The sample solution was introduced from the cathodic end of the tube.

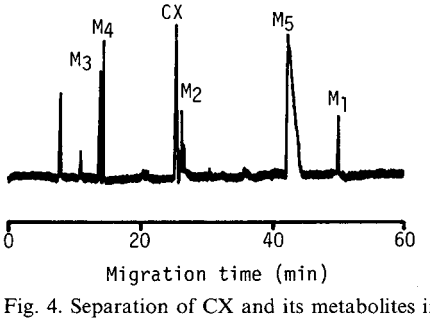

Fig. 4. Separation of CX and its metabolites in the CPDACS–methanol-containing carrier. Capillary, fused silica (75 cm × 50 μm I.D.); carrier, 20 m*M* phosphate buffer (pH 6.8) containing CPDAPS (0.15%, w/v) and methanol (20%, v/v); applied voltage, 30 kV. Other conditions as in Fig. 2. The sample solution was introduced from the anodic end of the tube.

mainly due to this effect, but the effect of addition of CPDAPS cannot be neglected for the separation of the M2–CX pair, as the resolution of this pair in phosphate buffer containing both CPDAPS and methanol was 1.75, whereas that in phosphate buffer containing only methanol was 1.35. The effect of CPDAPS was not predominent, but this amphoteric detergent played a subsidiary role. It seems that the cholamidopropyl part of the CPDAPS molecule interacted weakly with these compounds, and the slight difference in the magnitude of such an interaction between M2 and CX caused an improvement in their separation. The resolutions of the M3–M4 and M1–M5 pairs were much improved by addition of methonol but was not affected by addition of CPDAPS.

Electrokinetic chromatography mode. Terabe *et al.* [3] initiated micellar electrokinetic chromatography by addition of sodium dodecyl sulphate (SDS), an anionic surfactant, to the carrier. This mode permits separation based on solubilization of sample components to moving SDS micelles. However, no solubilization occurred in this work when SDS was added to 20 m*M* phosphate buffer (pH 6.8) at concentrations of 10—50 m*M*, as all components were only slightly hydrophobic under these conditions. The migration times of all these components were gradually increased with increasing SDS concentration, but the pattern of the electropherogram was the same as that in Fig. 2. The separations of the M3–M4 and M2–CX pairs were worse than those in the plain CZE mode (Fig. 2).

On the other hand, Terabe and Isemura [4] studied the separation of highly acidic compounds in a carrier containing polybrene, a basic polymer, and designated this mode ion-exchange electrokinetic chromatography. In this mode, the direction of electroosmotic flow is reversed owing to the change in sign of the electric charge on the capillary inner wall, caused by adsorption of this basic polymer. When this mode was applied in the present instance (Fig. 5), the migration order (CA, M4, M1 + M3, M5, M2, CX, in order of increasing migration times) was different from that in Fig. 2 (M3 + M4, CA, M2 + CX, M5, M1).

If a higher electronegativity of a component leads to a greater ability to bind to this basic polymer, as in ion-exchange chromatography, then components having larger numbers of carboxyl groups should give longer migration times. However, the results, especially the short migration time of M2, which has the largest number of carboxyl groups (three), were inconsistent with this prediction. There might be an unknown mechanism other than ion exchange operative in this system. In this mode the separation of M2 and CX was better than in the plain zone electrophoresis and micellar electrokinetic chromatography modes, but the separation of M1 and M3 was worse.

Overall, zone electrophoresis in the CPDAPS-containing carrier gave the best separation, permitting almost complete separation of CX and its metabolites.

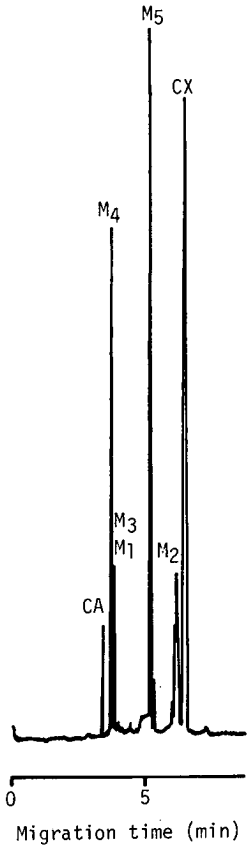

Fig. 5. Separation of CX and its metabolites in the polybrene-containing carrier. Capillary, fused silica (72 cm × 50 μm I.D.); carrier, 20 m*M* phosphate buffer (pH 6.8) containing polybrene (0.5%, w/v); applied voltage, 20 kV. Other conditions as in Fig. 2. The sample solution was introduced from the cathodic end of the tube.

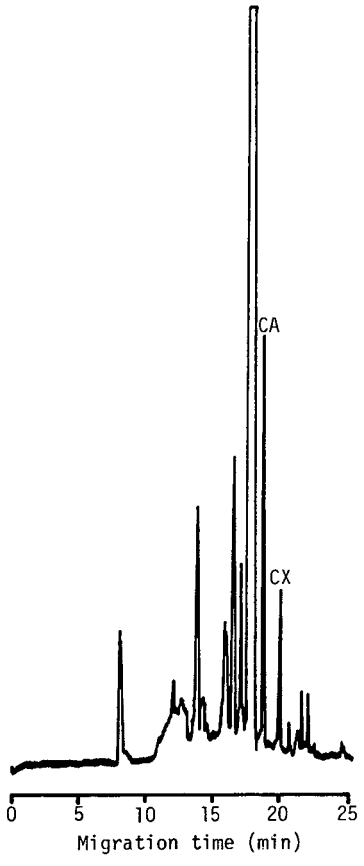

Fig. 6. Analysis of human urine spiked with CX and CA by plain zone electrophoresis. Capillary, fused silica (75 cm × 50 μm I.D.); applied voltage, 20 kV; detection, UV absorption at 295 nm. Concentration: CX, 30.0 μg/ml; CA, 85.1 μg/ml. Other conditions as in Fig. 1. The sample solution was introduced from the anodic end of the tube.

Determination of urinary CX

Orally administered CX is known to be absorbed from the intestine, transported into the circulatory system and excreted into urine almost without being metabolized. Therefore, the determination of the CX concentration in urine provides useful information on whether the CX level is properly controlled or not in the body.

The plain zone electrophoresis mode using 50 m*M* phosphate buffer (pH 6.8) as the carrier, applied to a urine specimen spiked with CX, together with CA as an internal standard, gave the electrophoretogram shown in Fig. 6. The peaks of both CX and CA were well separated from those of inherent urinary components.

Plots of the relative peak response of CX to CA (8.51 μg/ml) against CX concentration in urine gave a straight line almost passing through the origin ($y = 0.0166x - 0.0414$, $r = 0.996$) at least over the range 10–60 μg/ml, which covers the therapeutic range. The relative standard deviations ($n = 7$) at the 30 and 60 μg/ml levels were 3.6% and 2.9%, respectively. This method is simple, permitting the direct determination urinary CX.

REFERENCES

1 A. S. Cohen, D. R. Najarian, A. Paulus, A. Guttman, J. A. Smith and B. L. Karger, *Proc. Natl. Acad. Sci. U.S.A.*, 85 (1988) 9660.
2 Y. Namiki, T. Tanabe, T. Kobayashi, J. Tanabe, Y. Okimura, S. Koda and Y. Morimoto, *J. Pharm. Sci.*, 76 (1987) 208.
3 S. Terabe, K. Otsuka, K. Ichikawa, A. Tsuchiya and T. Ando, *Anal. Chem.*, 56 (1984) 111.
4 S. Terabe and T. Isemura, *Anal. Chem.*, 62 (1989) 650.
5 S. Fujiwara and S. Honda, *Anal. Chem.*, 59 (1987) 487.

Journal of Chromatography, 590 (1992) 369–372
Elsevier Science Publishers B.V., Amsterdam

CHROM. 23 801

Short Communication

Separation and preparative isolation of phenolic dialdehydes by on-line overpressured layer chromatography☆

A. Snini, A. Fahimi, Z. Mouloungui*, M. Delmas and A. Gaset

Laboratoire de Chimie des Agroressources, Ecole Nationale Superieure de Chimie de Toulouse INPT, 118 Route de Narbonne, 31077 Toulouse (France)

(First received April 15th, 1991; revised manuscript received October 14th, 1991)

ABSTRACT

The Reimer–Tiemann reaction carried out in a heterogeneous solid–liquid medium was found to give the isomeric dialdehydes 2-hydroxy-1,3-benzenedicarboxaldehyde and 4-hydroxy-1,3-benzenedicarboxaldehyde. The PRISMA model was employed to optimize the eluent mixture, and with careful choice of silica gel high-performance thin-layer chromatographic plates, the two isomers could be isolated and purified by on-line overpressured layer chromatography.

INTRODUCTION

The Reimer–Tiemann [1] reaction, involving condensation of phenol with chloroform in a basic medium, gives rise to salicylaldehyde (**2**) and *p*-hydroxybenzaldehyde (**3**). In the presence of a solid alkali metal hydroxide in chloroform–methanol–water, this reaction leads to the mono- and diformylation of phenol [2]. Apart from compounds **2** and **3**, 2-hydroxy-1,3-benzenedicarboxaldehyde (**4**) and 4-hydroxy-1,3-benzenedicarboxaldehyde (**5**) are also formed (Fig. 1).

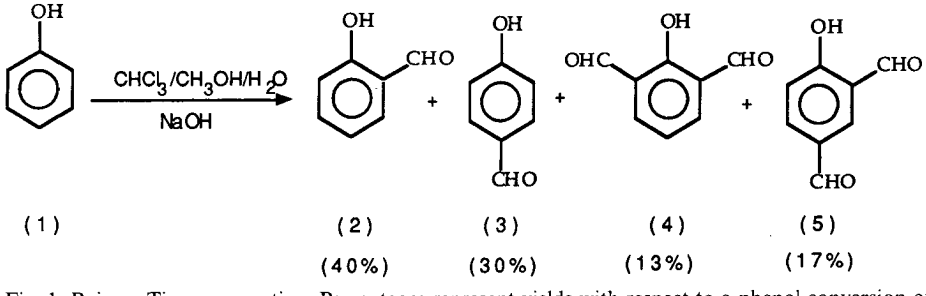

Fig. 1. Reimer–Tiemann reaction. Percentages represent yields with respect to a phenol conversion of 53%.

☆ Presented at the 18th International Symposium on Chromatography, Amsterdam, September 23–28, 1990.

0021-9673/92/$05.00

Although compounds **2** and **3** are readily separated by gas chromatography with a packed column [3], the complex mixture of dialdehydes cannot be separated by this method. We report here the use of on-line overpressured layer chromatography (OPLC) according to Tyihák *et al.* [4] for the rapid and efficient separation and purification of the phenolic dialdehydes. The advantages of this technique are the small amounts of eluent required, a short time for development, which is carried out in a closed chamber avoiding interaction with air, and the fact that detection and separation are carried out simultaneously.

EXPERIMENTAL

The ^1H NMR spectra of the dialdehydes were recorded on a Bruker WN 250-MHz NMR spectrometer using [$^2H_6$]acetone as solvent and tetramethylsilane (TMS) as internal reference. The IR spectra were recorded on a Perkin-Elmer Model 1710 spectrometer with samples in KBr potassium bromide disks.

The mass spectra of the two isomers were recorded using electron impact ionization on a Nermag R15-10 spectrometer (Delsi, Paris, France) coupled to a gas chromatograph equipped with a CP-Sil 5 quartz capillary column (25 m × 0.25 mm I.D., film thickness 0.2 mm) (Chrompack, Paris, France) under the following conditions: carrier gas, helium; temperature initally 100°C, then increased at 5°C/min to 220°C; input pressure, 0.25 bar.

High-performance liquid chromatographic (HPLC) separations were carried out on a Milton-Roy instrument with a LiChrosorb RP-18 (5-μm) column (25 cm × 0.46 cm I.D.) (Merck, Paris, France) using water–acetonitrile–acetic acid (8:2:0.02) as the mobile phase with a UV detector set at 254 nm (LDC Analytical, Roissy, France).

Separation by TLC was carried out on silica gel 60 F_{254} plates (5 × 7.5 cm, 0.2 mm thick layer) (Merck). A 0.5-μl volume of a solution containing a mixture (5%, w/w) of the compounds to be separated was placed 0.5 cm from the end of the plates, which were then placed in a closed glass tank (10 × 6 cm) previously saturated with vapour of the optimized eluent (diethyl ether–hexane–chloroform, 3:2:0.25). The plates were removed when the solvent front was 1 cm from the top of the plate. The plates were dried and the spots revealed under UV light (254 nm). Diethyl ether–hexane–chloroform (3:2:0.25) was found to give the best ΔR_F between compounds **4** and **5** (R_F = 0.41 and 0.29, respectively). TLC was employed to optimize the eluent mixture, which was subsequently employed for on-line OPLC.

TLC under pressure was carried out using a Chrompres 25 system (Factory of Laboratory Instruments, Budapest, Hungary) equipped with an automatic injector, fraction collector (Eurosas, Toulouse, France) and refractometer (LDC Analytical). Experiments were carried out using 20 × 20 cm silica gel 60 F_{254} HPTLC plates (Merck) (thickness 0.2 mm) on either 20 × 20 cm polyamide 11 F_{254} (Merck) (thickness 0.15 mm) or 20 × 20 cm alumina 150 F_{254} (Merck) (thickness 0.25 mm) sorbents. For the analytical separations, a standard mixture containing 47% of **1**, 21% of **2**, 16% of **3**, 7% of **4** and 9% of **5** was prepared in chloroform and 10-μl volumes of this mixture were injected. Prior to each separation, the plate was preconditioned with hexane at 1.5 ml/min for 15 min to eliminate air in the adsorbent layers. A flow-rate of 0.65 ml/min was used for all the analytical OPLC separations. The cushion pressure was kept at 16–18 bar during all separations. The mixture of **4** and **5** was separated by the systems illustrated in Fig. 2.

Phenol, methanol, chloroform and sodium hydroxide were obtained from Merck and were used as received. The solvents for HPLC and OPLC were

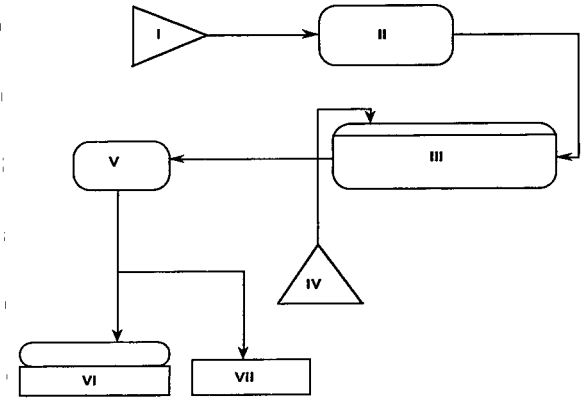

Fig. 2. Schematic diagram of analytical and preparative on-line OPLC system. I = Eluent micropump; II = automatic injector; III = Chrompres 25; IV = water micropump; V = refractometer; VI = fraction collector; VII = integrator.

of chromatographic grade (Merck). Water for HPLC was doubly distilled.

Synthesis

A 0.1-mol amount of phenol (9.41 g), 100 ml of chloroform, 25 ml of methanol and 20 ml of water were placed in a 250-ml flask fitted with a cooling system, thermometer and mechanical stirrer. The mixture was heated to 55–56°C and sodium hydroxide (1 mol; 40 g) was added in portions. The reaction was stopped 1 h after the final addition of sodium hydroxide. After acidification of the reaction mixture to pH 2–3, the reaction products were extracted by steam distillation and were obtained in analytical purity after separation by on-line OPLC. We only present here the spectral characteristics of the phenolic dialdehydes **4** and **5** as those of the monoaldehydes are known. The conversion of the starting phenol was 53%.

Physico-chemical characteristics of the phenolic dialdehydes

*2-Hydroxy-1,3-benzenedicarboxaldehyde (**4**).* Yield = 13%. M.p. = 119–120°C. IR: ν(OH) 3071 cm^{-1}, ν(C=O) 1680 cm^{-1}. ^1H NMR: δ (ppm), 11.9 (s, 1H, O*H*), 10.4 (s, 2H, C*H*O), 8.2 (d, 2H, J = 7 Hz, H^{-4}, H^{-6}) 7.3 (dd, 1H, J = 7 Hz, H^{-5}). Mass spectrum: *m/z* (%), 150 (M^+, 47), 149 (4.5), 122 (100), 121 (43), 93 (10.4). Analysis: calculated for $C_8H_6O_3$, C 64, H 4.03; found, C 64.04, H 4.06%.

*4-Hydroxy-1,3-benzenedicarboxaldehyde (**5**).* Yield = 17%. M.p. = 95–96°C. IR: ν(OH) 3080 cm^{-1}, ν(C = O) 1689, 1665 cm^{-1}. ^1H NMR: δ (ppm), 11.7 (s, 1H, O*H*), 10,3 (s, 1H, *p*-C*H*O), 10.1 (s, 1H, *o*-C*H*O), 8.5 (s, 1H, H^{-2}) 8.2 (d, 1H, J = *10 Hz, H^{-6}*), 7.3 (d, 1H, J = 10 Hz, H^{-5}). Mass spectrum: m/z (%), 150 (M^+, 98), 149 (100), 121 (16), 93 (24). Analysis: calculated for $C_8H_6O_3$, C 64, H 4.03; found, C 63.94, H 4.09%.

RESULTS AND DISCUSSION

Fig. 3 shows the OPLC of a standard mixture of the reaction medium of composition 47% phenol, 21% salicylaldehyde, 16% *p*-hydroxybenzaldehyde, 7% 2-hydroxy-1,3-benzenedicarboxaldehyde and 9% 4-hydroxy-1,3-benzenedicarboxaldehyde. The mixture was then separated in a two-stage process. First, compounds **1** and **2** were eliminated in a rotary evaporator. The dialdehydes **4** and **5** were recovered by steam distillation. Compound **3** remaining in the distillation flask was isolated by crystallization and recrystallization from toluene. Unsuccessful attempts were made to separate the dialdehydes by on-line OPLC on both polyamide or alumina sorbent layers. Better results were obtained with the silica gel HPTLC plates, which could be used three or four times before recycling. The composition of the eluent diethyl ether–hexane–chloroform (3:2:0.25) was optimized using the PRISMA model [5]. Sample and eluent injection and fraction recovery were automatic, and a refractometer was employed as a detector, placed between the Chrompres 25 and the fraction collector.

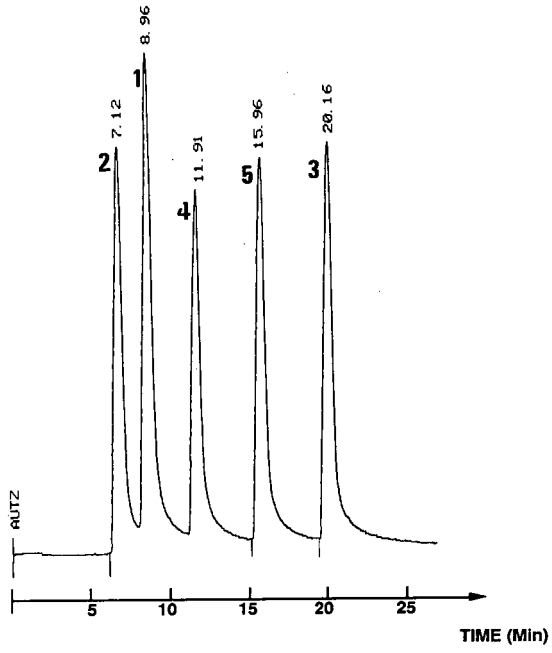

Fig. 3. Separation of a standard mixture on an HPTLC plate by on-line OPLC: 47% of **1**, 21% of **2**, 16% of **3**, 7% of **4** and 9% of **5**. Eluent flow-rate, 0.65 ml/min. for other conditions, see Experimental.

Given the migration time for each constituent of the mixture, the injection of the samples and the recovery of the dialdehydes could be readily programmed. For a load capacity of the HPTLC plates ranging from 20 to 30 mg, the phenolic dialdehydes **4** and **5** were isolated after 12 and 16 min, respectively (Fig. 4). It can be seen that on-line OPLC was

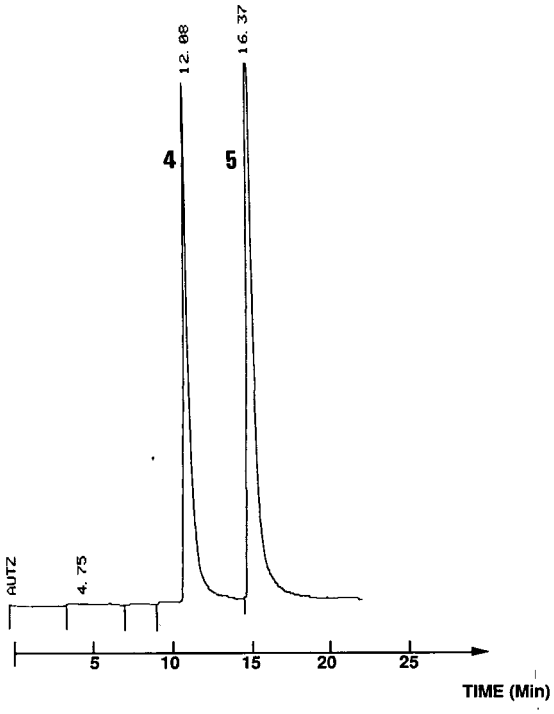

Fig. 4. Separation of dialdehydes **4** and **5** on an HPTLC plate by on-line OPLC. Eluent flow-rate, 0.65 ml/min. For other conditions, see Experimental.

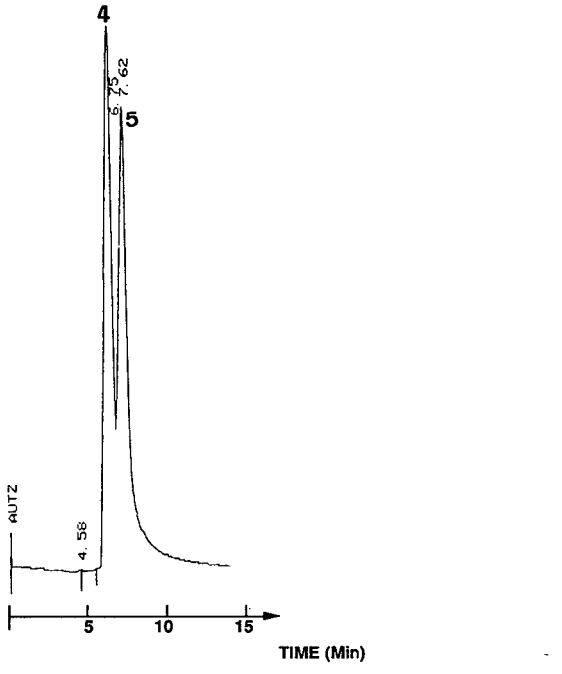

Fig. 5. Separation of dialdehydes **4** and **5** by HPLC. Eluent flow-rate, 0.8 ml/min. For other conditions, see Experimental.

a particularly efficient method for the separation and isolation of such a complex mixture, appearing much superior to HPLC (*cf.*, Fig. 5).

The physico-chemical characteristics of compounds **4** and **5** were determined by IR, ^{1}H NMR and mass spectrometry. pK_a values were determined by UV spectrophotometry. The two phenolic derivatives had similar pK_a values [6] (8.8 and 9, respectively), which accounts for the difficulty in separating them on an anion-exchange resin (Amberlite IRA 402) column.

Compounds **4** and **5** have been found to have marked antifungal activity toward *Candida albicans* and *Aspergillus* [7] and this activity is currently under investigation.

REFERENCES

1 H. Wynberg, *Chem. Rev.*, 60 (1960) 169.
2 A. Thoër, G. Denis, M. Delmas and A. Gaset, *Synth. Commun.*, 18 (1988) 2095.
3 Y. Yongjia and P. Zulan, *Hunan Shifan Daxue Zinan Kexue Xuebao*, 11 (1988) 133.
4 E. Tyihák, E. Mincsovics, H. Kalász and J. Nagy, *J. Chromatogr.*, 211 (1981) 451.
5 Sz. Nyiredy, in E. Tyihák (Editor), *Application of the "PRISMA" model for the Selection of Eluent Systems in Overpressured Layer Chromatography (OPLC)*, Labor MIM, Budapest, 1987, p. 1.
6 G. Denis, *Ph. D. Thesis*, INP, Toulouse, 1988.
7 A. Fahimi, unpublished results.

Journal of Chromatography, 590 (1992) 373–374
Elsevier Science Publishers B.V., Amsterdam

CHROM. 23 827

Book Review

Fluorometric analysis in biomedical chemistry —Trends and techniques including HPLC applications, edited by N. Ichinose, G. Schwedt, F. M. Schnepel and K. Adachi, Wiley, New York, Chichester, 1991, XIV + 225 pp., price £ 59.00, ISBN 0-471-52258-9.

This book is one of a series of volumes on chemical analysis dealing with various aspects of analytical chemistry and its applications, edited by J. D. Winefordner and I. M. Kolthoff.

Fluorimetric spectrometry covers the most important analytical applications of photoluminescence analysis, due to the sensitivity and the selectivity that are offered in the determination of trace amounts of substances. This book deals with basic principles and recent applications of fluorimetric analysis, mostly biochemically and biomedically oriented, including liquid chromatographic methods, all the chapters being authored by one or more of the four Editors.

After an introductory chapter by Schwedt (Clausthal University, Germany) on fluorimetric analysis, the physical properties of fluorescence, photoabsorption and emission phenomena, important parameters such as Stokes shift and quantum yield, the effect of influencing factors, the relationship with chemical structure and the possibilities of chemiluminescence and bioluminescence are treated by Ichinose (Hamamatsu University, Japan). Ichinose and Schwedt treat the principles of fluorescence measurements, including a full description of apparatus and arrangements, the measurement of fluorescence excitation and emission spectra and fluorescence calibration graphs.

Biochemical and biomedical applications of fluorescence analysis are provided next, in an extensive chapter. Schnepel (Stuttgart University, Germany) overviews the native fluorescence properties and potential of chemical derivatization with organic reagents for important biochemically active compounds, including amines (*e.g.*, pyrimidine, purine and indole derivatives), amino and imino acids, alkaloids, vitamins and related compounds and steroids (*e.g.*, estrogens, cholesterol, adrenal steroids). Biomedical and clinical analyses of free and total cholesterol, ammonia, tetracyclines, enzymes, bile acids, uric acid, galactose, fatty acids, inorganic phosphorus, DNA and intracellular pH determinations, amongst others, are described by Ichinose and Adachi (Hamamatsu University, Japan). The same authors illustrate the power of luminescence analysis in immunology (immunoassays), in medical diagnoses (*e.g.*, fluorimetric determination of δ-aminolevulinate dehydratase activity in human erythrocytes, diagnosis and management of diseases of tetrapyrrole metabolism, alkaline phosphatase), in obstetrics and gynaecology (*e.g.*, the assay of estrogens during pregnancy) and in other clinical fields (*e.g.*, inherent fingerprint luminescence detection by laser, flow-cytometric DNA analysis of living and dead cells, the continuous measurement of alcohol in biological fluids).

Finally, Ichinose, Schnepel, Schwedt and Adachi provide an extensive chapter dealing with the biochemical and biomedical applications of fluorimetric analysis using high-performance liquid chromatography. Amines, amino acids, vitamins, steroids, organic acids, alkaloids and thiols are determined after a pre- or post-column fluorescence labelling reaction. Some interesting recent developments in the fields of biomedical and clinical chemistry and fisheries biochemistry using high-performance liquid chromatography and fluorescence detection are described in detail for some specific compounds (*e.g.*, cerebrospinal fluid polyamine monitoring in central nervous system leukaemia, prostaglandins and thromboxanes, catecholamines and related compounds, urinary placental estriol, 5-hydroxyindole-3-acetic acid, urinary metanephrines and serum bile acids). Applications to the analysis of food

and feed samples are presented, with emphasis on the determination of biochemically relevant compounds such as ammonia and volatile amines, diamines, aliphatic amines, vitamin B_1, vitamin C, E and K_3, indoleacetic acid and mildiomycin.

This volume can be used as a theoretical and practical analytical handbook, providing a wealth of information on both the principles and applications of fluorescence spectrometry in life sciences via diagrams, tables, chemical structures of fluorophores and derivatization reactions, etc. It will be of appeal to a wide audience of analytically oriented biomedical, clinical and physical chemists and to academics who apply these methodologies in their research work.

Ghent (Belgium) Willy R. G. Baeyens

Author Index

Erratum

J. Chromatogr., 587 (1991) 81–84
Page 82, EXPERIMENTAL, *Fast protein liquid chromatography (FPLC)*, last sentence, (pH should read (pH 7).

Vol. 590, No. 2

Journal of Chromatography

NEWS SECTION

ANNOUNCEMENTS

19TH ANNUAL MEETING OF THE FEDERATION OF ANALYTICAL CHEMISTRY AND SPECTROSCOPY SOCIETIES (FACSS), PHILADELPHIA, PA, USA, SEPTEMBER 20–25, 1992

The 19th annual meeting of FACSS wil comprise invited and contributed papers, workshops and short courses, and a technical instrumentation exhibit, providing an expanded technical program with an emphasis on emerging technologies in analytical, spectroscopic and chromatographic sciences. Diverse analytical interests are respresented in the technical program which typically includes papers in the areas of: atomic spectroscopy, biotechnology and clinical chemistry, chemometrics, chromatography, electrochemistry, environmental analysis, infrared spectroscopy, lasers, mass spectrometry, nuclear magnetic resonance spectrometry, process analysis, raman spectroscopy, X-ray spectroscopy and surface analysis.

Contributed papers are solicited in all areas of analytical chemistry. The scientific program will also include various award symposia.

The deadline for submission of a title and a preliminary 100-word brief is March 4, 1992.

For further details, contact: FACSS, P.O. Box 278, Manhattan, KS 66502, USA. Tel.: (+1-301) 846-4797.

3RD INTERNATIONAL SYMPOSIUM ON FIELD-FLOW FRACTIONATION (FFF '92), PARK CITY, UT, USA, OCTOBER 5–7, 1992 AND FFF WORKSHOP V, SALT LAKE CITY, UT, USA, OCTOBER 3–4, 1992

Park City, Utah, will be the site of the 3rd International Symposium on field-flow fractionation to be held October 5–7, 1992. An optional extension of the workshop on Sunday, October 4, will greatly expand the opportunity for hands-on laboratory experience.

The Symposium will have presentations covering all aspects of FFF, ranging from recent theoretical and instrumental developments to applications in industry, biochemistry, and environmental studies. Recent advances in the separations and analysis of diverse types of biopolymers, synthetic polymers, colloids, and cell-sized particles by FFF will be surveyed.

Invited lectures along with contributed papers, posters, and discussion sessions will be scheduled. Titles and abstract of submitted papers and posters are due April 1, 1992. A few last-minute posters will be accepted as late as September 22, 1992.

The Symposium will be preceded by the FFF Workshop on Saturday, October 3, with an optional extension on Sunday, October 4, The Workshop is intended for those desiring a working knowledge of field-flow fractionation. Lecture topics will include

basic theory, principles of operation and optimization, and instrumental systems and characteristics. Enrollment will be limited to maintain an informal learning environment.

For further details, contact: Julie Westwood, FFF Research Center, Department of Chemistry, University of Utah, Salt Lake City, UT 84112, USA. Tel.: (+1-801) 581-5419; Fax: (+1-801) 581-4353.

3RD INTERNATIONAL SYMPOSIUM ON CHIRAL DISCRIMINATION, TÜBINGEN, GERMANY, OCTOBER 5–8, 1992

Scientists interested in the topic of chiral discrimination are invited to attend this symposium, which will present an excellent opportunity for discussion and inter-disciplinary exchange of information and experience.

The symposium will focus on recent developments in chiral discrimination phenomena and will highlight recent advances in the state-of-the-art. Contributions are solicited for the following topics, as well as in areas not listed here but appropriate to the theme of the symposium:

- Chiral discrimination in the solid state
- Chiral discrimination in separation methods
- Chiral discrimination in biological systems
- Chiral discrimination in biotechnology
- Chiral discrimination in pharmacology
- Chiral discrimination in catalysis and enzymology
- Mechanisms and models of chiral discrimination
- Legislative and miscellaneous aspects of chirality

The symposium will include plenary lectures by distinguished international scientists, invited lectures and contributed papers. The latter will be considered for oral presentation, and there will be a strong emphasis on poster presentation as the core of the scientific program. All presentations will be printed in a book of abstracts to be distributed during the symposium.

For further details, contact: Gesellschaft Deutscher Chemiker, GDCh, P.O. Box 90 04 40, D-6000 Frankfurt/Main 90, Germany. Fax: (+49-69) 791-7475.

3RD ANNUAL FREDERICK CONFERENCE ON CAPILLARY ELECTROPHORESIS, FREDERICK, MD, USA, OCTOBER 20–21, 1992

This meeting will include oral and poster presentations by individual conference participants, and optional enrollment in a definitive CE course. Invited speakers will provide expert overviews of the basic aspects and applications of capillary electrophoresis (CE) and micellar electrokinetic capillary chromatography (MECC), including instrument and column design, detection, modification buffer and factors that influence mobility, selectivity, resolution and optimization. Also, the application of CE to the separation of small ions as well as large biomolecules will be presented and discussed.

The submittal of abstracts is invited from investigators interested in presenting their work. A 200-word description of your research effort should be submitted for consideration by the Scientific Committee. Abstracts will be accepted as 20-minute talks or poster displays. The deadline for submission of abstracts is Friday, July 31, 1992.

Exhibitions of the most recent CE instrumentation and equipment will be on site throughout the duration of the conference.

There is no registration fee; however, registration is mandatory to ensure enrollment. Participation is limited.

A one-day definitive course on CE will be offered to interested participants on Monday, October 19, 1992. The instruction will include theory, instrumentation, buffer selection, optimization and applications. A nominal fee of US$ 100.00 will be charged for participation in this course (US$ 125.00 will be charged after October 1st). Course enrollment and payment are in addition to required registration.

For further details, contact: Margaret L. Fanning, Conference Coordinator, PRI, NCI-FCRDC, P.O. Box B, Frederick, MD 21702-1201, USA. Tel.: (+1-301) 846-1089; Fax: (+1-301) 846-5866.

ION-EX '93, WREXHAM, UK, APRIL 4–7, 1993

This Ion-Ex '93 conference will be devoted to the industrial, analytical and preparative applications of ion exchange processes and will be held at the North

East Wales Institute, Wrexham, Clwyd, April 4–7, 1993.

Topics which will be covered at the meeting will include: pharmaceutical analysis, water recycling and purification, the nuclear industry, electrochemical methods and capillary electrophoresis, inorganic ion exchangers, industrial applications, new materials, ion chromatography, environmental analysis, organic analysis, biological analysis, and ion exchange membranes, with plenary lectures being presented by Dr. B. Clarke (University of Bradford, UK), Dr. B. Croll (Anglian Water Services Ltd, UK), Dr. J.Lehto (University of Helsinki, Finland) Dr. M. Sadler (Consultant, UK), Professor M. Abe (Tokyo Institute of Technology, Japan) and Professor Ph. Gramain (Institut Charles Sadron, CNRS, France).

To accompany the meeting there will be an Industrial Exhibition of products and equipment by companies involved in this field.

For further details, contact: Ion-Ex '93, Conference Secretariat, Faculty of Science, The North East Wales Institute, Connah's Quay, Deeside, Clwyd, CH5 4BR, UK. Tel.: (+44-244) 831-531 ext. 245 or 276; Fax: (+44-244) 814-305.

COURSES

ANALYTICAL CHEMISTRY SHORT COURSES, LOUGHBOROUGH, UK

The following short courses will be held this summer at the Department of Chemistry, University of Technology, Loughborough, UK.

- ICP–MS; May 18–22, 1992.
- Separations for Biotechnology and Biochemistry; June 22–26, 1992.
- Radioisotope Techniques; June 29–July 3, 1992.
- High-Performance Liquid Chromatography; July 6–10, 1992.

For further details contact: Mrs. S. Maddison, Department of Chemistry, Loughborough University of Technology, Loughborough, Leics. LE11 3TU. Tel.: (+44-509) 222-575; Fax: (+44-509) 233-163.

AMSTERDAM SUMMERCOURSE ON CAPILLARY ELECTROPHORESIS, AMSTERDAM, NETHERLANDS, JULY 8–10, 1992

The Amsterdam CE Summercourse is meant to guide newcomers in the basic concepts of capillary electrophoresis. Among the potential fields of application we find pharmaceutical analysis, clinical analysis and biotechnology. In overview lectures experts in the field will show the possibilities of the technique, and provide the theoretical background required for a successful application. A choice of seminar topics will be offered on specialized aspects of CE. During the informal seminar sessions participants have the opportunity to discuss the application of CE in their own laboratory with the seminar leaders.

Commercially available instruments of all major manufacturers and laboratory instruments will be used in practical experiments by the participants. Experience can be obtained with various separation techniques. Participants can bring their own samples to study the feasibility of CE for their analyses.

Lecture/seminar topics will include: general introduction to capillary electrophoresis; optimization of CE separations; mass loadability and peak distortion; detection in CE; capillary gel electrophoresis; micellar electrophoresis and electrochromatography; CE of (small) inorganic and organic ions; CE of peptides and proteins; CE–MS coupling; capillary isotachophoresis; applications of CE in the pharmaceutical industry; applications of CE in biotechnology; and how to build your own CE instrument.

During the experimental sessions the participants can obtain practical experience with various aspects of CE. Different apparatus can be evaluated and compared.

The tuition fee will be approximately Dfl. 1600.00. The fee includes the course book and manual, lunches and refreshments and a course dinner. The number of participants is restricted and admittance will occur on the basis of the order of receipt of the registration form and payment.

For further details, contact: Dr. W.Th. Kok or Dr. J.C. Kraak, Laboratory for Analytical Chemistry, University of Amsterdam, Nieuwe Achtergracht 166, 1018 WV Amsterdam, Netherlands. Tel.: (+31-20) 525-6539/46/15; Fax: (+31-20) 525-5698.

NOMINATIONS FOR AWARDS

NOMINATIONS FOR THE TOMAS HIRSCHFELD STUDENT AWARDS

Nominations are requested for the Tomas Hirschfeld Student Awards, which will be presented at the 19th annual FACSS Conference in Philadelphia, PA, USA, September 20–25, 1992. Awards are given for the most outstanding papers submitted by graduate students in the field of analytical chemistry. The student nominees will present 20-minute papers at the 1992 FACSS Conference. To be considered for these awards, students must submit the title of their paper, two letters of nomination, including one from their graduate advisor, any reprints/preprints and a 250-word abstract to: Diane Landoll, FACSS National Office, P.O. Box 278, Manhattan, KS 66502, USA.

The deadline for submission of all materials is March 4, 1992.

The awardees' travel will be arranged and paid for by FACSS.

For further details, contact: F. Monte Evens, Conoco Inc., P.O. Box 1267, Ponca City, OK 74603, USA, Tel.: (+1-405) 767-3850; or, Ivan L. Glaze, American Cast Iron Pipe Co., P.O. Box 2727, Birmingham, AL 35202, USA, Tel.: (+1-205) 325-8979.

CALENDAR OF FORTHCOMING EVENTS

March 9–13, 1992
New Orleans, LA, USA
43rd Pittsburgh Conference and Exposition on Analytical Chemistry and Applied Spectroscopy

Contact: Mrs. Alma Johnson, Program Secretary, The Pittsburgh Conference, 300 Penn Center Boulevard, Suite 332, Pittsburgh, PA 15235-5503, USA.

April 6–8, 1992
Atlanta, GA, USA
ANATECH '92, 3rd International Symposium on Analytical Techniques for Industrial Process Control

Contact: ANATECH '92, Infosciences Inc., 3000 Dundee Road, Suite 313, Northbrook, IL 60062, USA. Tel.: (708) 291-9161; Fax: (708) 291-0097.

April 6–8, 1992
Nancy, France
PREP-92, 9th International Symposium on Preparative and Industrial Chromatography

Contact: PREP-92 Secretary, E.N.S.I.C.-L.P.C.I., 1 rue Grandville, B.P. 451, F-54001 Nancy Cedex, France. Tel.: (+33) 83300276; Fax: (+33) 83350811.

May 5–8, 1992
Liège, Belgium
4th International Symposium on Drug Analysis

Contact: Dr. J. Crommen, Drug Analysis '92-Liège, University of Liège, Institute of Pharmacy, rue Fusch 5, B-4000 Liège, Belgium. Tel.: (+32-41) 237002; Fax: (+32-41) 221855.

May 5–8, 1992
Munich, Germany
13th International Conference on Biochemical Analysis

Contact: U. Arnold, Nymphenburger Strasse 70, D-8000 Munich 2, Germany. Tel.: (+49-89) 1234500; Fax: (+49-89) 183258.

May 12–14, 1992
La Grand Motte, France
4th European Meeting of Groupe Français de Bio-Chromatographie

Contact: Groupe Français de Bio-Chromatographie, Unité d'Immuno Allergie, Institut Pasteur, 28 rue du Docteur Roux, 75724 Paris Cedex 15, France. Tel.: (+33-1) 45688000, ext. 7143; Fax: (+33-1) 43069835; Telex: 250609 F.

May 17–22, 1992
Kyoto, Japan
4th International Conference on Fundamentals of Adsorption

Contact: Prof. M. Suzuki, Conference Chairman, Institute of Industrial Science, University of Tokyo, 7-22-1 Roppongi, Minato-ku, Tokyo 106, Japan.

May 25–29, 1992
Baltimore, MD, USA
14th International Symposium on Capillary Chromatography

Capillary Chromatography

Contact: Dr. Leonard Schronk, Foundation for the ISCC, P.O. Box 663, Kennett Square, PA 19348, USA. Tel. and Fax: (+1-215) 692-4320.

June 1–4, 1992
Inuyama, Aichi, Japan
ISPAC, 5th International Symposium on Polymer Analysis and Characterization

Contact: Dr. Sadao Mori, Department of Industrial Chemistry, Faculty of Engineering, Mie University, Tsu, Mie 514, Japan. Tel: (+81-592) 32-1211, ext. 3843; Fax: (+81-592) 31-2252. Dr. Howard Barth, Dupont Company, Experimental Station, P.O. Box 80228, Wilmington, DE 19880-0228, USA. Tel: (+1-302) 695-4354; Fax: (+1-302) 695-1351.

June 9–12, 1992
Dortmund, Germany
22nd Roland W. Frei Memorial Symposium on Environmental Analytical Chemistry and Workshop on Detection in Environmental Analysis

Contact: Symposium Office IAEAC, M. Frei-Hausler, P.O. Box 46, CH-4123 Allschwil 2, Switzerland. Tel.: (+41-61) 632789; Fax: (+41-61) 4820805.

June 14–19, 1992
Baltimore, MD, USA
HPLC '92, 16th International Conference on Column Liquid Chromatography

Contact: HPLC '92, Ms. Shirley E. Schlessinger, 400 E. Randolph Drive, Suite 1015, Chicago, IL 60601, USA. Tel.: (312) 527-2011.

■ **July 8–10, 1992**
Amsterdam, Netherlands
Amsterdam Summercourse on Capillary Electrophoresis

Contact: Dr. W.Th. Kok or Dr. J.C. Kraak, Laboratory for Analytical Chemistry, University of Amsterdam, Nieuwe Achtergracht 166, 1018 WV Amsterdam, Netherlands. Tel.: (+31-20) 525-6539/46/15; Fax: (+31-20) 525-5698.

July 14–17, 1992
Montreal, Canada
CAC-92, 5th International Conference on Chemometrics in Analytical Chemistry

Contact: Int. Conf. on Chemometrics in Analytical Chemistry, c/o Department of Chemistry, Clarkson University, Potsdam, NY 13699-5810, USA. Tel: (+1-315) 268-3861 (Dr. Hopke); (+1-315) 268-2394 (Dr. Lavine); Fax: (+1-315) 268-6670.

■ **Aug. 23–26, 1992**
York, UK
Capillary Electrophoresis Training Course

Contact: Dr. Terry Threlfall, Industrial Liaison Executive, Department of Chemistry, University of York, Heslington, York YO1 5DD, UK. Tel.: (+44-904) 432576/432511; Fax: (+44-904) 432516.

Aug. 24–27, 1992
Jena, Germany
COMPANA '92, 5th Conference on Computer Applications in Analytical Chemistry

Contact: COMPANA '92, Friedrich Schiller University Jena, Institute of Inorganic and Analytical Chemistry, Steiger 3, Haus 3, O-6900 Jena, Germany. Tel.: (+37-82) 25467 or (+37-82) 25029.

■ **Aug. 26–28, 1992**
York, UK
International Symposium on Capillary Electrophoresis

Contact: Dr. Terry Threlfall, Industrial Liaison Executive, Department of Chemistry, University of York, Heslington, York YO1 5DD, UK. Tel.: (+44-904) 432576/432511; Fax: (+44-904) 432516.

Aug. 31–Sept. 3, 1992
Cincinnati, OH, USA
106th Annual International Meeting and Exposition of the AOAC

Contact: Margaret Ridgell, AOAC, 2200 Wilson Boulevard, Suite 400, Arlington, VA 22201-3301, USA. Tel.: (703) 522-3032; Fax: (703) 522-5468.

Sept. 13–18, 1992
Aix-en-Provence, France
19th International Symposium on Chromatography

Contact: G.A.M.S., 88 Boulevard Malesherbes, 75008 Paris, France. Tel.: (1) 45639304; Fax: (1) 49530434

■ **Sept. 20–25, 1992**
Philadelphia, PA, USA
19th Annual Meeting of the Federation of Analytical Chemistry and Spectroscopy Societies

Contact: FACSS, P.O. Box 278, Manhattan, KS 66502, USA. Tel.: (+1-301) 846-4797.

Sept. 21-24, 1992
Linz, Austria
International Ion Chromatography Symposium

Contact: Century Internaitonal, P.O. Box 493, Medfield, MA 02052, USA. Tel.: (+1-508) 359-8777; Fax: (+1-508) 359-8778.

□ **Oct. 3–4, 1992**
Salt Lake City, UT, USA
FFF Workshop V
Contact: Julie Westwood, FFF Research Center, Department of Chemistry, University of Utah, Salt Lake City, UT 84112, USA. Tel.: (+1-801) 581-5419; Fax: (+1-801) 581-4353.

□ **Oct. 5–7, 1992**
Park City, UT, USA
3rd International Symposium on Field-Flow Fractionation (FFF)
Contact: Julie Westwood, FFF Research Center, Department of Chemistry, University of Utah, Salt Lake City, UT 84112, USA. Tel.: (+1-801) 581-5419; Fax: (+1-801) 581-4353.

Oct. 5–8, 1992
Tübingen, Germany
3rd International Symposium on Chiral Discrimination
Contact: Gesellschaft Deutscher Chemiker, Abteilung Tagungen, P.O. Box 90 04 40, D-6000 Frankfurt 90, Germany. Fax: (+49-69) 791-7475

Oct. 6–9, 1992
Rome, Italy
ITP '92, 8th International Symposium on Capillary Electrophoresis and Isotachophoresis
Contact: Dr. Salvatore Fanali, Istituto di Cromatografia del C.N.R., P.O. Box 10, 00016 Monterotondo Scalo (Rome), Italy. Tel: (+39-6) 9005328/9005836; Fax: (+39-6) 9005849; Telex: 624809 CNR ML 1.

□ **Oct. 20–21, 1992**
Frederick, MD, USA
3rd Annual Frederick Conference on Capillary Electrophoresis
Contact: Margaret L. Fanning, Conference Coordinator, PRI, NCI-FCRDC, P.O. Box B, Frederick, MD 21702-1201, USA. Tel.: (+1-301) 846-1089; Fax: (+1-301) 846-5866.

Nov. 4–6, 1992
Montreux, Switzerland
9th Montreux Symposium on Liquid Chromatography–Mass Spectrometry (LC–MS, SFC–MS, CZE–MS, MS–MS)
Contact: Marianne Frei, IAEAC Secretariat, P.O. Box 46, CH-4123 Allschwil, Switzerland. Tel.: (+41-61) 632789; Fax: (+41-61) 4820805.

Nov. 29–Dec. 2, 1992
Syndey, Australia
12th International Symposium on HPLC of Proteins, Peptides and Polynucleotides
Contact: 12 ISPPP Sectretariat, GPO Box 128, Sydney NSW 2001, Australia. Tel.: (+61-2) 262-2277; Fax: (+61-2) 262-2323.

□ **April 4–7, 1993**
Wrexham, UK
Ion-Ex '93
Contact: Ion-Ex '93, Conference Secretariat, Faculty of Science, The North East Wales Institute, Connah's Quay, Deeside, Clwyd, CH5 4BR, UK. Tel.: (+44-244) 831-531 ext. 245 or 276; Fax: (+44-244) 814-305.

May 9–14, 1993
Hamburg, Germany
17th International Symposium on Column Liquid Chromatography
Contact: Gesellschaft Deutscher Chemiker, Abteilung Tagungen, P.O. Box 900440, Varrentrappstrasse 40-42, W-6000 Frankfurt am Main 90, Germany. Tel: (+49-69) 7917-360; Fax: (+49-69) 7917-475.

Sept. 5–11, 1993
Edinburgh, UK
EUROANALYSIS VIII, 8th European Conference on Analytical Chemistry
Contact: Miss P.E. Hutchinson, Analytical Division, The Royal Society of Chemistry, Burlington House, Piccadilly, London W1V 0BN, UK. Tel.: (071) 4378656; Fax: (071) 734-1227; Telex: 268001.

June 20–24, 1994
Bournemouth, UK
20th International Symposium on Chromatography
Contact: Executive Secretary, The Chromatographic Society, Nottingham Polytechnic, Burton Street, Nottingham, NG1 4BU, UK. Tel.: (0602) 500596; Fax: (0602) 500614.

PUBLICATION SCHEDULE FOR 1992

Journal of Chromatography and *Journal of Chromatography, Biomedical Applications*

MONTH	O 1991	N 1991	D 1991	J	F	M	
Journal of Chromatography	585/1	585/2 586/1 586/2 587/1	587/2 588/1+2	589/1+2 590/1 590/2	591/1+2 592/1+2 593/1+2	594/1+2 595/1	The publication schedule for further issues will be published later
Cumulative Indexes, Vols. 551–600							
Bibliography Section						610/1	
Biomedical Applications				573/1 573/2	574/2	575/1 575/2	

INFORMATION FOR AUTHORS

(Detailed *Instructions to Authors* were published in Vol. 558, pp. 469–472. A free reprint can be obtained by application to the publisher, Elsevier Science Publishers B.V., P.O. Box 330, 1000 AH Amsterdam, The Netherlands.)

Types of Contributions. The following types of papers are published in the *Journal of Chromatography* and the section on *Biomedical Applications:* Regular research papers (Full-length papers), Review articles and Short Communications. Short Communications are usually descriptions of short investigations, or they can report minor technical improvements of previously published procedures; they reflect the same quality of research as Full-length papers, but should preferably not exceed five printed pages. For Review articles, see inside front cover under Submission of Papers.

Submission. Every paper must be accompanied by a letter from the senior author, stating that he/she is submitting the paper for publication in the *Journal of Chromatography*.

Manuscripts. Manuscripts should be typed in double spacing on consecutively numbered pages of uniform size. The manuscript should be preceded by a sheet of manuscript paper carrying the title of the paper and the name and full postal address of the person to whom the proofs are to be sent. As a rule, papers should be divided into sections, headed by a caption (*e.g.*, Abstract, Introduction, Experimental, Results, Discussion, etc.). All illustrations, photographs, tables, etc., should be on separate sheets.

Introduction. Every paper must have a concise introduction mentioning what has been done before on the topic described, and stating clearly what is new in the paper now submitted.

Abstract. All articles should have an abstract of 50–100 words which clearly and briefly indicates what is new, different and significant.

Illustrations. The figures should be submitted in a form suitable for reproduction, drawn in Indian ink on drawing or tracing paper. Each illustration should have a legend, all the *legends* being typed (with double spacing) together on a *separate sheet*. If structures are given in the text, the original drawings should be supplied. Coloured illustrations are reproduced at the author's expense, the cost being determined by the number of pages and by the number of colours needed. The written permission of the author and publisher must be obtained for the use of any figure already published. Its source must be indicated in the legend.

References. References should be numbered in the order in which they are cited in the text, and listed in numerical sequence on a separate sheet at the end of the article. Please check a recent issue for the layout of the reference list. Abbreviations for the titles of journals should follow the system used by *Chemical Abstracts*. Articles not yet published should be given as "in press" (journal should be specified), "submitted for publication" (journal should be specified), "in preparation" or "personal communication".

Dispatch. Before sending the manuscript to the Editor please check that the envelope contains four copies of the paper complete with references, legends and figures. One of the sets of figures must be the originals suitable for direct reproduction. Please also ensure that permission to publish has been obtained from your institute.

Proofs. One set of proofs will be sent to the author to be carefully checked for printer's errors. Corrections must be restricted to instances in which the proof is at variance with the manuscript. "Extra corrections" will be inserted at the author's expense.

Reprints. Fifty reprints of Full-length papers and Short Communications will be supplied free of charge. Additional reprints can be ordered by the authors. An order form containing price quotations will be sent to the authors together with the proofs of their article.